LI
LABORATORY INVESTIGATION
THE BASIC AND TRANSLATIONAL PATHOLOGY RESEARCH JOURNAL
VOLUME 98 | SUPPLEMENT 1 | MARCH 2018

USCAP 2018

ABSTRACTS

GENITOURINARY PATHOLOGY

(894-1126)

107TH ANNUAL MEETING

GEARED TO LEARN

MARCH 17-23, 2018

Vancouver Convention Centre
Vancouver, BC, Canada

Published by
SPRINGER NATURE
www.ModernPathology.org

USCAP Creating a Better Pathologist
AN OFFICIAL JOURNAL OF THE UNITED STATES AND CANADIAN ACADEMY OF PATHOLOGY

EDUCATION COMMITTEE

Jason L. Hornick, Chair
Rhonda Yantiss, Chair, Abstract Review Board and Assignment Committee
Laura W. Lamps, Chair, CME Subcommittee
Steven D. Billings, Chair, Interactive Microscopy
Shree G. Sharma, Chair, Informatics Subcommittee
Raja R. Seethala, Short Course Coordinator
Ilan Weinreb, Chair, Subcommittee for Unique Live Course Offerings
David B. Kaminsky, Executive Vice President (Ex-Officio)
Aleodor (Doru) Andea
Zubair Baloch
Olca Basturk
Gregory R. Bean, Pathologist-in-Training
Daniel J. Brat
Amy Chadburn
Ashley M. Cimino-Mathews
James R. Cook
Carol F. Farver
Meera R. Hameed
Michelle S. Hirsch
Anna Marie Mulligan
Rish Pai
Vinita Parkash
Anil Parwani
Deepa Patil
Lakshmi Priya Kunju
John D. Reith
Raja R. Seethala
Kwun Wah Wen, Pathologist-in-Training

ABSTRACT REVIEW BOARD

Narasimhan Agaram
Christina Arnold
Dan Berney
Ritu Bhalla
Parul Bhargava
Justin Bishop
Jennifer Black
Thomas Brenn
Fadi Brimo
Natalia Buza
Yingbei Chen
Benjamin Chen
Rebecca Chernock
Andres Chiesa-Vottero
James Conner
Claudiu Cotta
Tim D'Alfonso
Leona Doyle
Daniel Dye
Andrew Evans
Alton Farris
Dennis Firchau
Ann Folkins
Karen Fritchie
Karuna Garg
James Gill
Anthony Gill
Ryan Gill
Tamara Giorgadze
Raul Gonzalez
Anuradha Gopalan
Jennifer Gordetsky
Ilyssa Gordon
Alejandro Gru
Mamta Gupta
Omar Habeeb
Marc Halushka
Krisztina Hanley
Douglas Hartman
Yael Heher
Walter Henricks
John Higgins
Jason Hornick
Mojgan Hosseini
David Hwang
Michael Idowu
Peter Illei
Kristin Jensen
Vickie Jo
Kirk Jones
Chia-Sui Kao
Ashraf Khan
Michael Kluk
Kristine Konopka
Gregor Krings
Asangi Kumarapeli
Frank Kuo
Alvaro Laga
Robin LeGallo
Melinda Lerwill
Rebecca Levy
Zaibo Li
Yen-Chun Liu
Tamara Lotan
Joe Maleszewski
Adrian Marino-Enriquez
Jonathan Marotti
Jerri McLemore
David Meredith
Dylan Miller
Roberto Miranda
Elizabeth Morgan
Juan-Miguel Mosquera
Atis Muehlenbachs
Raouf Nakhleh
Ericka Olgaard
Horatiu Olteanu
Kay Park
Rajiv Patel
Yan Peng
David Pisapia
Jenny Pogoriler
Alexi Polydorides
Sonam Prakash
Manju Prasad
Bobbi Pritt
Peter Pytel
Charles Quick
Joseph Rabban
Raga Ramachandran
Preetha Ramalingam
Priya Rao
Vijaya Reddy
Robyn Reed
Michelle Reid
Natasha Rekhtman
Michael Rivera
Mike Roh
Marianna Ruzinova
Peter Sadow
Safia Salaria
Steven Salvatore
Souzan Sanati
Sandro Santagata
Anjali Saqi
Frank Schneider
Michael Seidman
Shree Sharma
Jeanne Shen
Steven Shen
Jiaqi Shi
Wun-Ju Shieh
Konstantin Shilo
Steven Smith
Lauren Smith
Aliyah Sohani
Heather Stevenson-Lerner
Khin Thway
Evi Vakiani
Sonal Varma
Marina Vivero
Yihong Wang
Christopher Weber
Olga Weinberg
Astrid Weins
Maria Westerhoff
Sean Williamson
Laura Wood
Wei Xin
Mina Xu
Rhonda Yantiss
Akihiko Yoshida
Xuefeng Zhang
Debra Zynger

To cite abstracts in this publication, please use the following format: **Author A, Author B, Author C, et al. Abstract title (abs#). *Laboratory Investigation* 2018; 98 (suppl 1): page#**

894 Prostate Cancer with Cribriform Pattern (CFPC) is Associated with Adverse Clinical and Pathological Features in Prostate Biopsies (Bx) with Gleason Score (GS) 7 (3+4) Prostate Cancer (PC)

Eman Abdulfatah[1], *Dongping Shi*[2], *Rohith Arcot*[3], *Hui Guan*[3], *Elisabeth I Heath*[4], *Wael Sakr*[5]. [1]Wayne State University, Detroit, MI, [2]Wayne State University/Detroit Medical Center, Detroit, MI, [3]Wayne State University, [4]Karmanos Cancer Institute, Detroit, MI, [5]Wayne State University/Harper University Hospital, Detroit, MI

Background: Gleason grade 4 (GG4) PC has different architectural patterns with % of GG4 being an important prognosticator in patients(pts) with GS 7(3+4) PC. Recent reports indicate that CFPC may be an additional, independent adverse risk factor in this PC category. We aimed to explore the potential association of CFPC with aggressive clinicopathologic parameters in men with GS 7(3+4) PC on Bx.

Design: All pts diagnosed with Bx GS 7(3+4) PC between 2005-2011 in our institution were included. PSA at diagnosis, no. of positive cores, % of core involvement, % of GG4 and presence of CFPC were documented. The presence of CFPC was correlated with post treatment parameters; stage and margin status following radical prostatectomy (RP); biochemical recurrence(BR), distant metastasis(DM), progression free survival(PFS) and cancer specific mortality(CSM) for all pts. Statistical analyses were conducted using KM and regression analysis.

Results: 283 pts qualified for analyses. We classified 74%,53%,26% and 21% of GG4 as fused glands, poorly formed glands, glomeruloid and CFPC, respectively. At diagnosis, pts with CFPC had significantly higher PSA, more positive cores, higher % core involvement and higher % of GG4 (P=0.03,P=0.001,P=0.001 and P=0.001,respectively). Forty percent of pts were treated with RP, 55% by radiation therapy(RT), 3% cryoablation and 2% chose active surveillance.

After RP, GS was significantly upgraded for pts with CFPC(P=0.03). Median follow up was 89 (range 4-150)months. BR and DM were significantly higher in pts with CFPC compared to those without (P=0.001 & P=0.001,respectively). On univariate regression analysis, CFPC was a significant predictor of BR(P=0.001), DM(P=0.003) and CSM(P=0.01). On multivariate analysis, CFPC was an independent predictor of CSM(P=0.02). When stratifying pts based on treatment, CFPC was significantly associated with BR(P=0.03) and an independent predictor of CSM(P=0.02) after RP. Following RT, BR was also significantly higher in pts with CFPC(P=0.009).

On KM analysis, pts with CFPC had significantly shorter BR free survival and PFS(P=0.001 and P=0.008, respectively). PFS was also significantly shorter in pts with CFPC who underwent RP(P=0.04), while pts who received RT had shorter BRFS(P=0.001) and PFS(P=0.01).

Conclusions: Our data strongly suggest that CFPC, as a variant of GG4 PC, is significantly associated with poorer clinicopatholgic features. Accounting for this variant has the potential of influencing prognostic and management considerations.

895 Comparison of synchronous high grade prostate intraepithelial neoplasm, invasive adenocarcinoma and intraductal carcinoma of the prostate using NGS on LCM tissue

Andres Acosta[1], *Mohamed Rizwan Haroon Al Rasheed*[2], *Erica Vormittag*[3], *Dipti V Panchal*[4], *Magdalena Rogozinska*[4], *Andre Kajdacsy Balla*[5], *Frederick Behm*[4], *Gayatry Mohapatra*[4]. [1]UIC, Chicago, IL, [2]University of Illinois at Chicago, Chicago, IL, [3]University of Illinois at Chicago, Chicago, Illinois, [4]University of Illinois at Chicago, [5]Univ of Illinois, Chicago, IL

Background: IIntraductal carcinoma of the prostate (IDCP) is defined as malignant secretory cells spanning the lumen of ducts and acini and/or showing either significant nuclear pleomorphism or unequivocal comedonecrosis. This morphologic definition encompasses a wide spectrum of lesions that might include from cases with florid high-grade prostate intraepithelial neoplasia (HGPIN) to high-grade carcinoma confined to ducts. Adding uncertainty to the significance of this poorly defined category is the fact that, while associated with high-grade invasive carcinoma (IC) in the overwhelming majority of cases, IDCP has occasionally been found alone. To date, only limited (target-specific) genetic studies of IDCP have been performed. Here we compare synchronous HGPIN, IDCP and IC microdissected from 5 patients using a targeted solid tumor NGS panel.

Design: Formalin-fixed paraffin-embedded (FFPE) tissue from 6 patients with synchronous HGPIN, IC and lesions morphologically compatible with IDCP were retrieved. Two consecutive sections were obtained from each block for H&E staining and P63 immunohistochemistry (IHC), respectively. p63 IHC demonstrated IDCP in 5 of the 6 cases, which were sectioned, placed onto PEN-membrane slides and stained with toluidine blue for laser-capture microdissection (LCM). LCM was performed to isolate HGPIN, IDCP, and the major higher and lower grade components of IC using the p63 IHC as a guide. DNA and RNA were isolated and the corresponding libraries were prepared. NGS was performed on Ion S5XL sequencer using OCP 143-gene panel. Variants were called using Ion Reporter analysis tool (ThermoFisher).

Results: Sequencing results are presented in the table. Sequencing revealed a common set of aberrations present in all microdissected components. IDCP and IC show a similar genetic profile, which is more complex than that of concurrent HGPIN.

FOR TABLE DATA, SEE PAGE 403, FIG. 895

Conclusions: Our results show that synchronous HGPIN, invasive adenocarcinoma and IDCP within a single prostate share a group of core genetic abnormalities that are maintained throughout the process of tumor progression. Therefore, all the elements probably arise from a single precursor (HGPIN). The genetic makeup of IDCP closely resembles that of adjacent IC, supporting that IDCP represents ductal spread of coexisting IC. Alternatively, IDCP might arise as a result of duct-confined progression of HGPIN that subsequently develops invasion within a very short period of time, which would explain why IDCP is only exceptionally found alone.

896 Identification and validation of novel long non-coding RNA signatures of enzalutamide resistance in prostate cancer

John Aird[1], *Steven G Gray*[2], *Anne-Marie Baird*[2], *Marvin Chang Jui Lim*[3], *Ray McDermott*[4], *Stephen Finn*[5]. [1]St. James's Hospital, Dublin, [2]St. James's Hospital, [3]University of Dublin, Trinity College, [4]Adelaide and Meath Hospital incorporating The National Children's Hospital, [5]University of Dublin, Trinity College, Dublin

Background: Despite significant advances, castration resistant prostate cancer (CRPC) remains incurable. Sustained androgen-receptor (AR) signalling despite low levels of circulating androgens is a key feature of CRPC. New drugs like enzalutamide target the AR but drug resistance inevitably develops via sustained AR signalling. Although not yet fully understood, known mechanisms for sustained AR signalling include alternate AR splicing, AR gene overexpression/amplification and AR gene mutations.

Long non-coding RNAs (lncRNAs) are emerging as key modulators of gene expression and have been shown to be associated with drug resistance in cancer. Our hypothesis is that lncRNAs are associated with resistance to enzalutamide in prostate cancer.

Design: Using a model of spontaneous resistance to enzalutamide in LNCaP cells previously developed by Korpal *et al* (Cancer Discovery, September 2013) we profiled enzalutamide sensitive, and both weakly and strongly enzalutamide resistant clones for 40,173 well characterized lncRNAs using microarray technology. Differentially expressed lncRNAs with statistical significance were identified through Volcano Plot filtering. The threshold was fold change ≥ 2.0 and p-value ≤ 0.05. False discovery rates were adjusted from all the p-values by Benjamini-Hochberg method for multiple testing correction. Both highly upregulated and candidate lncRNAs with strong biological relevance (known association with CRPC or with androgen signalling) were validated using qPCR.

Results: Principal component analysis indicated significant differences between the sensitive and resistant cell lines. Genes of lncRNA transcripts that were significantly upregulated in enzalutamide resistant cells compared to enzalutamide sensitive cells included DGCR5, DPP10-AS1, FLJ26850, RP11-1C8.7, RP11-222K16.2 and RP11-38P22.2. A recent study by Zhai *et* al (Oncogene, September 2016) reported that RP11-38P22.2 encodes a lncRNA designated Suppressing Androgen Receptor in Renal Cell Carcinoma (SARCC). SARCC binds to the AR in renal cell carcinoma cells. Further validation experiments are on-going to assess the functional effect of modifying lncRNA levels on enzalutamide sensitivity.

Conclusions: LncRNAs are emerging as key players in the regulation of gene expression and the development of drug resistance. We have validated a lncRNA signature that is upregulated in enzalutamide resistant LNCaP cells in comparison to enzalutamide sensitive LNCaP cells.

897 Increased COX-2 immunostaining in Urothelial Carcinoma of the Urinary Bladder is associated with Invasiveness and Poor Prognosis

Jaudah Al-Maghrabi[1], *Wafaey Gomaa*[2], *Basim J Al-Maghrabi*[3], *Mohammed Abdelwahed*[4]. [1]King Abdulaziz University, Jeddah, Saudi Arabia, [2]Minia University, Al Minia, Al Minia, [3]University of Jeddah, Jeddah, Saudi Arabia, [4]University of Jeddah, Jeddah, Saudi Arabia

Background: Urothelial carcinoma of the urinary bladder [UCB] is the most common bladder cancer. Cyclooxygenase-2 [COX-2] mediates angiogenesis, cell survival/proliferation and apoptosis. This study investigates the relation of COX-2 immunostaining to UCB clinicopathological parameters.

Design: The study population includes 123 UCB and 25 urothelial mucosae adjacent to UCB. UCB samples were collected prior to the administration of any intravesical or systemic therapy. Tissue microarrays were designed and constructed and TMA blocks were sliced for further immunohistochemical staining. Immunohistochemical staining was done using a mouse anti-human COX-2 monoclonal antibody. A cut-off point of 10% was chosen as the threshold to determine low and high COX-2 immunostaining.

Results: COX-2 immunostaining is higher in UCB than in adjacent urothelium [p=0.033]. High COX-2 immunostaining is associated with high grade UCB [p=0.013], distant metastasis [p=0.031], lymphovascular invasion [p=0.008], positive muscle invasion [p=0.017], pT2 and above [p=0.003], and high anatomical stages [Stage II and above]. High COX-2 immunostaining is an independent predictor of higher tumour grade [p<0.001], muscle invasion [p=0.015], advanced pathological T [p=0.014], lymphovascular invasion [p=0.011], and distant metastasis [p=0.039]. High COX-2 immunostaining is associated with lower overall survival rate [p=0.019].

Conclusions: COX-2 immunostaining associated with invasiveness of UCB may be used as an independent prognostic marker. COX-2 may be a significant molecule in the development and progression of UCB. Molecular and clinical investigations are required to explore the molecular downstream of COX-2 in UCB and effectiveness of COX-2 inhibitors as adjuvant therapy along with traditional chemotherapy.

898 The Significance of Isolated Linear Tumor Nests within the Tunica Albuginea in Stage I Seminoma: A Multi-Institutional Study

Khaleel Al-Obaidy[1], *Chia-Sui Kao*[2], *David R Levy*[2], *Karen Trevino*[1], *Muhammad Idrees*[1], *Thomas Ulbright*[1]. [1]Indiana University School of Medicine, Indianapolis, IN, [2]Stanford University School of Medicine, Stanford, CA

Background: Linear arrays and small nests of tumor cells in the tunica albuginea that are remote from the main tumor have been suggested as a surrogate marker for lymphovascular invasion (LVI), a finding established to correlate with advanced stage. Nevertheless, no studies have specifically addressed this issue. We therefore sought to evaluate the clinical significance of this finding.

Design: We retrospectively reviewed the pathologic database of two institutions for patients with seminoma and pT1 or pT2 pathologic stage. Slides were reviewed and cases were then classified into three groups: pT1 tumors with discontinuous tumor cells (DTCs) within the TA (n=22), pT1 tumors without DTCs within the TA (n=60) and pT2 tumors with pure LVI and no TA involvement (n=11). Cases with rete testis, tunica vaginalis or epididymal invasion were excluded. Follow-up information was obtained from physicians' notes. Patients without follow-up data were excluded from the study.

Results: A total of 93 cases were found to fulfill the inclusion criteria. Patients with pT1 tumors and DTCs presented at a younger age when compared to patients with pT1 tumors and no DTCs (p=0.038) or those with pT2 tumors (p=0.047). The tumor size in pT2 patients or pT1 patients with DTCs was significantly larger than in pT1 patients without DTCs (p=0.009 and 0.038, respectively). No statistical significance existed in tumor size between pT1 patients with DTCs versus pT2 patients (p=0.41). Over an average follow-up of 53 months, tumor recurrence/clinical upstaging was observed in 18.1% (n=4) of pT1 patients with DTCs, 15% (n=9) of pT1 patients without DTCs and 45.5% (n=5) of pT2 patients. There was no significant difference in recurrence/upstaging between pT1 patients with DTCs versus pT1 patients without DTCs [OR: 1.25 (0.34 to 4.59) (p=0.72)] or versus pT2 patients [OR: 0.26 (0.05-1.3) (p=0.10)]. However, recurrence was significantly more frequent in pT2 patients compared to pT1 patients without DTCs [OR: 0.21 (0.05-0.84) (p=0.027)].

Conclusions: The presence of DTCs within the TA in patients with stage pT1 seminomas tend to occur at a significantly younger age when compared to patients with pT2 tumors and in larger tumors when compared to pT1 patients lacking DTCs. No statistical difference existed in recurrence/upstaging in pT1 tumors with DTCs tumors versus pT2 tumors. Our results are limited by small sample size in the DTC cohort but suggest that DTCs in seminoma are a possible surrogate for LVI. Larger studies are needed.

899 Is So-Called Oncocytic Papillary Renal Cell Carcinoma a Distinct Entity? A Multi-Institutional Morphologic, Immunohistochemical and Fluorescence In-Situ Hybridization Study

Khaleel Al-Obaidy[1], *John Eble*[1], *Liang Cheng*[1], *Sean R Williamson*[2], *Wael Sakr*[3], *Nilesh Gupta*[4], *Muhammad Idrees*[1], *David Grignon*[1]. [1]Indiana University School of Medicine, Indianapolis, IN, [2]Henry Ford Health System, Detroit, MI, [3]Wayne State University/Harper University Hospital, Detroit, MI, [4]Henry Ford Hospital, Detroit, MI

Background: Papillary renal cell carcinoma (PRCC) is the second most common type of RCC. It has been classified into type 1 and 2 based on cytology and architecture. In 2005, a potentially distinct type of PRCC, "oncocytic papillary renal cell carcinoma" was first introduced. However, to date no clear definition and insufficient data has been presented to support its designation as a separate entity. We evaluated the morphologic, immunohistochemical (IHC) and selected chromosomal characteristics of this entity.

Design: We retrospectively reviewed the pathologic characteristics of tumors diagnosed as PRCC from 2004-2017. For inclusion, the tumor had to have pure papillary or papillary/tubular architecture and be composed of cells with dense eosinophilic (oncocytic) cytoplasm with apically located nuclei. After application of these criteria, 14 cases (2 biopsies, 5 radical and 7 partial nephrectomies) were identified. IHC studies (CK7, CK AE1/AE3, EMA, MUC1, CD10, CD117, AMACR and vimentin) and FISH chromosomal (7, 17 and 3p) analysis were performed.

Results: Patients mean age was 65 years (range 46-80). Eight patients were women and 6 were men. Mean size was 1.6 cm (range 1-3). ISUP nuclear grade was most frequently 2 (n=8), followed by 1 (n=4) and 3 (n=2). All tumors were stage pT1a. All cases had branching papillae with thin fibrovascular cores, lined by low columnar cells with eosinophilic granular cytoplasm, apical nuclei with apical surface blebbing, regular nuclear contours, and in most inconspicuous nucleoli. Tubule formation (n=2) and cytoplasmic vacuoles (n=6) were also observed. 7 resected tumors had a pseudocapsule. Psammoma bodies, necrosis, mitoses and foamy macrophages were absent in all cases. Immunohistochemically, tumor cells were consistently and diffusely positive for AE1/AE3, EMA, MUC1 and CD10 (apical surface). CK7 was diffusely positive in 12 cases, expressed in <5% of cells in 1 case and was negative in 1 case. CD117 and vimentin were uniformly negative. AMACR expression was present in >50% of cells in 3 cases and 10% in 1 case. Trisomy 7 and/or 17 were detected in 36% of cases (n=5). No 3p deletions were detected.

Conclusions: The IHC profile with lack of vimentin expression and consistent MUC1 expression is not typical of usual PRCC. The frequency of trisomies is lower than expected in usual PRCC (up to 80% in our hands – data not presented). These findings suggest that so-called oncocytic papillary renal cell carcinoma may represent a unique tumor unrelated to usual PRCC.

900 Adenocarcinoma of the Rete Testis: Clinicopathologic and Immunohistochemical Characterization

Khaleel Al-Obaidy[1], *Thomas Ulbright*[1], *Muhammad Idrees*[1]. [1]Indiana University School of Medicine, Indianapolis, IN

Background: Adenocarcinoma of the rete testis is uncommon with approximately 60 cases reported. Due to rarity, its etiology, histogenesis, morphology and immunoprofile are not well characterized. We describe clinicopathologic and immunohistochemical characteristics of adenocarcinoma of the rete testis from our institution.

Design: Six cases of adenocarcinoma of the rete testis were retrieved from institutional records. All H&E stained slides were reviewed and immunohistochemical stains (CK7, CK20, AE1/AE3, PAX-8, inhibin, vimentin, S100, calretinin, WT-1, CK5/6, EMA) were performed on 4-mm-thick formalin fixed paraffin-embedded tissue sections of five cases. Follow-up information was obtained from patients' electronic records.

Results: The mean age at diagnosis was 64 years (range 55-76). Four of 6 tumors were right-sided. Hilar localization and transition from benign rete epithelium to malignant epithelium within the rete tubules were the most helpful criteria for diagnosis. Multiple histologic patterns were present in each case. All showed a variable proportion of glandular morphology, with slit-like to well-formed glandular structures. Other growth patterns included: papillary (6), solid (6), corded/trabecular (2), and nested (1). The cytoplasm was pale eosinophilic in all cases, with patchy clearing in 3. Tumors displayed frequent mitoses and geographic necrosis (n=3). All cases had hyalinized to partially fibrotic stroma. The immunostaining showed positivity for CK7 (5/5), AE1/AE3 (5/5), WT1 (5/5), EMA (4/4), PAX 8 (3/5), vimentin (4/4), CK5/6 (4/5) and Calretinin (2/5). Inhibin, CK20 and S100 were consistently negative.

Four patients developed retroperitoneal lymph node (RPLN) metastasis, 1 developed RPLN and lung metastases and 1 developed pulmonary and thoracic LN metastasis within one year of diagnosis. Three patients underwent RPLN dissection, two patients underwent chemotherapy alone and one patient had RPLN dissection and chemotherapy. Three patients died within four years of diagnosis. The remaining 3 patients were lost to long term follow up.

Conclusions: Adenocarcinoma of the rete testis is a rare malignant tumor with poor survival. Its rarity and poor morphologic and immunohistochemical characterization make the diagnosis challenging. Integration of clinicopathologic and immunohistochemical features is required to establish the diagnosis.

901 Targeting Androgen Receptor in Combination with Cisplatin: an Effective Treatment Strategy for Muscle Invasive Bladder Cancer

Mohammed Alghamdi[1], *Youssef Khafateh*[2], *Chendil Damodaran*, *Deeksha Pal*[3], *Ashish Tyagi*[3], *Mostafa Fraig*[4], *Houda Alatassi*[3]. [1]University of Louisville, Louisville, KY, [2]University of Louisville, Louisville, KY, [3]University of Louisville, [4]Univ of Louisville Hosp, Louisville, KY

Background: Bladder cancer is one of the major causes of cancer death in the United States and worldwide. Cisplatin is a key component of chemotherapeutic regimens employed in the treatment of advanced bladder cancer. Recently, androgen receptor (AR) activation has been associated with resistance to cisplatin treatment. The present study was envisaged to determine AR expression in human bladder cancer specimens and whether targeting AR alone or in combination of with cisplatin effectively suppresses the growth of muscle invasive bladder cancer.

Design: AR expression was determined in 50 human bladder cancer specimens and in a panel of bladder cancer cell lines. Cells grown in charcoal stripped media supplemented with dihydrotestosterone (DHT) were treated with cisplatin, enzalutamide (an AR inhibitor), or a combination of both. Cellular/phenotypic analysis including MTT assay, apoptotic assays, and migration as well as invasion assays and molecular analysis including western blotting and real-time PCR analysis were performed. Isobologram analysis for the combination was performed and analyzed with CompuSyn. Experiments were repeated in triplicate and analyzed with unpaired Student's t-test and one-way ANOVA *p≤0.05, **p≤0.01, ***p≤0.001.

Results: Thirty percent of the human bladder cancer specimens expressed AR. DHT treatment significantly (p=0.0001) induced cell growth in AR+ bladder cancer cells, suggesting functional AR status. Enzalutamide effectively inhibited the growth of AR+ bladder cell lines. Of particular interest, enzalutamide in combination with cisplatin synergistically inhibited the proliferation of MIBC cells. Combination index (CI) values for both cell lines TCCSUP (CI: 0.42, 1.25 + 5 μM), J82 (CI: 0.79, 2.5 + 5 μM) suggested that both drugs can act synergistically at low dosages. Treatment with the combination of cisplatin and enzalutamide also induced pro-apoptotic (Bax, Caspase 3) and DNA damage (pATM, pATR, pChk1, pHis) signaling and resulted in induction of apoptosis in AR+ bladder cancer cells. Significant inhibition of migratory as well as invasive potential in J82 and TCCSUP were also seen with the combination of enzalutamide and cisplatin.

Conclusions: The combination of cisplatin and AR inhibition effectively inhibits bladder tumor growth and migration, and holds promise as synergetic therapies for AR+ bladder cancer patients.

902 Pleomorphic Giant Cell Prostatic Adenocarcinoma (PGCA): A Series of 24 Cases

Abdullah M Alharbi[1], *Jonathan Epstein*[2], *Tamara L Lotan*[3]. [1]The Johns Hopkins Med Inst, Baltimore, MD, [2]The Johns Hopkins Med Inst, Baltimore, MD, [3]Johns Hopkins School of Medicine, Baltimore, MD

Background: Background: PGCA is rare with the only prior series consisting of 6 cases.

Design: We identified 22 cases from our consults and 2 cases from our own hospital. Paraffin blocks with lesional tissue were available in 6 cases for IHC (blocks from additional outside cases to be stained for final results).

Results: Men ranged in age from 43-90 years (mean 73). Diagnostic specimens consisted of needle biopsies (n=12); TURs (n=9), urethral/bladder biopsies (n=2), and radical prostatectomy (RP) (n=1). In all cases, there was usual acinar prostate adenocarcinoma (PCa.) where the highest grade in all cases was Gleason score 9-10 (Grade Group 5). Evaluable cases: On average, 85% of the involved cores had cancer with a maximum % cancer averaging 69%; on average, TURs had 88% of the area involved by cancer. PGCA was focal (<5% of cancer) (Figure 1). 2 of the needle biopsies showed extra-prostatic extension. Of 2 RPs, both had seminal vesicle invasion and positive margins with 1 having a positive lymph node. Of the 17 men with >2 years follow-up, 12 were dead with a median time to death of 9 months (mean 15.6 mos.). NKX3.1 labeled PGCA more than PSA and P501S (Table). In 2/6 cases, PGCA cells were negative for all 3 prostate markers. GATA3 was focally positive in the PGCA in 1/6 cases (also positive case in the usual PCa.). ki67 averaged 32% of the PGCA cells with a wide range. P53 was positive (>5%) in 2/6 cases of PGCA. PTEN was lost (Figure 2) with negative staining for ERG in all 6 PLGCA cases. Androgen receptor was positive in 4/6 cases in PGCA. In general, the degree of labeling for all the above markers in PGCA in a given case paralleled that seen in the associated usual PCa.

Case	NKX3.1 (%)	PSA (%)	P501S (%)	Ki67 (%)
1	0	0	0	30
2	50	<5	0	20
3	90	<1	<5	<5
4	100	0	<5	30
5	0	0	0	90
6	90	5	90	20

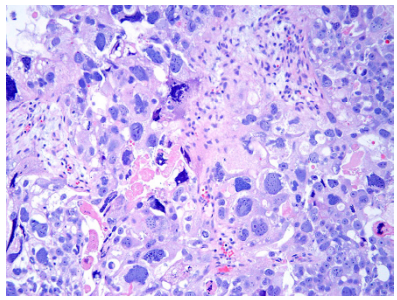

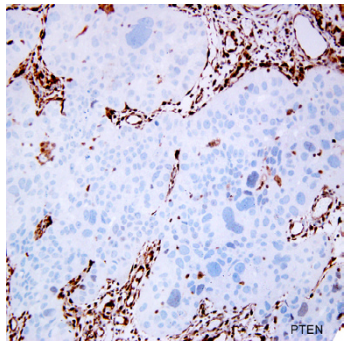

Conclusions: GCA is rare and accompanied by extensive usual prostate adenocarcinoma. Although the PGCA component is focal, it can mimic urothelial carcinoma. The associated usual PCa. is typically very high grade without significant glandular differentiation. Also, IHC can be misleading as PSA staining is often negative or focal in both the PGCA and usual PCa. components. NKX3.1 is the most sensitive prostate marker, but was still focal in 1 usual PCa. and negative in 2 PGCA. Loss of PTEN in all cases is consistent with the aggressive nature of these tumors. AR positivity in some cases including the PGCA raises the possibility of being responsive to ADT. Despite a dismal prognosis, there appears to be some long-term survivors such that prompt, accurate diagnosis is needed for the appropriate therapy.

903 Well-Differentiated Neuroendocrine Tumors of the Kidney. A Clinico-Pathologic Study of 15 Cases

Isabel Alvarado-Cabrero[1], *Raquel Valencia-Cedillo*[2], *Ana Elena Martin-Aguilar*[3], *Rafael Estevez-Castro*[4], *Ondrej Hes*[5]. [1]Mexican Oncology Hospital, Mexico, [2]Hospital de Oncología, CMN Siglo XXI IMSS, Cd Mexico, FDM, [3]Hospital de Oncología, CMN Siglo XXI, IMSS, [4]Laboratorio de Patología Dra. Rosario Castro. Santiago, República Dominicana, [5]Biopticka laborator, Plzen

Background: Primary renal well differentiated neuroendocrine tumors (WDNET) are exceedingly rare, with less than 100 cases being documented in world literature. The rarity of these tumors pose a diagnostic and therapeutic challenge.

The aim of this study is to discuss the clinicopathologic features and prognosis of 15 patients with primary renal WDNET.

Design: Of 3,800 patients who underwent partial or radical nephrectomy between 1999-2016 at our institution, 15 (0.39%) had primary renal WDNET. Pathologic parameters, TNM stage, and multifocality were evaluated. Immunostainings on all cases were performed with chromogranin, synaptophysin, CD56 and Ki-67. Clinical information was obtaining by reviewing the clinical records.

Results: Patient age ranged from 46 to 82 years (average 59y). The majority of specimens consisted of radical nephrectomies with or without associated lymph node dissection. None of these patients had carcinoid syndrome or a history of multiple endocrine neoplasia. Tumor size ranged from 4.5 to 11.8cm (average size: 7.1cm), all tumors were unifocal.

All tumors had histologic features similar to WDNET in other anatomical locations. All 15 neoplasms expressed at least 1 neuroendocrine marker. The Ki-67 index ranged from 0% to 5%.

Pathologic tumor stage included: T1b (n:2), T2a (n:6), T2b (n:3), T3a (n:3), T4 (n:1). At the time of surgery, the presence of metastases was

documented in 9 patients. Metastases were present in regional lymph node (4/9), bone (3/9), liver (1/9) and lungs (1/9). In addition, 2 patients developed liver metastases within 12 months of surgery. The mean follow-up period for all 15 patients was 29.2 months (range, 12.2-102 months). Five (33%) of the 15 patients died of their disease.

Conclusions: Primary kidney WDNET has similar morphologic features to those WDNET present at other anatomic sites.

Metastases are frequent.

Patients have a prolonged clinical course despite widely metastatic disease.

904 Tumor Microenvironment of Upper Tract Urothelial Carcinoma with Squamous Differentiation is Distinct from that of Upper Tract Urothelial Carcinoma without Evidence of Squamous Differentiation

Aileen Grace Arriola[1], *Sahar J Farahani*[2], *Priti Lal*[3]. [1]UT MD Anderson Cancer Center, Jersey City, NJ, [2]Hospital of the University of Pennsylvania, Philadelphia, PA, [3]University of Pennsylvania, Philadelphia, PA

Background: Upper tract urothelial carcinoma (UTUC) is an aggressive disease and the only current treatment is radical nephrectomy. Tumor microenvironment plays a significant role in the prognosis of cancer and is a promising target in cancer immunotherapy. One of the targets of immunotherapy is the signaling pathway of programmed death ligand-1 (PD-L1) binding to programmed death 1 receptor (PD-1) on the surface of tumor-infiltrating lymphocytes (TILs). While the tumor microenvironment of bladder cancer has been extensively studied, only a few have examined UTUC. In this retrospective study we performed a comprehensive clinical and histologic review of UTUC, with detailed analysis of TILs, expression of PD1 and PD-L1.

Design: 72 UT resections were identified (2000-2015) in our archives. Clinicopathologic data was collected and cases reviewed. Whole sections were stained for PD-L1 (Cell signaling 15165BF, clone E1J2J), PD-1 (Abcam 52587), and CD8. Immunohistochemical (IHC) expression of PD-L1 was documented in epithelial and lymphohistiocytic compartments where both papillary cores and peritumoral regions were evaluated. H scores were calculated (intensity X percentage) for PDL1. ≥1% membranous staining was considered positive. TILs by H&E were scored on a scale of 1-3. CD8 and PD-1+ lymphocytes were quantified manually in hotspot areas (average # of positive cells/10HPF). Clinicopathologic features were documented and statistical analysis performed.

Results: The morphologic characteristics of UTUC with squamous differentiation (SqD) were found to be significantly different from UTUC without SqD and included a larger average size (p=0.03), higher stage (p=0.04), and a significant increase in TILs in the peri-tumoral region (p=0.002). Furthermore, peritumoral TILs in UTUC-SqD revealed significantly increased expression of PD-1 (p=0.03) and the peritumoral lymphohistiocytic component revealed significantly increased PD-L1 expression (p=0.001). Finally, UTUC-SqD revealed significantly increased PD-L1 expression when compared to UTUC without SqD (p=0.02).

Conclusions: Our study suggests that the tumor microenvironment plays an important role in UTUC. The significantly higher PD-1+ TILs and PD-L1 expression in UTUC-SqD raises the potential difference in immunogenicity of these tumors that needs further validation in a larger cohort.

905 Primitive Neuroectodermal Tumor of the Urinary Bladder: A series of thirteen cases, a multi-institutional study

Manas Baisakh[1], *Suravi Singh*[2], *Debdarshi Rath*[3], *Soumya S Panda*[3], *Shilpy Jha*[4], *Dinesh Pradhan*[5], *Jasreman Dhillon*[6], *Matthew Geller*[7], *Jatin S Gandhi*[8], *Bonnie Balzer*[9], *Sambit K Mohanty*[10]. [1]Apollo Hospitals, [2]Prolife Diagnostics, Bhubaneswar, [3]IMS & SUM Hospital, [4]Vivekananda Hospital, Bhubaneswar, Odisha, India, [5]University of Pittsburgh Medical Center, [6]H. Lee Moffitt Cancer Ctr, Tampa, FL, [7]Winthrop University Hospital, Mineola, NY, [8]University of Tennessee Health Science Center, Memphis, TN, [9]Cedars-Sinai Medical Center, Los Angeles, CA, [10]Advanced Medical Research Institute and Hospital and Metropolis India Heath Care, Cuttack, Odisha

Background: Primitive neuroectodermal tumor (PNET) of the urinary bladder is a rare and aggressive small blue round cell neoplasm associated with specific type of genetic translocation and occurs in relatively older age group as compared to its bone and soft tissue counterpart. Given the rarity of this tumor, it is not entirely possible to establish the optimal therapeutic modalities, target-based therapy and prognostic biomarkers of this tumor, thus each case described in the literature serves to increase our knowledge and aid to elaborate strategies for treatment. Herein, we present thirteen new cases of primary PNET of the urinary bladder.

Design: Clinicopathologic parameters, including demographics, presentation, histology, immunohistochemical profiles, molecular signature, and management of 13 cases of PNET of the bladder were analyzed.

Results: The figure 1 illustrates the clinicopathologic parameters, including demographics, presentation, histology, immunohistochemical profiles, molecular signature, and management of the cases included in the study. Figure 2 depicts the histomorphology, immunohistochemistry for FLI1 and FISH assay (break-apart assay for EWSR1) of one of the cases. A multimodal approach was instituted in the cases, which included surgery supported by chemotherapy with cyclophosphamide, vincristine, and dactinomycin for all cases and addition of iphosphamide and etoposide for non-metastatic cases.

Clinicopathologic Profile of the Cohort of Cases

Case #	Age/Gender	Presenting symptoms	Tumor size (cm)	Metastasis	Surgical Intervention	CT	RT	Urinary Diversion	FLI1	CD99	Desmin	MyoD1	Myogenin	WT1	PAX 5	CATA 3	Vim	SYN	CC	CD56	EWSR1
1	46M	Gross hematuria	5.7	Liver, abdominal wall	TURBT, partial cystectomy	Adjuvant CT	Yes	IC	pos	pos	neg	neg	neg	neg	neg	weak pos	neg	pos	neg	pos	pos
2	78M	Gross hematuria	15	-	TURBT, radical cystectomy	Palliative CT	Yes	IC	pos	pos	neg	neg	neg	pos	neg	neg	neg	pos	pos	pos	pos
3	21F	Fever, acute urinary retention	4.4	Liver	TURBT, partial cystectomy	Adjuvant CT	No	IC	pos	pos	neg	neg	neg	neg	pos	neg	neg	pos	pos	pos	pos
4	58M	Fatigue, pancytopenia, cachexia	6	-	TURBT, partial cystectomy	Adjuvant CT	No	IC	pos	pos	neg	neg	neg	neg	neg	weak pos	neg	pos	neg	pos	pos
5	15F	Microscopic hematuria	11	Kidney	TURBT, radical cystectomy	Adjuvant CT	No	IC	pos	pos	neg	neg	neg	neg	neg	neg	neg	pos	pos	pos	pos
6	62M	Fever, dull aching lower abd pain, lump	8.9	-	TURBT, radical cystectomy	Adjuvant CT	No	IC	pos	pos	neg	neg	neg	neg	neg	neg	neg	pos	pos	pos	pos
7	18F	Microscopic hematuria	9.5	-	TURBT, partial cystectomy	Adjuvant CT	No	IC	pos	pos	neg	neg	neg	neg	pos	neg	neg	pos	pos	pos	pos
8	61M	Microscopic hematuria	14	-	TURBT, radical cystectomy	Adjuvant CT	No	IC	pos	pos	neg	neg	neg	neg	neg	neg	neg	pos	pos	pos	pos
9	21F	lower abd pain, gross hematuria	7	-	Partial cystectomy	Adjuvant CT	No	IC	pos	pos	Focally pos	neg	neg	neg	neg	weak pos	neg	pos	neg	pos	pos
10	81M	Dark urine, UTI, hydronephrosis	6.4	Lung, Liver	Partial cystectomy	Palliative, neoadjuvant CT	Yes	UR-M	pos	pos	neg	neg	neg	neg	pos	neg	neg	pos	pos	pos	pos
11	73M	renal failure, BL hydronephrosis	2.9	Lung, Liver	Radical cystectomy	Palliative, neoadjuvant CT	Yes	RE-M	pos	pos	Focally pos	neg	neg	pos	neg	neg	neg	pos	pos	pos	pos
12	59F	Lymphedema of legs	9	-	Radical cystectomy	Adjuvant CT	No	IC	pos	pos	neg	neg	neg	neg	pos	neg	neg	pos	pos	pos	pos
13	50F	Gross hematuria	4.8	-	Pleural fin surgery	Neoadjuvant CT	-	-	pos	pos	neg	neg	ND	neg	neg	neg	ND	pos	neg	pos	pos

Abbreviations used: TURBT: transurethral resection; CT: Chemotherapy; IC: Ileal conduit; N: Nephrectomy; Ure II: Urophalic II; EWSR1: EWSR1 breakapart FISH; NB: Not done.

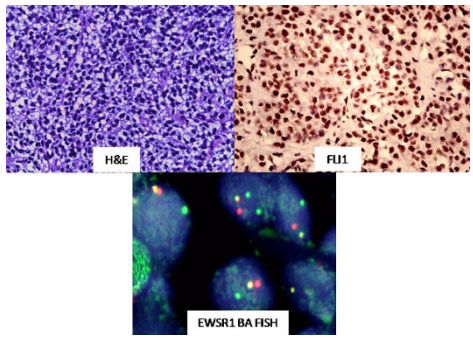

Conclusions: PNET is an extremely unusual malignant tumor of the urinary bladder. The definitive diagnosis is based on histomorphologic findings, immunohistochemical profile, and molecular analysis for specific translocation. With so few cases reported in the literature, it is not possible to establish definitve treatment guidelines for these group of neoplasms. Radical surgery and chemotherapy (adjuvant, neoadjuvant, or palliative), with or without radiation therapy is so far considered as the ideal form of treatment for such patients. Importantly, appropriate distinction of this entity from its morphologic mimics, including the round cell sarcomas/tumors and lymphoma is of paramount importance, as it carries distinctive therapeutic and prognostic implications. This cohort of thirteen cases would help in exapnding the diagnostic and therapeutic aramentarium of PNET of the bladder. Further studies with a larger cohort of patients with treatment information, clinical follow-up, and response to therapy are warranted to evaluate long-term outcomes of this group of tumor.

906 Distinct Mutational Profile of Metastatic Upper Tract Urothelial Carcinoma

Shaham Beg[1], *Verena Sailer*[2], *Brian Robinson*[1], *Andrea Sboner*[2], *Olivier Elemento*[3], *Himisha Beltran*[3], *Bishoy M Faltas*[2], *Juan Miguel Mosquera*[4]. [1]Weill Cornell Medicine, New York, NY, [2]Weill Cornell Medicine, [3]New York, NY, [4]Weill Cornell Medical College, New York, NY

Background: Upper tract urothelial carcinoma (UTUC) is a rare and aggressive cancer. A greater understanding of the molecular biology of this tumor and its natural history will aid the development of new therapeutic strategies. We report the molecular alterations in metastatic UTUC (mUTUC) in comparison to primary UTUC.

Design: 11 patients with UTUC were prospectively enrolled in our precision medicine clinical trial between February 2013 and May 2017. Whole exome sequencing (WES) of paired tumor & normal control samples was done on 15 metastases (lung, liver, mediastinum, lymph node, adrenal, bone and peritoneum). For comparison, 22 primary

UTUC (17 renal pelvis, 6 ureter) from 19 patients were analyzed. 8 of these cases were matched with mUTUC samples.

Results: Median age at diagnosis of mUTUC was 70 years. Most of their primary tumors were invasive (90%) and high grade (81%). Average time for metastasis development was 11 months. 72% cases had history of smoking. Average mutation count of 158 (range 12-495) per metastatic sample. One case showed very high mutation rate of 3507.

Most common mutated genes were *TP53* (38%), *KMT2D* (33.3%), *ALKP3* (28.2%), *ARID1A* (25.6%) and *MUC4, RBMLX3* & *CDKN1A* (20.5% each). Mutated genes enriched in mUTUC were *ALPK3, RBMXL3, PML, TNN* and *FBXW7* whereas mutations showing significant association with primary UTUC were in *BSN, MMP15* and *MAGI1.* Deletions of *CDKN2A* & *B* (34.8%) and *MTAP* (30.4%) were the most common somatic copy number variants (SCNV) in primary UTUC whereas *PPRAG* & *RAF* amplification (31.3% each) were most common in mUTUC.

Mutations in cell cycle control genes was more frequent in mUTUC compared to primary (81% versus 48%). p53 signaling genes were more commonly mutated in primary tumors (74% versus 56%). Genes showing alteration in other major pathways such as cell death and survival signaling, DNA damage response, invasion and metastasis and chromatin remodeling were similar in both primary and mUTUC (**Table1**). *TP53* was the only gene showing poor overall survival on univariate analysis.

Germline variants were seen in *MYL2, PMS2, PKP2, FBN1* and *RYR21* genes.

Table1: Mutated genes of major signaling pathways	
DNA damage response pathway	ATM,CHEK1,CHEK2,BRCA2,ATR,BRCA1,MSH2,MDC1
Cell cycle control genes	RB1,CDKN1A,E2F4,RBL1,E2F7, JAK2,E2F1,JAK1,CDKN2A,STAT5A
Chromatin Remodelling genes	ARID1A,CHD4,SMARCA4,HLTF,CHD3,ARID4A,BRD3,HDAC4,SMARCB1,BRD8,BAZ1A,CHD5,HDAC7,BRD9,CHD9
Invasion and metastatic pathway	MMP15,MMP1,MMP9,MMP3,MMP11,MMP26,ITGB3,ITGAV,MMP27
p53 signalling	TP53,TP53BP1,CDKN2A
Cell death & survival regulation signalling	TGFBR2,NFKB1,HLA-G,DIRAS3,APAF1,CASP8,CASP10,-CASP3,CASP7,ARL11,WWOX

Conclusions: Although spectrum of genes alterations in primary vs. mUTUC tumor were somewhat similar, there seem to exist differences in pathways involved. mUTUC showed greater involvement of cell cycle control genes compared to primary tumors. The latter were enriched for TP53 signaling gene mutations. mUTUC showed greater alteration of clinically significant genes which may be targeted

907 Differential prognostic impact of MYC and PCAT-1 copy number alterations and mRNA expression in intermediate risk prostate cancer: Experience from the Canadian Prostate Cancer Gene Consortium cohort

Shubha S Bellur[1], *Jessica Weiss*[2], *Melania Pintilie*[3], *Michael Frazer*[4], *Huang Vincent*[4], *Paul Boutros*[4], *Robert Bristow*[5], *Theodorus van der Kwast*[6]. [1]Toronto General Hospital, Toronto, ON, [2]Princess Margret Hospital, [3]University Health Network / Princess Margret Hospital, Toronto, ON, [4]Ontario Institute of Cancer Research, [5]Manchester Cancer Research Centre, [6]University Health Network, Toronto, ON

Background: The behavior of National Comprehensive Cancer Network (NCCN) intermediate risk (IR) prostate cancer is highly variable with a substantial proportion of men showing biochemical failure (BCF) despite treatment. Better predictors of disease outcome in this risk group would help provide optimal therapy with minimal side effects to individualize treatment. The striking association of 8q gains with metastatic hormone refractory prostate cancers raises the possibility that at least one 8q gene is associated with disease progression. We compared the prognostic impact of copy number alterations (CNA) of MYC and PCAT-1 with corresponding mRNA expression levels by RNA in situ hybridization (ISH) technology.

Design: Expression levels of MYC and PCAT-1 were visualized by RNA ISH using a tissue microarray (TMA) built from radical prostatectomy specimens who formed a part of the Canadian Prostate Cancer Gene Consortium (CPCGC) cohort. Their median follow up was 5 years. Immunostaining for MYC protein expression was also performed. Array data on MYC and PCAT-1 CNA and on mRNA levels of MYC and PCAT-1 from the corresponding tumor were compared with RNA ISH and MYC protein expression levels. Here we present the data from a subset of 103 cases.

Results: Median age was 62.20 years, median PSA was 6.6 ng/dl at diagnosis and 39 (38%) of the patients had BCF during follow-up. Eighty (78%) were clinical stage T1/T2a and 23 (22%) stage T2b /2c. Sixteen (16%) showed ISUP Grade Group 1, 66 (64%) Grade Group 2 and 21(20%) Grade Group 3. Association between MYC / PCAT-1 CNA and mRNA based on array as well as association between RNA expression by array and ISH were not significant. Univariate analysis showed prognostic impact on BCF only for 1) MYC CNA (HR = 3.63 (95% CI, 1.56-8.43); P-0.0014, 2) PCAT-1 CNA (HR=4.58 (95% CI, 1.98-10.61); P-0.0001) and 3) MYC array mRNA (HR = 0.41 (95% CI, 0.19-0.88); p-0.019). These variables continued to be independently significant on multivariate analysis. ISUP grade group and ISH measurements were not prognostic.

Conclusions: CNA of MYC and PCAT-1 were strong prognosticators of poor prognosis in our IR prostate cancer cohort, whereas increased MYC mRNA measured by array was associated with improved prognosis. Visually scored PCAT-1 and MYC RNA and MYC protein expression were not prognostic.

908 Prognostic Value of Cancer Extent Assessment in a Conservatively Treated Prostate Biopsy Cohort of 988 Men Using Prostate Cancer Death as Outcome

Luis Beltran[1], *Bernard North*[2], *Henrik Moller*[3], *Peter Scardino*[4], *Jack Cuzick*[5], *Daniel Berney*[6]. [1]Barts Health NHS Trust, London, [2]Queen Mary University of London, [3]Kings College, London, United Kingdom, [4]Memorial Sloan Kettering Cancer Center, New York, [5]Queen Mary University, London, United Kingdom, [6]Queen Mary University of London, London

Background: Prostate cancer (PC) extent in needle biopsies (NB) is a core data item in most reporting guidelines and can be calculated by a range of methods. Its value in predicting biochemical recurrence/adverse pathological features in prostatectomy has been widely documented but there are few studies using PC-specific death (DOD) as outcome. We have previously studied the prognostic value of PC extent in a cohort of men diagnosed between 1990-1996 and found that assessment of disease burden was statistically significant in predicting DOD in univariate and multivariate analysis. We wished to study this in a larger cohort, predominantly diagnosed by sextant biopsy.

Design: 988 cases of PC were identified from three cancer registries in the UK from men with clinically localized disease diagnosed by NB from 1990-2003. The endpoint was DOD. Clinical variables included PSA, age and clinical stage. Men treated radically within 6 months, those with objective evidence of metastases or who had prior hormone therapy were excluded. Follow up was through cancer registries up until 2012. Deaths were divided into DOD and those from other causes, according to WHO criteria. All biopsies were centrally reviewed by 2 uropathologists and assigned a Gleason score and Grade Group. PC extent was determined by # involved cores, % involved cores, maximum cancer length in core per case, total cancer length per case and % total cancer length per case. Cancer length was calculated both including and excluding uninvolved prostate tissue between neoplastic foci.

Results: In univariate analysis all methods of PC extent assessment have strong statistically significant prognostic value. % of involved cores is associated with the highest HR suggesting this measure is the strongest predictor. Whether uninvolved tissue is included or not in calculating cancer length appears to make very little difference. In multivariate analysis including Gleason score, PSA and clinical stage, no methods provided additional prognostic value.

	HR	P value	Harrell's c-statistic
No involved cores	1.16	0.00000011	0.61
% involved cores	1.25	$<2 \times 10^{-16}$	0.71
Maximum cancer length in core	1.11	4.38×10^{-12}	0.65
Maximum cancer length in core minus stromal gap	1.11	6.55×10^{-13}	0.66
Total cancer length in case	1.02	7.27×10^{-9}	0.66
Total cancer length minus stromal gap	1.02	2.56×10^{-9}	0.66
% total cancer length	1.02	$<2 \times 10^{-16}$	0.72
% total cancer length minus stromal gap	1.02	$<2 \times 10^{-16}$	0.72

Conclusions: Of the methods assessed, % of involved cores is not only the one associated with a strongest predictive value in univariate analysis but also one of the simplest to calculate; usually expressed as a fraction of # involved cores over the total. This observation questions the utility of systematically providing complicated and time consuming calculations of PC extent in biopsy reports, which are possibly of clinical relevance only in the context of active surveillance or in clinical trials.

909 PTEN and ERG status in a Case-Control Study of the Johns Hopkins Active Surveillance Cohort

Liana Benevides Guedes[1], *Carlos Eduardo Morais*[2], *Jessica L Hicks*[2], *Angelo DeMarzo*[3], *Mufaddal Mamawala*[2], *H. Ballentine Carter*[2], *Tamara L Lotan*[4]. [1]Johns Hopkins University School of Medicine, Baltimore, MD, [2]Johns Hopkins University School of Medicine, [3]Johns Hopkins University, Baltimore, MD, [4]Johns Hopkins School of Medicine, Baltimore, MD

Background: Up to 30% of patients with Gleason score 6 (GS6) prostate cancer placed on active surveillance protocols will eventually require definitive therapy, usually due grade reclassification following additional biopsy sampling. In addition to improved imaging techniques, ancillary molecular testing to help predict which GS6 tumors are at higher risk of reclassification could be helpful. Here, we examined PTEN and ERG status in a subset of a large active surveillance cohort with NCCN Very Low-Risk and Low-Risk prostate cancer.

Design: We designed a case-control study of the Johns Hopkins active surveillance cohort with available tissue for immunohistochemistry (IHC), including a control group of 72 patients with GS6 prostate tumors that had at least 8 years of follow-up and a minimum of two or more follow-up biopsies without reclassification to higher grade disease. The cases included 31 patients enrolled for active surveillance with GS6 tumors who reclassified to GS 3+4=7 or higher disease at needle biopsy within 2 years of follow-up and a separate group of 36 patients enrolled for active surveillance with GS6 tumors who reclassified to GS 4+3=7 or higher disease at biopsy or radical prostatectomy at any time during follow-up. PTEN and ERG IHC were performed using genetically validated protocols on the initial GS6 biopsy for all patients.

Results: The median age of the control group (n=72) was 66 (51-85) years at the time of the first diagnosis and these patients had a median of 6 (3-8) GS6 biopsies. The cases (n=67) had a median age of 67 (53-78) years and had a median of 2 (1-3) GS6 biopsies. The controls had a significantly lower volume of disease sampled at needle biopsy and a significantly higher fraction of Very Low-Risk disease compared to the cases. Measured on the initial GS6 biopsy, 1% (1/72) of the controls had PTEN loss versus 9% (6/67) of re-classified cases (p=0.31, Fisher's exact test). ERG was positive in 43% (28/65) of controls versus 50% (28/56) of the cases (p=NS, Fisher's exact test).

Conclusions: In the relatively strictly selected Johns Hopkins active surveillance cohort, PTEN loss is uncommon in the initial GS6 tumor sample. Though we observed a trend towards increased frequency of PTEN loss among the cases that were reclassified compared to the controls that were not, the low rate of PTEN loss in both groups may be due to the high fraction of patients with Very Low-Risk disease and may not justify the performance of this test in this clinical context.

910 Prospective Molecular and Morphological Assessment of Testicular Pre-Pubertal Type Teratomas in Post-Pubertal Men

Daniel Berney[1], *Amy Roe*[2], *Luis Beltran*[3], *Marianne Grantham*[4]. [1]Queen Mary University of London, London, [2]Bartshealth NHS Trust, [3]Barts Health NHS Trust, London, [4]Barts Health NHS Trust, London

Background: It has been recognised that some adult testicular teratomas, previously called by some 'Dermoids' are entirely benign. The WHO 2016 classifcation of testicular germ cell neoplasms included the new entity pre-pubertal type teratomas (Pre PTT) based on their morphological and molecular profile and the realisation that these lesions may occur in adults and require less surveillance. Differentiation from post-pubertal type teratomas (Post PTT) may be challenging. We wished to investigate morphological, clinical and molecular criteria used to diagnose these tumours in a prospective series.

Design: All cases of pure testicular teratoma assessed in our department or in consultation since the introduction of routine isochromosome 12p testing were reviewed. Pathological features of the tumor and stroma were examined as well as any immunochemistry performed and the results of molecular testing for isochromosome 12p.

Results: 31 cases of pure teratoma in post-pubertal men were reviewed. 20 cases (19 total and 1 partial orchidectomy) were diagnosed as post pubertal type teratomas on morphology and immunochemistry without molecular investigation (age 22-67). These tumors ranged in size from 12-90mm. 3/20 cases presented with clinical metastases. 8/20 cases showed immature areas including PNET. 10/20 cases showed GCNIS, 8 cases showed no GCNIS while in two cases this could not be assessed. 17 cases showed severe atrophy in the background parenchyma while 1 case could not be assessed. One case with neither GCNIS nor atrophy showed necrosis.

11 cases underwent molecular testing (age 24-64). The size of these lesions ranged from 2-20mm. One case positive for i(12p) also showed GCNIS but was tested as it was a tumour of pure muscular differntiation but was therefore diagnosed as a Post PTT. Of the remaining 10 cases diagnosed as Pre PTTs, 8 showed no i(12p) while in 2 tumors, testing failed. None of the tumours showed GCNIS or significant atrophy. Three of the pre PTTs showed small well differentiated neuroedocrine tumors from 1-2mm in size. One patient had an unrelated contralateral seminoma.

Conclusions: Both morphological and molecular features are of help in differentiating Pre from Post-PTTs. Pre-PTT may be diagnosed at any age and ancillary i(12p) is helpful in confirming the morphological suspisions. Although cases may be biased by referral practice, the high incidence of NETs only in the Pre-PTTs is confirmed. Optimal methods of follow up/surveillance are yet to be determined.

911 Urethral Squamous Cell Carcinomas are significantly more HPV associated and show morphological differences to Penile Squamous Cell Carcinomas

Daniel Berney[1], *Catherine Corbishley*[2], *Brendan E Tinwell*[3], *Ben Ayres*[4], *Nicholas A Watkin*[5], *Elzbieta Stankiewicz*[6]. [1]Queen Mary University of London, London, [2]London, [3]St George's University Hospitals NHS Foundation Trust, London, [4]St George's Hospital, London, [5]St George's Hospital, [6]Queen Mary University of London

Background: Urethral Squamous cell carcinomas (USCC) are extremely rare and not well characterised compared to penile squamous cell carcinomas (PSCC). A recent cohort of USCC from our center suggests that they differ from PSCC in morphology. We wished to investigate whether rates of HPV infection also differed between men with USCC and PSCC.

Design: Cases were identified at a tertiary referral centre for penile carcinoma. Wax blocks from 57 USCC cases were available for DNA extraction with a QIAamp DNA Mini kit. All cases were from men. Beta-globin PCR was performed using primers B1 and B19 to confirm the adequacy of the extracted DNA. Validated samples were tested for the presence of HPV DNA by a broad-spectrum HPV PCR method using short PCR fragment (SPF10) primers, which amplify a 65-base pairs (bp) fragment of the L1 open reading frame and HPV genotypes identified by the INNO-LiPA line probe assay. Results were compared with our previous cohort of 102 PSCCs.

Results: Of 57 USCCs, 25 (46%) were basaloid while 16 (28%) were of usual type. 8 (14%) were mixed basaloid /usual type. One was verrucous while the 6 remaining showed other mixed features. 55/57 tumors were positive for HPV. 53/55 of these (96%) were HPV type 16 positive, while 47/53 (89%) were positive for HPV 16 alone. Other high risk HPV types detected included HPV 58 (6/55) and HPV 53 (2/55). HPV18, 31,33, 52 56 & 67 were only detected in single cases. Of the basaloid tumors, 24/26 showed HPV 16, while 2/26 showed HPV 58 or a mixture of high risk types. Of the two HPV negative tumours, one was verrucous and the other of usual type. On comparison with the PSCC cohort there were statistically significantly higher rates of HPV infection overall, and of HPV type 16 and in both usual and basaloid subtypes.

Comparison of HPV and tumor type in USCC and PSCC

	All PSCC	All USCC	Usual Type PSCC	Usual Type USCC	Basaloid PSCC	Basaloid USCC
HPV Positive	57	55	38	15	10	26
HPV Negative	45	2	26	1	3	0
		p<0.0001		p=0.0092		p=0.03

Conclusions: USCCs are much more closely associated with HPV and HPV type 16 than PSCC. This suggests that while PSCC may arise without HPV infection, presumably due to other environmental influences, HPV infection is almost excusively the aetiological factor in the pathogenesis of urethral tumours and they appear to be more uniform in morphology and therfore possibly on molecular analysis. We suggest that the distal urethra, which has an intermediate epithelium between sqaumous and urothelial may be a sanctuary site for the HPV virus. HPV vaccination should be extremely effective in this rare tumor subtype.

912 Diagnostic Challenges Posed by Lesions of Adrenal Origin in the Assessment of Renal Tumor Histopathology

Wafi Bibars[1], *Sean R Williamson*[2], *Ondrej Hes*[3], *Kiril Trpkov*[4], *Rodolfo Montironi*[5], *Manju Aron*[6], *Seema Kaushal*[7], *Jae Y. Ro*[8], *Steven C Smith*[9], *Jeffrey Roux*[10], *Jatin S Gandhi*[11], *Mahul Amin*[12]. [1]University of Tennessee Memphis, Memphis, TN, [2]Henry Ford Health System, Detroit, MI, [3]Biopticka laborator, Plzen, [4]University of Calgary, Calgary, AB, [5]Univ. Politecnica delle Marche /Medicine, Ancona, Marche, [6]Keck School of Medicine, University of Southern Ca, Los Angeles, CA, [7]All India Institute of Medical Sciences, New Delhi, India, [8]Houston

Methodist Hospital, Cornell University, Houston, TX, [9]VCU School of Medicine, Richmond, VA, [10]Memphis, TN, [11]University of Tennessee Health Science Center Memphis, Memphis, TN, [12]Methodist University Hospital, Memphis, TN

Background: Intrarenal adrenal lesions are uncommon findings with variable clinical presentation that may range from an incidental abnormality discovered during nephrectomy, to symptomatic or asymptomatic radiologic lesions which result in nephrectomy. These findings may be broadly explained by either direct extension of an adrenal neoplasm into the kidney, or developmental abnormalities such as intrarenal ectopic adrenal tissue or renal-adrenal fusion that may develop neoplastic lesions. There is no comprehensive series of such cases that encompasses the spectrum of adrenal morphology and with emphasis on the differential with renal neoplasia.

Design: We collected a large series of lesions of adrenal origin that involved the kidney and performed a detailed clinicopathologic analysis focusing morphologically on aspects that may mimic renal neoplasia.

Results: 32 cases in the renal parenchyma /perinephric soft tissue were categorized as: 1. renal adrenal rests (n=16); 2. adrenal adenomas arising in the background of adrenal-renal fusion (n=7); 3. hyperplastic intrarenal adrenal rests resulting in pseudotumorous mass (n=3); 4. adrenocortical carcinomas secondarily involving the kidney (n=4); and 5. pheochromocytomas secondarily involving the kidney (n=2). Age ranged between 2 and 80 yrs. and lesions from 0.2 to 15 cm. Nested to trabecular architecture was present in almost all cases, with circumscription in 44%, and poor delineation/infiltration into the surrounding renal tissue in 56%. A clear cell predominant pattern was noted in 31% and an eosinophilic predominant pattern was present in 38%; 31% showed both eosinophilic and clear cells; 19% showed adrenal cortical and medullary tissue. 40% of the lesions were the primary indication for nephrectomy. 38% of lesions required diagnostic immunohistochemistry. A wide range of renal epithelial tumors, most commonly clear cell, chromophobe and unclassified renal cell carcinoma were in the differential diagnosis.

Conclusions: Although rare, lesions of adrenal origin involving the kidney show significant morphologic mimicry with a wide spectrum of adult renal neoplasia. Awareness of these diagnostic challenges should raise consideration for them especially when dealing with renal masses that do not have histology typical of renal epithelial neoplasia. Our experience underscores the importance of the communication with clinicians, correlation with imaging findings and immunohistochemistry to accurately characterize the cases for appropriate management.

913 The TNM 8th Edition: Validation of the Proposal for Organ-Confined (pT2) Prostate Cancer

Athanase Billis[1], *Leandro Freitas*[2], *Larissa B Costa*[3], *Icleia S Barreto*[3], *Amanda P Herculiani*[3], *Karina S Araujo*[3], *Daniele M Losada*[3], *Bruna C Zaidan*[3], *Ana V Costa*[3]. [1]State University of Campinas (Unicamp), Campinas, SP, [2]UNICAMP - Brazil, VALINHOS, São Paulo, [3]State University of Campinas (Unicamp), Campinas, São Paulo

Background: The 8th edition of the TNM has been updated and improved in order to ensure a high degree of clinical relevance. Organ-confined prostate cancer is now considered pT2 without subclassification. The aim of this study was to validate this major change.

Design: From a total of 530 patients submitted to radical prostatectomy (RP), 196 patients had organ-confined disease and negative surgical margins. We compared the behavior of unilateral vs bilateral tumors. From step sectioned prostates, each transversal section was subdivided into 2 anterolateral and 2 posterolateral quadrants. Tumor extent was evaluated by a semiquantitative point-count method: each quadrant of the transverse sections was drawn on paper and contained 8 equidistant points. Tumor extent was recorded as the total sum of the positive points of all transverse quadrants or as index tumor (dominant nodule) considering the maximum number of positive points in the largest single focus of cancer in the quadrants. We compared time to biochemical recurrence (TBCR) following RP of unilateral (pT2a/b) vs bilateral (pT2c) tumors considering total tumor extent (Group 1) or index tumor extent at least larger than 4 positive points (Group 2). Biochemical recurrence was considered PSA $\geq$ 0.2 ng/ml. For TBCR was used the Kaplan-Meier product limit analysis with the log-rank test for comparison between the groups. We also analyzed the equivalence of pT2 findings with the clinical staging.

Results: In Group 1, 43/196 (21.9%) tumors were unilateral and 153/196 (78.1%) bilateral. There was no significant different association with TBCR in Kaplan-Meier estimates comparing patients with unilateral vs bilateral tumors (log-rank, p=0.336) (Table). In Group 2, 79/97 (81.4%) tumors were unilateral and 18/97 (18.6%) bilateral. There was no significant different association with TBCR in Kaplan-Meier estimates comparing patients with unilateral vs bilateral tumors (log-rank, p=0.365). The clinical staging of the patients was 56.9%, 41.5%, and 1.6% for cT1c, cT2a/T2b, and cT2c, respectively.. There was a striking no correlation between clinical and pathological staging considering total tumor extent and poor correlation with index tumor extent.

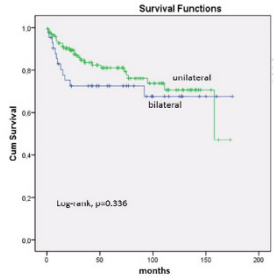

Conclusions: The findings of the study validate the TNM 8th edition for organ-confined prostate cancer. Substaging does not convey prognostic information and the correlation between cT and pT substaging is poor considering either total tumor extent or index tumor extent.

914 Is There a Bioenergetic Signature of Prostate Cancer According to Gleason Grading and Time of Biochemical Recurrence After Radical Prostatectomy?

Athanase Billis[1], *Wagner Favaro*[2], *Rogerio C da Silva*[3], *Alexandre Foratto*[4], *Leandro Freitas*[5], *Larissa B Costa*[6], *Icleia S Barreto*[6]. [1]State University of Campinas (Unicamp), Campinas, SP, [2]University of Campinas, Campinas, Brazil, School of Medical Sciences, State University of Campinas (Unicamp), Brazil, [4]School of Medical Sciences, State University of Campinas (Unicamp), Brazil, Campinas, São Paulo, [5]UNICAMP - Brazil, VALINHOS, São Paulo, [6]State University of Campinas (Unicamp), Campinas, São Paulo

Background: Unlike normal cells, glycolysis (GLY) is enhanced and mitochondrial oxidative phosphorylation (OXPHOS) capacity is reduced in various cancers. It has long been believed that glycolytic phenotype in cancer is due to a permanent impairment of OXPHOS. Although aerobic GLY is often found in malignant tumors, OXPHOS plays a major role in energy production in some cancers. The aim of the study was to investigate the mitochondrial bioenergetic signature of prostate cancer as a marker of Gleason grading and time to biochemical recurrence (BR) after radical prostatectomy (RP). We also developed a bioenergetic cellular index (BCI) which may reflect prognosis.

Design: We studied prostate samples from 4 groups (10 patients in each group): Group 1 (control): nodular hyperplasia; Group 2: Gleason score $\leq$ 6 in RP and no recurrence > 5 years after surgery; Group 3: Gleason score 7 and BR 2-5 years after RP; Group 4: Gleason score 8-10 and BR < 2 years after RP. All samples were submitted to immunohistochemical analyses for metabolic enzymes: GLUT 1, OHADH, LDH, Hsp60, and β-F1-ATPase**.** To evaluate immunoreactivity, a score was obtained based in number and intensity of positive cells. BCI was assessed by the β-F1-ATPase:Hsp60:LDH immunoreactivities score ratio.

Results: The results revealed two alternative pathways by which prostatic neoplastic cells negatively regulate mitochondrial activity. In Group 2 (low-grade tumors and no BR > 5 years after RP), there was no decrease in the labeling for β-F1-ATPase, which is consistent with repression of the mitochondrial proliferation program. In contrast, in Groups 3 and 4 (intermediary and high-grade tumors with BR after RP) there was a decrease in the specific regulation for β-F1-ATPase, which is consistent with selective repression of the expression of the components involved in mitochondrial bioenergetics function, leading to limitation of mitochondrial oxidative phosphorylation. In addition, intermediary and high-grade tumors, showed increase in the regulation of glycolytic pathway (GLUT 1 and LDH), as well as increased immunoreactivity for fatty acid oxidation pathway (OHADH). The BCI was significantly reduced in intermediary/high-grade *vs.* low-grade tumors, providing a bioenergetic signature for these tumors (Figure).

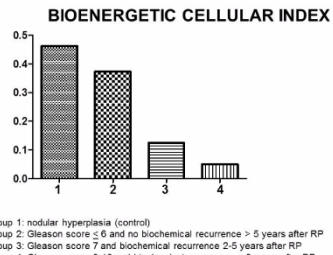

Conclusions: Down-regulated β-F1-ATPase and assessment of the bioenergetic cellular index related to Gleason grade and time to biochemical recurrence after RP may have prognostic value in prostate cancer.

915 Pathologist Call Rate Variation in 892 Prostatectomies Assessed Using Funnel Plots

Michael Bonert[1], *Bobby Shayegan*[2], *Serge Kajaer Koujanian*[3], *Samih Salama*[4], *Anil Kapoor*[2], *Ihab El-Shinnawy*[2]. [1]McMaster University, Hamilton, ON, [2]McMaster University, [3]McMaster University, Hamilton, ON, [4]Ancaster, ON

Background: Pathologist call rate (PCR) variation is traditionally assessed with kappa values in practice distant studies, and may be confounded by possible case and slide selection bias. Observational/population data may provide similar insights (based on the interpretation of all slides in a case), be less resource intensive to obtain and useful for directing continuous quality improvement (CQI). Useful population-based comparisons are predicated on (1) no significant referral bias or pathologist case selection, and (2) stable disease characteristics in the study population over time.

Design: All in house prostatectomy reports at two teaching institutions were retrieved for a six year period (2011-16). Gleason scores were converted to the World Health Organization grade groups (WHO1-5). Using custom computer code, PCRs for cancer grade (WHO1-5), positive margin (PM), lymph node metastasis (LNM), seminal vesicle invasion (SVI), extraprostatic extension (EPE) and lymphovascular invasion (LVI) were calculated, and plotted on funnels centered on the median call rate (MCR) of the pathology group with funnel edges defined by ±2 standard errors (SEs) (P=0.05) and ±3 SEs (P=0.001).

Results: Data could be extracted in 1,045 prostatectomies. Ten pathologists read at least 40 cases and together interpreted 892. The median call rates/ranges were 4%/0-30% for WHO1, 66%/42-84% for WHO2, 21%/10-36% for WHO3, 3%/0-20% for WHO4, 2%/0-19% for WHO5, 24%/12-34% for PM, 3%/1-6% for LNM, 12%/0-28% for SVI, 35%/11-72% for EPE and 6%/1-32% for LVI. The number of statistical outliers (P<0.001/P<0.05) in relation to the MCR were 2(P<0.001)/2(P<0.05) of 10 for WHO1, 5(P<0.001)/7(P<0.05) of 10 for WHO2, 0/3 of 10 for WHO3, 3/4 of 10 for WHO4, 2/2 of 10 for WHO5, 0/0 of 10 for PM, 0/0 of 10 LNM, 1/3 of 10 for SVI, 1/4 of 10 for EPE, and 1(P<0.001)/5(P<0.05) of 10 for LVI.

Conclusions: There is minimal PCR variation for PM and LNM in relation to EPE, SVI and LVI. PCR variation for WHO grade groups is considerable, and especially high for WHO2. As this process is mostly automated, resource use scales favorable with increased case volume and statistical power. The funnel plots were interpreted without difficulty and provided relevant information for individual pathologists in our group for directing CQI.

916 Multiparametric Magnetic Resonance Imaging Biopsies - Critical Review of Experience with 1,500 Prostate Biopsies from a Single Institution

Shaun Boyes[1], *Vamsi Parimi (Parini)*[2], *Stefan Pambuccian*[1], *Ian Hughes*[3], *Maria Picken*[4]. [1]Loyola University Medical Center, Maywood, IL, [2]New York University, New York, NY - New York, [3]Oak Park, IL, [4]Loyola Univ Med Ctr, Maywood, IL

Background: Prostate cancer (PCa) is the most common cancer affecting men in the United States. Systematic biopsies (SBx), sampling 6 regions of the prostate, are typically used to evaluate abnormal prostate specific antigen (PSA) levels. Over the past two years, multiparametric magnetic resonance imaging (mpMRI) is being utilized in our institution to enhance accurate diagnosis and avoid the negative sequelae of misdiagnosis. The mpMRI is interpreted using the Prostate Imaging Reporting and Data System (PIRADS), which is a five point scale with a rating of benign (1) to malignant (5). Utilizing mpMRI and PIRADS enables targeted biopsy (TBx) of radiologically suspicious prostatic lesions. The objectives of our study were 1. to evaluate experience with mpMRI targeted biopsies by comparing the rates of PCa detection per biopsy in SBx versus TBx over a two year period, 2. to determine the reason(s) for negative TBx.

Design: This single-institution retrospective study included 1,464 biopsies from 192 patients who underwent SBx and Tbx from 7/2015 through 7/2017. The percent of prostatic adenocarcinoma between SBx and TBx was analyzed over a two year period. All negative Tbx were subsequently reviewed in an effort to determine reasons for failure to detect carcinoma.

Results: Over a two year period, there were 1464 region specific needle core biopsies consisting of 1109 SBx and 355 TBx. The percent of PCa diagnosed histologically for SBx was 13.1%, and the percent of PCa diagnosed histologically for Tbx was 24.5% (Z-score -5.1337; p<0.00001),(table). Pathologic-radiologic review and correlation demonstrated atrophy and or significant chronic inflammation as a pitfall in radiologic interpretation in (40/98 patients) 40.8% of patients with negative TBxs. Among other reasons, most common were both urologist- (missing a small target) and radiologist-dependent (mis-interpretation of suspicious lesions).

7/2015 through 7/2017	Number of cores with PCa	Total Cores	Cores with PCa (%)
SBx	145	1109	13.1%
TBx	87	355	24.5%

Conclusions: The study shows that mpMRI-guided TBx has an statistically significant increased detection 24.5% over SBx 13.1% (p <0.00001). Atrophy and/or significant chronic inflammation emerged as a contributing factor in negative Tbx in 40.8% of patients in the study group. Additional explanations that may account for discordance between radiologic and pathologic correlation may be urologist-(missing a smal target) and radiologist-dependent (mis-interpretation of suspicious lesions).

917 Radical Prostatectomy (RP) Findings In Men with Low-Risk Prostate Cancer (PC) In a Contemporary Triethnic Population – Implications for Active Surveillance (AS)

Beth L Braunhut[1], *Rochelle Freire*[2], *Oleksandr Kryvenko*[1]. [1]University of Miami Miller School of Medicine, Miami, FL, [2]University of Miami Miller School of Medicine

Background: AS is a management option for men with low-risk (Grade Group (GG) 1, PSA <10 ng/mL, T1c-T2a) PC.

Design: We reviewed RPs in 175 (Hispanic (H) – 77; Black (B) - 33; White (W) – 65) consecutive men with low-risk PC in a triethnic population from 2013-2017. For patients with significant PC at RP, the misclassification was categorized from 1 (least significant) to 4 (most significant).

Results: In 3 ethnic groups (EG) the patients presented with comparable age, BMI, PSA, PSA density (PSAD). One patient had no PC on RP. All EGs demonstrated a greater incidence of posterior dominant tumor nodules (DTN) (H: 61.8%; W: 70.8%; B: 63.6%). Hispanics had a higher incidence of anterior DTN compared to W and B men. Anterior DTN volume was nearly twice larger than posterior for all EG (P <0.001). 66 men (37.9%) had insignificant PC (organ confined (OC), GG1, and DTN volume <0.5 ml) and 108 men (62.1%) had significant PC defined by volume (n = 30), grade (n = 30), or both (n = 47). One patient had a DTN <0.5 cm^3 GG1 disease, but was classified as having significant PC due to the presence of focal extraprostatic extension (fEPE). No patients had metastatic cancer in regional lymph nodes. There was no difference in the ethnic distribution of patients with significant vs insignificant PC. Patients with significant PC had significantly higher PSA, PSAD, more positive biopsy cores, and smaller glands. PSAD (r=0.37, p<0.001) predicted significant PC better than PSA (r=0.22, p=0.003). There was no statistical difference in anterior vs posterior DTN volume in patients with insignificant PC (p=0.7). In patients with significant PC, mean anterior DTN volume was significantly greater than posterior DTNV (1.18 cm^3 vs 0.87 cm^3, p=0.009). Patients with significant PC more commonly had posterior DTN, but anterior DTNs were more common than in those with insignificant PC (27.2% vs 12.1%, p=0.02). Among significant PC, 31 (28.7%) had category 1 misclassifications (GG1, DTNV >0.5 cm^3 and OC or any volume with fEPE), 54 (50%) had category 2 (GG2 and OC or fEPE), 12 (11.1%) had category 3 (GG2 and nfEPE), and 11 (10.2%) had category 4 (≥GG3). There was no difference between different EG.

Conclusions: PSAD outperformed PSA in predicting significant PC. 13.1% (23/175) of men with low-risk PC have cancer that is more likely to demonstrate aggressive behavior (category 3&4 significant PC). Our findings of similar RP outcomes in 3 EG are different compared to prior published data.

918 Refining the Diagnostic Criteria for Flat Urothelial Lesions Using International Society of Urological Pathology (ISUP) Imagebase

Qi Cai[1], *Lars Egevad*[2], *Cristina Magi-Galluzzi*[3], *Ming Zhou*[4]. [1]UT Southwestern Medical Center, Dallas, TX, [2]Karolinska University Hospital, Stockholm, SWE, [3]Cleveland Clinic, Cleveland, OH, [4]Clements University Hospital, Dallas, TX

Background: Flat urothelial lesions range from reactive to dysplasia and carcinoma in situ (CIS). The diagnosis is based mainly on morphology, which is subjective and affected by interobserver reproducibility. ISUP recently launched a "Pathology Imagebase" project in which GU pathology experts rendered diagnoses/grades on images of GU tumors, including flat urothelial lesions. These cases are published online as reference images, akin to Gleason diagram for prostate cancer. We sought to identify morphological features of flat urothelial lesions that correlated with at least 50% agreement among the experts.

Design: ISUP image library had 27 cases of flat urothelial lesions that were categorized into 3 majority diagnoses: reactive, dysplasia and CIS when ≥50% experts made the same diagnosis. "Dysplasia" also

include those cases with <50% agreement on CIS but ≥50% experts diagnosed them as either dysplasia or CIS. Blind to the diagnoses, authors evaluated the following features: thickness and polarity of urothelial cells, presence of discohesive cells, maturation, nuclear morphology, mitoses, and presence of significant inflammation in the urothelium. The presence of these features was correlated to the consensus diagnoses.

Results: Of 27 cases, the majority diagnoses were reactive in 7 (25.9%), dysplasia in 16 (59.3%) and CIS in 4 (14.8%). No cases achieved 100% consensus. Of the histological features studied, four, including loss of polarity (a), discohesive cells (b), loss of maturation (c) and presence of inflammation in the urothelium (d), showed significantly different incidence between "reactive" and "at least dysplasia", individually or in combination. For example, b and c were present in 11 and 8 "at least dysplasia", and in 1 and 0 "reactive" (p=0.027 and 0.051). a+b, b+c, b+d, c+d, b+c+d were present in 8, 8, 9, 8, and 8 "at least dysplasia", and in 0, 0, 0, 0 and 0 "reactive" (p=0.051, 0.051, 0.019, 0.051 and 0.051).

Conclusions: Using the ISUP Imagebase of flat urothelial lesions, we identified several histological features that are associated with the majority diagnosis. Discohesive cells and loss of maturation are features not emphasized previously. Therefore, these features should be emphasized when diagnosing flat urothelial lesions. In addition to being a reference image library, ISUP Imagebase contains abundant information that can be mined for standardizing diagnostic and grading criteria.

919 VEGFA mRNA Expression in TFEB-amplified Renal Cell Carcinoma and in TFEB-rearranged t(6;11) Renal Cell Carcinoma

Anna Caliò[1], *Matteo Brunelli*[2], *Diego Segala*[3], *Pedram Argani*[4], *Guido Martignoni*[3]. [1]University of Verona, [2]Dept of Pathology, Verona, Italy, [3]Verona, Italy, [4]Johns Hopkins Hospital, Ellicott City, MD

Background: Amplification of vascular endothelial growth factor A (VEGFA) has been recently reported in *TFEB*-amplified renal cell carcinomas regardless the level of *TFEB* amplification, which has potential therapeutic implications. We sought to determine VEGFA expression in a series of renal cell carcinomas with *TFEB* gene alterations, either amplification or rearrangement (t(6;11) renal cell carcinoma).

Design: Using Fluorescent In Situ Hybridization (FISH) analysis we identified 9 renal cell carcinomas (5 F, median ages: 41 years) with *TFEB* gene alterations. The expression of VEGFA mRNA was studied by *in situ* hybridization (RNAscope 2.5).

Results: *TFEB* gene rearrangement was demonstrated in 7 cases, the remaining 2 cases showed a high level of *TFEB* gene amplification (>10 copies of fluorescent signals) without evidence of rearrangement. Among the seven t(6;11) renal cell carcinomas (TFEB-rearranged cases), two showed increased *TFEB* gene copy number (3-4 copies of fluorescent signals) and behaved aggressively. Overall, VEGFA mRNA expression was observed in 5 of 9 cases (55%). Of these 5 positive cases for VEGFA staining, two cases showed high level *TFEB* amplification, one case showed *TFEB* rearrangement with increased *TFEB* gene copy number, while two showed *TFEB* gene rearrangement without increased copy number.

Conclusions: VEGFA mRNA expression occurs in *TFEB*-amplified renal cell carcinoma, but also in a subset of t(6;11) renal cell carcinoma demonstrating aggressive behavior, and in unamplified conventional t(6;11) renal cell carcinoma. VEGFA is a potential therapeutic target in aggressive *TFEB*-associated renal cell carcinoma.

920 The Heterogeneous Morphological Spectrum of Differentiated Penile Intraepithelial Neoplasia (D-PeIN). A Proposal of a Grading System

Sofía Cañete-Portillo[1], *Diego F Sanchez*[2], *Maria Jose Fernandez*[3], *Cecilia Lezcano*[4], *Elsa Velazquez*[5], *Luis A Delgadillo*[6], *Arturo Silvero-Isidre*[7], *Gabriel A Gauto*[8], *Tamara V Goossen*[7], *Sebastián Ocampos-Rojas*[9], *Cesar Urizar*[7], *Francisco Encina*[7], *Ingrid M Rodríguez*[10], *Maria L Cabanas*[11], *Enrique S Ayala*[12], *Antonio Cubilla*[13]. [1]Asuncion, [2]Instituto de Patologia e Investigacion, Asuncion, Central, [3]Facultad Politecnica, Universidad Nacional de Asuncion, San Lorenzo, Central, [4]Memorial Sloan-Kettering Cancer Center, New York, NY, [5]Miraca Life Sciences, Newton, MA, [6]Instituto de Patología e Investigación, Asunción, Paraguay, Asunción, Central, [7]Instituto de Patología e Investigación, Asunción, Paraguay, [8]Instituto de Patología e Investigación, Asunción, Paraguay, Fernando de la Mora, Central, [9]Instituto de Patología e Investigación, Asunción, Paraguay, Asunción , Capital, [10]Universidad Nacional de Asunción - Facultad de Ciencias Médicas, Asunción, Paraguay, [11]Instituto Nacional del Cancer, Lambare, [12]Instituto Nacional del Cancer, [13]Inst of Pathology, Asuncion

Background: Differentiated PeIN (D-PeIN), according to the WHO classification is a non-HPV-related precancerous lesion. It is the most common subtype of PeIN associated with invasive carcinomas in geographical regions endemic for penile cancer. We found no study addressing their morphological heterogeneity. The WHO classification of PeIN does not grade these lesions.

Design: Materials and methods: We evaluated 95 consecutive precancerous penile lesions diagnosed at the Instituto de Patología e Investigación in Asunción, Paraguay. Criteria for diagnosis were those of the 2016 WHO classification. 73 cases of D-PeIN were included (77%) and 22 warty/basaloid PeIN were excluded (23%). All lesions were associated with invasive squamous cell carcinomas.

Results: We found 3 distinctive patterns **1. Hyperplasia like (HL):** 26 cases (36%) that showed hyperkeratosis, acanthosis, extreme cell maturation, and minimal atypia restricted to one suprabasal cell layer. **2. Classical (CL):** 38 cases (52%). These cases showed hyperkeratosis, acanthosis, cell maturation, marked cell atypia involving the lower third of epithelial thickness, more than two basal cell layers. **3. Pleomorphic (PL),** corresponding to 9 cases (12%) with the following features: hyperkeratosis, acanthosis, mild to moderate maturation, and marked atypia with pleomorphic cells compromising more than two thirds of the epithelial thickness.

Conclusions: Differentiated PeIN comprises a heterogeneous spectrum of morphological patterns with different degrees of atypia. The differential diagnosis was with squamous hyperplasia and warty/basaloid PeIN. The diversity and predictable topography of the atypias in most cases may be the base for the proposal of a grading system for these lesions as follow: **grade 1** for **Hyperplasia-like (HL)** D-PeIN, **grade 2** for **Classical (CL)** D-PeIN, and **grade 3** for **Pleomorphic (PL)** D-PeIN. More studies using immunohistochemistry are necessary to validate this hypothesis.

921 Detection of HPV in Lichen Sclerosus (LS) Associated with Penile Intraepithelial Neoplasia (PeIN). A p16 and Laser Capture Microdissection (LCM)-PCR study of 21 lesions in 14 Patients

Sofía Cañete-Portillo[1], *Nuria Guimerà*[2], *Diego F Sanchez*[3], *Maria Jose Fernandez*[4], *Elsa Velazquez*[5], *David Jenkins*[6], *Wim Quint*[6], *Antonio Cubilla*[7]. [1]Asuncion, [2]Rijswijk, [3]Instituto de Patologia e Investigacion, Asuncion, Central, [4]Facultad Politecnica, Universidad Nacional de Asuncion, San Lorenzo, Central, [5]Miraca Life Sciences, Newton, MA, [6]DDL Diagnostic Laboratory, Rijswijk, Netherlands, [7]Inst of Pathology, Asuncion

Background: LS, a mixed epithelial/stromal condition of unknown etiology, is rarely reported in HPV-related penile precancerous lesions. Notwithstanding, some authors claim HPV may play a causative role in this disease. This is an HPV genotype detection study with focus on the epithelial component of LS associated with different subtypes of PeIN to explore this relationship.

Design: Material and Methods: We searched for the presence of specific HPV genotypes in 21 separate lesions from 14 patients. All cases had LS and an associated subtype of PeIN in the same area. We focused the analysis on the epithelia above the sclerotic stroma to prevent contamination from other tissues. Techniques for HPV detection were p16, whole tissue section PCR and LCM-PCR (*Fernández-Nestosa et al. Human papillomavirus genotypes in Condylomas, Intraepithelial Neoplasia and Invasive Carcinoma of the Penis using LCM-PCR: a study of 191 lesions in 43 patients. Am J Surg Pathol. 2017*).

Results: Patients' age ranged from 47 to 84 years with median of 65 years. Lesions were located in the foreskin (9 cases) or glans (12 cases). Data are shown in Table 1.

Table 1. HPV genotypes in epithelia of LS associated PeIN.

PeIN Subtype	No. of cases	HPV positive cases (%)	p16 positive cases	HPV genotypes
Differentiated	18	0 (0)	0	-
Warty	2	2 (100)	2	39,18
Basaloid	1	1 (100)	1	16

Conclusions: Whereas all cases had LS and PeIN in the same tissue region, HPV was negative in differentiated PeIN and positive in warty/basaloid PeIN. HPV genotypes were 39 and 18 for warty, and 16 for basaloid PeIN. These findings support the dual etiology of penile precancerous lesions, HPV- and non-HPV related, and suggest that the occasional presence of HPV in LS may be related to the associated precancerous lesion (PeIN) and not with the LS itself.

922 Lymphocytic Depleted Lichen Sclerosus (LS) is Preferentially Associated with Penile Neoplasia

Sofía Cañete-Portillo[1], *Diego F Sanchez*[2], *Adriano Piris*[3], *Cecilia Lezcano*[4], *Arturo Silvero-Isidre*[5], *Luis A Delgadillo*[6], *Jose Barreto*[5], *Ingrid M Rodríguez*[7], *Patricia Zarza*[5], *Sabrina Oneto*[8], *Tania Campagnoli*[5], *Lorena Gonzalez*[6], *Martin Mihm, Jr.*[9], *Elsa Velazquez*[10], *Antonio Cubilla*[11]. [1]Asuncion, [2]Instituto de Patologia e Investigacion, Asuncion, Central, [3]Brigham and Women's Hospital, Boston, MA, [4]Memorial Sloan-Kettering Cancer Center, New York, NY, [5]Instituto de

Patología e Investigación, Asunción, Paraguay, [6]Instituto de Patología e Investigación, Asunción, Paraguay, Asunción, Central, [7]Universidad Nacional de Asunción - Asunción, Paraguay, [8]Miami, FL, [9]Mihm Cutaneous Pathology Consultative Service, Boston, MA, [10]Miraca Life Sciences, Newton, MA, [11]Inst of Pathology, Asuncion

Background: LS is an epithelial/stromal dermatological condition of unknown etiology, frequently associated with penile neoplasia, especially non-HPV-related. Morphological features of LS are complex. Basal cell vacuolization, dermal fibrosis and lymphocytic infiltration are hallmarks of the lesion. It has been postulated that LS may represent a precancerous condition. In an evaluation of a large number of cases we identified distinctive morphological variants. The purpose of this study was to search for correlations of these variants with PeIN and invasive carcinomas.

Design: Material and methods: We selected 91 of 200 cases of LS with distinct homogeneous morphology and designated them as ***classical***, ***lichenoid***, and ***lymphocyte-depleted*** LS. Penile Intraepithelial Neoplasia and/or invasive squamous cell carcinoma were identified in 59 patients. **Classical LS** had a 3 layer band-like appearance with normal or hyperplastic epidermis, thick fibrosis in lamina propria, and an underlying deeply located dense lymphocytic infiltration. **Lichenoid LS** had a dense superficial sub-epidermal lymphocytic infiltration, with scant fibrosis. **Lymphocyte-depleted LS,** showed dense fibrosis but lymphocytic infiltration was scant or spotty, not dense. Statistical contrast was evaluated with the Fisher's exact test for categorical data.

Results: LS variants and their association with penile neoplasia are shown in Table 1.

Table 1. Variants of Lichen Sclerosus and associated lesions.

LS Variant	# of cases	Associated Lesions	
		Benign/ Non-atypical (%)	PeIN and/or invasive carcinoma (%)
Classical	13	12 (92)	1 (8)
Lichenoid	12	6 (50)	6 (50)
Lymphocytic depletion	66	15 (22)	52 (78)

($p < 0.0005$)

Conclusions: Morphological features of LS are complex. We identified 3 homogenous variants of LS: **classical, lichenoid, and lymphocyte-depleted**. The lymphocyte-depleted variant, which may represent a late stage of LS, was significantly associated with penile neoplasia. The finding suggests a role for the lymphocyte in the association of LS with penile neoplasia.

923 Histopathology of Radiation-Induced Urethral Strictures in Men with Prostate Cancer

Tiffany N Caza[1], *Michael V Hughes*[2], *Jeffrey A Spencer*[2], *Dmitriy Nikolavsky*[3]. [1]SUNY Upstate Medical University, Clay, New York, [2]SUNY Upstate Medical University, [3]SUNY Upstate Medical University, Syracuse, NY

Background: Treatment of prostate cancer by radiation therapy carries a risk of off-target injury to the membranous urethra. Forty percent of men with prostate cancer are treated with radiation post-prostatectomy. To date, only limited characterization of membranous strictures related to radiation have not been compared to those from other causes in the same location, such as mechanical trauma or congenital abnormalities. We hypothesize that there are histopathologic parameters unique to the irradiated cohort.

Design: 36 specimens from patients who underwent urethroplasty for membranous urethral strictures were identified, with 26 from patients without radiation exposure and 10 from irradiated patients. All specimens were reviewed for the following: tissue types (urothelium, squamous epithelium, striated muscle, nerve tissue, corpora spongiosum, and seminal vesicles), quantification of inflammatory cells (neutrophils/acute inflammation, lymphocytes/ chronic inflammation, foreign body giant cells), collagen density, collagen organization, hyalinized fibrosis, vascular density, spindle cell change, presence/absence of necrosis and/or hemorrhage, fat entrapment, and vacuolation/degenerative change of fibrous connective tissue. Frequency of histologic findings were evaluated by Chi Square analysis using Fisher's exact tests.

Results: Post-radiation strictures had a higher collagen density (100% vs. 58%, p=0.03), higher collagen organization (90% vs. 50%, p=0.01), with a trend towards increased hyalinized fibrosis (100% vs. 73%) when compared to membranous strictures without radiation. Post-radiation strictures also had a low vascularity, with 90% of strictures with <3 capillaries/hpf in the areas of highest vascular density vs. 15% for non-irradiated tissue (p=0.004). Spindle cell change was seen in 60% of post-radiation strictures, versus 38% without radiation. Radiation strictures had a trend towards a higher rate of necrosis (60% vs. 31%), fat entrapment (90% vs. 54%), and hemorrhage (80% vs. 65%). Fibrous connective tissue degenerative change with vacuolation was seen in 60% of radiation-induced strictures and was not observed without radiation (p=0.003).

Conclusions: Membranous urethral strictures caused by radiation have a greater amount of collagen fibrosis and show spindle cell change. There is lower tissue vascularity and increased necrosis. Increased tissue trauma with hemorrhage, fat entrapment, and fibrous connective tissue degeneration are also seen with radiation exposure.

924 De novo purine metabolic enzyme PAICS is overexpressed and plays a role in bladder cancer

Balabhadrapatruni V Chakravarthi[1], *Maria Del Carmen Rodriguez Pena*[1], *Sumit Agarwal*[1], *Darshan S Chandrashekar*[1], *Sai Akshaya Hodigere Balasubramanya*[1], *Fayez J Jabboure*[2], *Uttam Rao*[1], *Guru Sonpavde*[3], *Alcides Chaux*[4], *Jennifer Gordetsky*[1], *George J Netto*[1], *Sooryanarayana Varambally*[1]. [1]University of Alabama at Birmingham, Birmingham, AL, [2]University of Virginia, Charlottesville, VA, [3]Dana Farber Cancer Institute, [4]Centro para el Desarrollo de la Investigación Científica (CEDIC), Asunción, Central,

Background: Cancer cells utilize *de novo* purine and pyrimidine biosynthetic pathway as a source of their nucleotide needs. In this study, we show that PAICS, an enzyme involved in *de novo* purine biosynthetic pathway, is overexpressed in bladder cancer and plays a role in bladder cancer cell proliferation hence serving as an excellent potential therapeutic target.

Design: PAICS expression analyses.

Gene expression level of PAICS in bladder urothelial carcinoma (BLCA) and adjacent normal samples was obtained from The Cancer Genome Atlas (TCGA) using UALCAN (http://ualcan.path.uab.edu). Immunoblots were performed using bladder cancer patient samples and normal tissue samples. Immunohistochemistry (IHC) was carried out using PAICS antibody (GeneTex, CA, Cat# GTX83950). Two uropathologists evaluated IHC staining.

Cell Proliferation and tumor growth Assays

Cell proliferation was measured by cell counting after PAICS knockdown in bladder cancer cells. Tumor growth assay was performed using *chicken chorioallantoic membrane assay (CAM) using bladder cancer cell lines in which PAICS is knocked down.*

Statistical Analysis

Student's two-tail t-test was used for all experiments, P values <0.05 considered significant.

Results: *De novo* purine biosynthetic enzyme PAICS is over-expressed in bladder cancer

The transcriptome sequence analysis using TCGA bladder cancer dataset showed upregulation of PAICS in bladder urothelial carcinoma (**Fig. 1A, B**) Immunoblot analysis using PAICS-specific antibody indicated PAICS protein overexpression in bladder carcinoma but low in normal tissues (**Fig. 1C**). Additionally, PAICS showed stronger staining in bladder tumors (**Fig.1D**).

Role of PAICS in bladder cancer. Modulating PAICS expression in bladder cancer cell lines showed decreased cell proliferation (**Fig. 2A**), decreased colony formation (**Fig. 2B**), invasion (**Fig. 2C**). Furthermore, CAM assay showed decreased tumor growth when PAICS was removed from bladder cancer cell lines (**Fig. 2D**).

Figure 1

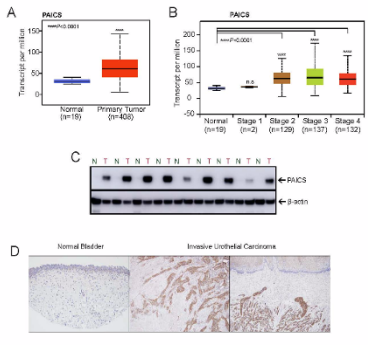

Figure 1. PAICS, a de novo purine biosynthetic pathway enzyme is over-expressed in aggressive bladder adenocarcinoma. **(A)** A boxplot showing relative expression of PAICS mRNA transcript in normal and, stage 1, 2, 3 and 4 of bladder cancer patients. **(B)** Boxplots represent PAICS expression level across normal bladder, mucosa and infiltrating bladder urothelial carcinoma (top) and across normal bladder and infiltrating bladder urothelial carcinoma (bottom). The data was retrieved from publicly available microarray datasets of bladder cancer with log2 median intensity using Cincomine array datasets. **(C)** Expression of PAICS in normal bladder and primary tumor samples from TCGA. **(D)** Immunohistochemical analysis of PAICS in normal bladder tissue and invasive urothelial carcinoma.

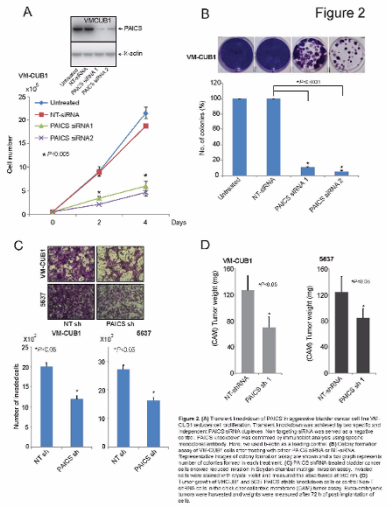

Conclusions: Our gene and protein expression analyses showed PAICS overexpression in muscle invasive bladder cancer. Further, our *in vitro* functional studies and *in vivo* CAM assay show that PAICS plays a critical role in bladder cancer progression. Collectively, our data suggests that targeting PAICS will provide a therapeutic option in aggressive bladder cancers.

925 Immunohistochemical Evaluation of Cell Cycle-Related Proteins in Squamous Cell Carcinomas Using Digital Image Analysis: Validation of the ImageJ immunoratio Plugin

Anahí Chaux[1], *George J Netto*[2], *Alcides Chaux*[1]. [1]Centro para el Desarrollo de la Investigación Científica (CEDIC), Asunción, Central, [2]University of Alabama at Birmingham (UAB), Birmingham, AL

Background: Digital image analysis for immunohistochemical expression of clinically-relevant proteins is aimed at decreasing interobserver variability and thus increase objectivity in their measurements. Open-source packages may provide an inexpensive approach for this task, but to date their validity has not been tested in squamous cell carcinomas.

Design: We built 4 high-density tissue microarrays (TMA) from 112 penile SCC. The following cell cycle-related proteins were evaluated: p53, Ki67, cyclin-D1 and MDM2. Percentage of positive tumor cells were estimated: (1) visually by naked eye; (2) digitally, using ImageJ (NIH), through the immunoratio plugin. Visual and digital percentages were analyzed using the Wilcoxon signed rank test and the Spearman σ correlation coefficient.

Results: The output of the ImageJ workflow is shown in Fig 1. Visually-estimated mean percentages were significantly higher than digitally-measured mean percentages for p53 (23.9 vs 3.2%, P<0.00001), Ki67 (24.2 vs 2.1%, P<0.00001), cyclin-D1 (24.9 vs 7.9%, P<0.00001), and MDM2 (4.3 vs 0.7%, P=1.5e-4). For p53, Ki67 and cyclin-D1, mean differences between visual estimates and digital measurements were greater in grade 3 tumors (Table 1). The overall correlation between visual estimation and digital measurement was high for p53 and cyclin-D1, moderate for Ki67, and weak for MDM2 (Table 2). When we stratified the correlation analysis by histologic grade we found that correlation coefficients were lower for grade 1-2 tumors and higher for grade 3 tumors (see Table 2).

Table 1

Marker	Grade 1	Grade 2	Grade 3
p53	11.4	21.3	22.9
Ki67	7.1	18.7	38.3
cyclin-D1	5.7	12.7	23.1
MDM2	4.9	5.3	2.2

Table 2

Marker	Overall correlation	Grade 1	Grade 2	Grade 3
p53	σ=0.75, P<0.00001	σ=0.54, P<0.00001	σ=0.74, P<0.00001	σ=0.77, P<0.00001
Ki67	σ=0.68, P<0.00001	σ=0.54, P=0.00005	σ=0.56, P<0.00001	σ=0.71, P<0.00001
cyclin-D1	σ=0.72, P<0.00001	σ=0.62, P<0.00001	σ=0.63, P<0.00001	σ=0.76, P<0.00001
MDM2	σ=0.38, P=4.8e-16	σ=0.26, P=0.04	σ=0.34, P<0.00001	σ=0.39, P<0.00001

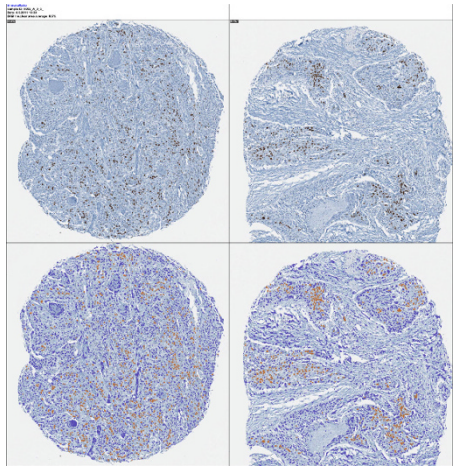

Conclusions: Percentages of positive tumor cells were significantly greater when using digital analysis compared to visual estimation by naked eye. Although the correlation was moderate to strong between both methods, the increased mean differences in the percentages for higher grades (probably related to nuclear pleomorphism) and the intragrade variability in the correlation coefficients limits the usefulness and potential clinical applicability of digital measurements of positive tumor cells in squamous cell carcinomas.

926 Non-malignancy pathologic findings and their clinical significance on targeted prostate biopsy in men with PI-RADS 4 / 5 lesions on prostate MRI

Fei Chen[1], *xiaosong meng*[2], *Brain Chao*, *Andrew B Rosenkrantz*, *Jonathan Melamed*[3], *Ming Zhou*[4], *Samir Taneja*, *Fang-Ming Deng*[3]. [1]NYU Langone Health, New York City, NY, [2]NYU Langone Health, [3]New York University Medical Center, New York, NY, [4]Clements University Hospital, Dallas, TX

Background: Traditional pathology reports of prostate biopsy mainly focus on presence of carcinoma but ignore other pathologic findings such as inflammation or hyperplasia. In the era of MRI-ultrasound fusion-targeted prostate biopsy (MRF-TB), where specific MRI regions of interest (ROI) are targeted for biopsy, these benign findings should be reported as they may guide decisions on when to repeat imaging or prostate biopsy. In this study, we reviewed MRF-TB prostate biopsies reported as negative for carcinoma to identify pathologic correlates to visible ROI on prostate MRI.

Design: From 2012 to2016, 1595 men underwent a total of 1813 pre-biopsy prostate MRI, followed by MRF-TB at our institution. We re-reviewed the prostate biopsy cores for all patients with PI-RADS 4 or 5 (PI-RADS 4/5) ROI but had no cancer detected on MRF-TB. Pathologic findings were separated into two groups: significant pathologic findings (SPF, such as inflammation, hyperplasia, ASAP/HGPIN) and no significant pathologic findings (NSPF) with or without cancer in same/adjacent site on systematic biopsy (SB). Patients with repeat MRI and follow-up MRF-TB evaluation.

Results: 497 men had PI-RADS 4/5 lesions out of 1595 initial biopsies. Of these 497 men, 101 (20%) had MRF-TB negative for carcinoma. Upon review, 54 had SPF and 47 had NSPF on MRF–TB.

Of 54 men with SPF on initial MRF-TB, 31 had repeat MRI, 23 of 31 men downgraded in which 16 had repeat MRF-TB with 1 had cancer detect. The other 8 of 31 men had persistent PI-RADS 4/5 lesions, 3 were detected cancer on repeat MRF-TB.

Of 47 men with NSPF on initial MRF-TB, 19 had PCa in the same/adjacent site on SB and were considered as missed on MRF-TB; of the other 28, 13 underwent repeat MRI. 8 of 13 downgraded with 0 had PCa in the repeat MRF-TB and 5 of 13 men with persistent PI-RADS 4/5 lesions, 3 had PCa detect on repeat MRF-TB. Altogether, 22/47 (47%) of the cases with NSPF in the initial MRF-TB were missed cancer.

Conclusions: 1/5 of the target biopsy cases on PI-RADS 4/5 ROI had negative cancer detection. Inflammation, nodular hyperplasia and HGPIN can account for some of the cases, and those were down-graded in followup MRI usually had a negative repeat biopsy. Cases with NSPF on MRF-TB for PI-RADS 4/5 lesions are likely (47%) missed PCa, high likelihood of persistent PI-RADS 4/5 ROI on repeat MRI and PCa detection on repeat biopsy. We suggest pathology findings beside cancer should be reported on MRF-TB biopsy as they can guide decisions on repeat imagine and biopsy.

927 Expression of Novel Neuroendocrine Marker Insulinoma-associated Protein 1 (INSM1) in Genitourinary High Grade Neuroendocrine Carcinomas: An Immunohistochemical Study of 34 Cases With Comparison to Chromogranin and Synaptophysin

Jie-Fu (Jeff) Chen[1], *Chen Yang*[2], *Dengfeng Cao*[2]. [1]Washington University in St. Louis, St Louis, MO, [2]Washington University School of Medicine, Saint Louis, MO

Background: Insulinoma-associated protein 1 (INSM1) is a transcription factor involved in the development of neuroendocrine cells and is directly regulating expression of chromogranin and synaptophysin. INSM1 has been recently shown to be a more sensitive marker than chromogranin and synaptophysin for pulmonary neuroendocrine tumors. However, no study has investigated INSM1 expression in genitourinary high grade neuroendocrine carcinomas (HGNECs). Here we evaluated INSM1 expression in 34 genitourinary HGNECs with comparison to chromogranin and synaptophysin for their sensitivity.

Design: Thirty-four (34) genitourinary HGNECs (kidney 4, bladder 24, prostate 6; 10 pure and 24 mixed with another non-neuroendocrine carcinomatous component; 26 small cell carcinomas and 8 mixed small cell and large cell neuroendocrine carcinomas) were studied. One paraffin block containing tumor from each case was used to generate unstained slides for immunohistochemical stainings with antibodies to INSM1 (Santa Cruz Biotechnology, Clone A8, 1:200 dilution), chromogranin (Ventana, clone LK2H10, prediluted) and synaptophysin (Cell Marque, Clone MRQ-40, prediluted). The immunohistochemical stainings were semi-quantitatively scored as 0 (<1% cells staining), 1+ (1-25%), 2+ (26-50%), 3+ (51-75%), and 4+ (76-100%). The percentage of tumor cells stained for each marker was visually estimated. The staining for INSM1 was nuclear and it was cytoplasmic for chromogranin and synaptophysin.

Results: Positive staining for INSM1, chromogranin, and synaptophysin was seen in 29/34 (85%, 1+ in 8, 2+ in 6, 3+ in 6, 4+ in 9), 29/34 (85%, 1+ in 7, 2+ in 6, 3+ in 4, 4+ in 12), and 31/34 (91%, 1+ in 3, 2+ in 1, 4+ in 27) genitourinary HGNECs, respectively (INSM1 vs chromogranin, p = 0.3703; INSM1 vs synaptophysin, p = 0.0003; chromogranin vs synaptophysin, p = 0.004). One tumor was negative for all three markers. The mean number of tumor cells stained for INSM1, chromogranin, and synaptophysin in genitourinary HGNECs was 43% (median 40%, range 0-90%), 48% (median 50%, range 0-100%), and 78% (median 98%, range 0-100%), respectively (INSM1 vs chromogranin, p < 0.00001; INSM1 vs synaptophysin, p < 0.00001; chromogranin vs synaptophysin, p < 0.00001).

Conclusions: INSM1 showed similar sensitivity to chromogranin for genitourinary HGNECs (85% vs 85%) but it labeled a lower number of tumor cells than chromogranin in these tumors. For genitourinary HGNECs, INSM1 is not as sensitive as synaptophysin which is the most sensitive marker.

928 Do We Need to Consider Tumor Volume and Prostate Weight in Quantifying Percentage of Gleason Pattern 4 in Radical Prostatectomies?

Bonnie Choy[1], *Dayana Delgado*[2], *Brandon Pierce*[2], *Gladell P Paner*[1]. [1]University of Chicago, Chicago, IL, [2]University of Chicago

Background: Studies showed a linear increase in PSA biochemical recurrence (BCR) with increasing percent of Gleason pattern 4 (GP4) in Gleason score (GS) 7 (Grade group 2-3) prostate cancers. In 2014, the International Society of Urological Pathology (ISUP) recommended reporting the percent GP4 for GS7 cancers. The aim of this study was to examine whether incorporating tumor volume (TV) and prostate weight (WT) in addition to GP4 help us better predict BCR for GS7 cancers after radical prostatectomy (RP).

Design: 386 RPs of GS 3+4=7 and GS 4+3=7 prostate cancers from a single institution's surgical pathology archives from 2003 to 2007 were reviewed. Percent GP4 and TV were determined. PSA biochemical recurrence (BCR) was used as the end point. Median follow-up was 62 months.

Results: We used data-driven modeling and tested different thresholds of GP4 to dichotomize this variable into "high" and "low" risk groups; GP4 40% was identified as the best cut-off (>40% GP4, HR 3.44, p<0.0001). We further divided each sub-risk group into "low" vs. "lowest" and "high" vs. "highest", 1-20% vs. 21-39% and 40-69% vs. ≥70%, respectively. Multivariate survival analysis of 1-20% vs. 21-40% (HR 2.08, p=0.05) and 41-70% vs. >70% (HR 5.76, p<0.0001) showed significant increase in BCR risk, demonstrating the increasing adverse effect of increasing GP4. TV alone, using 30% cutoff for "high" vs. "low" risk, was not a statistically significant predictor of BCR (HR 1.75, p=0.08). Taking into account both GP4 and TV (GP4 x TV; representing the volume of GP4), was still a significant predictor of BCR, where the "high" risk group (>7%) was associated with an increased risk of BRC, but to a lesser degree compared to GP4 alone (HR 2.15, p=0.017). Further incorporating WT to GP4 and TV (GP4 x TV x WT; representing the weight of GP4 in grams) continued to be significantly predictive of BCR (HR 2.35, p=0.035). Splitting of both GP4 and TV into 4 categories of risk showed similar results. Diagnostic evaluation of these 4 predictive models using a ROC curve showed TV and WT do not contribute any additional predictive power for BCR (χ^2=5.32, p=0.15).

Conclusions: This study showed that percent GP4 alone is predictive of BCR and incorporating percent TV and prostate WT diminishes the prognostic impact of percent GP4. Using formulas to incorporate TV and prostate WT to derive the amount of GP4 in RP, besides being impractical to use in routine practice, may not provide additional prognostic information beyond GP4 alone.

929 Post-renal Transplant Polyomavirus-associated Urothelial Carcinomas Are Aggressive High Grade Tumors with Altered RB/p53/p16 Pathway

Ying-Hsia Chu[1], *Weixiong Zhong*[2], *Djamali Arjang*[3], *Sanjay S Patel*[4], *Rong Hu*[5]. [1]University of Wisconsin Madison, Madison, WI, [2]Madison, WI, [3]University of Wisconsin Hospital and Clinics, [4]Brigham & Women's Hospital, Boston, MA, [5]University of Wisconsin Hospital and Clinics

Background: The role BK polyomavirus (BKV) in urological oncogenesis is unclear. BKV transforms cells in vitro via the binding of SV40 viral protein to pRb and p53. Isolated case reports have shown an association between BKV and urological malignancies in post-renal transplant patients, with one such report recently describing viral genome integration that aborted viral replication. We examined the clinicopathologic features of BKV-associated urological cancers in renal transplant recipients.

Design: Institutional database was queried for patients who received renal transplants between 01/1994-01/2014 and developed post-transplant urothelial carcinomas (UCs) and/or renal cell carcinomas (RCCs). As a control group, 24 high-grade invasive UCs from immunocompetent individuals were identified. Immunostains were done for SV40 large T antigen (SV40), pRb, p53 and p16. Positivity for p16 was defined as strong nuclear and cytoplasmic expression in >75% of cells. pRb and p53 expression was graded by percentage of tumor cells with strong nuclear positivity: 0, 1+(<25%), 2+(25-50%), 3+(50-75%) and 4+(>75%). Viral genome integration was studied by whole tumor genome sequencing. Viral replication was studied by electron microscopy (EM).

Results: Of 4772 renal transplant recipients between 01/1994-01/2014, 26(0.5%) and 26(0.5%) developed post-transplant UCs and RCCs respectively as of 03/2017. Tissue from 22 UCs and 19 RCCs was available. Six(27%) post-transplant UCs expressed SV40, thus deemed BKV-related. None of the post-transplant RCCs expressed SV40. BKV-related UCs (BKVUCs) occurred 8.9-19.1 years after transplantation, often (83%) with antecedent BKV infection. All 6 BKVUCs were high-grade and 4 were invasive, of which 2 patients died of tumor within two months of diagnosis, 1 died of an unrelated cause, and 1 remained tumor-free 6 years after diagnosis. All BKVUCs showed diffuse and strong (4+) expression of both p16 and p53. pRb expression was variable (1+ to 4+). In contrast, of high-grade invasive UCs from immunocompetent patients, none expressed SV40, 7(29%) were p16-positive, 7(29%) showed 4+ p53, and only 3(13%) diffusely expressed both p16 and p53 (P<0.05). Sequencing results indicate viral genome integration in BKVUC cases; PCR validation is underway. None of the 6 BKVUCs showed virion formation by EM.

Conclusions: A significant proportion of post-renal transplant UCs, but not RCCs, are BKV-related. BKV-related UCs are high-grade, aggressive tumors characterized by p16 and p53 overexpression.

930 Expression of p62 Correlates with Tumor Grade, Stage and Shortened Overall Survival in Transitional Cell Carcinoma (TCC) of the Urinary Bladder

Vaibhav Chumbalkar[1], *Siddhartha Dalvi*[2], *Christine Sheehan*[3], *Bhaskar Kallakury*[4], *Zarrin Hossein-Zadeh*[5], *Tipu Nazeer*[3]. [1]Albany, NY, [2]Delmar, NY, [3]Albany Medical College, Albany, NY, [4]Georgetown Univ Hosp, Washington, DC, [5]Georgetown University Hospital

Background: Bladder cancer is a common cancer with highest recurrence rate of any malignancy. Progression depends on tumor grade and stage. Autophagy has both tumor suppressor and enhancer roles with differential regulation of these roles. Adaptor molecules like p62 help in balancing these roles. Defective autophagy and accumulation of p62 are implicated in tumor promotion. Additionally, p62 also acts as a key pro-oncogenic signaling hub. We assessed p62 expression in bladder cancer and its correlation with grade, stage and prognosis.

Design: FFPE tissue sections from 46 TCCs were immunostained using mouse monoclonal SQSTM1/p62 antibody. Cytoplasmic (Cp62) and nuclear (Np62) p62 immunoreactivity was semiquantitatively assessed in the tumor and adjacent benign component (when present). Scoring was based on staining intensity and percentage of positive cells. Each case was then assessed as negative (N), tumor=benign (T=B), tumor>benign (T>B) and tumor < benign (T < B). Presence of Cp62 and Np62 immunoreactivity was also assessed within the tumor

microenvironment (Cp62tm and Np62tm, respectively). Additionally, a publicly available gene expression dataset (GSE48276) comprising of 116 patients was analyzed for p62 expression. Results were correlated with clinicopathologic variables.

Results: Immunohistochemical analysis showed Cp62tm in 15% tumors and correlated with high tumor grade (p=0.017) and advanced tumor stage (p=0.014). Cp62 overexpression was noted in 59% tumors and correlated with high tumor grade (p=0.036). Cp62 was increased (T>B) in 85%, decreased (TB) in 37%, decreased (T < B) in 5% tumors and the same (T=B) in 10% tumors and correlated with shortened survival (p=0.036). Np62tm was noted in 13% tumors and correlated with high tumor grade (p=0.003) and advanced tumor stage (p=0.003). Np62 overexpression was noted in 39% tumors and correlated with shortened survival (p=0.027). Np62 was increased (T>B) in 37%, decreased (T < B) in 5% tumors and negative in 58% tumors and correlated with shortened survival (p=0.008). Analysis of p62 gene expression showed higher expression in higher stage tumor (stage 0-II vs III-IV, p=0.002, Figure 1) and higher expression predicted short survival (43.7 vs 56.3 months, p=0.03, Figure 2).

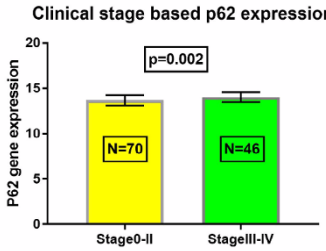

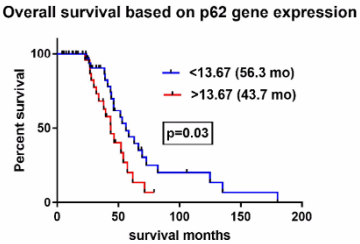

Conclusions: Gene expression of p62 as well as cytoplasmic and nuclear protein expression of p62 correlates with grade and stage of TCC of bladder and predicts survival. This study supports a role for targeting p62 as a potential therapeutic strategy.

931 Strong Association of PD-L1 Immunohistochemical Expression with Histologic Grade in Penile Squamous Cell Carcinomas

Margaret Cocks[1], *Diana Taheri*[2], *Mark Ball*[3], *Stephania M Bezerra*[4], *Maria Del Carmen Rodriguez Pena*[5], *Trinity J Bivalacqua*[6], *Rajni Sharma*[1], *Alan Meeker*[7], *Alcides Chaux*[8], *Arthur L Burnett*[6], *George J Netto*[9]. [1]Johns Hopkins Medical Institutions, Baltimore, MD, [2]Tehran University of Medical Sciences, Tehran, Tehran, [3]Johns Hopkins University, Baltimore, MD, [4]AC Camargo Cancer Center, Sao Paulo - SP, Sao Paulo, [5]University of Alabama at Birmingham, Birmingham, AL, [6]Johns Hopkins University, Baltimore, MD, [7]Johns Hopkins Univ/Medicine, Baltimore, MD, [8]Centro para el Desarrollo de la Investigación Científica (CEDIC), Asunción, Central, [9]University of Alabama at Birmingham (UAB), Birmingham, AL

Background: Penile squamous cell carcinoma (SCC) is a rare tumor for which few effective treatment options are available for advanced disease. Identifying novel molecular and immunotherapeutic targets is actively sought. Programmed death-ligand 1 (PD-L1) is a coinhibitory molecule that impairs the T-cell response by down-regulating T-cell proliferation and cytokine production. Tumor cells often up-regulate PD-L1 and thereby evade the host immune system. Immune-checkpoint inhibitors have been proven effective against several tumor types, but data on PD-L1 expression in penile SCC is scant with only rare studies from low-incidence areas. We evaluate PD-L1 expression in a larger dataset of patients with penile SCC from a high-incidence area.

Design: We built 4 tissue microarrays (TMA) from 112 tissue samples and evaluated PD-L1 immunohistochemical expression using a rabbit monoclonal anti–PD-L1 antibody. We estimated PD-L1 % of positive tumor cells and positive peritumoral lymphocytes. Comparisons between PD-L1 expression and histologic grade and subtype were carried out using the Mann-Whitney U and the Pearson chi-squared tests. Binomial logistic regression models (LRM) were used to estimate odds ratios (OR).

Results: We observed PD-L1 expression in 66% of TMA spots. We found a strong association between PD-L1 immunohistochemical expression and histologic grade (P=2.4e-10), with increasing percentage of positive tumor cells from grade 1 (median, 0%) to grade 2 (median, 1%) to grade 3 (median, 15%). PD-L1 positivity was also higher in high-grade tumors such as basaloid (median, 25%), warty-basaloid (median, 20%) and sarcomatoid carcinomas (median, 100%), with intermediate values in usual (median, 5%) and warty carcinomas (median, 5%), and low values in low-grade tumors such as papillary (median, 0%) and verrucous carcinomas (median, 0%) to a significant level (P=1.3e-14). Although to a lesser extent, we observed a similar trend for PD-L1 positivity in peritumoral lymphocytes, both for histologic grade (P=0.02) and subtype (P=4.4e-5). In unadjusted LRM, we observed increased OR for high-grade tumors when evaluating PD-L1 expression in tumor cells (P=1.1e-5) and peritumoral lymphocytes (p=0.09). In the adjusted LRM, increased OR remained significant for PD-L1 expression in tumor cells (P=8.1e-5) but not for peritumoral lymphocytes (P=0.52).

Conclusions: Our results provide support for the use of immune-check point inhibitors in patients with penile SCC, especially in those with high-grade tumors.

932 Intratumoral Infiltration of CD8+/Ki-67+ Lymphocytes is Stronger in Higher Grade Penile Squamous Cell Carcinomas

Margaret Cocks[1], *Diana Taheri*[2], *Mark Ball*[3], *Stephania M Bezerra*[4], *Maria Del Carmen Rodriguez Pena*[5], *Trinity J Bivalacqua*[6], *Rajni Sharma*[1], *Alan Meeker*[7], *Alcides Chaux*[8], *Arthur L Burnett*[6], *George J Netto*[9]. [1]Johns Hopkins Medical Institutions, Baltimore, MD, [2]Tehran University of Medical Sciences, Tehran, Tehran, [3]Johns Hopkins University, Baltimore, MD, [4]AC Camargo Cancer Center, Sao Paulo - SP, Sao Paulo, [5]University of Alabama at Birmingham, Birmingham, AL, [6]Department of Urology, Johns Hopkins University, Baltimore, MD, [7]Johns Hopkins Univ/Medicine, Baltimore, MD, [8]Centro para el Desarrollo de la Investigación Científica (CEDIC), Asunción, Central, [9]University of Alabama at Birmingham (UAB), Birmingham, AL

Background: Penile squamous cell carcinoma (SCC) is a rare genitourinary tumor for which the treatment options are limited in advanced disease. Immune-check point inhibitors have shown promising results, but knowledge about the immune response associated with penile SCC is scant. In this study, we evaluate the immunophenotype of intratumoral and peritumoral lymphocytes in a large series of penile SCC.

Design: We built 4 tissue microarrays (TMA) from 112 tissue samples. We evaluated the immunohistochemical expression of CD8, FOXP3 and Ki67 in intratumoral and peritumoral lymphocytes, counting the number of positive cells per high-power field (HPF). Comparisons between marker expression and histologic grade were carried out using the Mann-Whitney U and the Pearson chi-squared tests. Binomial logistic regression models (LRM) were used to estimate odds ratios (OR).

Results: We observed an intense inflammatory host response in 50% of TMA spots. The median number of intratumoral CD8+ lymphocytes was significantly higher (P=1e-5) in grade 3 tumors (6/HPF) compared to grade 2 (2/HPF) and grade 1 (1/HPF) tumors. We observed a similar trend for double CD8+/Ki67+ intratumoral lymphocytes (P=0.002). When considering peritumoral lymphocytes, the trend became non-significant for either CD8+ and double CD8+/Ki67+ lymphocytes (P>0.05). We found a strong association between Ki67+ in tumor cells and histologic grade (P=3.5e-9). Regarding FOXP3 expression, we did not observe a significant association with histologic grade for intratumoral lymphocytes, although we found decreasing counts of FOPXP3+ peritumoral lymphocytes with increasing histologic grades. Finally, the CD8-to-FOXP3 ratio was not associated with histologic grade, either in intratumoral or peritumoral lymphocytes. In unadjusted LRMs, we found increased OR for high grade when evaluating counts of CD8+ (P=1.6e-4) and double CD8+/Ki67+ (P=1.6e-3) intratumoral lymphocytes. In the adjusted LRM, this trend remained significant (P=6e-5 and P=0.05, respectively). Finally, we found decreased OR for counts of FOXP3+ peritumoral lymphocytes, in both unadjusted (P=0.07) and adjusted (P=0.04) LRMs.

Conclusions: Our results show that higher grade tumors elicit an increased infiltration of intratumoral CD8+ and CD8+/Ki67+ lymphocytes. Additionally, we also observed decreased counts of FOXP3+ peritumoral lymphocytes with increasing histologic grades. These findings provide support for exploring the use of immune-check points in patients with penile cancer.

933 Grade Group 2 Prostate Cancer with Poorly Formed Glands Alone on Needle Biopsy: Histologic Features and Pathologic Outcomes at Radical Prostatectomy

Paolo Cotzia[1], *Hikmat Al-Ahmadie*[1], *Ying-Bei Chen*[1], *Anuradha Gopalan*[1], *S. Joseph Sirintrapun*[2], *Satish Tickoo*[3], *Victor Reuter*[1], *Samson W Fine*[1]. [1]Memorial Sloan Kettering Cancer Center, New York, NY, [2]New York, NY, [3]Memorial Sloan Kettering CC, New York, NY

Background: Modern application of prostate cancer grading has resulted in more narrowly-defined pattern 3 and expanded definition of pattern 4. Poorly formed glands (PFG) are the most commonly encountered pattern 4 morphology, yet suffer from poor interobserver reproducibility. Descriptions of PFG on needle biopsy (NB) and subsequent pathologic outcomes at radical prostatectomy (RP) are limited.

Design: We reviewed 285 matched NB and RP performed at our institution. PFG were identified as having attenuated, small and/or compressed lumina, almost invariably associated with an incomplete ring of nuclei. We evaluated total tumor/PFG quantification and localization of PFG (interspersed v. distinct clustering) on NB [nine levels for each biopsy] and presence/localization of PFG, association with other pattern 4 subtypes and final Grade Group (GrdGrp) on paired RP specimens.

Results: 25 (9%) cases showing GrdGrp 2 with PFG alone were identified; 18/25 had one core with PFG and 7/25 had 2 cores. Tumor involved 5 to 90% (0.5 to 13 mm) of evaluated cores, with %pattern 4 ranging from 5 to 40%, corresponding to 3 to 30 PFG. PFG interspersed among pattern 3 glands were seen in all cases; 8 (32%) also showed distinct clustering of PFG. 18/25 cases showed 1-9 additional cores with GrdGrp 1.

A PFG component was identified in all RPs, with 92% anatomic concordance with NB. PFG were the sole pattern 4 subtype in 11 (44%) cases; among 14 cases with PFG + other pattern 4 subtype, PFG was the dominant subtype in 6. 23/25 (92%) RPs had interspersed PFG within tumor nodules, 7 of which also showed distinct clustering. RP GrdGrp was 2 in 23 and 3 in 2 cases, respectively.

- Grade Group 2 with PFG alone was an uncommon finding in this NB series.
- The presence of PFG in NB strongly correlates with PFG in subsequent RP and therefore should be recognized and graded.
- In this cohort, PFG were interspersed with well-formed pattern 3 glands in all NB cases and similarly seen in subsequent RP.
- Further study in a larger cohort with long-term clinical follow-up is underway to expand on these associations.

934 Concomitant Loss of PBRM1 and BAP1 Protein Expression is an Important Prognostic Event in Early Stages of Clear Cell Renal Cell Carcinoma.

Isabela W da Cunha[1], *Walter H da Costa*[2], *Aline F Fares*[3], *Stephania M Bezerra*[4], *Luciana Schultz*[5], *Gustavo C Guimaraes*[2], *Stenio C Zequi*[3]. [1]A.C Camargo Cancer Center, Sao Paulo SP, [2]A. C. Camargo Cancer Center, [3]A.C. Camargo Cancer Center, [4]AC Camargo Cancer Center, Sao Paulo - SP, Sao Paulo, [5]Instituto de Anatomia Patológica, AC Camargo Cancer Center, Santa Barbára D'Oeste, SP

Background: Between 20% and 30% of patients with clinically localized renal cell carcinoma (RCC) will develop metastases after undergoing a potentially curative nephrectomy. Identifying this high-risk group of patients remains a clinical challenge. The incorporation of molecular markers into conventional models is anticipated to enhance their predictive accuracy. Recent analyses of clear cell RCC revealed frequent mutations including PBRM1 and BAP1. These genes encode proteins that regulate chromatin and most reported somatic mutations result in loss of function, indicating that these proteins function as tumor suppressors. Our purpose was to evaluate the prognostic impact of immunohistochemical expression of BAP1 and PBRM1 in patients with early stage (pT1-pT2N0M0) in clear cell RCC.

Design: Four hundred and forty-one consecutive patients treated surgically for stages I and II (TNM-AJCC 2010) ccRCC between 1990 and 2016 were selected. All cases were reviewed for uniform reclassification and the most representative tumour areas were selected for the construction of a tissue microarray (TMA). Sixty-two patients had frozen tumoral tissue available in the tumor bank of our institution for qRT-PCR analysis.

Results: Of the 441-immunostained ccRCC specimens, 91 (20.6%) and 107 (24.3%) showed negative-expression of PBRM1 and BAP1, respectively. Fifty-eight (13.2%) showed negative-expression of both markers (PBRM1-/BAP-). There was an association between the markers expression pattern and classical parameters, such as pT stage (p <0.001), tumor size (p < 0.001) and tumour grade (p < 0.001). Both PBRM1 and BAP1 negative-expression were associated with lower rates of disease- specific survival (DSS) and recurrence-free survival (RFS). When patients were grouped into presence of positive-expression of one or both markers vs. PBRM1- /BAP1- patients, DSS and rates were 95.3% vs. 77.6%, respectively (P < 0.001). PBRM1-/BAP1- group presented a higher risk of cancer specific death (HR = 2.631; p = 0.009) and disease recurrence (HR = 3.203; p < 0.001) in multivariate analysis.

	PBRM1	PBRM1		BAP1	BAP1	
Variable	Negative expression n (%)	Positive expression n (%)	p value	Negative expression n (%)	Positive expression n (%)	p value
Gender						
Male	57 (62.6)	222 (63.4)	0.903	63 (58.9)	216 (64.7)	0.301
Female	34 (37.4)	128 (36.6)		44 (41.1)	118 (35.3)	
Surgery						
Nephron-sparing	34 (37.4)	240 (68.6)	<0.001	43 (40.2)	231 (69.2)	<0.001
Radical Nephrectomy	57 (62.6)	110 (31.4)		64 (59.8)	103 (30.8)	
pT Stage						
pT1a	29 (31.9)	207 (59.1)	<0.001	35 (32.7)	201 (60.2)	<0.001
pT1b	38 (41.8)	116 (33.1)		46 (43.0)	108 (32.3)	
pT2a	18 (19.8)	20 (5.7)		18 (16.8)	20 (6.0)	
pT2b	6 (6.6)	7 (2.0)		8 (7.5)	5 (1.5)	
Tumor size (cm)	6.78	5.96	<0.001	6.52	6.00	<0.001
ISUP grade						
Low grade	40 (44.0)	246 (70.3)	<0.001	48 (44.9)	238 (71.3)	<0.001
High grade	51 (56.0)	104 (29.7)		59 (55.1)	96 (28.7)	
LVI						
No	84 (92.3)	341 (97.4)	0.029	99 (92.5)	326 (97.6)	0.021
Yes	7 (7.7)	9 (2.6)		8 (7.5)	8 (2.4)	
Necrosis						
No	73 (80.2)	306 (87.4)	0.090	93 (86.9)	286 (85.6)	0.873
Yes	18 (19.8)	44 (12.6)		14 (13.1)	48 (14.4)	
Sarcomatoid Features						
No	88 (96.7)	347 (99.1)	0.105	105 (98.1)	330 (98.8)	0.636
Yes	3 (3.3)	3 (0.9)		2 (1.9)	4 (1.2)	
Clinical Situation						
Alive with no disease	66 (72.5)	318 (90.9)	<0.001	74 (69.2)	310 (92.8)	<0.001
Alive with disease	6 (6.6)	9 (2.6)		13 (12.1)	2 (0.6)	
Death due to cancer	16 (17.6)	16 (4.6)		17 (15.9)	15 (4.5)	
Death (other causes)	3 (3.3)	7 (2.0)		3 (2.8)	7 (2.1)	

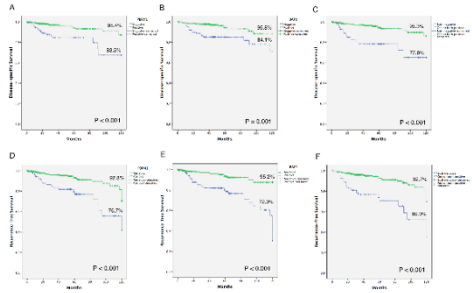

Conclusions: Patients with early stage tumors that present concomitant loss of both PBRM1 and BAP1 demonstrated worse survival rates and represent a relevant risk group for tumor recurrence and death.

935 Efficacy And Utility of Intraoperative Frozen Section Analysis In Robot Assisted Radical Prostatectomies: What Should Pathologists And Urologists Know?

Lagnajita Datta[1], *Kanika Taneja*[2], *Sean R Williamson*[3], *Nilesh Gupta*[1]. [1]Henry Ford Hospital, Detroit, MI, [2]Henry Ford Health System, Detroit, MI, [3]Henry Ford Health System, Detroit, MI

Background: Preservation of sphincter integrity and neurovascular bundles with negative resection margins in Radical Robot Assisted

Prostatectomy (RARP) is a challenge. Nerve sparing leads to higher rates of positive surgical margins (PSMs), which an independent risk factor for biochemical recurrence. Intraoperative frozen section (IFS) is used to balance these goals by lowering PSMs. In this study, utility and efficacy of IFS was investigated.

Design: Data and pathology slides of 99 patients undergoing IFS during RARP in 2015 were analyzed. Anatomical site of IFS was noted and compared with corresponding paraffin sections and final margins (FMs) of main prostatectomy specimen, divided into 6 categories (C) and analyzed (Table 1). IFS site was compared with previous biopsy findings.

Results: We retrieved 99 patients, who had IFS during RARP, of which most were of low stage and grade (57% Grade Group 1 or 2 and 58% pT2) (Table 2). IFS was positive for carcinoma in 12 patients (13%), 2 of which were reinterpreted as negative on paraffin sections (C4). Negative IFS in 3 cases was reinterpreted as positive on paraffin sections (C1). The remainder 93 were concordant with concordance rate of 95%. IFS helped in getting negative FM in 76 (78%) patients in C3 and C6 who then underwent nerve sparing RARP. In 4 patients of C6, IFS converted a positive to negative FM. Out of these 4, 3 had high Grade Groups of 4 and 5. The rest of 22 (25%) cases in C2 and C5 had positive FM in spite of IFS. C2 and C5 had cases with higher stage, EPE and SV invasion as compared to C3. IFS site matched previous biopsy tumor location in 75 patients, out of which 19 had positive FM. IFS site did not match in 13 cases of whom 7 had positive FM.

Table 1

Categories (C)	Definition	Number of cases
C1	IFS -, Paraffin +, FM +	3 (Included in C5)
C2	IFS -, Paraffin -, FM +	12
C3	IFS -, Paraffin -, FM -	71
C4	IFS +, Paraffin -, FM +	2 (Included in C5)
C5	IFS +, Paraffin +, FM +	10
C6	IFS +, Paraffin +, FM -	4

IFS: Intraoperative frozen section margin,
Paraffin: Corresponding paraffin section of IFS,
FM: Final margin in main prostatectomy specimen

Table 2

Variables	IFS patients	C1	C2	C3	C4	C5	C6
Number (%)	99(100)	3 (3)	12 (12)	72 (74)	2 (2)	10 (10)	4 (4)
Age (years), mean	63	60	66	62	57	62	66
Gleason grade group (%)							
1	11 (11)	0	0	10 (14)	0	1 (10)	0
2	45 (46)	2 (67)	7 (58)	33 (46)	1 (50)	4 (40)	1 (25)
3	21 (21)	1 (33)	2 (17)	15 (21)	1 (50)	4 (40)	0
4	6 (6)	0	0	4 (6)	0	0	2 (50)
5	15 (15)	0	3 (25)	10 (14)	0	1 (10)	1 (25)
Pathological stage (%)							
pT2a	5 (5)	0	1 (8)	4 (6)	0	0	0
pT2c	52 (53)	1 (33)	5 (4)	42 (58)	1 (50)	3 (30)	2 (50)
pT3a	27 (26)	1 (33)	3 (25)	18 (25)	1 (50)	5 (50)	1 (25)
pT3b	14 (14)	1 (33)	3 (25)	8 (1)	0	2 (20)	1 (25)
Extraprostatic extension(EPE) (%)	35 (36)	2 (67)	6 (50)	21 (29)	1 (50)	7 (70)	2 (50)
Seminal vesicle (SV) invasion (%)	14 (14)	1 (33)	3 (25)	8 (1)	0	2 (20)	1 (25)
Lymph node involvement (%)	5 (5)	1 (33)	0	2	0	2 (20)	1 (25)
Extra nodal involvement (%)	3 (3)	1 (33)	0	1	0	1 (10)	1 (25)

Conclusions: We found high concordance between frozen and corresponding paraffin sections. IFS was useful in majority of patients (78%), particularly in 4 patients of C6 where a positive was converted into negative FM, 3 of whom had high Grade Groups. Thus, IFS might be of greater value in reducing PSM in patients with higher grades. IFS failed to achieve negative FM in 22 cases (25%). Of these 22, 13 (60%) were higher stage. Extensive sampling and multiple IFS may be necessary to reduce PSM in higher stage tumors. Significant difference in rate of PSM between patients who had matched IFS and previous biopsy tumor location and unmatched cases (19/75 versus 7/13) was noted. Better correlation between IFS site and previous biopsy findings might lower PSM rate.

936 A Novel Dual Immunohistochemical Stain to Characterize Sloughed Cells in Testicular Biopsies for Infertility

Hari P Dhakal[1], *Jennifer J Coleman*[2], *Christopher Przybycin*[1]. [1]Cleveland Clinic, Cleveland, OH, [2]Cleveland Clinic, Cleveland, OH

Background: Evaluation of testicular biopsies from azoospermic men requires recognition of phases of germ cell maturation as organized architecturally within the seminiferous tubule, as well as distinguishing the inability to generate mature spermatozoa (germ cell aplasia or maturation arrest) from normal spermatogenesis, which may be associated with a reversible obstruction. While traditional fixatives (e.g. Bouin's) have provided exquisite nuclear detail and preserved the architectural integrity of the seminiferous tubule, formalin fixation has yielded biopsies with relatively poor nuclear detail and frequent luminal sloughing of cells, making it difficult to assess sperm maturation. One clone of the anti-DOG1 antibody was recently found to be expressed in late germ cells (Salama et al, USCAP 2015 abstract #1016). We developed a dual stain including DOG1 and SF-1 to mark late germ cells and Sertoli cells, respectively, in both sloughed and intact cells.

Design: Consecutive testicular biopsies (N=28) from men with azoospermia were classified by H&E morphology and stained with a dual SF-1 (Perseus)/DOG1 (Cell Marque) immunostain.

Results: Architectural disruption of seminiferous tubules with sloughing of cells into the lumens was noted in all biopsies, at least focally. SF-1 was expressed in sloughed Sertoli cells; DOG1 in sloughed late (post-spermatogonial) germ cells. The immunophenotype of the sloughed cells could be used in concert with the morphologic findings to diagnose the cases as shown in Table 1. Figure 1 shows sloughed cells composed of SF-1 (+) Sertoli cells (brown nuclear expression), DOG1 (+) late germ cells (red cytoplasmic expression), and SF-1(-)/DOG1(-) early germ cells in a case of normal spermatogenesis. The sloughed cells in Figure 2 (Sertoli only syndrome) are only SF-1 (+) Sertoli cells.

Diagnostic group	Morphology	Immunophenotype of sloughed cells
Normal spermatogenesis (N=5)	Full spectrum of maturation to mature spermatids in most tubules	SF-1(+)/DOG1(+)
Hypospermatogenesis (N=5)	Decreased number of tubules progressing to mature spermatids	SF-1(+)/DOG1(+)
Maturation arrest (late) (N=2)	Germ cells present, but no maturation beyond a given point	SF-1(+)/DOG1(+)
Sertoli cells only (N=15)	No germ cells present	SF-1(+)/DOG1(-)
"End-stage testis" (N=1)	Extensive tubular hyalinization	N/A

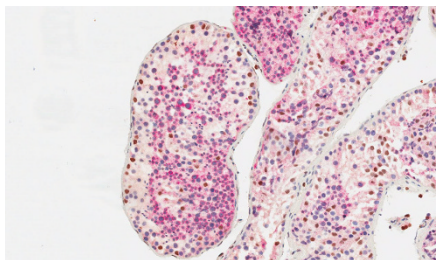

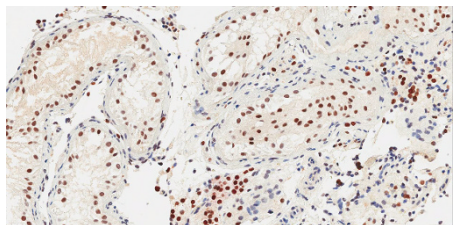

Conclusions: This dual SF-1/DOG1 immunostain can supplement morphology in the assessment of architecturally suboptimal testicular biopsies.

937 Gene Biomarker Signature for Distinguishing Urothelial Carcinoma from Squamous Cell Carcinoma

Jasreman Dhillon[1], *Yin Xiong*[2], *Anthony Magliocco*[1], *Soner Altiok*[3]. [1]H. Lee Moffitt Cancer Ctr, Tampa, FL, [2]Moffitt Cancer Center, [3]Moffitt Cancer Center, Tampa, FL

Background: Urothelial carcinoma (UC) can mimic a poorly squamous cell carcinoma (SCC) and it may be difficult to distinguish the two especially in metastatic sites. It is important to distinguish the two cancers for proper patient management. These two cancers have an overlapping immunohistochemical profile (both positive for CK5/6, CK7, p63 and p40). GATA3 although relatively specific for UC, can be expressed in SCC. Hence, we decided to develop biomarker signature to distinguish the two.

Design: A total of 161 UC cases and 38 head and neck (H&N) SCC cases and 268 lung SCC cases from Moffitt Cancer Center (MCC) Total Cancer Care (TCC) database were used as the training dataset. The gene expression data was derived from HuRSTA chips, each with 60607 probe sets for 26356 unique genes. Unpaired t-test was performed to identify significantly differentially expressed genes for UC vs. SCC from lung and H&N SCC. The top 19 most differentially expressed genes were selected for PCA (Principal Component Analysis). The first and second principal component (PC1 and PC2) of the 19 genes were used as the signature which was first self-validated on the training dataset with

157 out of 161 UCs correctly identified as UC and 302 out of 306 SCCs correctly identified as SCC (sensitivity = 97.52%; specificity = 98.69%). The signature was further validated on publicly available external datasets at GEO datasets, with 96 cases of H&N SCC from GSE31056, 18 lung SCCs from GSE10245 and 93 UC from GSE31684, total of 207 cases.

Results: This signature correctly identified 112 of the 114 publically available SCCs with gene data (96 H&N and 16 lung) as SCC and all of 93 publically available UCs with gene data as UC. From our in-house samples, it correctly identified 157 of 161 UCs as UC and 302 of 306 SCCs as SCC [Table 1]. Hence, with PC1 cutoffs <-5.1036 and PC2 <2.147621, we could correctly classify 250 of 254 UCs and 414 of 420 H&N and lung SCCs. The accuracy of this gene-signature to distinguish the types of cancer is shown in Figure 1.

Data Source	No. of Samples	Cancer Type	Classified as UC	Classified as SCC	Accu-racy
TCC	161	UC	157	4	97.52%
TCC	306	SCC lung + HN	4	302	98.69%
GEO	96	SCC HN	0	96	100%
GEO	93	UC	93	0	100%
GEO	18	SCC lung	2	16	88.89%

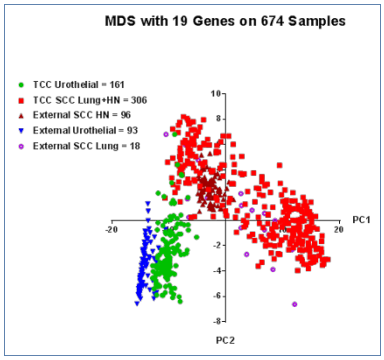

Conclusions: This 19-Gene biomarker signature can help in distinguishing UCs from SCCs of H&N and lung primaries. This will make a significant impact on patient management and outcome.

938 Integrated Proteomic and Peptidomic Analysis to Identify Biomarkers of Aggressive Behaviour in Early-Stage Renal Cell Carcinoma

Ashley Di Meo[1], *Ihor Batruch*[2], *Marshall Brown*[2], *Michael A Jewett*[3], *Antonio Finelli*[3], *Eleftherios P Diamandis*[2], *George M Yousef*[4]. [1]Toronto, ON, [2]The Advanced Centre for Detection of Cancer at the Lunenfeld-Tanenbaum Research Institute of Mount Sinai Hospital, Toronto, Canada, [3]Princess Margaret Cancer Centre, Toronto, Canada, [4]The Li Ka Shing Knowledge Institute of St. Michael's Hospital, Toronto, Canada

Background: Renal cell carcinoma (RCC) is the most lethal urologic malignancy of the adult kidney. Over recent decades the global incidence of RCC has increased, primarily due to the incidental detection of early stage, small renal masses (SRMs). RCC-SRMs can be either progressive (grow rapidly and metastasize) or non-progressive (do not significantly increase in size over time). There are no biomarkers to predict behaviour of SRMs, leading to significant number of unnecessary nephrectomies. Non-invasive biomarkers able to predict aggressive behaviour are urgently needed.

Design: We performed an integrated urinary proteomic and peptidomic analysis in patients with progressive and non-progressive clear cell RCC-SRMs. We analyzed protein and peptide fractions separately on the Q-Exactive mass spectrometer. We performed survival analysis and protease prediction analysis. Overall survival data were obtained from The Cancer Genome Atlas (TCGA).

Results: A total of 2,589 unique proteins were identified by proteomic analysis. In addition, peptidomic analysis identified a total of 20,760 unique endogenous peptides arising from 1,418 proteins. We identified twelve candidate proteins that could significantly differentiate progressive from non-progressive clear cell RCC-SRMs. Charged multivesicular body protein 2a (CHMP2A, AUC: 0.97), Carcinoembryonic antigen-related cell adhesion molecule 1 (CEACAM1, AUC: 0.88), Integral membrane protein 2B (ITM2B, AUC:0.88), and ferritin light chain (FTL, AUC: 77) expression was significantly elevated in progressive versus non-progressive clear cell RCC-SRMs. Moreover, CHMP2A (p=0.02) and FTL (p=0.001) expression significantly correlated with overall survival. We identified sixty-four endogenous peptide candidate that were significantly elevated in progressive versus non-progressive clear cell RCC-SRMs. Several proteases were predicted to be dysregulated in aggressive SRMs, including CTSS, MEP1A, MME, CMA1, CTSL, HTRA2, CTSE, and CTSB.

Conclusions: Taken together, elevated proteomic and peptidomic urinary levels represent potential prognostic biomarkers for progressive and non-progressive renal lesions. Moreover, bioinformatic analysis, identified several proteases that may have a role in disease progression.

939 Diagnostic Challenges of Prostatic Intraductal Carcinoma: A Pilot Survey Study from a Cohort of Trainees and Practicing General Surgical Pathologists

Ziad El-Zaatari[1], *Jae Y. Ro*[2], *Mukul Divatia*[3], *Steven Shen*[1]. [1]Houston Methodist Hospital, Houston, TX, [2]Houston Methodist Hospital, Cornell University, Houston, TX, [3]Houston Methodist Hospital, Houston, TX

Background: Prostatic intraductal carcinoma (IDC) has recently been recognized as an entity most often resulting from intraductal spread of high-grade prostate carcinoma. The finding of IDC on prostate biopsy thus necessitates more aggressive clinical management. It is important for pathologists to recognize this entity and to differentiate it from various benign or malignant mimickers.

Design: We designed a survey comprised of photomicrographs of H&E stained sections. Pathology residents, fellows, and practicing general surgical pathologists were asked to provide a diagnosis for each picture, and diagnoses were compared to those made by an expert genitourinary (GU) pathologist. The pictures included 4 cases of IDC, 4 cases of high-grade prostatic intraepithelial neoplasia (HGPIN), and 15 cases of benign and malignant possible mimickers, including atypical cribriform lesion (3), ductal adenocarcinoma (1), invasive prostate carcinoma (2), clear cell cribriform hyperplasia (2), normal central zone glands (5), seminal vesicle/ejaculatory duct (1), and transitional cell metaplasia (1).

Results: For IDC, the overall percent agreement with the expert pathologist diagnosis was 61% for trainees and 44% for practicing surgical pathologists. The most frequent alternate diagnoses made in lieu of IDC were ductal adenocarcinoma, invasive prostatic carcinoma, atypical cribriform lesion, high grade PIN, clear cell cribriform hyperplasia, and urothelial carcinoma involving ducts. Frequencies of each diagnosis made by either trainees or practicing surgical pathologists are shown in [Table 1].

Table 1 - Diagnoses Made by Survey Participants in Lieu of IDC (with GU Expert as Reference)

Diagnosis	Trainees	Pathologists
Ductal Adenocarcinoma	29%	50%
Invasive Prostate Carcinoma	43%	10%
Atypical Cribriform Lesion	14%	20%
High Grade PIN	-	10%
Clear Cell Cribriform Hyperplasia	14%	-
Urothelial Carcinoma Involving Ducts	-	10%

Conclusions: Although well- established criteria for the diagnosis of IDC are furnished in published literature and used by GU pathologists, diagnosing this entity can pose a challenge for trainees and general surgical pathologists. Our study highlights several possible mimickers which may confound the diagnosis of IDC. Suggested strategies that aid in achieving improved recognition of IDC and diagnostic consensus include further education regarding adherence to specified criteria, careful distinction from mimickers in the differential diagnosis, supplementation by ancillary immunohistochemical studies, and consultation with GU pathologists.

940 Divergent Histology and Aggressive Pathologic Features at Transurethral Resection of Bladder Tumor Correspond to Response Failure (as Compared to Success) with Neoadjuvant Chemotherapy: A Seven Year Retrospective Review of Cases Following Radical Cystectomy/ Cystoprostatectomy for Urothelial Carcinoma

Carla L Ellis[1], *Bradley C Carthon*[2], *Adeboye O. Osunkoya*[3]. [1]Emory University, Atlanta, GA, [2]Emory University, [3]Emory Univ/Medicine, Atlanta, GA

Background: There is limited data in the pathology literature regarding the long term natural history of urothelial carcinoma (UCa) following neoadjuvant chemotherapy and subsequent radical cystectomy or cystoprostatectomy. We have previously shown that failure of neoadjuvant therapy is associated with poor clinical outcome and a higher incidence of disease recurrence. We now seek to determine if divergent histology and aggressive pathologic features at the time of pre-surgical transurethral resection of bladder tumor (TURBT) are associated with neoadjuvant failures (as compared to successes) in the subsequent radical resection specimens.

Design: A search of our pathology data system was performed. All radical cystectomy and cystoprostatectomy specimens in patients who received neoadjuvant chemotherapy for UCa were reviewed in the 7 year period between 2009 and 2016, and analyzed in terms of: the presence or absence of divergent histologic features and aggressive pathologic features (angiolymphatic invasion, perineural invasion or carcinoma in situ) in the pre-resection TURBT, demographic information (age and gender), pathologic stage and grade, and type/cycle duration of neoadjuvant therapy. Successes were defined as patients with no evidence of residual UCa (ypT0N0M0) at radical resection and failures as patients with evidence of residual UCa at the time of resection.

Results: A total of 163 cases (39 successes, 24% and 124 failures, 76%) were reviewed. All patients had at least 3 cycles of neoadjuvant chemotherapy (range: 3-6 cycles), most commonly with gemcitabine and cisplatin. The average age was 69 years (range: 39-92 years). Fifty-five of 163 (34%) patients were female. The vast majority of patients (141/163, 87%) had a pre-surgical pathologic stage of pT2. Six of 39 (15%) successes and 66/124 (53%) failures showed divergent histology (squamous, glandular, sarcomatoid features or components of micropapillary or small cell carcinoma) and/or aggressive pathologic features (angiolymphatic invasion, perineural invasion, carcinoma in situ) at pre-surgical TURBT (p-value = 0.000033).

Conclusions: We now demonstrate that the presence of aggressive features at TURBT is associated with failure of neoadjuvant chemotherapy. This finding is statistically and clinically significant, as the presence of these divergent histologic features and aggressive pathologic features (when described at the time of TURBT) may necessitate more aggressive therapy or longer/more frequent clinical follow up.

941 Multifocal extracapsular extension of prostate cancer: a third subtype with worse prognosis than focal and established prostate cancer

Lama Farchoukh[1], *Rajiv Dhir*[2], *Thu Tran*[3], *Sheldon I Bastacky*[3]. [1]UPMC, Pittsburgh, PA, [2]UPMC, Shadyside, Pittsburgh, PA, [3]University of Pittsburgh Medical Center, Pittsburgh, PA

Background: Extracapsular extension (ECE) of prostate cancer (PRCA) in a radical prostatectomy (RP) specimen is a poor prognostic factor. ECE has been divided into 'focal' (F) (ECE tumor dimension < 0.8 mm) and 'established' (E) (≥0.8 mm) subtypes. We investigated the prognostic utility of a third category, 'multifocal' (MF), comprising more than one focus of ECE (< 0.8 mm). Tumors in this MF category would have been otherwise classified as F subtypes according to current binary classification.

Design: We conducted a retrospective analysis of biochemical recurrence and prognostic pathological variables of 673 men with stage pT3a/pT3b prostate cancer (seminal vesicle invasion, angiolymphatic invasion, positive nodes, Gleason score, pathological stage and volume of PRCA) to determine recurrence probability and pathological features of ECE subtypes.

Results: The type of ECE had significant effect on recurrence with progressively lower PFP (Log Rank, Breslow tests: p<0.0001) and higher recurrence probability from F to E to MF (p < 0.002). MF and E tumors had similar pathological characteristics except for a significantly larger tumor volume in MF specimens (p < 0.002). MF and E tumors exhibited worse prognostic features (p<0.0001) and higher hazards ratio than F (3.52 and 3.07, respectively with 95% confidence interval). In multivariate analysis, E and MF were independent prognostic factors (p=0.005 and p<0.0001) with the greatest adverse prognostic significance associated with MF.

TABLE 1. Radical prostatectomy specimen Gleason score, tumor percentage as an estimate of total tumor volume, number and percentages of positive surgical margins, seminal vesicle involvement and lymph node metastasis at each prostate tumor classification.

Abbreviations: Rec, biochemical recurrence; SVI, seminal vesicle involvement; +ALI, angiolymphatic invasion; +SM, positive surgical margins; +LN, lymph node metastases; X^2, Chi-square test.

		Rec	+SVI	+ALI	+SM	+LN	Stage		Gleason score	Tumor (%)
ECE	N	N (%)	N (%)	N (%)	N (%)	N (%)	pT3a N(%)	pT3b N(%)	Median (range)	Median (range)
F	322	76 (23.6)	25 (7.8)	13 (4)	59 (18.3)	9 (2.8)	297 (92.2)	25 (7.8)	7(6-9)	12.5 (1-80)
E	258	126 (48.8)	75 (29.1)	30 (11.6)	52 (20.2)	36 (14)	183 (70.9)	75 (29.1)	7(6-10)	17.5(1-85)
MF	93	63 (67.7)	34 (36.6)	16 (17.2)	25 (26.9)	16 (38.7)	59 (63.4)	34 (36.6)	7(6-10)	25(1-90)
	FvsE	P<0.0001								
	FvsMF									
	EvsMF	P<0.002	NS	NS	NS	NS	NS	NS	NS	P<0.002
		X^2	X^2	X^2	X^2	X^2	X^2	X^2	t-test	t-test

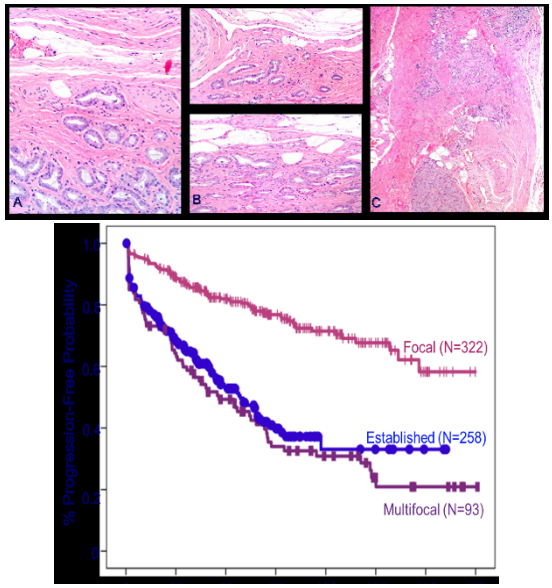

Conclusions: Identification of MF provides important prognostic clinical information associated with increased likelihood of recurrence compared to F and E tumors

942 High Risk HPV Positive Flat Lesions of The Penis with No or Minimal Atypias May Represent Hitherto Unrecognized HPV Driven Early Precancerous Changes. A P16 and Laser Capture Microdissection (LCM)-PCR Study of 26 Lesions in 10 Patients

Maria Jose Fernandez[1], *Nuria Guimerà*[2], *Diego F Sanchez*[3], *Sofía Cañete-Portillo*[4], *Elsa Velazquez*[5], *David Jenkins*[6], *Wim Quint*[6], *Antonio Cubilla*[7]. [1]Facultad Politecnica, Universidad Nacional de Asuncion, San Lorenzo, Central, [2]Rijswijk, [3]Instituto de Patologia e Investigacion, Asuncion, Central, [4]Asuncion, [5]Miraca Life Sciences, Newton, MA, [6]DDL Diagnostic Laboratory, Rijswijk, Netherlands, [7]Inst of Pathology, Asuncion

Background: In a recent HPV genotype detection study of penile precancerous lesions using LCM-PCR, we found non-atypical or minimally atypical flat lesions with variable morphology difficult to classify which were positive for low and high risk HPV. The WHO classification of HPV-related Penile Intraepithelial Neoplasia (PeIN) does not consider low grade lesions. The aim of this study was to describe the morphology of these unusual lesions with correlation to specific HPV genotypes and p16.

Design: Material and Methods: 26 flat lesions in 10 patients were evaluated. Eight of them were in the vicinity of PeIN or invasive carcinoma. They were, previous to HPV detection, variously diagnosed as squamous hyperplasia, differentiated or warty PeIN, differentiated PeIN vs warty PeIN, condylomas vs hyperplasia, or flat condylomas. HPV was detected using a LCM-PCR technique performed at the DDL laboratory (Fernandez-Nestosa et al Am J Surg Path 41:820-832, 2017).

Results: Median age was of 60 years. The foreskin was the most common site (21 cases or 77%) followed by the glans (2 cases), shaft (2 cases), and coronal sulcus (one case). Microscopic features on review for this study varied from non-atypical squamous hyperplasia (6 cases) to minimally atypical differentiated PeIN (14 cases), and flat condylomas (7 cases). High risk HPV was detected in 16 of 26 lesions (62%), 10 of which were HPV 16. Other detected genotypes were 66, 39, 35 (high risk HPV), and 6, 11, 44, 68, 74 (low risk HPV). High risk HPV were more common in lesions with the phenotype of differentiated PeIN (79%) or squamous hyperplasia (50%) and less common in flat condylomas (29%). The majority of high risk HPV-positive cases were also positive for p16.

Conclusions: HPV positive non-atypical or minimally atypical squamous flat lesions in the vicinity of classical PeIN and carcinoma were morphologically heterogeneous and difficult to classify. Many of them were unexpectedly positive for high risk HPV and p16, indicating that, independently of their features and low grade morphology, they may represent hitherto unrecognized HPV driven precancerous lesions.

943 Impact of Zone of Origin in Anterior-Dominant Prostatic Tumors: Long-Term Biochemical Recurrence-Free Survival in an Anatomically Well-Annotated Series

Samson W Fine[1], *Hikmat Al-Ahmadie*[1], *Emily Vertosick*[1], *Daniel Sjoberg*[1], *Andrew Vickers*[1], *Ying-Bei Chen*[1], *Anuradha Gopalan*[1], *S. Joseph Sirintrapun*[1], *Satish Tickoo*[1], *Victor Reuter*[1]. [1]Memorial Sloan Kettering Cancer Center, New York, NY

Background: It has been argued that transition zone (TZ) prostate cancers (PCa) should be considered separately from peripheral zone (PZ) PCa because the former have an overall more favorable prognosis. In the modern era, approximately 25% of PCa seen at radical prostatectomy are anterior–dominant. While TZ PCa may be of large volumes and associated with high serum prostate specific antigen, most reports have maintained that TZ PCa show lower grade and stage than PZ PCa. In a previous evaluation of anterior–dominant prostatic tumors, in which zone of origin was assigned after careful topographic review, we found comparable pathologic features (grade, stage and margin status) between TZ and anterior PZ PCa. The long-term clinical outcomes of anterior–dominant PCa have not been well studied.

Design: The study cohort included 197 patients who underwent radical prostatectomy between 2000 and 2004 and had anterior–dominant PCa previously categorized as TZ, anterior PZ, both TZ and anterior PZ or of indeterminate zone. We assessed whether tumor localization was associated with biochemical recurrence (BCR).

Results: Of the 197 patients, 97 (49%) were located in anterior PZ, 70 (36%) in TZ, 14 (7%) in both and 16 (8%) of indeterminate zone. Grade Group (GrdGrp) distribution was similar for anterior PZ and TZ PCa (GrdGrp 1, 2, 3, 4 and 5: 34%, 54%, 10%, 0% and 2% versus 34.5%, 54%, 11.5%, 0% and 0%); similar rates of extraprostatic extension (anterior PZ: 11%, TZ: 10%) and margin positivity (anterior PZ: 14%, TZ: 13%) were also observed.

Median follow-up time among survivors was 9.5 years (IQR 7.2, 12.7). 19 patients had BCR: 10 with anterior PZ tumors and 5 with TZ tumors. Estimated 5 and 10 year BCR–free survival was 91% (95% CI 83-96%) and 89% (95% CI 80-94%) for anterior PZ and 94 (95% CI 84-98%) and 92% (95% CI 82-97%) for TZ tumors. On univariate analysis, there was no evidence of a difference in BCR-free survival between TZ and anterior PZ PCa (p=0.5).

Conclusions: In this large cohort of topographically-annotated anterior–dominant PCa, in addition to similar pathologic outcomes at radical prostatectomy between PCa of different zonal origins, we found no significant difference in biochemical recurrence–free survival on long-term follow-up. If corroborated in other series, these results suggest that previous studies showing differences between TZ and PZ PCa may have been influenced by posterior PZ PCa, which account for the majority of PCa.

944 Pathologic Characteristics of the Hereditary Renal Cell Carcinomas Associated with Birt-Hogg-Dubé Syndrome

Mitsuko Furuya[1], *Ikuma Kato*[2], *Yoji Nagashima*[3], *Naoto Kuroda*[4], *Hisashi Hasumi*[5], *Masaya Baba*[6], *Masahiro Yao*[5], *Yukio Nakatani*[7]. [1]Yokohama City University Graduate School of Medicine, Yokohama, Kanagawa, [2]Yokohama City University Graduate School of Medicine, Yokohama, Kanagawa, [3]Tokyo Women's Medical University, Tokyo, [4]Kochi Red Cross Hospital, Kochi City, Kochi, [5]Yokohama City University, [6]Kumamoto University, [7]Chiba University Hospital, Chiba, Japan

Background: Birt-Hogg-Dubé (BHD) syndrome is an autosomal dominant disorder caused by germline mutation of *FLCN*. The affected families are at risk of renal cell carcinomas (RCCs), fibrofolliculomas and pulmonary cysts (Fig. 1). Although current WHO classification does not define BHD-RCC as a specific entity, differential diagnosis between BHD-RCCs and sporadic counterparts is important because the affected individuals frequently develop multiple RCCs. It is difficult for pathologists to suggest whether the patient with RCC potentially has genetic mutation of *FLCN* or not. The aim of the study is to find useful markers for differential diagnosis between BHD-RCCs and histology-matched sporadic counterparts.

Design: The morbidity of BHD-RCCs and *FLCN* mutations were investigated in 170 different BHD families composed of 437 individuals. Histopathologic characteristics of 76 surgically resected BHD-RCCs were investigated.

Results: We have identified 40 mutation patterns including 11 novel ones. Thirty-six percent of mutation carriers over 40 years of age developed RCCs. Chromophobe RCC and hybrid oncocytic/chromophobe tumors accounted for 78 % of BHD-RCCs (Fig. 2). Normal-looking cortices often contained epithelial cell nests and complicated cysts. Somatic mutations of *FLCN* were identified in 40% of BHD-RCCs. Loss of heterozygosity (LOH) patterns were detected in 10%. Copy number variation analysis revealed little gain/loss in BHD-RCCs, and numerous LOH regions existed as uniparental disomy. FISH analysis for the centromeric regions of chromosomes 2p, 3p, 6p and 17q revealed disomic in BHD-RCCs whereas frequently monosomic in sporadic counterparts.

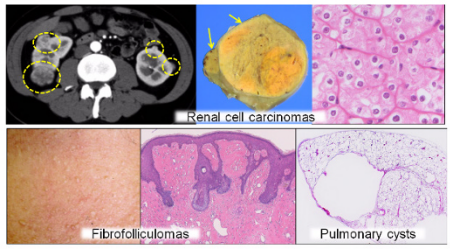

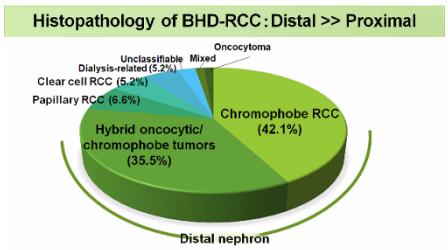

Conclusions: The collective data demonstrate characteristic features of BHD-RCCs that are distinctively different from sporadic counterparts, which will be informative for pathologists to determine whether the cases should be considered for further genetic testing.

945 HPV Genotyping of Penile Carcinomas by Real-Time Polymerase Chain Reaction (qPCR) and Multi-color Melting Curve Analysis (MMCA) of formalin fixed paraffin embedded (FFPE) Tissue

Manoj Gadara[1], *Ravi Kothapalli*, *Genevra Magliocco*[2], *Philippe E Spiess*, *Anthony Magliocco*[3], *Jasreman Dhillon*[3]. [1]Moffitt Cancer Center, [2]University of California, San Diego, [3]H. Lee Moffitt Cancer Ctr, Tampa, FL

Background: Penile carcinoma accounts for 0.4% to 0.6% of all malignancies in men. A subset of penile carcinomas are HPV related. Methods commonly utilized for detecting HPV in tissue sections are immunohistochemical (IHC) stain p16 and HPV In situ hybridization (ISH). In this study, FFPE tissue from penile cancer cases was tested for presence of HPV by qPCR and MMCA.

Design: 38 cases of penile cancer were tested. The tumors were stained with IHC p16. HPV ISH (types 16, 18, 31, 33, 35, 39, 45, 51, 52, 56, 58 and 66) was performed. 200 ng of DNA was extracted from each FFPE tissue using QIAamp DNA, FFPE tissue Kit. High risk HPV (HR HPV) genotyping was determined using the MeltPro HR HPV Genotyping Assay that is based on qPCR and MMCA and screens for 14 HR HPV types (16, 18, 31, 33, 35, 39, 45, 51, 52, 56, 58, 59, 66, and 68). A case was considered true positive when at least 2 of the 3 tests or all 3 tests were positive; false positive when only 1 test was positive.

Results: 15 (39 %) cases were p16 positive of which 3 cases were negative for HPV by ISH and qPCR. These 3 cases were considered to be false positive (8 %). 23 (61 %) cases were p16 negative. These were also negative by HPV by ISH and qPCR. There were 3 (8%) false positive cases by ISH that tested negative for p16 as well as qPCR. False positive cases for p16 and HPV ISH were mutually exclusive. qPCR did not have any false negative or false positive cases (Table 1). There were 12 (31.5 %) cases that tested positive for HPV by qPCR. Genotyping of these viruses is provided in Table 2.

Table 1. Comparison of HPV results by p16, HPV ISH and qPCR

Test Performed (n = 38)	Positive Test Result	Negative Test Result	False Positive	False Negative
P16	15	23	3	0
HPV ISH	15	23	3	0
qPCR	12	26	0	0

Table 2. HPV Genotyping by qPCR

HPV Type	Number of Positive Cases (%) 12 (100%)
16	9 (75%)
18	1 (8%)
35	1 (8%)
51	1 (8%)

Conclusions: qPCR is a highly sensitive and specific technique for detection of HPV in FFPE tissues

1. In p16 negative cases, there is no value of reflex HPV ISH or qPCR testing as p16 negative tumors are always HPV negative (100% negative predictive value)

2. In our cohort, HPV 16 is the most common genotype in penile carcinomas

946 Adenocarcinoma of the Rete Testis: Reappraisal of Diagnostic Criteria in the Light of Recent Immunohistochemical Advances

Jatin S Gandhi[1], *Ondrej Hes*[2], *Eva Maria Comperat*[3], *Rodolfo Montironi*[4], *Maurizio Colecchia*[5], *Isabel Alvarado-Cabrero*[6], *Michelle S Hirsch*[7], *Santosh Menon*[8], *Gladell P Paner*[9], *Abbas Agaimy*[10], *Wafi Bibars*[11], *Jonathan Epstein*[12], *Mahul Amin*[13]. [1]University of Tennessee Health Science Center Memphis, Memphis, TN, [2]Biopticka Laborator, Plzen, [3]Paris, [4]Univ. Politecnica delle Marche /Medicine, Ancona, Marche, [5]Fondazione IRCCS Istituto Nazionale dei Tumori di Milano, Milan, Italy, [6]Mexican Oncology Hospital, Mexico, Mexico, [7]Brigham and Women's Hospital, Boston, MA, [8]Tata Memorial Hospital, Mumbai, Maharashtra, [9]University of Chicago, Chicago, IL, [10]Friedrich-Alexander University Erlangen-Nuremberg, Erlangen, Bavaria, [11]University of Tennessee Memphis, Memphis, TN, [12]The Johns Hopkins Med Inst, Baltimore, MD, [13]Methodist University Hospital, Memphis, TN

Background: Infiltrating adenocarcinoma with tubulopapillary architecture in the paratestis engenders the differential diagnosis of a rete testis adenocarcinoma (RTA), malignant mesothelioma (MM), ovarian-type carcinoma of the tunica vaginalis, epididymal adenocarcinoma, and metastatic adenocarcinoma. Of these, RTA is an extremely rare neoplasm reported in the literature only as anecdotal case reports. PAX 8 is a lineage specific transcription factor that is essential for the development of Wolffian and Mullerian ducts and is now established as a diagnostic marker for renal and Mullerian tumors. A recent study demonstrated consistent expression of PAX 8 in normal male genital tract tissue including the rete testis, epididymis, vas deferens and ejaculatory ducts, consistent with their derivation from the Wolffian ducts. The goal of this study was to evaluate PAX8 and other biomarkers in RTA.

Design: 9 cases of RTA were identified based on previously published criteria, most of which are exclusionary in nature, including 1) absence of an extra scrotal tumor, 2) tumor centered on the testicular hilum, 3) morphology incompatible with other tumors of testicular or paratesticular origin, and 4) immunohistochemical exclusion of other possibilities, particularly MM and metastases. Immunohistochemistry, including but not limited to PAX8, was performed on all cases.

Results: Median patient age was 49 years (range 11–75) with almost equal distribution of laterality. Tumor size varied from 1.5-3.5 cm (mean 2.5 cm). An infiltrating adenocarcinoma with tubulopapillary architecture was seen in all cases; variations included spindled morphology and squamous differentiation. Necrosis and psammoma bodies were frequently present. All tumors showed a characteristic intra-rete growth pattern and diffusely expressed PAX8. Metastases to the lung and supraclavicular lymph nodes were observed.

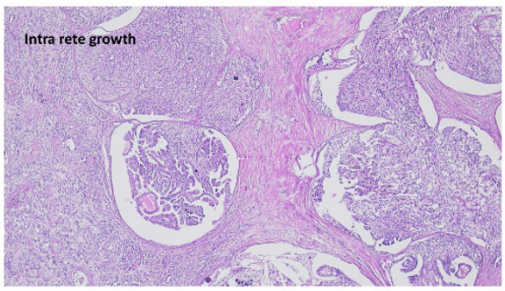

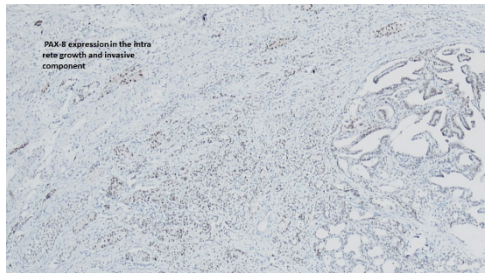

Conclusions: Our series, the first to date on these tumors, allows us to refine diagnostic criteria for the rare RTA, adding to the previously published four criteria. New inclusion criteria we propose include 1) the presence of a prominent intra-rete growth pattern, and 2) immunohistochemical positivity for PAX8. Establishment of definitive inclusionary diagnostic criteria will allow us to accurately recognize these rare tumors and enable further study; molecular studies are underway in our laboratory.

947 TMPRSS2:ERG Fusion Positive and TMPRSS2:ERG Wild Type Relapsed and Metastatic Castrate Resistant Prostate Cancer Differ in Genomic Signatures and Opportunities for Targeted and Immunotherapies

Laurie Gay[1], *Jon Chung*[2], *Julia A Elvin*[3], *Jo-Anne Vergilio*[4], *James Suh*[5], *Eric Severson*[6], *Shakti Ramkissoon*[7], *Sugganth Daniel*[2], *Siraj Ali*[3], *Garrett M Frampton*[2], *Ryan Hartmaier*[2], *Lee Albacker*, *Alexa B Schrock*[3], *Vincent A Miller*[2], *Philip M Stephens*[2], *Jeffrey S Ross*[1]. [1]Foundation Medicine, Cambridge, MA, [2]Foundation Medicine, [3]Foundation Medicine, Inc, Cambridge, MA, [4]Foundation Medicine, Inc, Cambridge, MA, [5]Foundation Medicine, Inc., Morrisville, NC, [6]Foundation Medicine, Inc, Morrisville, NC, [7]Foundation Medicine, Morrisville, NC, [8]Cambridge, MA, [9]Foundation Medicine, Cambridge, MA

Disclosures:
Laurie Gay: *Employee*, Foundation Medicine, Inc.
Jon Chung: *Employee*, Foundation Medicine, Inc.
Jo-Anne Vergilio: *Employee*, Foundation Medicine, Inc.
James Suh: *Employee*, Foundation Medicine, Inc.
Eric Severson: *Employee*, Foundation Medicine, Inc.
Shakti Ramkissoon: *Employee*, Foundation Medicine, Inc.
Siraj Ali: *Employee*, Foundation Medicine, Inc.
Ryan Hartmaier: *Employee*, Foundation Medicine, Inc.
Alexa Schrock: *Employee*, Foundation Medicine, Inc.
Philip Stephens: *Employee*, Foundation Medicine, Inc.
Jeffrey Ross: *Employee*, Foundation Medicine, Inc.

Background: *TMPRSS2:ERG* fusions have been described in up to 50% of early stage acinar prostatic adenocarcinomas with variable clinical significance as to prognosis and responsiveness to hormonal and systemic chemotherapies. We performed comprehensive genomic profiling (CGP) to learn whether sub-categorization of *TMPRSS2* fusion status would impact therapy opportunities in patients with clinically advanced castrate resistant disease (CRPC).

Design: DNA was extracted from 40 µm of FFPE sections of 2,424 CRPC. CGP was performed on hybridization-captured, adaptor ligation-based libraries to a mean coverage depth >600X for up to 315 cancer-related genes. The results were analyzed for all classes of genomic alterations (GA) including short variant (SV) base substitutions and insertions and deletions; select rearrangements; and copy number changes. Tumor mutational burden (TMB) was determined on 1.1 Mbp of sequenced DNA and microsatellite instability (MSI) was determined on 114 loci.

Results: All (100%) CRPC sequenced had failed multiple systemic hormonal and cytotoxic/radiation therapy regimens. The 755 (31%) *TMPRSS2*+ CRPC had a median age of 66 years (range 36 to 87 years) and the 1,669 *TMPRSS2*- CRPC median age was 65 years (34 to 85 years). The mean GA/sample for the two groups similar (Table). *TMPRSS2*+ CRCPC features significantly greater *TP53* and *PTEN* GA and *TMPRSS2*- CRPC featured higher *MYC* and *ATM* GA. Differences in *BRCA2* and *RB1* GA were not significant. The mean TMB was not different between the groups and, although *TMPRSS2*- CRPC had higher frequencies of higher TMB levels, these frequencies were very low. Although quite rare for both groups, MSI-High status was more frequently identified in *TMPRSS2*- CRPC.

	TM-PRSS2:ERG+ CRPC (755)	TM-PRSS2:ERG- CRPC (1,669)	Signifi-cance
Median Age in years	66	65	
GA/tumor	4.5	4.3	NS
TMPRSS2 Fusions	100%	0%	
TP53	55%	39%	P<0.0001
PTEN	45%	27%	P<0.0001
AR	25%	22%	NS
MYC	9%	14%	P=0.0004
BRCA2	8%	10%	NS
ATM	4%	7%	P=0.0032
RB1	8%	6%	NS
MSI-High	1%	3%	P=0.01
TMB median (mut/Mb)	1.7	2.7	NS
TMB Mean (mut/Mb)	5.10	5.65	NS
TMB ≥ 10 mut/Mb	3%	6%	P=0.04
TMB ≥ 20 mut/Mb	2%	4%	P=0.01

Conclusions: At 31%, the frequency of *TMPRSS2*+ CRPC cases appears lower that the 46% seen in early stage disease (TCGA data) suggesting that, when present, this biomarker may be linked to a favorable prognosis for the disease. When CRPC is separated into *TMPRSS2:ERG* fusion status, significant genomic differences emerge which may have impact on therapy selection.

948 Collecting Duct Carcinoma of the Kidney: a Comprehensive Genomic Profiling Study

Laurie Gay[1], *Julia A Elvin*[2], *Jo-Anne Vergilio*[3], *Shakti Ramkissoon*[4], *Eric Severson*[5], *Sugganth Daniel*[6], *Siraj Ali*[7], *Jon Chung*[6], *Alexa B Schrock*[8], *Vincent A Miller*[6], *Philip M Stephens*[6], *Jeffrey S Ross*[1]. [1]Foundation Medicine, Cambridge, MA, [2]Foundation Medicine, Inc, Cambridge, MA, [3]Foundation Medicine, Inc, Cambridge, MA, [4]Foundation Medicine, Morrisville, NC, [5]Foundation Medicine, Inc, Morrisville, NC, [6]Foundation Medicine, [7]Cambridge, MA, [8]Foundation Medicine, Cambridge, MA

Disclosures:
Laurie Gay: *Employee*, Foundation Medicine, Inc.
Jo-Anne Vergilio: *Employee*, Foundation Medicine, Inc.
Shakti Ramkissoon: *Employee*, Foundation Medicine, Inc.
Eric Severson: *Employee*, Foundation Medicine, Inc.
Siraj Ali: *Employee*, Foundation Medicine, Inc.
Jon Chung: *Employee*, Foundation Medicine, Inc.
Alexa Schrock: *Employee*, Foundation Medicine, Inc.
Philip Stephens: *Employee*, Foundation Medicine, Inc.
Jeffrey Ross: *Employee*, Foundation Medicine, Inc.

Background: Collecting duct carcinoma (CDC) is a rare form of malignancy arising in the renal medulla which progresses rapidly and appears resistant to current systemic therapies. We queried whether comprehensive genomic profiling (CGP) could uncover opportunities for targeted and immunotherapies for this challenging disease.

Design: DNA was extracted from 40 microns of FFPE specimen from 46 cases of relapsed, refractory and metastatic CDC and a control group of 626 clinically advanced clear cell RCC (ccRCC). CGP was performed using a hybrid-capture, adaptor ligation based next generation sequencing assay to a mean coverage depth of 874X. Tumor mutational burden (TMB) was calculated from a minimum of 1.11 Mb of sequenced DNA as previously described and reported as mutations/Mb. Microsatellite instability status (MSI) was determined by a proprietary algorithm. The results were analyzed for all classes of genomic alterations (GA), including base substitutions, insertions and deletions (short variants; SV), fusions, and copy number changes including amplifications (amp) and homozygous deletions.

Results: All 14 (100%) SCCB cases were confirmed on routine histology and included 32 (70%) male and 14 (30%) female patients with a median age of 55 years (range 28 to 90 years). All (100%) of CDC were clinically advanced Stage IV tumors with the primary CDC used for CGP in 70% of cases and a metastasis biopsy was sequenced in 30%. All (100%) CDC were intermediate (Grade 3) or high grade (Grade 4). The 46 CDC had a lower GA/tumor of 1.8 compared to 2.7 GA/tumor in the ccRCC control group (Table). *VHL* and *TSC1* alterations were more frequent in ccRCC and *SMARCB1*, *NF2, RB1* and *RET* GA were more frequent in CDC. The median TMB was low for both tumor types (1.8 for CDC and 2.7 for ccRCC) with very low frequencies of ≥20 mut/Mb. No (0%) of CDC were MSI-high and 1 (<1%) of ccRCC were MSI-High.

GA	CDC (46 cases)	ccRCC (626 Cases)	Significance
Mean GA per tumor	1.6	2.7	P=0.04
VHL	0%	78%	P<0.0001
SMARCB1	19%	1%	P<0.0001
NF2	14%	2%	P=0.0007
RB1	5%	1%	P=0.02
EGFR	5%	3%	NS
RET	5%	0%	P=0.0003
TP53	5%	12%	NS
TSC1	0%	8%	P=0.04
TSC2	3%	1%	NS
TMB > 10/>20	5%/0%	<1%/<1%	NS

Conclusions: In addition to their histologic differences, the frequencies and types of GA seen in CDC differ significantly from that seen in ccRCC. The opportunities for biomarker driven targeted therapies for CDC appear limited with opportunities to target GA in growth TKGFR and MTOR pathway. Similarly, the relatively low TMB and absence of MSI-High status in CDC also predicts that these tumors may be resistant to immunotherapies. Further study of the genomic features of CDC appear warranted.

949 Characterization of PD-L1 Expression in Penile Squamous Cell Carcinoma

Lan Gellert[1], *Chanjuan Shi*[2], *Giovanna A Giannico*[3], *Omar Hameed*[3]. [1]Vanderbilt Univ Med Ctr, Nashville, TN, [2]Vanderbilt University, Nashville, TN, [3]Vanderbilt University Medical Center, Nashville, TN

Background: Programmed death-ligand 1 (PD-L1) is a cell surface glycoprotein and it has been shown to be a promising therapeutic and prognostic biomarker in several malignancies. The aim of this study was to investigate PD-L1 expression in penile squamous cell carcinoma and correlate its expression with various clinicopathologic factors and disease outcome.

Design: PD-L1 expression was evaluated by immunohistochemistry (clone E1L3N) in 123 patients with penile squamous cell carcinoma between 1998 and 2013 on tissue microarrays. PD-L1 positivity was defined as the presence of any extent of membranous staining in ≥ 1% of tumor cells. P16 status was available from our previous study. Clinical data were collected from patients' electronic medical record including age, stage, histologic grade, lymph node status, lymphovascular invasion, local recurrence and overall survival. Statistical analysis was performed using Stata software v.13.1.

Clinical and pathologic variables are summarized in Table 1. Of the 123 cases, PD-L1 expression was identified in 37 cases (30%). PD-L1 status was found to be significantly correlated with pathologic stage (p = 0.03) and nodal metastasis (p=0.02). No statistically significant associations were found between PD-L1 status and age (p=0.14), p16 status (p = 0.69), histologic grade (p=0.06), lymphovascular invasion (p = 0.23) and margin status (p = 0.37). The median follow-up time was 30 months. On multivariate analysis, using Cox proportional hazards model, PD-L1 expression was significantly associated with local recurrence (p=0.03) and overall mortality (p=0.01) after controlling for p16 status, pathologic stage, histologic grade, nodal metastasis and margin status.

Results:

Clinicopathologic variables by PD-L1 status

Variable	PD-L1 (-) (%)	PD-L1 (+) (%)	Total	p value
Overall	86(70%)	37(30%)	123	
Age(yrs)				
<=60	37(43%)	15(41%)	52	0.14
>60	49(57%)	22(59%)	71	
Histologic grade				
well diff	43(50%)	10(27%)	53	0.06
moderately diff	32(37%)	20(54%)	52	
poorly diff	11(13%)	7(19%)	18	
P16				
negative	38(47%)	19(53%)	57	0.69
positive	42(53%)	17(47%)	59	
Pathologic stage				
pTis/pTa	19(22%)	1(3%)	20	0.03
pT1	25(29%)	14(38%)	39	
>=pT2	42(49%)	22(59%)	64	
LVI				
negative	78(91%)	30(81%)	108	0.23
positive	8(9%)	7(19%)	15	
Nodal metastasis				
negative	58(67%)	16(43%)	74	0.02
positive	28(33%)	21(57%)	49	
Margin				
negative	56(65%)	27(73%)	83	0.37
positive	30(35%)	10(27%)	40	

Conclusions: PD-L1 expression is present in a proportion of penile squamous cell carcinoma. It is often associated with high risk clinicopathologic factors and worse clinical outcomes. These findings suggest a potential role for anti-PD-L1/PD-1 immunotherapy for patients with advanced penile squamous cell carcinoma.

Table I: A Cytogenetic Subgroups of Pure Type II pRCC*

	Group 1 (trisomy 7 *and* 17 and loss of Y chromosome)*		Group 2 (+7 *or* +17)*		Group 3 (absence of +7 or +17, and concomitant loss of 3p *and* 14)*		Group 4 Other		Total Cases
Sarcomatoid Features	Absent (%)	Present (%)	Absent (%)	Present (%)	Absent (%)	Present (%)	Absent (%)	Present (%)	
Low ISUP grade									
Male	14 (34%)		8 (38%)				3 (14%)		25
Female	2 (5%)		2 (10%)						4
									29
High ISUP grade									
Male	21 (51%)		10 (24%)		1 (17%)	3 (50%)	14 (67%)	3 (14%)	52
Female	4 (10)		1 (5%)		1 (17%)	1 (17%)	1 (5%)		8
									60

Table I: B Cytogenetic Subgroups of Mixed Type II pRCC

	Group I		Group II		Group III		Group IV		Total cases
Sarcomatoid Features	Absent	Present	Absent	Present	Absent	Present	Absent	Present	
Low ISUP grade									
Male	1								1
Female	1								1
									2
High ISUP grade									
Male	9		1			1	4		14
Female	1								
									18

* [Marsaud et al, 2015]

Tabe II: Outcomes of pRCC Type II and Mixed

Type 2 pRCC						
	No Follow-up	No recurrence/metastasis	Recurrence	Metastasis	Deceased	Total
Group I	11	29		1		41
Group II	6	12	1	1	1	21
Group III	1	0		3		4
Group IV	7	6		3	4	20
Total	25	47		8	5	85
						Total
Type 2 pRCC mixed						
Mixed	No follow-up	No recurrence/metastasis	Recurrence	Metastasis	Deceased	Total
Group I	3	9			1	13
Group II	1					1
Group III						
Group IV	1	5		1	1	8
Total						22

950 Cytogenetic Analysis of Papillary Renal Cell Carcinoma Type II: a Novel Subgroup

Yipeng Geng[1], *Josephine Aguilar-Jakthong*[2], *Anthony Sisk*[3], *Quintero Fabiola*[4]. [1]UCLA, Los Angeles, CA, [2]UCLA Pathology and Laboratory Medicine, Los Angeles, CA, [3] Tarzana, CA, [4]UCLA

Background: Papillary renal cell carcinoma (pRCC) is the second most common renal cell carcinoma and is classified into 2 types. Type 2 pRCC is morphologically and cytogenetically heterogeneous. There are currently 3 cytogenetic subgroups correlating to prognosis (Table I). We propose a 4th subgroup that may further characterize these tumors and identify patients with poor prognosis. In addition, because there is limited data on mixed type 2 pRCC, we compare tumor characteristics in the proposed subgroup to those of pure type 2 pRCC.

Design: Data from all patients diagnosed with type 2 pRCC between January 2002 and August 2017 was collected. We compared demographics, histologic features and karyotype. Tumors are classified into ISUP high (III/IV) and low (I/II) grade, then further classified into the three proposed subgroups (Table 1), and the remaining cases into a fourth subgroup.

Results: From a set of 160 patients with pRCC type 2, 136 (85%) were diagnosed with pure type 2 pRCC, of which 89 tumors had abnormal karyotype results and were classified into the four subgroups. 86% (n=21) of Group 4 are high-grade with 16% of those with sarcomatoid features. Thus, Group 4 patients had a significant correlation to high-grade tumors compared to Group 1 and 2, 85% vs. 58% ($p<0.05$) (Table I). 61 of the 89 patients had follow-up. 58% of Group 4 had metastases or expired, compared to 3%, 14% in group 1 and 2 ($p<0.05$), and 100% in 3 (Table 2),

The remaining 24 (15%) patients were diagnosed with mixed pRCC, of which 18 tumors had karyotype and were classified into the 4 subgroups. All Group 4 were high-grade (Table I). Comparing mixed and pure type 2 tumors, more mixed tumor were high-grade than pure type 2 (89% vs. 61%, $p<0.05$). Also, sarcomatoid features were only seen in groups 3 and 4 in both pure type 2 and mixed tumors.

Also, men have a significantly increased risk for high-grade tumors than women for type 2 (66% vs. 17%,$p<0.05$) and mixed type ($p<0.05$). Women present at a younger age (<50) than men ($p<0.05$).

Conclusions: We propose an additional cytogenetics subgroup, which our data has shown to have: 1) high occurrence of trisomy 16 or 12, or both, with low frequency (in 0-4 cases) of concurrent duplication 1q or 5q, or loss 3p or 9p or 14, known to be associated with aggressive tumors, 2) more high-grade lesions -few with sarcomatoid features, 3) higher stage and metastases/deaths than Groups 1 and 2. Thus, patients that are classified into this group may require more aggressive management.

951 Updated Immunohistochemistry Characterization of Well-Differentiated Neuroendocrine Tumors of the Kidney

Claudia Ormenisan Gherasim[1], *Sara Higgins*[1], *Melanie Johncilla*[1], *Michelle S Hirsch*[1]. [1]Brigham and Women's Hospital, Boston, MA

Background: Well differentiated neuroendocrine tumors (WDNET, i.e., so-called carcinoid tumors) are frequently encountered in the lung and gastrointestinal (GI) tract. In contrast, primary WDNETS of the kidney are extremely rare, and have been reported in horseshoe kidneys or associated with teratoma. Because of the rarity of these renal neoplasms, a metastasis from other sites must always be considered. Previous studies have shown expression of numerous biomarkers, including polyclonal PAX8 (pPAX8), a marker frequently used for renal epithelial tumors, and TTF1 in GI and pulmonary WDNETs, respectively. The goal of this study was to evaluate traditional, as well as more recently described biomarkers for WDNETs in tumors arising from the kidney to help determine if any can be used to reliable predict primary site.

Design: Six WDNETs in the kidney were retrieved and re-evaluated by H&E to confirm classic morphologic features. Clinical and radiographic evaluation excluded metastatic disease from other primary sites. Immunohistochemistry (IHC) was performed on all cases using general NET biomarkers (synaptophysin, chromogranin), GI NET biomarkers (pPAX8, PAX6, NKX2.2, CDX2, ISL1, PDX1) and a pulmonary NET biomarker (TTF1).

Results: Four patients were female and two were male. Tumors ranged from 2.8 cm to 7.5 cm, with 2 cases showing extension in perirenal soft tissues. Two cases were associated with a horseshoe kidney, and one of these also contained adjacent teratoma. All six cases (100%) were positive for synaptophysin, chromogranin and NKX2.2; the latter is a new biomarker previously described in WDNETs of the GI tract. There was no expression in any (0/6) cases for CDX2

or TTF1. pPAX8 was positive in 4/6 cases, three focal (50%) and 1 diffuse (17%). Three cases (50%) were focally positive for PAX6, the remaining 3 were negative. ISL1 and PDX1 showed variable weak staining in 80% and 40% of cases, respectively. 4 of 6 patients are alive with no evidence of metastatic WDNET; one patient died of disease and one died of other causes.

Conclusions: Morphologic features as well as the presence of chromogranin and synaptophysin confirm the diagnosis of a WDNET in the kidney. There are no specific biomarkers, including pPAX8, to support a renal primary; however, the absence of CDX2 and TTF1 argue against metastatic GI and lung WDNETs, respectively. Additionally, NKX2.2, cannot be used to differentiate GI and renal WDNETs as it is diffusely immunoreactive in tumors both sites.

952 Adult Renal Cell Carcinoma in Female Patients

Claudia Ormenisan Gherasim[1], *Paola Dal Cin*[1], *Angelica Castillo*[1], *Michelle S Hirsch*[1]. [1]Brigham and Women's Hospital, Boston, MA

Background: Approximately 65,000 new kidney tumors are diagnoses annually, accounting for ~2.6% of all cancers. Kidney carcinomas represent the 6th most common tumor in men, versus the 8th most common tumor in women, and represent up to 3% of deaths. The majority (~85%) of tumors in the kidney are renal cell carcinomas (RCCs), which occur more frequently in men than women (M:F ratio 3:2). However, in the most recent 2016 WHO classification of renal tumors, new subtypes of RCC that occur more frequently in women have been described. This study evaluates the incidence of renal epithelial tumors (RET) in adult females in a single institution.

Design: A retrospective search over a 5 year period from 2010-2015 of all adult nephrectomy specimens for tumor at a single institution was performed; cases were non-selective and consecutive. Renal pelvis urothelial carcinomas, lymphomas, sarcomas, and metastases were excluded. Pathologic and genetic findings were reviewed.

Results: Overall, 974 RET were identified. 724 cases were in men and 250 cases were in women; the latter accounting 26% of cases. 18 cases were benign and 232 were malignant (ie, RCC). Size of the tumors ranged from 0.3 to 24 cm (mean 5.29 cm).The majority of cases were clear cell RCC (CCRCC) (N=159) followed by papillary RCC (PRCC) (N=24), accounting for 64% and 10% of cases. The remaining breakdown of subtypes is found in Table 1. Sarcomatoid and/or rhabdoid differentiation was present in 21/232 cases (9%). Stage breakdown was as follows: 87 pT1a, 59 pT1b, pT2a 17, pT2b 5, pT3a 50, pT3b 6, pT3c 2, pT4 6. Lymph node and distant metastases were present at nephrectomy in 15 (6.5%) and 11 (4.7%) cases, respectively, including 2 Xp11.2 RCCs and a FH-deficient RCC. Immunostains were performed in 53 cases (21.2%) and cytogenetics and/or FISH was attempted in 231 cases (92.4%). The latter yielded a result in 147 cases (63.6%). Tissue was sent for next generation sequencing in 104 cases (41.6%).

Table 1: Breakdown of RET Subtypes

	ChRCC	UN-CRCC	CCT-PRCC	XP11.2 RCC	CDCA	MTSCC	FHRCC	TCEB1 RCC	Be-nign RET
# of Cas-es	18	11	11	4	2	1	1	1	18
% of All Cas-es	7.2%	4.4%	4.4%	1.6%	<1%	<1%	<1%	<1%	7.2%

Conclusions: RET in females account for <1/3 of all cases in our institution. The incidence of RET subtypes in females is generally similar to that seen in men. However, the percent of CCRCCs might be slightly lower than previously reported as CCTPRCCs, Xp11.2 RCC and MTSCC are better recognized, and the latter two subtypes may occur more frequently in women than men. Further evaluations of the pathologic and molecular findings are currently in process.

953 Cytokeratin Staining in Yolk Sac Tumor: Back to Basics

Claudia Ormenisan Gherasim[1], *Sara Higgins*[1], *Michelle S Hirsch*[1] [1]Brigham and Women's Hospital, Boston, MA

Background: Adult mixed germ cell tumors (MGCTs) are comprised of varying amounts of embryonal carcinoma (EC), yolk sac tumor (YST), seminoma, choriocarcinoma and teratoma. There are many histologic patterns of YST and recognizing this component can be difficult in a subset of cases. In our experience, the diffuse embryoma pattern, where the YST 'hugs' the EC in a fashion that we refer to as "spooning", is frequently underrecognized. AFP and Glypican3 (Glyp3) are the 2 most frequently used biomarkers for YST; however, both have issues with sensitivity and specificity. The goal of this study was to reevaluate a panel of immunostains to determine the best approach for recognizing small amounts of YST.

Design: Orchiectomy specimens diagnosed with MGCTs were reviewed, and 11 cases that contained diffuse embryoma YST were chosen for evaluation. Immunostaining for AFP, Glyp3, AE1/AE3 (CK), GATA3, OCT3/4, EMA, inhibin, CDX2, CD30 and SOX2 was performed. Findings were scored as negative, focal or diffuse in the areas of YST. Attention was also given to staining in non-YST germ cell tumor components.

Results: The YST was strong and diffusely CK positive in all 11 cases. Glyp3 was positive in all YSTs, diffusely in 73% and focally in 27%. AFP was negative in 1 YST and positive in 10; diffusely in 3 cases (27%) and focally in 7 cases (64%). GATA3 was diffusely positive in 2 YSTs (18%) and focal in 7 (64%); 2 YSTs were negative for GATA3. YST was focally positive for CDX2 in most cases (75%); 1 was negative and 1 diffusely positive. OCT3/4, CD30, SOX2, EMA, and inhibin were negative in all evaluated cases. In contrast, EC was negative for CK in 9 cases, and showed focal weak staining in 2 cases. Trophoblast and teratoma also demonstrated some CK, but were morphologically distinguishable from the YST. In contrast to YST, GATA3 was strong and diffuse in all trophoblast, and the teratoma was positive for EMA in epithelial components. EC was positive for OCT3/4, CD30 and SOX2, and negative for Glyp3 and GATA3.

Conclusions: Specific morphologic features, including 'spooning', can be sufficient to distinguish YST from other germ cell components in many MGCTs. When immunostains are needed, CK AE1/AE3 remains the most sensitive and specific biomarker for distinguishing YST from EC. As CK can also stain teratoma and choriocarcinoma, one could consider Glyp3, followed by GATA3 or AFP as additional biomarkers in a subset of cases. However, one should be aware that some YSTs will be negative for these biomarkers.

954 Determination of Expression of PDL1 in the Morphologic Spectrum of Renal Cell Carcinoma. Its possible Role In New Modalities of Treatment

Sara M Gil[1], *Xu Naizhen*[2], *Ramaprasad Srinivasan*[3], *Marston Linehan*[3], *Maria J Merino*[4]. [1]NIH, Silver Spring, MD, [2]NIH, Bethesda, MD, [3]NIH, [4]NIH/NCI, Bethesda, MD

Background: Immunotherapy is a well-known form of therapy for advanced Cancers such as lung, melanoma and colon cancer. In Renal Cell Carcinomas (RCC), the role of Immunotherapy is being study and it might depend on the tumor expression of PD-L1. Programmed Death-Ligand 1 (PD-L1) is an antibody that is expressed on the surface of certain tumor types. It binds to the PD-1 protein on cytotoxic T-cells, which inhibits the antitumor immune response. Few studies have investigated PD-L1 expression in Kidney Cancer. The aim of this study is to evaluate PD-L1 expression in the morphologic spectrum of renal cell carcinomas, for its possible use in the treatment of kidney cancers.

Design: Ninety-seven cases of RCC composed of 14 Clear Cell, 9 Papillary type 1, 3 SDHB, 31 HLRCC, 12 Chromophobes, 7 Oncocytomas, 7 Hybrid tumors, 3 TFE3, 1 TFEB and 2 undifferentiated were studied using formalin-fixed, paraffin-embedded (FFPE) tissue. Sections of 4-mm thickness were stained for PD-L1 with rabbit anti–PD-L1 antibody; (Cell Signaling. Danvers, MA) and evaluated for membranous staining.

Results: 70% of the 97 samples were negative for PDL1 and 29% were positive. The majority of the positive cases were HLRCC (57.1%), followed by papillary type 1 (14.2%), TFE3 (7.14%) and Chromophobe (7.14%). Interestingly, the group of tumors corresponding to clear cell carcinoma, which in our study the majority was of hereditary VHL type was the least associated with positive staining for PDL-1.

Conclusions: Our study suggests that high grade aggressive forms of cancer such as HLRCC may be high expressers of PDL1, in contrast, VHL related clear cell carcinomas which did not express PDL1. It is possible that immunotherapy could be an excellent alternative for aggressive forms of kidney cancer.

955 Immunohistochemical Analysis of Primitive Neuroectodermal Tumors Arising in Germ Cell Neoplasms of the Testis Supports a "Central-Type PNET" Subclassification

Krzysztof Glomski[1], *Sara Higgins*[2], *Claudia Ormenisan Gherasim*[2], *Esther Oliva*[3], *Michelle S Hirsch*[2]. [1]Massachusetts General Hospital, Cambridge, MA, [2]Brigham and Women's Hospital, Boston, MA, [3]Massachusetts General Hospital, Boston, MA

Background: Primitive neuroectodermal tumors (PNETs) of the genitourinary tract are rare, but both peripheral-type (p) and central-type (c) PNETs have been described in men and women. Genital pPNETs are identical to Ewing sarcoma(ES)/PNET of other tissue sites with chromosome 22 (ch22) abnormalities, while cPNETs are distinct neoplasms that are associated with teratoma, lack ch22 changes and manifest neuronal, glial, or ependymal differentiation. In the testis, most PNETs are central type; however, diagnostic distinction between pPNET and cPNET is not typically made, and instead 'PNET' is a general term for all tumors with an expansile growth of undifferentiated small round blue cells. Recently, NKX2.2 was shown to be expressed in ES/

pPNET of soft tissues with high specificity and sensitivity. The goal of this study was to determine if NKX2.2 immunostaining could classify testicular PNETs into central or peripheral type.

Design: 7 malignant germ cell tumors with a component of PNET were identified: 6 testis tumors and 1 in a retroperitoneal lymph node dissection post-chemotherapy. Clinical and morphologic parameters were evaluated. Areas of "PNET" in all tumors were immunostained (IHC) for a variety of biomarkers, including, but not limited to NKX2.2, Synaptophysin, GFAP, S100, SALL4, Nestin, FLI1, and CD99.

Results: Average patients age was 36 years (range 22-55). Primary tumor size ranged from 1.6 to 11.3 cm (mean 7.1). 2 patients were pT1, 3 pT2 and 1 pT3. A teratoma component was present in all cases, and the amount of PNET ranged from 5% to 98% of the total tumors. 3 cases contained stratified columnar rosettes and 4 had small round blue cell morphology without further differentiation. By IHC, 6 PNETs were positive for Synaptophysin and 3 focally positive for GFAP. NKX2.2 was focally positive in 2 of 7 tumors. Areas of 'immature teratoma' were also negative for NKX2.2. Additional IHC results can be seen in Table I.

	NKX2.2 (N=7)	Synapto (N=7)	GFAP (N=7)	S100 (N=6)	Nestin (N=7)	FLI1 (N=5)	CD99 (N=5)	SALL4 (N=4)
# Diffusely Positive (%)	0 (0%)	2 (29%)	0 (0%)	0 (0%)	3 (43%)	3 (60%)	0 (0%)	3 (75%)
# Focally Positive (%)	2 (29%)	4 (57%)	3 (43%)	2 (33%)	3 (43%)	1 (20%)	2 (40%)	0 (0%)
# Negative (%)	5 (71%)	1 (14%)	4 (57%)	4 (67%)	1 (14%)	1 (20%)	3 (60%)	1 (25%)

Conclusions: All PNET of the testis in this study were associated with teratoma, as often seen in cPNETs of the ovary. Furthermore, NKX2.2 was predominantly negative in this cohort, a staining pattern more supportive of a cPNET phenotype. CD99 was not consistently expressed in our cohort, as previously reported in other studies of cPNET; however, GFAP and Nestin positivity support cPNET classification. The distinction between central- and peripheral-type PNETs of the testis should be considered, as this distinction may carry prognostic and therapeutic implications.

956 Programmed Death Ligand 1 Expression in Micropapillary Urothelial Carcinoma of the Bladder: Role for Immune Checkpoint Inhibitors

Abigail Goodman[1], *Adeboye O. Osunkoya*[1]. [1]Emory Univ/Medicine, Atlanta, GA

Background: There is now increasing evidence supporting the role of immune checkpoint inhibitors in the management of patients with malignant melanoma and other malignancies. Programmed Death Ligand-1 (PD-L1) plays a pivotal role in regulating host immune responses. However, PD-L1 expression in micropapillary urothelial carcinoma (UCa) has not been well characterized. In this study, we sought to analyze the expression of PD-L1 in a large cohort of patients with micropapillary UCa of the bladder.

Design: A search was performed through our Urologic Pathology files and expert consult files of the senior author for cases of micropapillary UCa of the bladder. Only cases with available tissue blocks were selected. Immunohistochemical stains for PD-L1 was performed on all cases. Cases were considered negative for PD-L1 when less than 1% of cells had positive expression.

Results: Thirty-six cases were identified. The mean patient age was 70 years (range: 39–87 years). There was a male predominance. The pathologic stages were as follows: 1 case of pTa, 8 cases of pT1, 8 cases of pT2, 13 cases of pT3a, 5 cases of pT3b, and 1 case of pT4a. Other pathologic parameters were as follows: 22/36 (61%) cases had angiolymphatic invasion, 16/36 (44%) cases had lymph node metastasis, and 10/16 (63%) of those had extra-nodal extension. Six of 36 (17%) cases had positive PD-L1expression in the tumor cells. One of the 6 (17%) cases with PD-L1 immunoreactivity was pT1 the other 5 (83%) cases with PD-L1 expression were categorized as pT3. Of these 5, 2 (40%) were pT3a and 3 (60%) were pT3b. PD-L1 expression was present in cases with and without angiolymphatic invasion and lymph node metastasis. Positive PD-L1 expression was also noted in a subset of patients who failed platinum based neoadjuvant chemotherapy.

Conclusions: This is one of the largest studies to date on the expression of PD-L1 in micropapillary UCa of the bladder. There is clearly a role for immune checkpoint inhibitors such as recently FDA approved anti- PD-L1 agent Atezolizumab in the management of a subset of patients with micropapillary UCa of the bladder. In addition, a subset of patients who have failed platinum based neoadjuvant chemotherapy for micropapillary UCa may also benefit from Atezolizumab or other similar agents.

957 Neuroendocrine Differentiation in the Setting of Prostate Cancer: Contemporary Assessment of 76 Consecutive Cases From a Single Institution

Anuradha Gopalan[1], *Hikmat Al-Ahmadie*[1], *Ying-Bei Chen*[1], *S. Joseph Sirintrapun*[2], *Satish Tickoo*[3], *Victor Reuter*[1], *Samson W Fine*[1]. [1]Memorial Sloan Kettering Cancer Center, New York, NY, [2]New York, NY, [3]Memorial Sloan Kettering CC, New York, NY

Background: There have been recent attempts to classify the morphology of neuroendocrine (NE) differentiation in prostate cancer (PCa) in light of increasing incidence of "NE"/aggressive PCa, especially in patients treated with potent next-generation anti-androgen therapy. Contemporary series with pathologic characterization and comprehensive clinical annotation are limited.

Design: We searched institutional databases (2012 to mid-2017) for in-house cases with history of PCa and evidence of NE differentiation at any time during the disease course. All available slides/charts were reviewed.

Results: 85 cases were initially identified; 9 were excluded based on insufficient evidence of either prostatic origin or NE differentiation; of the remaining 76 cases, 30 were primary to prostate and 46 were metastases. Locations of metastatic lesions included: liver [n=14], lymph node [n=9], bone [n=5], CNS [n=4], lung [n=3], other sites [n=11].

61/76 (80%) cases with morphologic NE differentiation by histology or immunohistochemistry (IHC) were identified post-therapy: 7 with radiation therapy (RT), 22 with hormonal/androgen–deprivation therapy (ADT) and 32 with both RT+ ADT. Of 54 patients who received ADT [either alone or in combination with RT]: 31 received Lupron/Casodex alone, 4 received abiraterone alone, 18 received a mix of conventional and next-generation ADT; in 1 patient exact ADT was unavailable.

Morphologic breakdown:

23 cases of pure high-grade NE carcinoma (HGNEC)/small cell carcinoma (SmCC): 3/23 primary, 20/23 metastatic.

10 cases of combined high-grade PCa and HGNEC/SmCC: 9/10 primary, 1/10 metastatic.

15 cases of PCa with diffuse NE differentiation, all in metastatic sites. These cases were characterized by sheet-like growth of cells with abundant cytoplasm and prominent nucleoli, yet diffuse positivity for at least one prostatic and one NE IHC marker.

11 cases of PCa with patchy NE differentiation, displaying more than single cell positivity for NE IHC marker(s): 5/11 primary, 6/11 metastatic.

6 cases of PCa with focal NE marker positive cells: 3/6 primary, 3/6 metastatic.

11 cases of PCa with Paneth cell-like change: all in primary disease; 9/11 post-therapy.

- The majority of NE differentiation in this contemporary series was seen after therapy.
- HGNEC/small cell carcinoma and PCa with diffuse NE differentiation are overwhelmingly seen in the metastatic setting.
- Combined high grade PCa+HGNEC and Paneth cell-like change are overwhelmingly seen in the localized setting.

958 Dual Staining of Karyopherin Alpha 2 and Cytokeratin 20 in the Evaluation of Urothelial Carcinoma in situ of the Bladder

Jennifer Gordetsky[1], *Maria Del Carmen Rodriguez Pena*[1], *Soroush Rais-Bahrami*[1], *George J Netto*[1], *Guru Sonpavde*[2], *Sooryanarayana Varambally*[1]. [1]The University of Alabama at Birmingham, Birmingham, AL, [2]Dana Farber Cancer Institute

Background: Urothelial carcinoma *in situ* (CIS) is a flat lesion that contains cytologically malignant cells. The diagnosis of CIS can be difficult, as reactive changes to the urothelium can cause significant cytologic atypia. We investigated the utility of dual KPNA2/CK20 immunohistochemical staining in the identification of urothelial CIS.

Design: A retrospective search was performed of our surgical pathology database identifying radical cystectomy/cystoprostatectomy specimens with CIS and dysplastic urothelium. Additionally, benign urothelium was identified in patients with no history of bladder cancer including, benign urothelium with minimal inflammation, benign urothelium with moderate/severe inflammation, and benign urothelium with radiation-induced cystitis. Dual immunohistochemical staining for KPNA2 and CK20 was evaluated for intensity and distribution in urothelial cells.

Results: We obtained 68 urothelial specimens (25 benign, 22 CIS, 21 dysplasia). In non-umbrella cells, KPNA2 showed no staining in 25/25

(100%) benign urothelial cases (minimal inflammation 7/25, 28%, moderate/severe inflammation 12/25, 48%, and radiation cystitis 6/25, 24%). KPNA2 showed weak staining of umbrella cells in 2/25 (8%) cases of benign urothelium. CK20 was positive in 9/25 (36%) benign cases, all of which showed strong, exclusive umbrella cell staining. KPNA2 was positive in non-umbrella cells in 22/22 (100%) cases of CIS and in 16/21 (76%) cases of urothelial dysplasia. CK20 was positive in non-umbrella cells in 17/22 (77%) cases of CIS and in 4/21 (19%) cases of urothelial dysplasia.

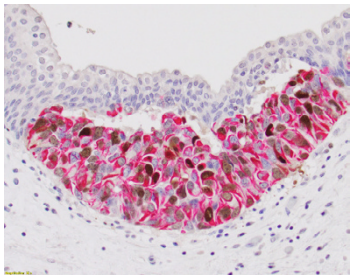

Conclusions: KPNA2/CK20 dual immunohistochemical staining is a novel combination marker for urothelial carcinoma *in situ* and may have a role in distinguishing reactive change from urothelial dysplasia.

959 What is the Best Method For Evaluating Gleason Score and Tumor Extent for MRI/US Fusion Targeted Biopsy?

Jennifer Gordetsky[1], *Luciana Schultz*[2], *Kristin Porter*[3], *Jeffrey Nix*[3], *Soroush Rais-Bahrami*[3]. [1]The University of Alabama at Birmingham, Birmingham, AL, [2]Instituto de Anatomia Patológica, AC Camargo Cancer Center, Santa Barbára D'Oeste, SP, [3]University of Alabama at Birmingham

Background: Multiparametric MRI/ultrasound targeted biopsy (TB) typically samples multiple cores from each MRI lesion of interest. Pathologists can evaluate the extent of cancer involvement and Gleason score using a per-core or aggregate method. These different methods could potentially lead to differences in percentage of cancer involvement and/or Gleason score. To see which method best corresponds with MRI and prostatectomy findings, we compared different methods of histologic evaluation of MRI/US TBs.

Design: We reviewed patients who underwent MRI/US TB and radical prostatectomy. TB cores were evaluated for prostate cancer Grade Group and percent tumor extension by two methods. Individual core method (IC): Grade Group for each TB was based on the core with the highest score. Tumor extension for each TB was determined by the core with the highest extent of tumor. Aggregate cores method (AG): Tumor from all cores was aggregated as a part of the final Grade Group and percentage of tumor involvement. Each method was compared to MRI lesional volume, MRI lesional density (lesion volume/prostate volume), and findings on radical prostatectomy.

Results: We identified 47/544 patients who underwent MRI/US TB followed by prostatectomy. The average age and PSA was 64 years and 10.7 ng/ml, respectively. Patients had an average of 2.2 MRI lesions and 4.8 TB cores. The maximum extent of cancer reported by each method changed in 43/63 (68.3%) lesions. Extent of tumor measured by the AG method showed significant correlation with MRI target lesion volume (p=0.04) and cancer proven lesional density (p=0.03), while the IC method was not significant. Extent of tumor on TB was associated with extraprostatic extension (EPE) on prostatectomy by the AG method (p=0.04), but not by the IC method. This performance was particularly better in the subgroup of patients with Grade Group ≤3 (p=0.008). When applying a cut-off of 50% core involvement, there was a disagreement in 12/47 (25.5%) patients, who had >50% tumor extent by the IC method and <50% by the AG method. Of these, 3/12 showed EPE on prostatectomy, rendering the AG method a better predictor of EPE (p=0.017, AUC<0.48). A change in Grade Group occurred in only 2 patients when comparing methods (both downgraded from Grade Group 3 to Grade group 2 by the AG method).

Conclusions: For multiple cores obtained via a MRI/US TB, an aggregate method for tissue evaluation better correlates with target lesion volume, cancer proven lesional density, and EPE on prostatectomy.

960 Progression to Sarcomatoid Bladder Cancer is Associated with Dysregulation of Chromatin Remodeling and Cell Cycle Circuits

Charles Guo[1], *Tadeusz Majewski*[2], *Li Zhang*[3], *Jolanta Bondaruk*[1], *Ashish Kamat*[4], *Colin Dinney*[4], *David McConkey*[5], *Bogdan Czerniak*[6]. [1]UT-MD Anderson Cancer Center, Houston, TX, [2]M. D. Anderson Cancer Center, Houston, TX, [3]University of Cincinnati, Cincinnati, OH, [4]The University of Texas MD Anderson Cancer Center, [5]Johns Hopkins University, [6]UT MD Anderson Cancer Ctr, Houston, TX

Background: The progression of conventional bladder cancer to sarcomatoid carcinoma (SARC) is associated with a mesenchymal phenotypic change and enhanced clinical aggressiveness. We aimed to analyze the expression profile of SARC and define the features contributing to clinical behavior.

Design: We analyzed the expression profiles of RNA extracted from paraffin embedded tumor tissue of 28 patients with bladder SARC and a reference set of 89 conventional urothelial carcinomas (UC) using Illumina HT-12v4 DASL chips. The genome expression profiles and pathway analyses were performed and related to clinical and pathological data.

Results: We showed that SARC was characterized by the genome-wide dysregulation of the expression pattern affecting more than 6000 genes. Among the top upregulated genes were FAM101B, UHRF1, and PHC2, all of which were members of a chromatin remodeling super family. SARC was also characterized by upregulation of multiple oncogenic pathways including RhoA, cell cycle, molecular mechanisms of cancer, and CBX5 targets. Consistent with their epithelial to mesenchymal transition (EMT) SARC demonstrated a striking loss of genes associated with epithelial/urothelial differentiation and the activation of EMT genes including SNAIL, TWIST, and ZEB. Only a small subset of SARC (n=12) expressed basal markers, and the majority (n=16) did not express either luminal or basal markers (double-negative). Patients with SARC had a poorer median survival than those with conventional UC (11 months vs.24 months), and double-negative SARC was associated with a poorer prognosis than basal SARC (10 months vs. 18 months). A subset of predominantly double negative SARC were characterized by overexpression of immune signature genes including those involved in immune checkpoint blockade suggesting that they may respond to immunotherapy.

Conclusions: Progression to SARC is associated with widespread dysregulation of chromatin remodeling and cell cycle circuits. SARCs, which are purely mesenchymal, represent the most aggressive variant of the disease.

961 Clear Cell Renal Cell Carcinomas with PDGFRA/KIT (4q12) Co-amplification and PDGFRB (5q32) Amplification

Sounak Gupta[1], *Shabnam Zarei*[2], *William R Sukov*[2]. [1]Memorial Sloan Kettering Cancer Center, New York, NY, [2]Mayo Clinic, Rochester, MN

Background: Chromosome 5q gains are common in clear cell renal cell carcinoma (CC-RCC), and have been reported in 15-69% of cases. As few studies have sought to identify key oncogenic drivers on 5q, we analyzed the 5q31-5q35.3 amplicon. *PDGFRB emerged as* a candidate targetable oncogene. Herein, we have studied amplifications (Amp) of *PDGFRB* (5q32) and its heterodimerization partner *PDGFRA* (4q12) in CC-RCC.

Design: The cBioPortal platform was used to analyze TCGA data for 537 CC-RCC. Copy number (CN) status of *PDGFRB* was analyzed by FISH in 151 institutional cases of CC-RCC, and SNP genomic microarray was performed in a subset of cases.

Results: Analysis of the 5q31-5q35.3 amplicon in the TCGA CC-RCC cohort for candidate oncogenes (*FLT4, MAPK9, SQSTM1, MAML1, FGFR4, NPM1, ITK, PDGFRB, CSF1R*), for CN changes and mRNA expression, revealed 85 (of 537, 16%) cases with 5q31-5q35.3 Amp. *PDGFRB* Amp was identified in 74 (of 537, 14%) cases. Common *PDGFRB* Amp-associated CN alterations included losses of chromosome 3p (70 of 74, 95%) and 14q (29 of 74, 39%).

The mean age at diagnosis for TCGA CC-RCC patients was 59 years, 24 (of 74, 32%) cases were =>pT3, 26 (of 74, 35%) had documented metastasis, and 15 (of 74, 20%) patients died of disease over a mean follow up of 43 months. FISH analysis of a validation cohort revealed Amp/high level polysomy (5-10 copies/nucleus) in 17 (of 151, 11%) cases of CC-RCC. In this cohort, the mean age at diagnosis was 68 years, 7 (of 16, 44%) cases were =>pT3, 4 (of 16, 25%) had documented metastasis at diagnosis or follow up, and 5 (of 14, 36%) patients died of disease over a mean follow up of 104 months.

PDGFRA Amp was identified in 3 (of 537, 0.6%) CC-RCC in the TCGA cohort. A single case had a *PDGFRA/KIT* (4q12) co-Amp, with mRNA expression =>94th percentile of all cases. A second case of *PDGFRA/KIT* co-Amp was identified by SNP genomic microarray, which was performed on a subset of CC-RCC, and showed a >16fold CN change. Both cases were =>pT3, showed sarcomatoid change, with one case invading beyond Gerota's fascia (pT4). The latter patient had disease progression at 6 months and died of disease related complications at 10 months of follow up.

Conclusions: Our study highlights the importance of global chromosomal copy number analysis for advanced stage CC-RCC to identify cases with *PDGFRA/KIT* and *PDGFRB* Amp, a subset of which behave aggressively. Further studies are needed to define clinical outcomes and response to targeted therapy in these molecular subtypes of CC-RCC.

962 Invasive High Grade Urothelial Carcinoma Arising in a Background of Urothelial Carcinoma with an Inverted Growth Pattern: A Contemporary Clinicopathologic Analysis of 65 Cases

Christina M Gutierrez[1], *Adeboye O. Osunkoya*[2]. [1]Emory University, Atlanta, GA, [2]Emory Univ/Medicine, Atlanta, GA

Background: Urothelial carcinoma (UCa) associated with an inverted/endophytic growth pattern can occasionally mimic inverted papilloma and may also pose diagnostic challenges when being evaluated for invasion. Making these distinctions are important for timely and appropriate treatment to improve patient survival and outcomes. Only a few studies have analyzed the clinicopathologic features of invasive high grade UCa arising in a background of UCa with an inverted growth pattern.

Design: A search was made through our urologic pathology files and consult cases of the senior author for cases of invasive high grade UCa arising in a background of UCa with an inverted growth pattern. Clinicopathologic parameters including extent of invasion, variant histology, presence of UCa in situ, and follow-up information was obtained.

Results: Sixty-five cases were included in the study. The mean patient age was 69 years (range: 38-95 years) and 52/65 (80%) patients were male. Fifty one of the 65 (78%) cases invaded the lamina propria, 14/65 (22%) cases invaded the muscularis propria (detrusor muscle). Adjacent UCa in situ was present in 25/65 (38%) cases. Variable patterns of invasion were present, and in some cases within the same tumor. In addition, micropapillary urothelial carcinoma was present in 5/65 (8%) cases. Clinical follow-up was available in 55/65 (85%) patients with a mean duration of 17 months (range: 0.5-60 months). Eight of 14 (57%) patients with muscularis propria (detrusor muscle) invasion had subsequent radical cystoprostatectomy or cystectomy. Forty-two of 55 (76%) patients developed recurrent UCa, 5/55 (9%) progressed with metastatic disease, and 10/55 (18%) patients subsequently died of disease.

Conclusions: This is the largest study to date of invasive high grade UCa arising in a background of UCa with an inverted growth pattern. This study further emphasizes the fact that it is very important to distinguish these tumors from benign mimickers of UCa. Recognition of invasive foci is also critical in view of the potentially high frequency of recurrence, and the possibility of advanced disease in a subset of these patients.

963 Correlation of Invasive Front Inflammation, PD-L1 Expression and Immunohistochemical Subtype In High Grade Urothelial Carcinoma of Bladder

Elan Hahn[1], *Anjelica J Hodgson*[2], *Bin Xu*[3], *Michelle Downes*[4]. [1]Laboratory Medicine and Pathobiology, University of Toronto, Toronto, ON, Canada; Sunnybrook Health Sciences Centre, Toronto, ON, Canada, [2]The University of Toronto, Toronto, ON, [3]Sunnybrook Health Sciences Centre - University of Toronto, Toronto, ON, [4]Sunnybrook Health Sciences Centre, Toronto, ON

Background: Characterization of the immune microenvironment is increasingly important as our understanding of the tumour immune milieu advances. Invasive front inflammation is prognostically significant in high grade urothelial carcinoma of bladder (HGUC) and PD-L1 (programmed cell death ligand 1), an immune inhibitory ligand, is a predictive biomarker in several malignancies. In a parallel fashion, our knowledge of molecular subtyping of urothelial carcinoma has advanced, and it has been shown that muscle-invasive bladder cancers can be immunohistochemically classified into luminal and basal molecular subgroups. Both chemotherapy sensitivity and prognosis may vary between these groups. With this in mind, we sought to evaluate invasive front inflammation, immunohistochemical subtype, and PD-L1 expression in a cohort of HGUC.

Design: 235 cases of HGUC treated by cystectomy were retrospectively identified and reviewed. Pathologic variables were recorded and disease free survival was calculated. Invasive front inflammation was scored for each case (high/low). 207 cases were used to construct a triplicate core tissue microarray (TMA). TMA sections were sequentially stained with CK5/6 and GATA-3 and classified as luminal, basal or double negative phenotype. Additional TMA sections were stained with SP263 and SP142 PD-L1 antibodies, and were subsequently scored as positive/negative using recommended cut offs. Statistical analysis of oncologic outcome, invasive front inflammation, tumour subtype, and PD-L1 expression was performed.

Results: 36.6% of cases had high invasive front inflammation. The cases were immunohistochemically classified as: luminal – 82% (n = 167), basal – 14% (n = 29), and double negative – 4% (n = 9). PD-L1 positivity was seen in 21% (n = 43) and 9% (n = 18) using SP263 and SP142 respectively. PD-L1 positivity strongly associated with high invasive front inflammation (p = 0.003 [SP263] and < 0.001 [SP142]) and basal subtype (p = 0.004, SP263 and 0.038, SP142). There was a trend between basal subtype and high invasive front inflammation (p = 0.093). Oncologic outcome was not associated with PD-L1 status (p>0.0.5) with a trend towards worse outcome in basal subtype (p=0.078).

Conclusions: PD-L1 expression was identified in a subset of HGUC and was significantly associated with both high invasive front inflammation and basal subtype. Our findings suggest that PD-L1 therapy could be used neoadjuvantly in basal subtype HGUC.

964 The Tumor-Immune Microenvironment and PD-L1 Expression in Acinar Prostatic Adenocarcinoma

Elan Hahn[1], *Bin Xu*[2], *Stanley K Liu*[3], *Danny Vesprini*[4], *Michelle Downes*[5]. [1]Laboratory Medicine and Pathobiology, University of Toronto, Toronto, ON, Canada; Sunnybrook Health Sciences Centre, Toronto, ON, Canada, [2]Sunnybrook Health Sciences Centre - University of Toronto, Toronto, ON, [3]Sunnybrook Health Sciences Centre, [4]Sunnybrook Health Sciences Centre, Toronto, ON, Canada; University of Toronto, Toronto, ON, Canada, [5]Sunnybrook Health Sciences Centre, Toronto, ON

Background: Tumor-induced immunosuppression plays a role in the development and progression of cancer. Of interest is the interaction between PD-1 and PD-L1 which can be targeted through immune checkpoint blockade, however there is limited data surrounding the composition of the immune milieu in prostate cancer. The objective of this study was to characterize the immune cell infiltrate in acinar prostate cancer, and to examine the relationship between immune cell composition and tumor grade group (GG) and stage.

Design: 21 therapy naïve radical prostatectomy cases were reviewed and the Gleason score, GG and stage were confirmed. A representative slide of the dominant nodule was selected and manually assessed for tumor-infiltrating lymphocytes (TIL) over 20 high-power fields (hpf). Sequential slides were stained for CD3, CD8, FOXP3, CD20, CD68, CD163, CD4, CD45, PD-1, and PD-L1 (SP263). Manual counting was performed in 20 hpf and averaged for each case. PD-L1 was assessed in tumor and lymphocytes with a 5% cut-off applied. Cases were divided into > or ≤ GG2 and > or ≤ pT2. Statistical analysis was performed using Student's two-tailed t test.

Results: 14 cases were ≤ GG2 and 11 ≤ pT2. Marked heterogeneity in lymphocyte composition was noted across cases. No significant difference in TIL count or lymphocyte markers was observed between groups. 5/21 cases were PD-L1 high (1 in tumor cells, 4 in immune cells, 24%). The overall mean CD4 counts were higher than the CD8 counts (20 vs 13), ratio= 1.54. In cases > GG2 and > pT2 a similar level of CD68 and CD163 expression was noted, in comparison to ≤ GG2 and ≤ pT2 where the CD163 was elevated compared with CD68. A statistically significant difference was seen in CD68 expression across GG (p=0.044) with a trend towards significance in stage (p=0.072).

Conclusions: The immune infiltrate in acinar prostate cancer is heterogeneous from case to case and is not significantly associated with GG or stage. PD-L1 was positive in a quarter of cases. CD4 expression is higher than CD8. The lower GG and stage cases showed a predominant M2 macrophage phenotype, whereas the higher GG and stage cohort showed increased, though similar, mean CD68 and CD163 expression. These findings suggest a pro-inflammatory or "cold" immunophenotype with increased activity of the alternative pathway of macrophage activation.

965 Variants and Concomitant Tumor Morphologies Associated with Gene Expression Subtypes of Bladder Cancer (BC) in Radical Cystectomy (RC) Specimens

Lisa Han[1], *Randy F Sweis*[1], *Gary D Steinberg*[1], *Gladell P Paner*[1]. [1]University of Chicago, Chicago, IL

Background: Luminal (LS), basal (BS), and claudin-low (CLS) molecular subtypes of bladder cancer have been previously characterized using a gene expression signature (BASE47) (Damrauer et al. 2014). However, detailed histomorphologic characterization of these different molecular subtypes remains incomplete and most previous analyses were performed on limited tumor samples only. To our knowledge, detailed histologic analysis of RC in its entirety, including bladder mucosa away from main tumor and LN metastasis has not been done. RC specimens from a single institution were retrieved and a comprehensive morphologic analysis was performed.

Design: 48 invasive BCs (≥T2) from a single institution were classified as LS (n=14), non-luminal (BS [n=18], and CLS [n=16]) subtypes by a gene set predictor (BASE47) defined by prediction analysis of microarrays. CLS is considered a subtype of BS. The RC specimens including LN dissection of these BC were retrieved and the histopathological findings of the main tumor (2016 WHO), other bladder regions and LN metastases were reviewed by one of the authors blinded to the molecular subtypes.

Results: Pure and mixed variants morphology of any amount are identified in 34 (71%) of specimens. Squamous differentiation is more common in non-luminal (BS/CLS) vs. LS (47% vs. 29%) and more

pronounced (squamous >30% in 47% vs. 7%, p=0.040). Sarcomatoid change is identified exclusively in non-luminal subtypes (24%). Micropapillary is identified in LS (2) and BS (4) with concomitant sarcomatoid only in BS (2). Other variants included small cell carcinoma (1, LS), glandular (1, CLS), osteoclast-like (1, BS), lymphoepithelioma-like (1, CLS), lipoid (2, BS), clear cell (1, L). Distinct foci of markedly pleomorphic cells (with/without giant, bizarre, or multinucleated cells) were more common in non-luminal than LS (7% vs. 62%, p<0.001). Invasive tumor was multifocal in LS (21%), BS (13%) and CLS (38%). Concomitant CIS away from the main tumor was identified in LS (36%), BS (44%) and CLS (38%). Marked pleomorphism in CIS was not identified in LS, but found in BS (4/8) and CLS (3/7). Lymph node metastasis was present in LS (57%), BS (44%) and CLS (12.5%), and the histology corresponded to the primary tumor including variants morphologies.

Conclusions: This study identifies new morphologic correlates of molecular subtypes of BC. Non-luminal BC is associated with squamous morphology, sarcomatoid change, and marked cellular pleomorphism including in CIS away from the main tumor.

966 MRI/Ultrasound Fusion-guided Biopsy Helps Improve the Accuracy of Tumor Grading in Prostate Cancer

Yansheng Hao[1], *Kenneth Haines*[2], *Qiusheng Si*[2]. [1]The Mount Sinai Hospital, New York, NY, [2]The Mount Sinai Hospital

Background: Targeted magnetic resonance (MRI)/ultrasound fusion biopsy has been broadly used together with standard (12-core) biopsy for prostate cancer screening in the past few years. However, the efficacy of MRI/ultrasound fusion compared to standard biopsy has only been assessed by limited studies, which is further investigated in this study.

Design: Retrospective data from 400 consecutive cases with simultaneous targeted and standard prostate biopsies, performed at a single institution, between January 01, 2014 and May 30, 2017 was collected. Information from the subsequent radical prostatectomy, if performed, was also collected.

Results: The average patient age was 64.5 years (r=37-86) and average PSA was 7.83 ng/mL (r=0.4-145 ng/mL). Prostatic adenocarcinoma was identified in the targeted biopsy in 222 cases (55.5%) and in the standard biopsy in 250 cases (62.5%) cases. There was exact diagnostic agreement on the absence of cancer, and if cancer was present, the Gleason Prognostic Grade Group, between the two groups in 259 of the 400 cases (64.8%). Within the 150 negative results by standard biopsy, targeted biopsy detected 22 tumors (14.7%). Compared to grade group detected by standard biopsy, targeted biopsy upgraded to higher grade levels (Grade 1: 20.2%, Grade 2: 11.4%, Grade 3: 14.7%). This effect of targeted biopsy was significantly different in 212 first biopsy cases (new tumor 7.8%, Grade 1: 20.75%, Grade 2: 10.9%, Grade 3: 15%) and 121 cases with prior negative history (new tumor 20%, Grade 1: 22.58%, Grade 2: 16.7%, Grade 3: 25%) (p=0.048). The agreement with the final grading (from 108 patients who underwent prostatectomy) was 55 (50.9%) and 52 (48.1%) in targeted and standard biopsies respectively, whereas it was 74 (68.5%) with combination of 2 types of biopsies. The targeted and standard biopsies had comparable efficacies in detecting longest focuses of tumor. The longest focuses detected by either types of biopsies were closely correlated to the involvement percentage of whole prostate (targeted: r=0.369, p=0.006; standard: r=0.536, p<0.0001).

All cases		Upgrading by Targeted biopsy			
		First biopsy	Previous negatvie biopsy	Previous positive biopsy	
Stan-dard biopsy	Negative	14.7%	7.8%	20.0%	25.0%
	Grade 1	20.2%	20.8%	22.6%	16.7%
	Grade 2	11.4%	10.9%	16.7%	8.3%
	Grade 3	14.7%	15.0%	25.0%	0.0%
	Grade 4	0.0%	0.0%	0.0%	0.0%
	Grade 5	0.0%	0.0%	0.0%	0.0%

Conclusions: Combined with standard biopsy, targeted biopsy helps to detect new tumors and achieve more accurate tumor grade. This effect of targeted biopsy is significantly affected by the history of prior biopsies. The targeted and standard biopsies have comparable efficacies in detecting longest focuses of tumor, which are closely correlated with the involvement percentage in the whole prostate.

967 Urothelial Carcinoma Variants: Comparison of PELP1 and GATA3 Immunostains

Lakshmi Harinath[1], *Shweta Patel*[2], *Edward Lynch*[3], *Jan F Silverman*[4]. [1]Allegheny General Hospital, Pittsburgh, PA, [2]Allegheny Health Network, Pittsburgh, PA, [3]Allegheny General Hospital, [4]Allegheny General Hospital, Allegheny Health Network, Pittsburgh, PA

Background: Urothelial carcinomas (UC) can have a broad range of morphologic appearance and immunohistochemistry (IHC) is frequently used in order to make an accurate diagnosis. GATA 3 is a zinc finger transcription factor that is a useful marker in urothelial as well as breast carcinomas. PELP1 is a novel nuclear hormone coregulator that is associated with development of breast carcinoma. Recent studies have identified PELP1 as a more sensitive marker than GATA3 for triple negative breast carcinomas, while PELP1 was found to have a higher frequency of expression and a stronger staining intensity as compared to GATA3. The staining patterns of PELP1 and GATA3 have not been evaluated in UC variants.

Design: We examined 20 cases of previously diagnosed invasive UC variants (5 micropapillary, 4 glandular, 2 squamous, 2 sarcomatoid, 2 clear cell, 1 signet ring, 1 plasmacytoid, 1 squamous and sarcomatoid, 1 glandular and squamous, 1 micropapillary and squamous) in biopsy and cystoprostatectomy specimens. We stained all of the slides with GATA3 and PELP 1 antibody and graded the intensity of staining and the percentage of tumor cells expressing these proteins. The staining intensity was graded from weak (1+) to strong (3+). The percentage of cells that expressed these antibodies was rated as less than 25%, 25-50%, 50-75% and above 75%.

Results: We found that in 14 (70%) of cases, GATA 3 and PELP1 protein expression were concordant in different histologic variants. In 5 (25%) cases, PELP1 stained more diffusely as compared to GATA3, although the staining intensity appeared to be less than GATA3 due to the characteristic delicate nuclear staining pattern. In 1 (5%) case of micropapillary variant, GATA3 showed a stronger intensity and stained an increased number of tumor cells.

Conclusions: We believe that this is the first study comparing PELP1 and GATA3 staining in UC variants. PELP1 and GATA3 have equivalent staining in most of the histologic variants of UC. However, a potential advantage of PELP1 antibody is the more positive diffuse staining as compared to GATA3 in a small percentage of our cases. Since heterogeneity of GATA3 staining could be source for a false negative staining, we believe that adding PELP1 antibody in the work up of metastatic UC variants can be of value.

968 Clinical Significance of Urothelial Carcinoma Ambiguous for Muscularis Propria Invasion on Initial Transurethral Resection of Bladder Tumor

Oudai Hassan[1], *Fatima G Cuello*[2], *Alexander S Marwaha*[3], *Andres Matoso*[4]. [1]Bloomfield Hills, MI, [2]The Johns Hopkins Hospital, Baltimore, MD, [3]The Johns Hopkins Hospital, Baltimore, MD, [4]Johns Hopkins Hospital, Baltimore, MD

Background: Urothelial carcinoma (UCa) with muscularis propria (MP) invasion has a much worse prognosis than those with only invasion of the lamina propria (LP). In a subset of cases, the initial transurethral resection of a bladder tumor (TURBT) is ambiguous for MP invasion (AMP). These patients usually undergo a repeat TURBT in an attempt to definitively classify the depth of invasion. The clinical significance of a diagnosis on AMP in the initial TURBT has not been studied before.

Design: The cohort included all in-house consequtive cases of invasive urothelial carcinoma on initial TURBT between 1999-2017 that underwent radical cystectomy (RC). The cases were grouped based on the depth of invasion in the initial TURBT as follows: invasion of the LP (INLP), invasion of MP (INMP) and ambiguous for MP invasion (AMP). AMP was defined as tumor with extensive invasion displaying thin muscle bundles where it is difficult to determine with certainty if those muscle bundles represent muscularis mucosae or MP. Pathological stage at RC and survivial were recorded. Cases with any amount of small cell carcinoma were excluded.

Results: The average age at diagnosis was 65 years old in INLP (n=127; 30%), 68 in INMP (n=267; 62%), and 66 in AMP (n=34; 8%). RC showed tumor involving MP in 25/127 (19.5%) of INLAM in the initial TURBT vs. 58/267 (21.2%) of INMP (P=0.7), and 13/34 (37.7%) of AMP (P=0.04). Perivesical invasion was present in 34/127 (26.8%) of INLP in the initial TURBT, vs. 128/267 (47.8%) in INMP (P<0.001), and 12/34 (35.3%) in AMP (P=0.4). Invasion of pelvic organs was present in 11/127 (8.7%) of INLP in the initial TURBT vs. 43/267 (16%) in INMUS (P=0.06), and 3/34 (8.9%) in AMP (P=0.8). Lymph nodes were positive in 29/123 (24%) of INLP, vs. 85/245 (37%) of INMP (P=0.04), and 6/28 (21%) in AMP(P=1). The average followup was 38 months (range 0-144). 18/127 (14%) of INLP patients died of disease, vs. 110/267 (41%) of INMP (P<0.001), vs. 6/34 (18%) on AMP (P=0.8).

Conclusions: The majority of patients with AMP on intial TURBT have pT2 or above disease at RC (28/34; 82%), but less extravesical extension, invasion of pelvic organs, positive lymph nodes or disase

specific mortality than those with INMP.

969 The Clinical Significance of a Small Component of Choriocarcinoma in Testicular Mixed Germ Cell Tumor (MGCT)

Oudai Hassan[1], *Aline C Tregnago*[2], *Jonathan Epstein*[2]. [1]Bloomfield Hills, MI, [2]The Johns Hopkins Med Inst, Baltimore, MD

Background: The 2016 *WHO Classification of Tumours of the Urinary System and Male Genital Organ* states: Choriocarcinoma is the most aggressive form of germ cell tumor, with a proclivity for early hematogenous spread and high stage at presentation, yet the significance of limited choriocarcinoma in a MGCT is unknown.

Design: MGCT with ≤5% choriocarcinoma at radical orchiectomy (RO) (2000-2016) from our consult service were studied.

Results: Clinicopathologic information was available for 30 men. Median follow up was 41 mos. (1-168 mos.). Median tumor size was 4.5 cm. (1.1-8.0 cm.). 22/30(73%) cases were pT1, 6/30(20%) cases pT2, and 2/30(7%) cases pT3. 4/30(13%) cases had lymph node metastases and 2/30(7%) cases had distant metastases at the time of RO. In 28 cases with RO we had information on immediate adjuvant treatment: 12/28(43%) active surveillance, 4/28(14%) retroperitoneal lymph node dissection (RPLND), 9/28(32%) chemotherapy (Chemo), 2/28(7%) RPLND followed by Chemo, and 1/28(4%) resection of a distant metastasis. Pre-operative serum hCG levels ranged between 0.1-60,715 MIU/ml (median: 485). The TNM staging system stratifies hCG into 3 levels: <5000 MIU/ml; 5,000-50,000; and >50,000. One patient had an hCG level of 6,367 MIU/ml and another 60,715 MIU/ml with remaining cases <5000 MIU/ml. The patient with >60,000 serum hCG had pT3N2M1b disease. 4/30(13%) patients had elevated serum markers after surgery, 3 of them normalized following Chemo while the fourth one continued to have elevated serum AFP levels after Chemo. All patients were alive at last follow up. 7/31(22.6%) patients subsequently developed metastatic disease to lymph nodes or distal organs, with the metastases consisting mainly of teratoma and yolk sac tumor. Embryonal carcinoma was present in two metastatic sites. One lung metastasis was suggestive for choriocarcinoma. Definitive choriocarcinoma was not present in any of the metastasis, although 2 men with metastases at presentation (including case with preoperative >60,000 serum hCG) were treated with Chemo without sampling the metastases.

Conclusions: A small component of choriocarcinoma in a MGCT is typically associated with relatively low level elevations of serum hCG levels, and is not associated with aggressive disease. Our findings support the TNM staging system which uses levels of serum markers (hCG, AFP, LDH) as surrogates for extent of disease along with pathological stage rather than the histologic subtype of MGCT for staging prognostic purposes.

970 SPOP mRNA Downregulation Is Associated with the Presence of TMPRSS2-ERG Fusion and PTEN Loss in Prostate Cancer

Silvia Hernández-Llodrà[1], *Laura Segalés Tañà*[2], *Nuria Juanpere*[3], *Marta Lorenzo*[4], *Raquel Albero*[5], *Lluís Fumadó*[4], *Lluís Cecchini*[4], *Belen Lloveras*[6], *Josep Lloreta*[4]. [1]Pompeu Fabra University, [2]Universitat Pompeu Fabra, Barcelona, Catalunya, [3]Hospital del Mar-Parc de Salut Mar, Barcelona, Spain, [4]Hospital del Mar-Parc de Salut Mar-IMIM, [5]Hospital del Mar-Parc de Salut Mar-IMIM, Barcelona, Spain, [6]Hospital del Mar, Barcelona

Background: *ERG* rearrangements and loss of *PTEN* are frequent and concomitant events in prostate cancer (PrCa) that cooperate in progression. The E3 ubiquitin ligase adaptor speckle-type POZ protein (SPOP) targets ERG protein for ubiquitin-proteasome degradation. SPOP is frequently dysregulated in PrCa, via either somatic mutations or mRNA downregulation, suggesting an important tumor suppressor function. Moreover, *SPOP* mutations are associated with an increase in ERG protein levels, but these mutations appear to be mutually exclusive with *ERG* rearrangements in a subset of PrCa. The objective of this study is to analyze the prevalence of *SPOP* alterations in PrCa and to determine the relationship between *SPOP* status, *ERG* rearrangement and *PTEN* loss with the different clinical and pathological variables of prostate cancer.

Design: *SPOP*, *TMPRSS2-ERG* rearrangement and *ERG* mRNA expression were analyzed by RT-qPCR in 82 PrCa tumors, and *PTEN* in 73 tumors of the same series (Parc de Salut MAR-Biobank, Barcelona, Spain). *GADPH* was used as internal control and 3 benign frozen prostate samples were used to normalize the thresholds of *SPOP*, *TMPRSS2-ERG* rearrangement and *ERG* (ΔΔCt). In addition, *SPOP* mutational analysis was also performed by direct sequencing in all samples.

Results: *TMPRSS2-ERG* rearrangement was detected in 59,8%, *ERG* overexpression in 58.5%, *PTEN* loss in 39.7% and *SPOP* expression loss in 26.8% tumors. *SPOP* mutations were found in 5 PrCa (6.1%) and were mutually exclusive with *TMPRSS2-ERG* (p=0,0087). Conversely, about 82% of tumors with loss of *SPOP* expression harbored a *TMPRSS2-ERG* rearrangement (p=0.0136) and a 77.3% overexpressed *ERG* (p= 0.0370). In addition, 75% of tumors with *SPOP* downregulation showed also *PTEN* expression loss (p=0.00015), and 65% showed the *ERG*-overexpression/*PTEN*-loss combination (p=0.0012). *SPOP* alterations (mutation plus expression loss), were more frequent in GG5 (55.5%) than in GG1 to 4 (26.3% to 31.3%) but without statistical significance. ERG+/PTENwt/SPOPwt phenotype was found in 43% of GG1 and in 18.6% of GG2-5 tumors (p=0.077).

Conclusions: *SPOP* mutations are mutually exclusive with *TMPRSS2-ERG* rearrangement. However, loss of *SPOP* expression is associated with *TMPRSS2-ERG*, with *ERG* overexpression and with the *ERG*-overexpression/*PTEN*-loss phenotype. Although *SPOP* mutations may represent an alternative, *ERG-wt* pathway, loss of *SPOP* expression is actually associated with *ERG* fusion and *PTEN* loss in prostate tumors. (FIS/CarlosIII/FEDER/PI15/00452).

971 Basal Subtype Bladder Tumours Demonstrate a "Hot" Immunophenotype

Anjelica J Hodgson[1], *Bin Xu*[2], *Michelle Downes*[3]. [1]The University of Toronto, Toronto, ON, [2]Sunnybrook Health Sciences Centre - University of Toronto, Toronto, ON, [3]Sunnybrook Health Sciences Centre, Toronto, ON

Background: The immune response is recognized as an important predictive and prognostic parameter in multiple solid organ malignancies however, its role and significance in high grade urothelial carcinoma of the bladder (HGUC) is yet to be fully elucidated. In this study, we aimed to immunophenotypically profile the inflammatory milieu of a cohort of HGUC, and to correlate these findings with molecular subtype.

Design: 235 cases of HGUC treated by cystectomy were retrospectively identified and reviewed. Clinical and pathologic variables were recorded. 207 cases were used to construct a triplicate core tissue microarray (TMA). Haemotoxylin and eosin stained sections were used to classify tumour infiltrating lymphocytes (TILs) as encompassing < 5% of the tumour area (low) or > 5% of the tumour area (high). Tumour sections were stained for CK5/6 and GATA3 to classify cases as luminal or basal subtype. Further sequential sections were stained for CD20, CD3, CD4, CD8, FOXP3, PD-1 and PD-L1 (SP142 and SP263). Immune cell staining was assessed as hotspot counts (1 representative 40x field/core with results averaged across all cores). PD-L1 staining was scored as positive or negative using recommended cut offs for each antibody. Statistical analysis was performed using Students two tailed t test.

Results: 194 cases were evaluable for subtyping by immunohistochemistry, where 29 cases were designated as basal (15%) and 165 as luminal (85%). Basal subtype HGUC showed greater TILs than luminal subtype HGUC(p=0.009). PD-L1 expression was seen in 9.3% (SP142) and 20.8% (SP263) of cases. Statistically significant associations between basal subtype and CD8 (p= 0.008), PD-1 (p=0.001) and PD-L1 expression (p=0.008 SP142 and p=0.014 SP263) were noted. In addition, basal HGUC showed lower CD4/CD8 (p=0.047) and increased CD8/FOXP3 ratios (p=0.031) compared to luminal subtype cases. No difference in CD20 expression was noted.

Conclusions: Basal subtype HGUCs show a characteristic "hot" immunophenotype with increased PD-1 and CD8 expression and higher CD8/FOXP3 ratios compared to the luminal subtype HGUC. In addition, increased PD-L1 expressing cells were present within the basal tumour immune microenvironment. These findings are similar to data in other organ systems and highlight the potential utilization of T cell typing to aid in identifying and stratifying patients with HGUC who may benefit from targeted therapy.

972 Local Tumor Recurrence Following Partial Nephrectomy

Chad Hruska[1], *Gang Wang*[2], *Pheroze Tamboli*[3], *Firas G Petros*[4], *Christopher G Wood*[4], *Surena F Matin*[4], *Miao Zhang*[5]. [1]MD Anderson Cancer Center, Houston, TX, [2]MD Anderson Cancer Center, Houston, TX, [3]UT-MD Anderson Cancer Center, Houston, TX, [4]MD Anderson Cancer Center, [5]Bellaire, TX

Background: Local tumor bed recurrence is a known complication following partial nephrectomy (PN). The factors involved with tumor recurrence are not well understood. Given the growing interest in non-surgical management options for clinical T1 renal masses, a better understanding of these factors will enable the pathologist to provide the most significant prognostic information to the clinician and guide patient care. In this study, we examine the clinicopathologic characteristics of local tumor recurrences following PN.

Design: We retrospectively reviewed the medical records of 2,556 PN cases performed in the institution between May 2002 and January 2017. Local tumor recurrence was strictly defined as detection of a new enhancing lesion within the surgical defect or within the same region as the PN site. A total of 60 patients (2.3%) with local tumor recurrence were identified. A comparison group was formed by selecting 163 random PN cases with no evidence of recurrence after at least ten

years of follow-up. Univariate and multivariate cox regression models were used to evaluate time to recurrence and predictive factors for local tumor bed recurrence.

Results: The clinicopathologic factors associated with local tumor recurrence are: male patients (73% vs. 55%, p=0.01), have a solitary kidney (27% vs. 4%, p<0.01), bilateral disease at presentation (23% vs. 10.4%, p=0.02), larger tumor size (m=3.8 cm vs. 3.0 cm, p<0.01), clear cell RCC (87% vs. 58%, p<0.01), patients with von Hippel-Lindau (VHL) syndrome (10% vs. 0%, p<0.01), high pathologic stage (>=T3a, 22% vs. 3%, p<0.01), multiple lesions (23% vs. 2%, p<0.01), distance from parenchymal margin less than or equal to 1 mm (52% vs. 10%, p<0.01). The median time between PN and local tumor recurrence was 30 months (5 – 177 months). Eight patients with local tumor recurrence (13%) died of disease and& seven of these patients developed metastatic disease. No patients died of disease or had metastases in the control group.

Conclusions: Our study showed the preoperative factors associated with local tumor recurrence following PN are: gender, tumor size, clear cell subtype, multi-focal disease, VHL syndrome. Intra/post-operative factors are: high pathological stage (>=pT3) and close surgical margins (<=1 mm). Our study is the first to identify pre and post-operative factors associated with recurrence among a relatively large cohort of patients using stricter, and perhaps more relevant definition of local tumor bed recurrence.

973 Primary Neuroendocrine Tumors of the Kidney: A clinicopathologic analysis of 17 cases. Does the grading system matter?

Chad Hruska[1], *Kanishka Sircar*[2], *Pheroze Tamboli*[2], *Priya Rao*[3]. [1]MD Anderson Cancer Center, Houston, TX, [2]UT-MD Anderson Cancer Center, Houston, TX, [3]UT MD Anderson Cancer Center, Houston, TX

Background: Primary neuroendocrine tumors (NET) of the kidney are rare neoplasms. There is limited data documenting the prognosis of these tumors. Current grading systems are designed for NETs from other sites & are often applied to renal NETs. We describe the clinicopathologic findings of renal NETs & address the applicability of current grading systems from other organ sites to renal NETs.

Design: We identified 17 cases with clinical follow up. Histologic parameters including Ki-67 index & mitotic counts were performed on all cases. Tumors were graded according to two separate systems: the 2015 World Health Organization (WHO) criteria for pulmonary NETs & the American Joint Committee on Cancer (AJCC) criteria for NETs of the gastrointestinal tract.

Results: Clinical follow up & Ki-67 index were available for all patients (pts). The average age was 52 yrs (range 35-70). The average tumor size was 8.3 cm (range 2.5 to 15.5). Other parameters studied included geographic necrosis (n=5), extrarenal extension (n=6), & LVI (n=7). Ten patients showed LN metastases; 12 pts had distant metastases, including liver (n=8), lung (n=3), bone (n=2), adrenal (n=1), and omentum (n=1). The Ki-67 proliferation index was determined by manual count of 500 cells (n=11) or by quantitative image analysis (n=4) with an average of 12.7% (range 0% to 55%). The data is summarized in Table 1. At last follow-up, 9 pts were alive & 8 were deceased, 4 pts showed no evidence of disease, 2 pts developed tumor recurrence (local n=1, distant n=1), & 11 pts had residual disease after treatment. Log-rank test analysis showed no significant differences in overall survival for the pulmonary (p=0.142) or GI (p=0.569) NET grading systems.

Case #	T size (cm)	Necrosis (Y/N)	Mitotic count (mitoses per 2 mm^2)	Ki-67 index	Original diagnosis	Reclassification based on lung NETs	Reclassification based on GI NETs
1	4.0	N	0	1.2	Carcinoid	Typical carcinoid	G1
2	4.0	N	1	0	Carcinoid	Typical carcinoid	G1
3	5.5	N	1	1.2	Carcinoid	Typical carcinoid	G1
4	14.0	Y	1	2.0	Atypical carcinoid	Atypical carcinoid	G1
5	6.5	N	1	1.9	Atypical carcinoid	Typical carcinoid	G1
6	3.7	N	0	0.8	Carcinoid	Typical carcinoid	G1
7		N	1	1.6	Carcinoid	Typical carcinoid	G1
8		N	2	0	Carcinoid	Atypical carcinoid	G2
9	2.5	N		2.9	Carcinoid	NA	G2
10	7.0			16.0	Carcinoid	NA	G2
11	14.5	Y		10.0	Carcinoid	Atypical carcinoid	G2
12	12.0	Y	34	27.6	Small cell neuroendocrine carcinoma	Small cell neuroendocrine carcinoma	G3/Small cell neuroendocrine carcinoma
13	15.0	Y		41.1	Small cell neuroendocrine carcinoma	Small cell neuroendocrine carcinoma	G3/Small cell neuroendocrine carcinoma
14	15.5	Y		28.5	Intermediate grade neuroendocrine carcinoma	NA	G3
15	2.6	Y		55.0	Small cell neuroendocrine carcinoma	Small cell neuroendocrine carcinoma	G3/Small cell neuroendocrine carcinoma
16	4.7	N	3		Carcinoid	Atypical carcinoid	G2
17	13.5	N	1		Carcinoid	Typical carcinoid	G1

*NA- Not available

Conclusions: Renal NETs are rare neoplasms with a strong propensity to metastasize to lymph nodes & distant organ sites. While frank small cell carcinoma in the kidney rarely poses diagnostic difficulty due to consensus in nomenclature, there is a wide spectrum of reporting terminologies used for the more low grade appearing NETs. The terminology currently used for GI NETs may be more appropriate for renal NETs, as the term "carcinoid" has been abandoned in the favor of using the terminology of "neuroendocrine tumor", thus underscoring the aggressive biologic potential and propensity for metastasis in even "low grade" renal NETs.

974 Syntaphilin is a Biphasic Biomarker of Aggressive Behavior in Prostate Cancer: Decreased Central Tumor Expression is Associated with Metastasis

Michael J Hwang[1], *Peter Humphrey*[2], *Marie E Robert*[3]. [1]Yale University School of Medicine, Hamden, CT, [2]Yale University, New Haven, CT, [3]Yale University School of Medicine, New Haven, CT

Background: Molecular biomarkers that can reliably identify aggressive and metastatic prostate cancer are not presently available. Syntaphilin (SNPH) is a cytoskeletal protein that regulates mitochondrial trafficking in neurons. Recent evidence suggests that SNPH may be expressed in cancer, promoting cell proliferation while inhibiting tumor cell invasion and metastasis (https://doi.org/10.1172/JCI93172). In this study, we examined the expression and role of SNPH in adenocarcinoma of the prostate in relation to grade, the invasive front, and clinico-pathologic parameters.

Design: The pathology database was searched for radical prostatectomy specimens and metastases with a diagnosis of prostatic adenocarcinoma. The 2015 modified ISUP Gleason scheme was used in assigning Gleason scores. Anti-SNPH antibody immunostain (Sigma #HPA04939) was performed on one selected slide for each case. The SNPH intensity was graded on a 0-3+ semi-quantitative scale for each Gleason pattern (GP) by two pathologists. In addition, the invasive front (external rim of cancer abutting benign tissue), and the central bulk (central portion of cancer excluding the invasive front) were graded. An H score was calculated based on the percentage and intensity of SNPH-stained cells in each GP and location. The relationship of SNPH staining to Gleason pattern, clinico-pathologic findings, and development of metastasis was analyzed.

Results: 29 Grade Group (GG) 1 and 60 GG 2-5 prostatectomy specimens with 15 paired lymph node or visceral metastasis were studied. GG 1 was analyzed separately, as a lesion associated with

a favorable prognosis. SNPH H scores increased with increasing GP; and GP 5 scores were significantly greater than GP 3 and GP 4 scores ($p<0.001$). Significantly increased SNPH expression was found at the invasive tumor front, compared to the central tumor bulk in all primary tumors ($p<0.0001$, Fig 1). The presence of metastases was significantly associated with both lower central bulk ($p=0.027$) and total gland ($p=0.029$) H scores (Fig 2). In addition, invasive front and overall SNPH H scores in GG 1 tumors were lower than in GG 2-5 cases ($p=0.004$).

Biphasic Syntaphilin Immunostain in Prostate Cancer

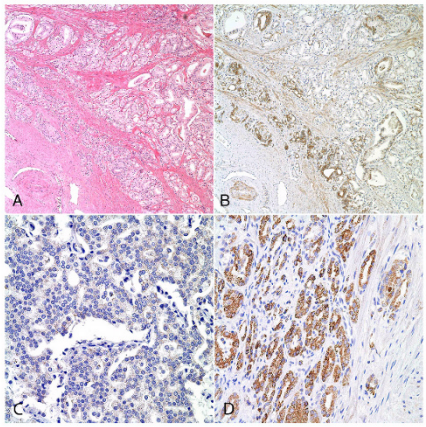

A. Medium magnification view of edge of tumor with central portion at upper right and invasive front at lower left. **B.** Same with SNPH immunostain. **C.** High magnification view of SNPH stain in central portion showing faint, barely perceptible intensity. **D.** High magnification view of invasive front with strong granular SNPH staining.

Comparison of SNPH Central Tumor H Scores in Patients With and Without Metastases

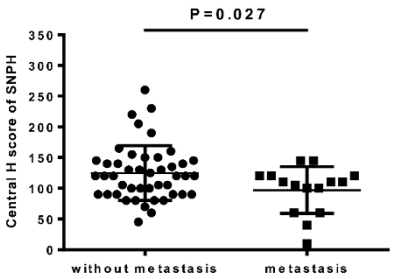

Patients with metastatic prostate cancer had significantly lower central SNPH staining than those without metastasis. Together, these results support a dual role of SNPH as suppressor of metastasis and mediator of tumor cell proliferation.

Conclusions: SNPH is a novel, biphasic marker of aggressive prostate cancer. High-grade tumors express high levels of SNPH, especially at the invasive front, whereas decreased SNPH expression in the central tumor bulk correlates with metastasis. SNPH may be a potential biomarker for disease progression in prostate cancer.

975 Epithelial-mesenchymal transition as a mechanism of the acquired tyrosine kinase inhibitor resistance in clear cell renal cell carcinoma

Hee Sang Hwang[1], *Heounjeong Go*[2], *Ja-Min Park*[3], *Sun Young Yoon*[3], *Jae-Lyun Lee*[4], *Se Un Jeong*[5], *Yong Mee Cho*. [1]University of Ulsan College of Medicine, Asan Medical Center, Seoul, Korea [2]Seoul Nat'l Univ/Medicine, Seoul, Korea, [3]Asan Institute for Life Sciences, Asan Medical Center, [4]University of Ulsan College of Medicine, Asan Medical Center, Seoul, Korea, [5]Asan Medical Center, Seoul, Korea

Background: Tyrosine kinase inhibitors (TKIs), such as sunitinib, have been widely accepted for the treatment of metastatic clear cell renal cell carcinoma (ccRCC) patients. However, even the response is favorable, most of the patients eventually experience disease progression despite the TKI treatment. The mechanism underlying the TKI resistance has not been fully explained in ccRCC.

Design: Ten TKI-treated metastatic ccRCC cases, of which tumor samples have been harvested before the treatment and immediately after the disease progression, were enrolled. Gene expression profiles and copy number variations of the matched pre- and post-treatment tumor samples were investigated using Human Transcriptome Array 2.0 and OncoScan CNV assay kits, respectively. Sunitinib-resistant ccRCC cell lines were generated by long-term treatment of ccRCC cell lines with sunitinib-containing media, and then their gene expression was evaluated.

Results: The proportion of sarcomatoid component was significantly increased in progressed tumor sample. Gene transcript levels related to the cell cycle and epithelial-mesenchymal transition (EMT) phenomenon were significantly upregulated in the progressed tumor samples compared to those of pre-treatment samples. Gene set enrichment analysis showed that *MYC* targets, p38-MAPK, TNF-alpha, and *mTOR* pathway gene sets were significantly enriched in the progressed tumor samples. Several chromosomal regions of copy number gains were also shown in the progressed tumor samples. Sunitinib-resistant ccRCC cell lines were successfully generated. Alteration of the EMT-related genes was also demonstrated in a sunitinib-resistant ccRCC cell line, which showed an enhanced invasion properties compared to the parent cell line. siRNA-induced inhibition of upregulated EMT-related genes significantly suppressed the invasion capacity of TKI-resistant cell lines.

Conclusions: Both the progressed ccRCC cases and sunitinib-resistant ccRCC cell lines demonstrated an alteration of EMT-related gene expression, which may contribute to the TKI resistance of ccRCC.

976 Mismatch Repair and BRAF (V600E) Genes Mutations in Patients with Bilateral Testicular Germ Cell Tumors: A Clinicopathologic and Immunohistochemical Study

Muhammad Idrees[1], *Karen Trevino*[1], *Thomas Ulbright*[1], *Khaleel Al-Obaidy*[1]. [1]Indiana University School of Medicine, Indianapolis, IN

Background: DNA mismatch repair (MMR) deficiency and microsatellite instability (MSI) are associated with cisplatin resistance in human germ cell tumors (GCTs). BRAF mutation has been implicated in the pathogenesis of several solid tumors and is associated with MSI. The role of MSI and BRAF mutations in patients with unilateral TGCT is controversial and its role in patients with bilateral disease has not been investigated. We studied the clinicopathologic characteristics and the immunohistochemical expression status of MMR and BRAF in patients with bilateral TGCTs.

Design: A retrospective search was performed for in-house patients who had TGCTs between 2001-2016 and subsequently for patients with bilateral disease within this cohort. Of 319 cases, 13 were identified as bilateral. Clinical information and follow up were collected from physician notes. Immunohistochemical staining for MMR (MLH1, MSH2, PMS2 and MSH6) and mutant BRAF was performed on 4 micron thick sections from paraffin-embedded tissue. Nuclear staining was recorded as positive expression for each MMR immunostain. Negative nuclear staining for BRAF was considered absent mutation.

Results: Bilateral TGCTs were found in 4% of patients in our institution. The mean age at the first and subsequent tumors diagnoses were 26.9 and 28.3 years, respectively. 11 patients had metachronous disease and the mean period between the tumors was 4.9 years (range 1-11). Of those 11 patients, 4 had bilateral mixed GCTs; 4 patients had MGCT initially and later developed seminoma in the other testis; 2 patients who initially had seminoma subsequently developed MGCT in the contralateral testis. Finally, 1 patient had initial seminoma and contralateral germ cell neoplasia in-situ. Of the two patients with synchronous GCTs, 1 had a MGCT and contralateral non-seminoma and the other had seminoma and an opposite MGCT. In metachronous cases, the initial tumor was pT1 in 42% and the subsequent one was pT1 in 87.5%. Recurrence was observed in 4 patients. No disease progression occurred after chemotherapy in any case. MLH1, PMS2, MSH2 and MSH6 showed expression in all cases. No BRAF mutation was found.

Conclusions: While MMR protein deficiency is implicated in cisplatin resistance in patients with TGCTs and BRAF mutation is found in several other solid tumors, our study found no association between the development of bilateral TGCTs and the MMR/MSI pathway or BRAF mutation. In our cohort, subsequent metachronous tumors behaved much more indolently.

977 Immunohistochemistry of Androgen Receptor and Related Signaling Pathways in Bladder Cancer as Prognosticators

Satoshi Inoue[1], *Taichi Mizushima*[2], *Hiroki Ide*[3], *Takashi Kawahara*[2], *Guiyang Jiang*[2], *George J Netto*[4], *Hiroshi Miyamoto*[5]. [1]University of Rochester, Rochester, NY, [2]University of Rochester, [3]Keio University, [4]University of Alabama at Birmingham (UAB), Birmingham, AL, [5]University of Rochester, Rochester, NY

Background: Recent preclinical evidence suggests a critical role of androgen receptor (AR) signals in urothelial tumor outgrowth. We have also demonstrated that androgens activate several transcription factors and other molecules via the AR pathway in bladder cancer (BC) cells. The current study aims to determine the expression status of AR, as well as such molecules including phospho-ATF2 (pATF2), phospho-

ELK1 (pELK1), phospho-ERK (pERK) and phospho-NFκB (pNFκB), and phospho-FOXO1 (pFOXO1), their activated and inactivated forms, respectively, in BC and its prognostic significance.

Design: We immunohistochemically stained for AR/pATF2/pELK1/pERK/pFOXO1/pNFκB in 129 BC and paired non-neoplastic bladder tissue specimens. We then evaluated the relationship between the expression of each protein and clinicopathologic features of our patient cohort.

Results: AR, pATF, pELK1, pERK, pFOXO1, and pNFκB were positive in 45%, 33%, 66%, 26%, 55%, and 66% of BCs, respectively, which were significantly lower (AR: 75%, *P*<0.001) or higher (pATF2: 14%, *P*=0.004; pELK1: 35%, *P*<0.001; pERK: 10%, *P*<0.001; pFOXO1: 24%, *P*<0.001; pNFκB: 50%, *P*=0.029) than in benign urothelial tissues. Thirty (60%) of 50 low-grade *vs.* 28 (35%) of 79 high-grade BCs (*P*=0.007) and 43 (55%) of 78 non-muscle-invasive (NMI) *vs.* 15 (29%) of 51 muscle-invasive (MI) BCs (*P*=0.006) were immunoreactive for AR. By contrast, pNFκB expression was considerably up-regulated in high-grade (73% *vs.* 54%, *P*=0.035) or MI (76% *vs.* 59%, *P*=0.057) BCs. There were no significant associations between pATF2/pELK1/pERK/pFOXO1 expression and tumor grade or stage. Kaplan-Meier analysis revealed significant associations between pELK1 positivity and recurrence of NMI tumors (*P*=0.043) as well as between the positivity of AR (*P*=0.013), pATF2 (*P*=0.028), pELK1 (*P*=0.045), pERK (*P*=0.017), pFOXO1 (*P*=0.041), or pNFκB (*P*=0.001) and progression of MI tumors. Multivariate analysis further identified pATF2 (HR=3.390, *P*=0.002), pELK1 (HR=2.693, *P*=0.021), and pNFκB (HR=6.424, *P*=0.003) as independent prognosticators in patients with MI tumor.

Conclusions: Compared with non-neoplastic urothelium, significant increases in the expression of all 5 AR-related proteins in BC were seen. The current results also support our preclinical findings indicating correlations of AR/ATF1/ELK1/ERK/NFκB activation or FOXO1 inactivation with urothelial tumor progression. Furthermore, all of these proteins, especially pATF2/pELK1/pNFκB overexpression, were found to serve as predictors of poor prognosis.

978 Clinical Significance of Percentage of Gleason Pattern 5 as a Tertiary Pattern In Prostate Cancer at Radical Prostatectomy

Mohsin Jamal[1], *Daniel Schultz*[2], *Sean R Williamson*[3], *Mireya Diaz-Insua*[4], *Hans Stricker*[4], *James Peabody*[4], *Craig G Rogers*[4], *Nilesh Gupta*[4]. [1]Henry Ford Hospital, Detroit, MI, [2]Henry Ford Hospital, [3]Henry Ford Health System, Detroit, MI, [4]Henry Ford Health System

Background: In 2005 ISUP consensus recommendations, although primary and highest Gleason grades were recommended for needle biopsies, it was the consensus of the group that for a radical prostatectomy (RP) specimen one assigns the Gleason score (GS) based on the primary and secondary patterns with a comment as to the tertiary pattern. Recent publications have suggested using 5% cut off for tertiary grade. We sought to determine the prognostic value of percentage Gleason pattern 5 (GP5) as a tertiary pattern in RP specimens and what constitutes an appropriate cut-off for tertiary vs secondary grade.

Design: Between a period of 2010 and 2014, 2248 patients underwent RP. 176 cases showing tertiary pattern 5 and were included in the study. Data collected included pT stage, percentage of all Gleason patterns, tumor volume, margin status, angiolymphatic invasion, lymph node involvement and biochemical recurrence (BCR) after surgery.

Results: Mean age of the patients was 64 years. We stratified 176 patients into eight groups based on percentage of Tertiary pattern 5 (GP5). G1: GS 3+4=7 with GP5 <5%, G2: GS 3+4=7 with GP5 5% - <10%, G3: GS 3+4=7 with GP5 10% - <15%, G4: GS 4+3=7 with GP5 <5%, G5: GS 4+3=7 with GP5 5% - <10%, G6: GS 4+3=7 with GP5 10% - <15%, G7: GS 4+3=7 with GP5 ≥15% and G8: 4+4=8 with GP5 <5%.

In order to quantify the importance of reporting tertiary Gleason pattern 5, the ROC curve showed utility of adding tertiary Gleason pattern 5 to the grade group in predicting BCR. The ROC indicates that the optimal cutoff value for percentage of tertiary Gleason pattern 5 lies between 5% and 10% (Figure 1). The percentage of tertiary GP5 was statistically significantly related to BCR (χ^2, p=0.003). The tertiary GP5 correlated significantly with seminal vesicle invasion (SVI), angiolymphatic invasion (AI) and final RP stage in GrGp3 tumors (Table 1).

Table 1. Association of categorical pathology outcomes in GS 4+3=7 tumor with percentage of tertiary pattern 5 in RP

Pathologic outcomes in Gleason score 4+3=7 tumors with tertiary pattern 5	p-value
Organ confined	0.15
Extraprostatic extension	0.15
SVI	0.004
Margin +	0.54
Lymph node +	0.14
AI	0.034
pT Stage	0.031

p-value based on Fisher exact test statistic.

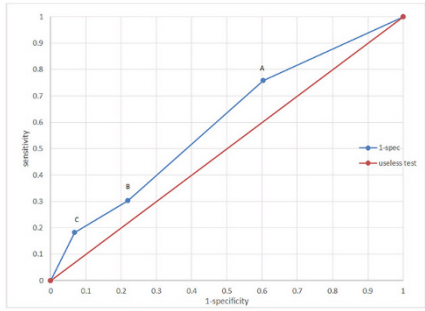

Figure 1: ROC curve with % tertiary Gleason pattern 5 cut-offs. A: 5%, B. 10%, C. 15%.

Conclusions: 1. The percentage of tertiary GP5 correlates significantly with BCR. Tertiary grade cut off value falls between 5-10% and any percentage of tertiary GP5 should be included as a secondary pattern.

2. Percentage of tertiary GP5 is an important parameter that should be reported on all RP cases with Gleason score 7 especially in GS 4+3=7 tumors, given its independent prognostic value.

3. In GS 4+3=7, tertiary GP5 correlated significantly with seminal vesicle invasion, angiolymphatic invasion and pT-stage.

4. Additional studies are needed to determine the role of higher Gleason pattern percentages in tumors other than Gleason score 7.

979 Morphologic and Molecular Characterization of Renal Medullary Carcinoma: A study of 18 cases

Liwei Jia[1], *Maria I Carlo*[2], *Hina Khan*[3], *Gouri J Nanjangud*[2], *Satshil Rana*[2], *A. A Hakimi*[2], *Amit K Verma*[4], *Hikmat Al-Ahmadie*[5], *Samson W Fine*[5], *Anuradha Gopalan*[5], *S. Joseph Sirintrapun*[6], *Satish Tickoo*[7], *Victor Reuter*[5], *Benjamin A Gartrell*[8], *Ying-Bei Chen*[5]. [1]MSKCC, New York, NY, [2]Memorial Sloan Kettering Cancer Center, [3]Montefiore Medical Center, [4]Albert Einstein College of Medicine, [5]Memorial Sloan Kettering Cancer Center, New York, NY, [6]New York, NY, [7]Memorial Sloan Kettering CC, New York, NY, [8]Montefiore Medical Center, Bronx, NY

Background: Renal medullary carcinoma (RMC) is a rare but highly aggressive form of renal cancer occurring in patients with sickle cell trait or disease. Uniform loss of SMARCB1 (INI1) expression, a core unit of the SWI/SNF complex, is a key diagnostic feature of these tumors. However, the molecular mechanism underlying SMARCB1 loss remains unclear in RMC.

Design: The retrospective study included 18 patients diagnosed with RMC and confirmed to have sickle cell trait at two institutions from 1996 to 2016. We reviewed the morphologic features of all cases and assessed the expression of SMARCB1 and OCT3/4 by immunohistochemistry (IHC). We developed a 3-color fluorescence in situ hybridization (FISH) assay to examine the status of *SMARCB1* locus and utilized targeted next-generation sequencing (NGS) platforms for molecular analysis.

Results: Mean age of patients at diagnosis was 24 years (range 7-46 y) with a male to female ratio of 2:1. Metastatic disease was detected in 9 (50%) at initial diagnosis, 8 underwent nephrectomy and others had diagnostic biopsies. In nephrectomies, reticular/microcystic growth was the dominant pattern in 5 (63%), whereas solid growth dominated in the other 3. At metastatic sites, biopsies most commonly revealed infiltrating tubules, solid cords or individual cells in a desmoplastic stroma (7/10, 70%). By IHC, all 18 cases showed a loss of SMARCB1 while OCT3/4 was positive in 8/16 (50%) cases including very focal staining (<5%) in 3. FISH analysis in 16 cases revealed 10 (62%) harboring *SMARCB1* translocation in one allele and concurrent hemizygous loss of the other allele, 3 (19%) showing homozygous loss of *SMARCB1*, and 3 (19%) without structural or copy number alterations involving *SMARCB1* despite the protein loss. NGS revealed a pathogenic somatic mutation of *SMARCB1* in one of the 3 cases that were negative by FISH. Two additional cases not analyzed by FISH were found to have *SMARCB1* homozygous deletion or copy

number loss by sequencing. No recurrent somatic mutations of other genes were identified. Tumors in the 3 subsets with different FISH findings exhibited morphologic overlap.

- This study is the largest molecular analysis of RMC to date.
- We demonstrate that different molecular mechanisms underly the loss of SMARCB1 expression in RMC.
- Biallelic inactivation of *SMARCB1* occurs in a large majority of cases either via concurrent hemizygous loss and translocation disrupting *SMARCB1* or by homozygous loss.

980 Clear Cell Renal Cell Carcinoma with Prominent Papillary Architecture: a Rare Morphologic Variant Supported by Molecular Evidence

Liwei Jia[1], *Gowtham Jayakumaran*[1], *Hikmat Al-Ahmadie*[1], *Samson W Fine*[1], *Anuradha Gopalan*[1], *S. Joseph Sirintrapun*[1], *Satish Tickoo*[1], *Victor Reuter*[1], *Ying-Bei Chen*[1]. [1]Memorial Sloan Kettering Cancer Center, New York, NY

Background: Clear cell renal cell carcinoma (ccRCC) is the most common histologic subtype of RCC and shows a wide spectrum of morphology. However, well-formed true papillae are considered rare in ccRCC. The differential diagnosis includes clear cell papillary RCC, MiT family (TFE3/TFEB) translocation RCC, and papillary RCC etc. Our study aimed to characterize and better classify a rare subset of RCCs with clear cytoplasm, high-grade nuclei, and prominent papillary architecture, but negative for TFE3/TFEB fusion.

Design: We retrospectively identified 13 cases of RCC with clear cytoplasm, high-grade nuclear features, and prominent papillary architecture from archival materials of our institution and TCGA papillary RCC (2 cases) public databases. The diagnosis of MiT family translocation RCC was excluded by TFE3/TFEB immunohistochemistry (IHC) and/or fluorescence in situ hybridization (FISH). Tumors were evaluated morphologically, immunophenotypically, and molecularly by targeted next-generation sequencing (NGS) and other methods (TCGA cases).

Results: Mean age of patients was 55 years (range 32-72y), and all were men. At nephrectomy, tumor size ranged from 2.9 to 14.5 cm (median: 8.25 cm), and 4 were pT1, 3 pT2, and 6 pT3. Two pT2 and one pT1 case had small vessel invasion. At a median follow-up of 35 months (range 7-109 mths), 2 patients (15%) died of disease, 8 (61%) developed metastasis, while 5 (38%) were free of disease at the last follow-up. Ten cases (77%) consisted mainly of papillary growth (60% or greater), 3 cases (23%) showed non-dominant, but distinct large areas of papillary growth. Acinar architectural pattern suggestive of ccRCC was either focal (≤20%) (n=11) or lacking (n=2). CA-IX was immunoreactive in 8/10 (80%), but only 5/8 (63%) showed diffuse, membranous staining. CK7 was positive in 3/9 (30%) whereas AMACR was positive in 6/8 (75%). Molecular analysis of 8 cases revealed a *VHL* mutation and concurrent 3p loss in 7/8 (88%) cases. While the remaining case is *VHL* wildtype, it had 3p loss and a *TET2* (Tet Methylcytosine Dioxygenase 2) truncating mutation that could lead to DNA hypermethylation. No trisomy 7/17 or *MET* mutations were found in these cases.

Conclusions: Molecular analysis of a rare subset of RCCs with clear cytoplasm, high-grade nuclei, and prominent papillary architecture, but negative for TFE3/TFEB translocations, reveals characteristic molecular features of ccRCC and supports their classification as a rare morphologic variant of ccRCC.

981 The Nested Variant of Urothelial Carcinoma Displays Immunophenotypic Features of Luminal Bladder Tumors

Steven Johnson[1], *Armen Khararjian*[2], *Francesca Khani*[3], *Brian Robinson*[3], *Jonathan Epstein*[4], *Sara E. Wobker*[5]. [1]University of North Carolina School of Medicine, Chapel Hill, NC, [2]Baltimore, MD, [3]Weill Cornell Medicine, New York, NY, [4]The Johns Hopkins Med Inst, Baltimore, MD, [5]UNC Chapel Hill, Chapel Hill, NC

Background: Nested variant of urothelial carcinoma (NVUC) is a rare subtype of invasive UC that is clinically aggressive, but paradoxically low-grade in morphology. Few groups have analyzed its immunophenotype, and gene expression profiling studies have not investigated if NVUC displays a basal or luminal subtype. We aim to characterize NVUC with immunohistochemical (IHC) analysis using markers with differential expression in basal (CK5/6, CK14) and luminal (GATA3, FOXA1) molecular subtypes, high and low grade UC and other prognostic IHC markers.

Design: Searches of pathology archives from three institutions identified 19 cases diagnosed as NVUC from 2000 to 2017. H&E-stained slides from each case were reviewed to confirm diagnosis. Sections were stained with 10-antibody panel (GATA3, FOXA1, CK5/6, CK14, p16, FGFR3, HER2, Cyclin D1, MYC, p53) and expression was analyzed by two pathologists. IHC markers were given a score 0-6 for percent-positive tumor cells (0 = 0%, 1 = 1-10%, 2 =11-30%, 3 = 31-50%, 4 = 51-70%, 5 = 71-99%, 6 = 100%) and 0-3 for stain intensity (0 = none, 1 = weak, 2 = moderate, 3 = strong). Scores were added for a maximum of 9, with a total score ≥ 6 defined as positive. p53 nuclear staining of ≥ 50% tumor cells was defined as abnormal.

Results: Specimens consisted of radical (n=13) or transurethral resections (n=6), and all but two cases (89%) were staged ≥ pT2. All tumors were positive for GATA3 and most expressed the luminal marker FOXA1 (84%). The basal markers CK5/6 and CK14 were minimally reactive, positive in 4 (21%) and 0 (0%) cases, respectively. The majority of cases (63%) displayed a composite immunophenotype (GATA3+, FOXA1+, CK5/6-, CK14-) characteristic of the luminal subtype. Few cases were positive for p16 (26%), FGFR3 (26%), and cyclin D1 (26%), most consistent with high-grade bladder tumors. All but one showed wild type p53 staining, and MYC was universally negative. HER2 expression was variable, with IHC scores ranging from 0 (n=7) to 7 (n=1).

Conclusions: Our results suggest that NVUC possesses a luminal molecular phenotype. While NVUC is associated with advanced stage, expression of luminal features has been associated with improved patient outcomes over the basal-like phenotype and is often responsive to chemotherapy. We also show evidence of high grade features by IHC, despite low grade cytology in NVUC. Due to prognostic and potential treatment implications, future aims include RNA gene expression profiling of these tumors to confirm the IHC findings.

982 Universal Lynch Syndrome Screening Should Be Performed in Upper Tract Urothelial Carcinomas

Jennifer Ju[1], *Anne Mills*[2], *Stephen Culp*[3], *Helen Cathro*[4]. [1]University of Virginia, Charlottesville, VA, [2]Charlottesville, VA, [3]University of Virginia, [4]UVA School of Medicine-Pathology, Charlottesville, VA

Background: Lynch Syndrome (LS) is defined by germline mutations in DNA mismatch repair (MMR) genes, and affected patients are at high risk for multiple cancers. Reflexive testing for MMR protein loss by immunohistochemistry (IHC) is currently recommended only for colorectal and endometrial cancers. However, upper tract urothelial carcinoma (UTUC) is the third most common malignancy in patients with LS, with a 20% lifetime risk. A previous study found that 50% of random UTUC patients with MMR loss (all MSH2 or MSH6) also had a history of other LS-associated cancers (LS-AC), consistent with likely LS. Our project sought to assess the frequency of MMR loss in UC at our institution by IHC, as well as possible predictive factors for loss, in order to evaluate the utility of reflexive IHC.

Design: H&E slides from 117 UTUC patients diagnosed from 2010-2017 were reviewed, and IHC for MSH2, MSH6, and PMS2 was performed on full sections. Cases with PMS2 loss were additionally stained for MLH1. A tissue microarray of 160 bladder UC (BUC) cases diagnosed from 1985-2004 was also stained. BUC cases with MMR protein loss on the microarray were repeated on full sections. MMR proteins were considered lost when tumor nuclei lacked staining completely, with a positive internal control.

Results: 8.5% of UTUC showed MMR loss (8 MSH6 alone; 1 MSH2 and MSH6; 1 MLH1 and PMS2; n=117) compared to 0.6% (1 MSH6 alone; n=160) of BUC (p=0.001). All 11 cases of UC MMR loss occurred in patients > 60 years. While 5 UTUC cases with MMR loss had no other cancers by chart review, 3 presented with other LS-AC and 2 had non-LS-AC. Most patients in the study were smokers and had a family history of cancer. Although 33.3% of cases with MMR loss had a lymphocytic infiltrate >30/10 HPF, 82.1% of UTUC with >30/10 HPF retained MMR.

Conclusions: UTUC accounts for only 5-10% of UC; however, our study shows that UTUC has significantly more loss of MMR than BUC at 8.5% versus 0.6% (p=0.001), almost all with loss of MSH6 alone. Age < 60 years, personal cancer history, family cancer history, smoking status and lymphocytic infiltrate were not predictive. 30.0% of UTUC patients with MMR loss in our study also had other LS-AC. Combining our results with those of a prior study suggests that 2.6-4.3% of cases of UTUC may represent LS. LS accounts for 2-6% of both colorectal and endometrial cancers. As LS likely accounts for a similar percentage of UTUC, we suggest that reflexive MMR IHC screening for all UTUC be included in diagnostic guidelines.

983 ERG, Prostein and PTEN Expression and their Relationship with Epithelial-Mesenchymal Transition, Stemness and Apoptosis Molecules in Prostate Cancer

Nuria Juanpere[1], *Silvia Hernández-Llodrà*[2], *Marta Lorenzo*[3], *Silvia de Muga*[3], *Joan Gil*[2], *Raquel Albero*[4], *Ivonne Vázquez*[5], *Lluís Fumadó*[3], *Lluís Cecchini*[3], *Belen Lloveras*[6], *Josep Lloreta*[3]. [1]Hospital del Mar-Parc de Salut Mar, Barcelona, Spain, [2]Pompeu Fabra University, [3]Hospital del Mar-Parc de Salut Mar-IMIM, [4]Hospital del Mar-Parc de Salut Mar-IMIM, Barcelona, [5]Consorci Sanitaria Parc de Salut Mar, Hospital del, Barcelona, [6]Hospital del Mar, Barcelona

Background: In an ERG+ subset of prostate cancer (PrCa), we reported that combined ERG expression, Prostein loss and PTEN loss (3-hit) is associated with high grade and stage PrCa and shorter PSA progression-free survival, while ERG expression alone is related to lower Grade Group tumors. Loss of E-cadherin and β-catenin membrane expression are markers of epithelial-mesenchymal transition (EMT). CD44, an adhesion molecule expressed in prostate basal cells, has been reported in a subpopulation of prostate stem cells with tumor-initiating and metastatic potential. Bcl-2 protein has anti-apoptotic effects and has been involved in PrCa chemoresistance. The aim of the present study has been to investigate by means of immunohistochemistry the relationship between ERG, Prostein and PTEN expression and E-cadherin, β-catenin, CD44 and Bcl-2 -as markers of EMT, stemness and apoptosis regulation, respectively- in a series of PrCa.

Design: A TMA series with 220 radical prostatectomies (with a mean of three cores per case) selected retrospectively from the files of the Parc de Salut MAR Biobank (MARBiobanc, Barcelona, Spain) was stained with antibodies against ERG, Prostein, PTEN, E-cadherin, β-catenin, Bcl-2 and CD44. The results were assessed by a team led by two pathologists.

Results: From 64 cases with Prostein loss, 29 (45.3%) were associated with E-cadherin loss in contrast with 19/136 Prostein wild type (*wt*) cases (13.6%) (p< 0.0001). From 73 PrCa with PTEN loss 26 (35.6%) were associated to E-cadherin loss *vs* 22/127 PTEN *wt* cases (17.3%) (p= 0.0035). From 21 cases with the 3-hit, 15 (71.4%) were associated to E-cadherin loss compared to 33/179 non-3-hit cases (13.4%) (p< 0.0001). From 65 cases with Prostein loss, β-catenin was lost in 25 (38.4%) *vs* 34/138 Prostein *wt* cases (24.6%) (p= 0.042). From 98 ERG+ PrCa, Bcl-2 expression was found in 44 (44.7%) *vs* 31/108 ERG- cases (26.7%) (p= 0.015). Finally, from 85 ERG- PrCa, 58 were CD44+ (68.2%) vs 35/67 ERG+ PrCa (52.2%) (p= 0.044).

Conclusions: In our PrCa series, Prostein loss, PTEN loss and the "triple hit" (ERG+/Prostein-/PTEN-) are significantly associated with changes in adhesion molecules involved in epithelial-mesenchymal transition (E-cadherin, β-catenin). These changes are probably related to the higher aggressiveness of this subset of tumors. Interestingly, Bcl-2 is more commonly expressed in ERG+ tumors and, on the other hand, CD44 is significantly related only to the ERG- PrCa subset.

FIS/Carlos III/FEDER/PI15/00452, Spanish Ministry of Health.

984 The Role of Tumor Infiltrating Neutrophils in Clear Cell Renal Cell Carcinoma

Jennifer Kalina[1], *Basile Tessier-Cloutier*[2], *Ruth Katz*[3], *Julian J Lum*[4], *Nils Pavey*[5], *Mahsa Marzban*[6], *David D Twa*[6], *Zaidi Tanweer*[7], *Davide Salina*[8]. [1]University of British Columbia, Vancouver, BC, [2]British Columbia Cancer Agency, Vancouver, BC, [3]M. D. Anderson Cancer Center, Houston, TX, [4]British Columbia Cancer Agency, [5]British Columbia Cancer Agency, Victoria, BC, [6]University of British Columbia, [7]MD Anderson Cancer Center, [8]Royal Jubilee Hospital

Background: Tumor promoting inflammation is an emerging hallmark of cancer and also a therapeutic target. Malignant cytokine production, like G-CSF, is known to promote angiogenesis and suppress NK cells and cytotoxic T-cells by recruiting neutrophils. Effectors released from neutrophils, include matrix metalloproteases, citrullinated histones and elastase, likely support the metastatic dissemination of tumor cells by degrading cell adhesion proteins including E-cadherin. We review a clinically annotated cohort of clear cell renal cell carcinoma (CCRCC) cases to assess the presence of neutrophils and their function as part of the tumor microenvironment.

Design: We reviewed a cohort of 90 cases of CCRCC, including primary and metastatic sites, from 3 centers. Both surgical resection and fine needle aspiration (FNA) specimens were analyzed. TINs were scored on a scale of 0-4 (0: negative, 1: low TIN, 2-4 high TIN) based on neutrophils scored either in histological section or cytology by two pathologists. TIN count was correlated with tumor characteristics including size of tumor, Fuhrman's nuclear grade and immunohistochemistry. RStudio (v1.0.153) was used to performed survival analysis using the survival package (v2.41-3) for R (v3.3.3). Significance was determined using the log-rank test.

Results: Among the 53 CCRCC resections, TIN count was high (score 2-4) in 20 (38%) cases and low (score 0-1) in 33 cases (62%). The presence of TIN was significantly associated with worse overall survival (p=0.009) independently of tumour grade and stage. Of the 37 primary CCRCCs sampled via FNA, 20 cases had high TIN count versus 17 cases that demonstrated a low TIN count. High TIN count in FNA samples was strongly associated with distant metastasis (p=0.0003) and shorter overall survival (p=0.0003). On surgical resected material, immunohistochemistry showed loss of E-cadherin in viable tumour cells in areas with high TIN. The activated neutrophils release elastase and citrullinated histones into the tumor microenvironment.

Conclusions: Our preliminary results show that TIN is an independent prognostic factor in CCRCC, which has the potential to be assessed at the time of first biopsy/FNA. Neutrophils act directly on tumour tissue by releasing elastase which successfully breaks down cell-cell adhesion and likely facilitates dissemination. Further analysis is required to correlate prognosis and disease progression to neutrophil function biomarkers.

985 Ki-67 is an Independent Predictor of Prostate Cancer Death in Routine Sections: Potential Use in Active Surveillance

Solene-Florence Kammerer-Jacquet[1], *Amar Ahmad*[2], *Henrik Moller*[3], *Peter Scardino*[4], *Luis Beltran*[5], *Jack Cuzick*[6], *Daniel Berney*[7]. [1]Service Anatomie Pathologique, Rennes Ille-et-Vilai, [2]Queen Mary University of London, [3]Kings College, London, United Kingdom, [4]Memorial Sloan Kettering Cancer Center, New York, [5]Barts Health NHS Trust, London, [6]Queen Mary University, London, United Kingdom, [7]Queen Mary University of London, London, United Kingdom

Background: Standard clinical parameters fail to accurately differentiate indolent from aggressive prostate cancer (PC). Our previous studies have shown that immunohistochemical (IHC) testing for Ki-67 in tissue microarray studies improved prediction of PC death in a cohort of conservatively treated clinically localised PC. However there have been few studies examining this in routine histopathological sections. Here, we present results in a more contemporary needle biopsy cohort with Ki-67 assessment in whole biopsies with long term follow-up and prostate cancer death as an outcome to demonstrate the practicability of use in a routine clinical setting.

Design: PC biopsy cases were identified in the UK, between 1990 and 2003, treated conservatively. Prostate-specific antigen (PSA), tumour extent and serum PSA were available. Biopsy cases were centrally reviewed by two uropathologists and Gleason grading and Grade groups conformed with contemporary ISUP criteria. Follow-up was through cancer registries up until 2012. Deaths were divided into those from PC and those from other causes as per WHO criteria. IHC was performed on a single platform to reduce pre-analytical variables. The percentage of Ki-67 in tumour cells was evaluated by immunohistochemistry (IHC) and available for 756 patients. This percentage was used in analysis of time to death from prostate cancer using a Cox proportional hazards model.

Results: In univariable analysis, the hazard ratio (HR) (95% confidence intervals) for continuous Ki-67 was 1.08 (1.06, 1.10) χ_1^2=47.975, P<0.001. In multivariable analysis, Ki-67 added significant predictive information to that provided by Grade Groups, extent of disease and PSA HR (95% CI) =1.04 (1.02, 1.06) $\Delta\chi_1^2$=13.703, P<0.001. In Grade Groups 1 and 2 (n=427), Ki-67 was an independent statistically significant predictor of time to death from prostate cancer, HR (95% CI) =1.1 (1.04, 1.16), χ_1^2=9.017, P=0.003.

	Univariable					Multivariable		
Variable	HR (95%CI)	LR χ^2	p-value	c-index*		HR (95%CI)	LR χ^2†	p-value
Grade Group 1-5	1.68 (1.50, 1.89)	74.562	<2e-16	0.716		1.38 (1.20, 1.59)	74.562	<2.2e-16
Continuous Ki-67	1.08 (1.06, 1.10)	47.975	4.32e-12	0.665		1.04 (1.02, 1.06)	19.850	8.38e-06
Extent of tumour	1.25 (1.18, 1.33)	59.955	9.66e-15	0.690		1.11 (1.04, 1.19)	14.286	0.0002
PSA	1.22 (1.15, 1.29)	36.908	1.24e-09	0.660		1.06 (0.99, 1.13)	2.771	0.096
LR χ_4^2 (p-value)						111.469 (<2e-16)		
c-index* (95%CI)			0.757 (0.707, 0.808)					

* Harrell's c-index † Terms added sequentially (first to last)

Conclusions: The Ki-67 index was studied in the largest conservatively treated prostate cancer cohort with long-term follow-up and contemporary assessment of grade. This study demonstrates Ki-67 as a robust, viable and practicable prognostic biomarker that could be useful for clinical practice. Unlike earlier cohorts, the results maintained significance in Grade Groups 1 and 2 which suggest that Ki-67 may be used routinely in patients being considered for active surveillance. Ki-67 should now be compared with commercially available tests as it represents a cheaper and simpler alternative.

986 T-cell Density is Associated with ERG, PTEN and p53 Molecular Status in Primary Prostate Cancer

Harsimar Kaur[1], *Liana Benevides Guedes*[2], *Jiayun Lu*[3], *Laneisha Maldonado*[1], *Logan Reitz*[4], *John R Barber*[6], *Jessica L Hicks*[6], *Angelo DeMarzo*[7], *Corinne Joshu*[3], *Karen Sfanos*[1], *Tamara L Lotan*[8]. [1]Johns Hopkins School of Medicine, [2]Johns Hopkins University School of Medicine, Baltimore, MD, [3]Johns Hopkins Bloomberg School of Public Health, [4]Johns Hopkins School of Medicine, Alpharetta, GA, [5]Johns Hopkins Bloomberg School of Public Health, Baltimore, MD, [6]Johns Hopkins University School of Medicine, [7]Johns Hopkins University, Baltimore, MD, [8]Johns Hopkins School of Medicine, Baltimore, MD

Background: The inflammatory microenvironment plays an important role in the pathogenesis and progression of a variety of tumors and correlates with clinical outcomes in some settings. We evaluated the association of tumor-associated T-cell density with clinical-pathologic variables, tumor molecular subtype and oncologic outcomes in surgically-treated prostate cancer.

Design: Two cohorts of primary prostate tumors were evaluated, including one cohort enriched for African-American ancestry (n=309) and one cohort designed to examine association of biomarkers with metastasis in prostate cancer (n=311). Tissue microarrays (TMA) were immunostained for CD3, CD8 and FOXP3 as well as ERG, PTEN and p53 using previously genetically validated protocols. One cohort was also queried for alternative *ETS* translocations via RNA *in situ* hybridization. For CD3, CD8, and FOXP3, automated image analysis for T-cell density in 3-4 0.6 mm diameter TMA tumor spots was performed for each case.

Results: In a validation set of 29 cases, CD3+ cell density measured on TMA spots was correlated with CD3+ density measured on standard histologic sections (r=0.73). Across both TMA cohorts, CD3+ cell density was not significantly associated with most clinical pathologic variables, including tumor grade, stage and racial ancestry. There was no significant correlation between CD3 density and biochemical recurrence or survival on univariate and multivariate analysis. However, in both cohorts, CD3+ cell density was significantly higher in tumors with ETS/ERG expression, PTEN loss or p53 nuclear accumulation compared to those without the respective molecular alterations ($p<0.05$ for all comparisons).

Conclusions: Higher CD3+ cell density is associated with specific molecular alterations in prostate cancer, however there is no significant correlation between CD3+ cell density and clinical-pathologic parameters or clinical outcomes in these cohorts.

987 Morphologic and Clinical Review of 62 Renal Tumors in 30 Patients with Familial Kidney Cancer Syndromes

John M Kennedy[1], *Aaron M Udager*[2], *L. Priya Kunju*[3], *Madelyn Lew*[4], *Arul Chinnaiyan*[5], *Scott Tomlins*[6], *Angela Wu*[7], *Rohit Mehra*[6]. [1]University of Michigan, Ann Arbor, MI, [2]University of Michigan Medical School, Ann Arbor, MI, [3]University of Michigan Hospital, Ann Arbor, MI, [4]Dexter, MI, [5]Plymouth, MI, [6]University of Michigan, Ann Arbor, MI, [7]Ann Arbor, MI

Background: Most renal cell carcinomas (RCC) occur sporadically, although a small subset are associated with hereditary syndromes (HS). Due to the rarity of each individual HS, there are few comprehensive studies investigating the clinicopathologic features of these tumors. The present study is a retrospective review at our institution to further characterize the clinicopathologic spectrum of HS tumors.

Design: The medical record was searched for renal biopsies/resections of HS patients seen at a single large academic institution since 2000. The search yielded 62 renal biopsies/resections from 30 patients with HS, including Von-Hippel Lindau (VHL), Birt-Hogg-Dube (BHD), tuberous sclerosis (TS), hereditary leiomyomatosis and renal cell carcinoma (HLRCC), and succinate dehydrogenase deficiency (SD). Twenty-four patients with 41 tumor biopsies/resections were available for morphologic review.

Results: See table 1 for summary of tumor type, stage, grade, and multifocality for each HS. Morphologic features for each HS are described below. VHL: 86% of resections (n=21) had cystic CCRCC and/or atypical clear cell lined cysts. 40% of patients (n=10) had tumorlets within benign renal parenchyma of at least one resection specimen. BHD: 25% of resection specimens (n=4) available for review showed background renal oncocytosis. TS: All resections (n=3) available for review demonstrated background cysts. Features of epithelioid AML and AML tumorlets were seen in 67% of cases (n=3). Clinical and pathologic data for patients with HLRCC and SD is being analyzed currently. Of all masses biopsied in HS patients (n=24), 8% of cases led to a new diagnosis of HS by molecular testing. Indications for biopsy in patients with a HS diagnosis included radiosurveillance of a renal mass (79%) and confirmation of successful radioablation treatment (8%). One biopsy on a patient without a HS diagnosis did not prompt testing, but later clinical information led to SD testing. Additional biopsy data and subsequent patient management is currently being analyzed.

Table 1. Tumor type, stage, grade, and multifocality for renal tumors of hereditary syndromes.

Hereditary syndrome	# of resections	Resections available for morphologic review	Tumor type	Stage (of RCCs)	Grade (of RCCs, excluding ChRCC)	Multifocal
VHL	22	21	CCRCC (91%)	T1 (96%)	Gr2 (45%)	RCC (77%)
			CCPRCC (4.5%)	T4 (4%)	Gr3 (55%)	
			ChRCC (4.5%)			
BHD	8	4	CCRCC (12.5%)	T1 (100%)	Gr2 (100%)	HOT (75%)
			ChRCC (37.5%)			RCC (0%)
			HOT (50%)			
TS	5	3	AML (80%)	T1 (50%)	Gr2 (50%)	AML (80%)
			TS-associated RCC (20%)	T2 (50%)	Gr3 (25%)	RCC (50%)
			RCC-unclassified (40%)		Gr4 (25%)	
			CCRCC (20%)			

CCRCC = clear cell renal cell carcinoma; CCPRCC = clear cell papillary renal cell carcinoma; ChRCC = chromophobe renal cell carcinoma; HOT = hybrid oncocytic tumor; AML = angiomyolipoma; TS-associated RCC = tuberous sclerosis-associated RCC.

Conclusions: Renal tumors associated with HS frequently have characteristic morphologies unique to each HS. Multifocality is common in both benign and malignant tumors of HS patients. Both VHL and BHD related-RCCs are identified at low stage (T1), most likely due to radiologic surveillance of HS patients. Renal biopsies rarely led to a new diagnosis of HS, but play an important role in the surveillance of renal masses in HS patients.

988 Testicular Lymphomas: An Institutional Experience

Binny Khandakar[1], *Rifat Mannan*[2], *Songyang Yuan*[3]. [1]Mt Sinai St Luke's Roosevelt Hospital, New York, NY, [2]The Johns Hopkins Hospital, [3]Mt Sinai Beth Israel, New York, NY

Background: Testicular lymphoma is a rare neoplasm, representing 1% to 2% of all non-Hodgkin lymphomas (NHLs) and approximately 5% of all testicular neoplasms. It is predominantly a disease of the elderly and is the most common testicular tumor in men over the age of 60. We sought to identify the clinical and pathologic features of testicular lymphomas diagnosed at our institute.

Design: The database was searched and 40 cases of testicular lymphomas were included for the series. The data was analyzed systematically for age, laterality, side, lymphoma subtype, IHC findings, and molecular findings.

Results: Right testis was involved in 53% cases [n=18/34]. Bilateral involvement was seen in 2; 1 testis was inguinal. Average age was 59.5 years [range, 10-84]. Majority were B-cell lymphomas [95%, n=38], comprising DLBCL [65%, n=26], Burkett's like [10%, n=4], blastic lymphoma/leukemia [7.5%, n=3], plasmablastic lymphoma [5%, n=2], Burkitt's lymphoma [5%,n=2], and CD5-neg blastoid mantle cell lymphoma [5%,n=2]. The remaining 2 cases[5%] were T-cell lymphoma. Burkitt's like, DLBCL & T-cell lymphomas were commoner in older age group [range: Burkitt's like, 44-84 years; DLBCL, 31-82 years; T-cell, 70-80 years] compared to blastic lymphoma/leukemia [18-29 years], Burkitt's [10, 35 years]. The blastic lymphomas were B-cell origin. Non-GCB subtype of DLBCL [n=17] was commoner than GCB subtype [n=10, non-GCB vs n=7 GCB]. 10 cases of DLBCL were both BCL2 and BCL6 positive [n=5, GCB; n=5, non-GCB]. MUM1 was expressed in 28% of GCB [n=2]. CD5 expression was found in ABC subtype [n=1] with co-expression of myc, BCL6 and BCL2. MIB1 LI ranged from 60->90% in both the DLBCL subtypes. 1 case of CD-5 negative mantle cell lymphoma showed t (11;14)(q13:q32.3).

Conclusions: Testicular lymphomas are uncommon. Different subtypes affect different age group. T-cell lymphoma is very rare and affects the old. CD-5 expression and co-expression of myc, and BCL2 was uncommon in the current series.

989 Testicular & Penile Pathology in Gender Affirmation Surgery (GAS)

Binny Khandakar[1], *Rifat Mannan*[2], *Jess Ting*[3], *Songyang Yuan*[4]. [1]Mt Sinai St Luke's Roosevelt Hospital, New York, NY, [2]The Johns Hopkins Hospital, [3]Mount Sinai Hospitals, [4]Mt Sinai Beth Israel, New York, NY

Background: GAS is becoming a widely performed procedure in the US in patients with gender dysphoria. Transgender individuals

seeking male to female (M-F) transition routinely receive pre-surgery cross-hormone therapy. Testicular & penile pathology in specimens received for GAS is not widely described. We sought to analyze the morphologic changes in orchiectomy & penectomy specimens received for M-F GAS.

Design: This retrospective study (2016-2017) included random bilateral routine orchiectomy (n=64) & accompanying modified penectomy (n=19) specimens. H&E slides were reviewed for histologic changes in testis & penis. Controls included testes from non-tumoral areas of orchiectomies for testicular neoplasia. Findings were compiled.

Results: Average age was 32 years (range, 20-61 years). Average testicular size was 4.0 cm (range, 2.5-7.2 cm), with 7 (11%) measuring <3.0 cm in diameter. Average testicular weight was 28.6 gm. On microscopy, 42 testes (65.6%) showed spermatogenesis arrest, at the level of spermatogonia/primary spermatocyte, with no mature sperm in seminiferous tubules (ST). Another 12 (18.8%) showed hypospermatogenesis, with presence of few mature sperms. Complete absence of spermatogenesis was observed in remaining 10 (15.6 %). Sertoli cell only was observed in 1. Severe & diffuse atrophy of STs with complete hyalinization was seen in 20 (31%). Tubular basement membrane showed varying degrees of thickening: mild (n=18, 28%), moderate (n=14, 22%), and severe (n=20, 31%); it was normal in 12 (19%). Leydig cells were markedly reduced in 34 (53%), with presence of rare cells in the interstitium. Remaining 30 (47%) appeared to have adequate number of Leydig cells. Changes in interstitium included edema & hyalinization. Epididymal changes included peritubular fibrosis & epithelial hyperplasia. None showed any neoplastic change, including germ cell neoplasia in-situ. Incidental ectopic adrenal rest was found in 1. Penile specimens showed mild interstitial fibrosis (n=9, 47%) & mild periurethral chronic inflammation (n=2, 11%).

Conclusions: The current series describes detailed histopathologic findings in testes & penises for GAS in a large number of specimens. There was variable impairment of spermatogenesis, including maturation arrest, hypospermatogenesis & complete absence of spermatogenesis. There were also changes in interstitium and epididymis, with non-specific changes in the penis. Observed changes can be attributed to pre-surgery hormone therapy or a change in tissue biology.

990 Molecular Status of Intraductal Carcinoma of the Prostate Occurring as an Isolated Finding or with Gleason 6 Carcinoma at Radical Prostatectomy

Francesca Khani[1], *Sara E. Wobker*[2], *Brian Robinson*[1], *Jessica L Hicks*[3], *Angelo DeMarzo*[4], *Jonathan Epstein*[5], *Tamara L Lotan*[6]. [1]Weill Cornell Medicine, New York, NY, [2]UNC Chapel Hill, Chapel Hill, NC, [3]Johns Hopkins University School of Medicine, [4]Johns Hopkins University, Baltimore, MD, [5]The Johns Hopkins Med Inst, Baltimore, MD, [6]Johns Hopkins School of Medicine, Baltimore, MD

Background: Intraductal carcinoma of the prostate (IDC-P) almost invariably occurs concurrent with high grade invasive prostatic carcinoma, and is likely to represent retrograde spread of invasive carcinoma in many cases. ERG expression and PTEN loss are common in IDC-P in this setting and almost always concordant with the invasive carcinoma. In rare cases, IDC-P may occur as an isolated finding at radical prostatectomy or in association with low grade (Gleason score 6) invasive adenocarcinoma. In these unique cases, we hypothesized that IDC-P is likely to be a true precursor lesion. Here, we characterized these cases for ERG and PTEN status.

Design: We obtained 4 cases where IDC-P was an isolated finding and 11 cases where IDC-P occurred with only Gleason 6 invasive carcinoma at radical prostatectomy from our consultation practice and institutional archives. IDC-P was defined using WHO 2016 criteria. All cases of invasive carcinoma were graded using the Grade Group system. ERG and PTEN immunostaining were performed using genetically validated protocols on the IDC-P and concurrent invasive carcinoma (available in 82% or 9/11 of the cases).

Results: Overall, ERG was expressed in only 7% (1/15) of the IDC-P and PTEN was lost in 53% (8/15). The rates of ERG positivity and PTEN loss were significantly lower in these cases compared to our previously published series of IDC-P occurring at radical prostatectomy with predominantly Gleason score ≥ 7 invasive carcinoma (p=0.01 and p=0.03). Of the cases of concurrent Gleason score 6 invasive carcinoma, 22% (2/9) were ERG-positive and 0% (0/9) had PTEN loss. Overall, 33% (3/9) cases were discordant for ERG status in the IDC-P compared to the invasive tumor (2 were ERG- in IDC-P and ERG+ in the invasive component). Similarly, 44% (4/9) were discordant for PTEN status in the IDC-P compared to invasive tumor (all had PTEN loss in the IDC-P and intact PTEN in the invasive tumor). 56% (5/9) were discordant for ERG or PTEN status in IDC-P and invasive tumor components.

Conclusions: IDC-P occurring as an isolated finding or in association with low grade invasive carcinoma is frequently ERG-negative and may be molecularly distinct from IDC-P occurring with concurrent high grade invasive carcinoma. The frequent discordance for PTEN and ERG status in the concurrent IDC-P and Gleason 6 carcinomas suggests that they may arise from separate clones in many cases.

991 Automatic Prostate Cancer Diagnosis and Gleason Pattern Recognition using Deep Neural Networks

Kyungeun Kim[1], *Taebum Lee*[2], *Hyeseon Hwang*[3], *Sangjun Oh*[4], *Kyuhyoung Choi*[4], *Sun Woo Kim*[4], *Choi Yoon-La*[2]. [1]Kangbuk Samsung Hospital, Sungkyunkwan University School of Medicine, Seoul, Seoul, [2]Samsung Medical Center, Sungkyunkwan University School of Medicine, [3]Deep Bio Inc., Seoul, South Korea, Seogwipo-si, Jeju, [4]Deepbio, Seoul, South Korea

Background: Due to astonishing development in deep learning, such improvement on automatic histological image analysis is expected. It may be very helpful for pathologists to diagnose, if the predicted regions and Gleason patterns are marked on the whole slide images (WSIs). This study investigates how a classifier based on deep neural networks can accurately detect prostate cancer and recognize the Gleason patterns on WSIs.

Design: This study included 602 WSIs of prostate needle biopsy specimen with H&E staining. Among them, 534 WSIs were used for training and the remains were used for validation. All WSIs were split into square patches with size of 240 by 240 pixels, and each patch was labeled as Gleason pattern 3, 4 or 5 as well as normal tissue by a pathologist. The patch classifier, an artificial neural net of 147 layers and 142M parameters to be learned, was composed of two branches, one for the original patch itself and the other for the surrounding region of 720 by 720 pixels. Each branch of the network was based on ResNet, and their outputs were concatenated at the top layers.

Results: The training set contained 372,311, 15,584, 41,410 and 9,903 patch images for normal prostate, Gleason pattern 3, 4 and 5, respectively. When applying the trained net to WSIs of test set, the cancer detection of each slide was performed with high sensitivity, specificity, positive and negative predictive values of 91.9%, 91.7% 95.4% and 85.8%, respectively. The Gleason pattern recognition showed sensitivity of 88.1%, 94.2% and 86.7 %, and specificity of 95.5%, 87.8% and 94.1% in Gleason pattern 3, 4 and 5, respectively. The negative predictive values were also high with 99.4%, 98.9% and 99.4% in Gleason pattern 3, 4 and 5, respectively. However, the positive predictive values for each Gleason pattern showed 56% at maximum, so further studies including more images should be needed for more accurate Gleason pattern recognition.

Conclusions: In this early application of deep learning in diagnosing prostate cancer, our results revealed that the deep neural networks can detect prostate cancer areas in WSIs and classify histologic images into Gleason patterns with high accuracy, suggesting that a deep learning based prostate cancer detector can be used as an assistant tool for pathologists.

992 Clinicopathological Characteristics of Acquired Cystic Disease-Associated Renal Cell Carcinoma with Metastasis

Fumiyoshi Kojima[1], *Jatin S Gandhi*[2], *Joe Kaminsky*[3], *Ibu Matsuzaki*[4], *Kenji Warigaya*[5], *Masakazu Fujimoto*[6], *Akinori Iba*[7], *Toshio Shimokawa*[8], *Eiichi Morii*[9], *Isao Hara*[7], *Shin-ichi Murata*[4], *Mahul Amin*[10]. [1]Wakayama Medical University, Wakayama, [2]University of Tennessee Health Science Center, Memphis, TN, [3]UTHSC, Memphis, [4]Wakayama Medical University, Wakayama, [5]Department of Diagnostic Pathology, Wakayama Medical University, [6]Wakayama Medical School, Human Pathology, Wakayama, [7]Wakayama Medical University, [8]Wakayama Medical University Hospital, [9]Osaka University, [10]Methodist University Hospital, Memphis, TN

Background: ACD-RCC develops in the acquired cystic kidney under hemodialysis. ACD-RCC usually has a favorable prognosis; however, anecdotal cases with metastasis have been reported. While the morphology of primary tumors is described in the very few reported series, there has been no systematic study to date of a series of cases in which the morphology and immunophenotype of metastatic ACD-RCC has been evaluated. In this study we elucidate clinicopathological characteristics of ACD-RCC with metastasis (ACD-RCC, m+) compared to ACD-RCC without metastasis (ACD-RCC, m-) in an attempt to identify adverse prognostic features.

Design: We retrieved slides from 22 patients with 40 ACD-RCCs and evaluated the following: age, sex, laterality, duration of hemodialysis, tumor size, infiltrative growth, architectural pattern, intratumoral oxalate crystal deposition, perinephric invasion, lymphovascular invasion, coagulative necrosis, WHO/ISUP grade, and sarcomatoid differentiation. The histologic features of metastases were correlated with the primary tumor. A comprehensive panel, PAX8, GATA3, carbonic anhydrase IX, CD10, RCC marker, CK7, AMACR, c-kit (CD117), kidney specific cadherin, CK34βE12, and S100A1 was performed in the primary and metastatic tumors.

Results: 7 of 22 ACD-RCCs cases had metastasis; material on 6 cases was available for review. Most cases with or without metastasis were in males with over 10 years history of hemodialysis. Adverse histologic features in tumors with metastasis compared to those

without metastasis were as follows: infiltrative growth (57% vs. 7%); perinephric extension (28% vs. 0%); WHO/ISUP grade 3 (71% vs. 21%) and coagulative necrosis (57% vs. 4%). Interestingly, we found oxalate crystal deposition in 2 metastatic lesions. PAX 8, RCC antigen and S100A1 were frequently expressed in metastatic sites indicating diagnostic utility in this setting. 71% of patients with metastases died due to disease; no patients without metastasis died due to renal cell carcinoma.

Pathological findings and statistical tests of acquired cystic disease-associated renal cell carcinoma (ACD-RCC)

	ACD-RCC with metastasis	ACD-RCC with no metastasis	**p-value (< 0.05)**
maximum diameter (cm)	3.38[1] (1.19)[2]	2.1[1] (0.80)[2]	0.085
invasive growth (+ / -)	4 / 3[3]	1 / 14[3]	0.021
proliferation pattern (crib / pap / tub)	2 / 3 / 1[3]	10 / 3 / 2[3]	0.348
extrarenal invasion (+ / -)	2 / 5[3]	0 / 15[3]	0.091
necrosis (+ / -)	4 / 3[3]	4 / 11[3]	0.343
intratumoral oxalate crystal (+ / -)	3 / 4[3]	9 / 6[3]	0.651
Grade (WHO / ISUP) (2 / 3)	2 / 5[3]	9 / 6[3]	0.283

[1]average, [2]standard deviation, [3]number of cases

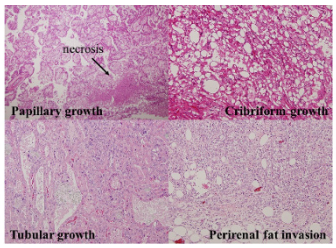

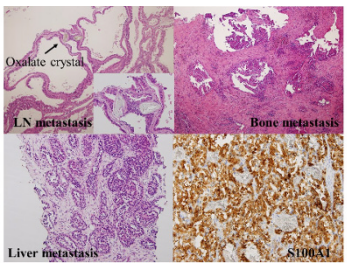

Conclusions: We report the first series of ACD-RCC focusing on histopathologic features of tumors with metastasis. The presence of oxalate crystals in metastatic tumors suggests their participatory role in the progression of these tumors and warrants further study. Our data suggests that ACD-RCC with infiltrative growth, perinephric extension, and coagulative necrosis are more commonly associated with metastatic outcome and these patients should be candidates for closer clinical follow-up.

993 Adrenal cortical carcinomas: A microsatellite instability-high tumor?

Yumi Kojima[1], *Chad Hruska*[1], *Kanishka Sircar*[1], *Mouhammed Habra*[1], *Miao Zhang*[1]. [1]The University of Texas MD Anderson Cancer Center, Houston, TX

Background: Adrenal cortical carcinoma (ACC) is uncommon tumor with less than 50% 5 year survival. Current treatment for ACC is limited. Recently, targeted therapy with pembrolizumab has been approved by the FDA for any tumors with mismatch repair deficiency and/or tumors that express PD-1/PD-L1; however, the status of microsatellite instability (MSI) markers in ACC is unknown. In this study, we examined the MSI markers, PD-1 and PD-L1 expression in ACCs immunochemically.

Design: We constructed a tissue microarray (TMA) with 46 cases of ACCs. Patients with adenoma (n=15), atypical adenomas (n=11), and normal adrenal tissue (n=13), of matched age/gender, were included as controls. Immunohistochemical stains were performed on the TMA with MLH1, PMS2, MSH2, MSH6, PD-1, and PD-L1.

Results: There were 44 female and 43 male patients, with a mean age of 39 yrs (range:19yrs-86 yrs). The average tumor size of ACC is 12 cm (range:4.5-22.5 cm), significantly larger than the control group (avg 4 cm; range: 2.1 cm - 10 cm, p<0.01). The Weiss score of ACCs ranges from 4 to 9, significantly higher than the control group (0-2, p<0.01). The average quantitative Ki-67 (qki-67) proliferation index is 11.8% in ACC group (range:5.15%-33.9%), significant higher than the control group (avg 0.273%, range: 0.03% - 0.8%, p<0.01). Out of 46 ACCs, 19 cases showed loss of at least one MSI marker immunohistochemically; 6 cases showed loss of two MSI markers (MLH1/PMS2, MSH2/MSH6, PMS2/MSH6) and 1 case showed loss of three MSI markers (MSH2, MSH6 and PMS2), significantly higher than the control group (p<0.01). 2 ACC cases were positive for PD-1, while 3 ACC cases were positive for PD-L1. PD-1 and PD-L1 were negative in the control group. 17 patients in the ACC group died of disease with a mean survival of 57 months (range:7 months-120 months), while no patient in the control group died of disease (follow up, 60-120 months). A Cox regression analysis found a significant prediction for overall survival when using qKi-67, tumor size, and Weiss score. PD-1/PDL-1 and MSI expression status were not significant predictors for overall survival.

Conclusions: Our study is the first large scale study to address the MSI and PD-1/PDL-1 expression status in ACCs. Although MSI loss or staining with PD-L1/PD-1 does not confer a change in the overall survival rate, it does allow for use of specific targeted treatment that may change the overall survival of these patients, warranting a new treatment modality in clinical practice for ACC patients.

994 Plasmacytoid Variant of Bladder Cancer: Immune and Molecular Pathologic Profiling

Myriam Kossai[1], *Camelia Radulescu*[2], *Julien Adam*[3], *Yanish Soorojebally*[2], *Nicolas Signolle*[4], *Mathilde Sibony*[5], *Yves Allory*, *Thierry Lebret*, *Mathieu Rouanne*[2]. [1]Hopital FOCH, Suresnes, Haut de Seine, [2]Hopital FOCH, [3]Gustave Roussy, Villejuif, IDF, [4]Gustave Roussy, Villejuif, France, [5]Hopital Cochin

Background: Plasmacytoid Urothelial Carcinoma (PUC) is a rare but increasingly recognized pathologic subtype of bladder cancer associated with an aggressive behavior. A molecular classification of bladder cancer highlights two main molecular subtypes referred as basal and luminal with distinct clinical outcomes and sensitivities to chemotherapy. These 2 subtypes have been correlated with specific immunohistochemical (IHC)markers (GATA3 and KRT20 for the luminal sutype; KRT5/6 for the basal subtype). We aimed to assess these markers in a cohort of PUC. Giving the striking results of FDA approved immune checkpoint blockade therapies in advanced UC, we studied the immune microenvironment of PUC.

Design: Immunohistochemical analysis was performed using antibodies detecting: p63, GATA3, KRT5/6, KRT20, HER2 and E-cadherin expression on bladder tumor specimen from 32 PUC and 30 pathologic stage-matched pure high grade conventional UC. Clinico-pathological variables were documented and compared between PUC and pure UC. Progression-free survival was compared between both groups. The density of CD8+ tumor-infiltrating lymphocytes was digitally analyzed based on whole tissue sections obtained from transurethral resection of the bladder tumor at diagnosis. PD-L1 expression (clone 28-8) was evaluated in tumor (TC) and immune cells (IC).

Results: PUC were pure (42%) or mixed (58%), generally associated with conventional UC. The immune infiltrate, defined by the density of intra tumor lymphocytes, was significantly weaker in the PUC group compared to matched controls (p<0.05). PD-L1 expression in immune cells (p=0.9) was weak in PUC and no expression in tumor cells, was found, contrary to pure UC controls (p=0.03). The intratumoral positive CD8 cell density was not significantly different in both groups (p=0.6). PUC highly expressed GATA3 (100%, p=0.34) and CK20 (61%, p=0.12) whereas KRT5/6 (23%; p<0.05) and p63 (42%; p<0.05), E-cadherin (p<0.05) expression were significantly lower compared to the control group. Overexpression of HER2 was found in 9 cases out of 32 (28%, p=0.37) and in 5 controls (17%). Compared to the control population, PUC had a worse progression-free survival (p=0.3).

Conclusions: Plasmacytoid urothelial carcinoma harbored a luminal profile with a high frequency of HER2 overexpression. Our results suggest that patients may not represent good responder to PD-1/PD-L1 blockade therapy alone, but a treatment combining platinum-based chemotherapy and immune checkpoint blockade might be efficient.

995 Racial Disparity in Expression of NF-κB and GDF15 in Prostate Cancer and Accompanying Benign Prostatic Epithelium: Dependence on Stage and Grade

Oleksandr Kravtsov[1], *M. Scott Lucia*[2], *Benjamin Rybicki*[3], *Jim R Lambert*[4], *Kenneth A Iczkowski*[5], *Kathleen C Torkko*[4]. [1]Medical College of Wisconsin Affiliated Hospitals, Milwaukee, WI, [2]University of Colorado, Aurora, CO, [3]Henry Ford Hospital, Detroit, MI, [4]University of Colorado Denver, [5]Medical College of Wisconsin, Milwaukee, WI

Background: Growth differentiation factor 15 (GDF15, PDF, NAG-1) is a stress-induced anti-inflammatory cytokine with immunomodulatory functions. High GDF15 is associated with prostate cancer progression [PMID:12894347]. NF-κB is a transcription factor of the Rel family that regulates pro-inflammatory gene expression and gets constitutively activated in androgen-independent prostate cancer, increasing anti-

apoptotic bcl-2 and angiogenesis. Prostatic GDF15 expression had been shown to correlate inversely with inflammatory lesions in the prostate and suppress NF-κB activity [PMID:25327758]. In this study we examined the levels of NF-κB and GDF-15 in tissue microarrays from African-American (**AA**) and White (**W**) prostate cancer patients.

Design: TMAs of 161 AA prostatectomies and 205 W were stained with goat polyclonal antibody to GDF15 or rabbit monoclonal antibody to NF-κB. Cases were matched for grade (p=.8) and stage (2, 3a, or 3b) (p=.3); mean W age 62.2, AA age 60.7 (p=.03). The 3-12 evaluable punched cores of PC and benign prostate/case were evaluated by 2 pathologists on a 0-3+ scale. Mann-Whitney test was used for racial disparities. Kruskal-Wallis test was used for stagewise and gradewise comparisons.

Results: Regardless of race, median GDF15 reactivity was 3 in PC and 1 in benign; NF-κB was 1.5 in PC and 1 in benign (all p <.005). GDF15 expression negatively correlated with NF-κB in tumor (r=.207, p=.008) and in all tissues (r=.192, p=.0003) for W but not for AA. For tumor-tumor and benign-benign comparisons of both antigens by race, only benign glands showed a significant difference, with higher NF-κB in benign epithelium of AA men compared to W men (p=.01). 41.4% of AA had reactivity >1 in benign glands but 30.2% of W did (p=.03).

Stagewise and gradewise: In W men, GDF15 expression in PC trended from 3 down to 2 with rising stage (p=.02) and from 3 down to 2.5 with grade (p=.58); NF-κB trended from 1.37 up to 2.00 with stage (p=.28) and 1.5 up to 2.25 with grade (p=.07); all 4 of these trends were absent in AA.

Conclusions: GDF-15 and NF-κB protein levels are inversely related in W but not AA men. There was higher NF-κB in benign glands in AA (possibly correlating with AA's more frequent prostatic inflammation [PMID:9605645]), coupled with less of a decrease in GDF15 and less of an increase in NF-κB with worsening tumor in AA. Higher benign gland NF-κB may account for less ability to mount an immune response to cancer in a segment of AA population and may explain their worse cancer outcome.

996 NKX3.1: A Potential Marker for Sertoli Cells

Arash H Lahouti[1], *Eugene Santagada*[2], *Beverly Wang*[3], *Guang-Qian Q Xiao*[4], *Pamela Unger*[5]. [1]Lenox Hill Hospital, New York, NY, [2]Lenox Hill Hospital, [3]UC Irvine Medical Center, Orange, CA, [4]USC-Keck Medical Center, Los Angeles, CA, [5]New York, NY

Background: NK3 Homeobox1 (NKX3.1) is an androgen-regulated homeoprotein expressed by tissues of male urogenital system, including prostate, seminal vesicle, and testis. The NKX3.1 gene has an important role in normal differentiation of prostatic epithelium and its loss of function has been implicated in prostate tumorigenesis and tumor progression. While tissue microarray studies have shown expression of NKX3.1 in normal testis, the cells of origin and the role of NKX3.1 gene in testis is largely unknown. An older study suggested NKX3.1 positivity in normal germ cells and Intratubular germ cell neoplasia, while weak or absent staining was seen in seminomas and embryonal carcinomas. In this study, we aimed to characterize expression of NKX3.1 in non-neoplastic testis and a variety of testicular tumors.

Design: Immunohistochemical staining using monoclonal antibodies for NKX3.1 was performed on 46 adult testis specimens obtained from January 2012 to August 2017. NKX3.1 positivity was scored based on extent (0-5%:0, >5-25%:1+, >25-50%: 2+, >50%: 3+) and intensity (weak: 1+, moderate-strong:2+) of nuclear staining.

Results: Patient age ranged from 26 to 88 years (mean: 43±15). Twenty-five specimens were obtained from patients with neoplastic diseases (13 classic seminomas, 6 mixed germ cell tumors, 2 embryonal carcinomas, 2 Leydig cell tumors, 1 Sertoliform cystadenoma, and 1 adenomatoid tumor) and 21 from non-neoplastic conditions (17 infertility work-up and 4 acquired disorders). In the non-neoplastic testis, NKX3.1 stain highlighted Sertoli cells in all cases (42/42; 2+: 83%, 1+: 17%; extent: 2-3+ in all). Similarly, all 3 Sertoli cell nodules showed diffuse and strong expression (3+, 2+). Neither Leydig cells nor non-neoplastic germ cells expressed the NKX3.1. In neoplastic testis, the NKX3.1 was only expressed focally (1+) in the glandular elements of 2 out of 3 teratoma specimens (67%; one case showed 1+ and one showed 2+ staining). NKX3.1 was not detected in seminoma (0/14), embryonal carcinoma (0/6), yolk sac tumor (0/2), intratubular germ cell neoplasia (0/13), Leydig cell tumor (0/2), Sertoliform cystadenoma (0/1) and adenomatoid tumor (0/1).

Conclusions: NKX3.1 gene expression is restricted to the Sertoli cells in adult testis. This finding may add to understanding the biology of testis. Further studies are now needed to explore NKX3.1 positivity in Sertoli cell tumors.

997 Clinicopathologic Characteristics of Fumarate Hydratase-Deficient and Hereditary Leiomyomatosis and Renal Cell Carcinoma-Associated Renal Cell Carcinoma: A Series of 10 Cases

Hubert Lau[1], *Sean R Williamson*[2], *Christian Kunder*[3], *Alice C Fan*[4], *Chia-Sui Kao*[3]. [1]Stanford University Med. Ctr., Stanford, CA, [2]Henry Ford Health System, Detroit, MI, [3]Stanford University School of Medicine, Stanford, CA, [4]Stanford University Med Ctr

Background: Hereditary leiomyomatosis and renal cell carcinoma-associated renal cell carcinoma (HLRCC-RCC) is a rare and recently described entity. We aim to analyze the use of fumarate hydratase immunohistochemistry (FH IHC) in identifying HLRCC-RCC and provide a comprehensive study of renal tumors that are FH-deficient, either by IHC or presence of a germline *FH* mutation.

Design: 20 renal tumors with prominent viral inclusion-like nucleoli and perinucleolar halo were initially identified. FH IHC was performed on all cases. All available clinicopathologic data was recorded.

Results: 9 tumors showed complete loss of FH staining (1 had confirmed germline *FH* mutation), and 1 with retained FH staining had a confirmed germline *FH* mutation. Of these 10, papillary was the most common pattern (80%), followed by solid (60%), cribriform (40%), tubular (40%), collecting duct carcinoma (CDC)-like (30%), tubulopapillary (30%), tubulocystic (30%), sarcomatoid (10%), and cystic (10%). Papillary was the dominant pattern in 40%, solid was dominant in 30%, and sarcomatoid, cribriform, and tubulopapillary were each dominant in 10%. These cases were consistently negative for CK7 (7/7) and mostly negative for p63 (6/7) and GATA3 (6/7). Clinical data were available for 7 cases. 1 was originally diagnosed as HLRCC-RCC; others were originally diagnosed as unclassified RCC (3), CDC (2), and papillary RCC (1). Patient age ranged from 37 to 65 years (median, 44 years), M:F=4:3, tumor size ranged from 3.6 to 17 cm (median, 5.1 cm), and tumor stage was mostly ≥ pT3a (86%). 57% of patients had a history of early-onset uterine leiomyomas or family history of RCC. After a mean follow-up time of 30 months (range, 1 to 99 months), 29% of patients died of disease, 29% had disease progression, and 42% had no evidence of disease.

Conclusions: FH IHC is not 100% sensitive for HLRCC-RCC, as rare cases with confirmed germline *FH* mutations may show retained FH staining. Thus, even with retained FH staining, genetic counseling and testing for a germline *FH* mutation may be indicated if the clinical history and morphologic features suggest HLRCC-RCC. FH IHC is also unlikely to be 100% specific for HLRCC-RCC, as sporadic FH-deficiency has been described, although it remains unclear how frequently. Patterns other than papillary may predominate, and FH-deficient/HLRCC-RCC should be included in the differential diagnosis with CDC and urothelial carcinoma; negative CK7, p63, and GATA3 staining is helpful in distinguishing it from the latter two.

998 TFE3 expression in renal cell carcinoma is correlated with poor prognosis regardless of its gene translocation status

Hyun Jung Lee[1], *Dong Hoon Shin*[2], *Kim So Young*[3], *Chung Su Hwang*[4], *kim young Keum*[5], *Ahrong Kim*[6], *Won Young Park*[7], *Lee Jung Hee*[3], *Jee Yeon Kim*[1]. [1]Busan, Korea, [2]Pussan National University Yang-San Hospital, Yang-San, Korea, [3]Pusan National University Yang-San Hospital, [4]Yang-San, [5]Pusan National University Hospital, [6]Pusan, KOR, [7]Pusan National University, Busan, Korea

Background: Xp11.2 translocation renal cell carcinoma was first recognized in pediatric and young adult patients, and it has been delineated by the 2016 World Health Organization as a distinc classification of MiT family translocation renal cell carcinoma. Morphologic features, clinical significance of TFE3 expression, frequency of gene translocation, and even diagnostic criteria of translocation renal cell carcinoma have been the subject of a limited number of reports.

While the gold standard test for TFE3 translocation is fluorescent in situ hybridization (FISH), detecting TFE3 using immunohistochemistry is faster and cheaper. It shows high sensitivity and there are cases exhibiting TFE3 positivity by immunohistochemistry but negativity by FISH. However, there have been a few studies regarding the significance of TFE3 expression in RCC regardless of FISH results. We speculated that the intensity and distribution of TFE3 expression in RCCs may have correlations with clinicopathologic parameters such as prognosis, *TFE3* translocation status, morphology, and others.

Design: Among 190 consecutive cases, we selected 185 RCC patients as TRCC candidates who treated at our hospital between 2011 and 2015 whose clinical data and paraffin blocks are available. Clincal data were obtained for each selected patient. Slides were reviewed by two pathologists and histologic subtypes of these RCCs were reclassified according to the criteria proposed in the 2016 WHO classification. Immunohistochemical staining was performed for TFE3 ans Cathepsin K in 185 cases and FISH analysis was done for molecular test. TCGA dataset of renal cell carcinoma was evaluated for validation of TFE3 expression and survival analysis.

Results: Of 17 cases expressing strong nuclear TFE3 signal, FISH analysis showed break-apart signal in 15 cases (88.2%). In 45 which showed no or weak TFE3 expression, 6 samples were translocation-positive by FISH assay. In the survival analysis, high TFE3 expression was significantly correlated with decreased progression free survival (p=0.002). In the TCGA dataset, among 412 samples, TFE3 mRNA overexpression was associated with poor progression free survival and poor overall survival.

Analysis of prognostic factors for survival				
	Univariate analysis		Multivariable analysis	
Variables	HR (95% CI)	P-value	HR (95% CI)	P-value
Age> 50	1.67 (0.49, 5.68)	0.410	1.13 (0.31, 4.16)	0.857
Gender, female	0.57 (0.19, 1.70)	0.316	0.31 (0.08, 1.31)	0.114
WHO/ISUP nuclear grade (3, 4: high)	3.58 (1.48, 8.66)	0.005	1.37 (0.49, 3.83)	0.545
pT stage (III, IV: high)	13.19 (5.08, 34.08)	<0.001	9.69 (3.42,27.44)	<0.001
High TFE3 expression	4.00 (1.46,10.94)	0.002	4.17 (1.16, 14.99)	0.029
High Cathepsin-K expression	1.17 (0.39, 7.25)	0.482	1.04 (0.23, 1.04)	0.959

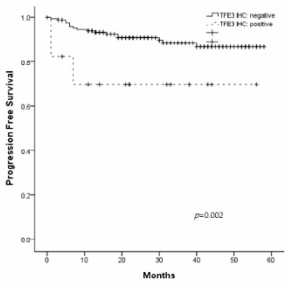

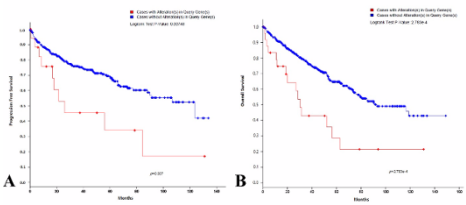

Conclusions: This study highlights that increased TFE3 expression in RCC is associated with poor progression free survival regardless of its gene translocation status. Unexpectedly, high rate of TFE3 expression and TFE3 translocation was revealed from our study and this finding should be studied and validated further.

999 Aberrant Expression of Uroplakin II and GATA-3 in Bladder Cancer Mimickers: Caveats in the Use of a Limited Panel to Determine Cell of Origin in the Bladder

Mariah Leivo[1], *Emily Ross*[2], *David Tacha*[3], *Donna Hansel*[4]. [1]San Diego, CA, [2]UC San Diego, La Jolla, CA, [3]Biocare Medical, Pacheco, CA, [4]UCSD, La Jolla, CA

Background: Uroplakin II (UPII)-targeting antibodies have been recently developed and have been shown to be more sensitive and specific for urothelial carcinoma than prior uroplakin III antibodies. UPII is highly specific for urothelial cell origin and is frequently used as a marker to determine site of origin in primary or secondary lesions involving the bladder. To date, however, no studies have been performed to test the expression of UPII in mimickers of bladder cancer seen on histopathology and we sought to test expression of UPII with and without GATA-3 stain in this population.

Design: We evaluated the expression of UPII and GATA-3 in conventional nephrogenic adenoma (n=8), papillary nephrogenic adenoma (n=6), endometriosis/endosalpingosis (n=4), inflammatory myofibroblastic tumor (n=4), ectopic prostate tissue (n=3) and malakoplakia (n=2). UPII and GATA-3 antibodies were obtained from Biocare Medical (Pacheco, CA) and used at predilute concentrations. Slides were reviewed by two pathologists and results correlated.

Results: Samples from 8 females and 19 males were used for analysis, with average patient age of 64 years (median 69 years). Weak immunoreactivity for UPII was identified in 5/27 mimickers (19%), including in 3 cases of papillary nephrogenic adenoma, 1 case of conventional nephrogenic adenoma, and in the luminal cell layer of 1 case of ectopic prostate tissue. By contrast, GATA-3 was expressed in 12/27 mimickers (44%) that included the basal cell layer of 2 cases of ectopic prostate cancer, 6 cases of nephrogenic adenoma, 2 cases of inflammatory myofibroblastic tumor (weak), and in 2 cases of endometriosis. No case showed dual immunoreactivity for UPII and GATA-3.

Conclusions: Strong immunoreactivity for UPII remains a specific marker for urothelial cell of origin, although weak staining may be seen in a significant proportion of mimickers. GATA-3 stains a greater number and broader spectrum of mimickers. However, no case was dual positive for UPII and GATA-3. These findings support a panel-based approach to the immunohistochemical analysis of possible bladder cancer mimickers, if required.

1000 Somatic TP53 Mutations in Cancerous and Non-Cancerous Bladder: Early Clones Revealed by Ultra-Deep Sequencing

Sherry Lian[1], *Nancy Kiviat*[1], *Rosana Risques*[1], *Maria Tretiakova*[2]. [1]University of Washington, [2]University of Washington, Seattle, WA

Background: *TP53* mutations play a crucial role in pathogenesis of urothelial carcinomas (UC) occurring at early stage of carcinoma in situ (CIS). UC carcinomas are often synchronous and metachronous and are believed to originate monoclonally from extensive premalignant fields. To investigate premalignant *TP53* mutated clones in bladder tissue, we took advantage of the extreme accuracy of Duplex Sequencing (DS). DS error rate is <1 in 10^7, compared to 1 in 100 of conventional NGS. This allows detection of low frequency mutations with high sensitivity. Our goal was to identify *TP53* mutations in UC and matching benign urothelium and to compare them with *TP53* mutations in normal bladder (biological background mutations).

Design: Ultra-deep DS was performed in DNA extracted from fresh-frozen bladder tissues from 5 patients with UC (pT1-2) and 5 age-matched autopsy patients without any history of urinary tract pathology. For the 5 patients with UC, the samples included tumor and matched benign bladder mucosa (>5 cm away from UC). CIS was available for 1 patient. DS uses random molecular tags inserted in the sequencing adaptors allowing to identify reads corresponding to each strand of DNA and to perform internal error correction. We used DS to sequence the coding region of *TP53* at an average depth of 2,000x.

Results: DS detected low frequency (< 1 in 1000) *TP53* mutations in all 16 samples. These biological background mutations were similarly prevalent in cancerous and normal tissue from UC patients as well as in tissue from normal controls. In agreement with prior findings in other tissues, biological background mutations were "cancer-like" (missense, deleterious, and clustered in hotspots). Three of 5 UC cases had clonal high frequency *TP53* driver mutations in exons 4, 6 and 7. The same *TP53* mutations were also present at lower frequency in the benign mucosa and in CIS (Fig. 1). Two remaining UC cases presented only *TP53* mutations at a low frequency suggesting a different driver gene.

Fig. 1 TP53 mutations in bladder cancer and adjacent normal

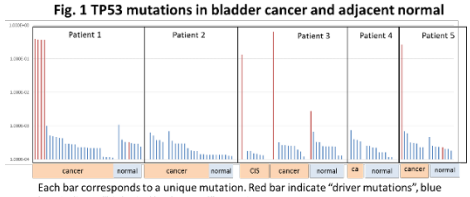

Each bar corresponds to a unique mutation. Red bar indicate "driver mutations", blue bars indicate "biological background" mutations.

Conclusions: Biological background mutations were prevalent in cancerous and non-cancerous bladder from patients with UC as well as in normal control tissues. These mutations were 'cancer-like' and have been previously reported as an aging effect. In addition to these background mutations, driver TP53 mutations were detected in a subset of UC with or without CIS, and consistently reproduced at lower frequency in distant benign mucosa, indicating the clonal origin of UC from a distant histologically normal precursor clone.

1001 Female Urethral Carcinoma: Analysis of 29 Cases and Proposal for a New Staging System

Brett M. Lowenthal[1], *Sounak Gupta*[2], *Manju Aron*[3], *John Cheville*[4], *Donna Hansel*[5]. [1]UPMC-Presbyterian Hospital, San Diego, CA, [2]Memorial Sloan Kettering Cancer Center, New York, NY, [3]Keck School of Medicine, University of Southern Ca, Los Angeles, CA, [4]Mayo Clinic, Rochester, MN, [5]UCSD, La Jolla, CA

Background: Female urethral carcinoma is an extremely uncommon form of cancer. Limited studies have been undertaken to evaluate this carcinoma and to assess the application of AJCC staging criteria on

this entity. We undertook a comprehensive pathology and clinical outcomes analysis of 29 cases, which represents one of the largest series of this entity analyzed to date.

Design: Resection cases were obtained from 3 institutions. All slides were re-evaluated by three pathologists to assess for histopathological findings and depth of invasion. Clinical records were analyzed to obtain demographic and outcomes data.

Results: Twenty-nine women with urethral carcinoma were identified. Average age was 71 yrs (median 73 yrs). Specimens included 12 anterior exenterations, 13 urethrectomies, and 4 limited resections. Tumors ranged from non-invasive lesions to carcinomas 5.5 cm (average 3.0 cm). Subtypes included 16 urothelial carcinomas, 5 clear cell adenocarcinomas, 5 adenocarcinomas NOS, and 3 squamous cell carcinomas. Four cases had lymph node metastasis at resection. Review of 7th and 8th edition AJCC staging criteria was limited when carcinomas invaded beyond periurethral muscle and did not account for the anterior extension of carcinoma. We used anatomic landmark subdivisions for urethra carcinoma stage (UCS) 0: non-invasive; UCS1: subepithelial and peri-urethral muscle; UCS2: adventitia; UCS3: dense (fibro)muscular tissue posterior and large caliber vessels anterior; UCS4: lamina propria of the vaginal wall, anterior peri-pubic fat, or bladder involvement. The number of cases in each category included: UCS0 3 cases; UCS1 3 cases; UCS2 9 cases; UCS3 5 cases; UCS4 8 cases. Carcinoma subtype did not cluster with UCS stage. Follow-up was available for 28 patients (average 109 mo; median 65 mo). Twelve patients (12/28; 43%) were alive without disease or dead from other causes. However, 7 patients were alive with advanced disease and 8 patients were dead of disease (15/28; 54%). Patients who did not progress to recurrence and/or death had a significantly higher rate of UCS0 and UCS1 cases (5/12) versus those who progressed (1/15; P=0.03); conversely, UCS3 and 4 cases were higher in those who progressed (8/15; 53%) versus those who did not (4/12; 33%; P=0.30).

Conclusions: Female urethral carcinoma is a highly aggressive disease, independent of subtype. Staging stratification along anatomic landmarks can be readily performed and may enhance outcomes prediction in this population. Additional studies on an expanded group

1002 Expression Profiles of ERG, SPINK1, ETV1 and ETV4 in Early Onset Prostate Cancer: An Immunohistochemical and RNA In-Situ Hybridization Study on Whole Mount Slides

Zhichun Lu[1], *Nallasivam Palanisamy*[2], *Daniel Schultz*[3], *Sean R Williamson*[2], *Shannon Carskadon*[4], *Mireya Diaz-Insua*[4], *Craig G Rogers*[4], *Hans Stricker*[4], *James Peabody*[4], *Jeong Wooju*[4], *Nilesh Gupta*[5]. [1]Henry Ford Health System, Detroit, MI , [2]Henry Ford Health System, Detroit, MI, [3]Henry Ford Hospital, [4]Henry Ford Health System, [5]Henry Ford Hospital, Detroit, MI

Background: ETS family gene fusions are commonly seen in prostate cancer. ERG is more frequently overexpressed, followed by ETV1, ETV4, and ETV5. SPINK1 overexpression has been described in prostate cancer (PCa), but its prognostic value is controversial. All these alterations are generally mutually exclusive in PCa, but its expression profiles and the probable roles in young onset PCa have not been thoroughly explored.

Design: A total of 153 Radical prostatectomy (RRP) specimens of patients younger than 55 year-old were retrieved from our institution. SPINK1 and ERG were detected by using immunohistochemical staining, ETV1 and ETV4 were detected by RNA in-situ hybridization. Expression of ERG, SPINK1, ETV1, and ETV4, and their association with various recorded clinicopathologic parameters were analyzed.

Results: Age ranged from 33 to 55 years (Mean: 49). 70 (46%) Caucasians (CA), 61 (40%) African Americans (AA). Pre-operative PSA ranged from 0.6 to 52.7ng/ml (Mean: 7.15). 66(43%) patients had positive family history of PCa. Follow up period ranged from 1 to 123.7(Mean: 30.5) months. Biochemical Recurrence (BCR) was seen in 7/144 (5%).

ERG expression was seen in majority of cases: 93/152 (61%) followed by SPINK1 in 73/152 (48%), ETV1 in 10/128(8%) and ETV4 in 3/48(6%). 37 cases (24%) showed both ERG and SPINK1 positivity. Table 1 lists association of these alterations with various clinicopathologic parameters.

Out of 10 cases that were positive for ETV1, 6 cases showed additional marker positivity in whole mount sections: 2 cases (ERG+/SPINK1+) & 2 cases (ERG+/SPINK1-). 3/4 cases with isolated ETV1+ were non-organ confined, remainder 7 cases were organ confined.

ETV4 was positive in 3 cases (all AA patients), 2 cases showed additional marker positivity as follows: 1 case was SPINK1+ and 1 case was both ERG and SPINK1 positive. 2/3 cases were non-organ confined.

Table 1: Relationship of ERG and SPINK1 with age, race and stage

	ERG			SPINK1		
	Negative	Positive	P-value	Negative	Positive	P-value
Age: ≤45: 43 (28%)	10	33	0.0134	29	14	0.016509
46-55: 109 (71%)	49	60		50	59	
Race: CA: 69 (45%)	18	51	0.00678	44	25	0.0000049
AA: 61(40%)	33	28		20	41	
Pathology Stage:						
≤pT2:112(73%)	37	75	0.029607	64	48	0.032804
≥pT3a:40(26%)	21	19		15	25	

Higher frequency of ERG expression was seen in younger aged patients (≤ 45 years old), CA patients and organ confined tumors

1. SPINK1 is often seen in AA patients and associated with non-organ confined disease

2. ERG and SPINK1 expression observed in 24% cases within different regions of a same tumor or different tumors within prostate gland. The clinical significance of this finding is uncertain as remains to be determined.

3. No association of any of the studied alteration was seen with BCR

4. Overall, tumors in young pts are low grade and stage and majority behave in an indolent fashion with low BCR rates.

1003 Characteristics of Secondary Tumors in Patients with Multifocal Prostate Cancer and Its Implications in Focal Therapy: A Study of 102 Whole Mount Robotic Radical Prostatectomies

Zhichun Lu[1], *Kanika Taneja*[2], *Mireya Diaz-Insua*[3], *Sean R Williamson*[4], *Craig G Rogers*[3], *Hans Stricker*[3], *James Peabody*[3], *Jeong Wooju*[3], *Nilesh Gupta*[5]. [1]Henry Ford Health System, Detroit, MI, [2]Henry Ford Health System, Detroit, MI, [3]Henry Ford Health System, [4]Henry Ford Health System, Detroit, MI, [5]Henry Ford Hospital, Detroit, MI

Background: Focal therapy protocols often target the dominant tumor nodule (T1) as those are often implicated in progression of the disease. Prostate cancer is often multifocal and some of these tumors may not be treated during focal therapy. The aim of our study is to determine the characteristics of these secondary tumor nodules (T2) on whole mount robotic radical prostatectomy to help define focal therapy protocols.

Design: A total of 102 consecutive robotic radical prostatectomy (RRP) performed at a single institution were reviewed. Pathologic data recorded on each tumor nodule included Grade group (GG), tumor size, location, distance to prostate capsule, and distance from the margin. Overall pT stage, tumor volume (TV), margin and lymph node status were noted.

Results: Age ranged from 45 -78 years with mean of 63 years. 68 (67%) cases had multifocal disease (average 2 tumors).

1. Of the 68 cases with multiple tumors, two thirds (n = 41) of secondary tumors showed Grade group 2 or higher and one third (n = 27) showed Grade group of 1. Table 1 summarizes the Grade group of all the tumors.

2. The volume of the dominant nodule was significantly larger than that of secondary nodules (p-v=0.015).

3. The distance of the dominant nodule to the capsule is smaller than in the second nodule 0.7 ± 1.2 mm (p=0.002) (Table 2).

4. Distribution of size of secondary nodules is provided in Table 3.

5. More than half of the secondary nodules involved the mid location, followed by one third cases involving the apex and a minority of cases involving the base. More than two thirds of these tumors involved the posterior half of the prostate gland.

Table 1. Grade Group distribution of each nodule group.

Nodule	N	GG1	GG2	GG3	GG4	GG5
T1	102 (100%)	9 (4 tert)	43 (7 tert)	28 (10 tert)	10 (1 tert)	12 (2 tert)
T1wo	34 (33%)	1 (1 tert)	12 (1 tert)	12 (4 tert)	3	6 (1 tert)
T1w	68 (67%)	8 (3 tert)	31 (6 tert)	16 (6 tert)	7 (1 tert)	6 (1 tert)
Tumor 2	68 (67%)	29 (2 tert)	32	7 (1 tert)	0	0
Tumor 3	32 (31%)	20	12	0	0	0
Tumor 4	11 (11%)	6	5	0	0	0

Numbers indicate counts of cases with that particular GG. Number of cases with a tertiary Grade is indicated within parentheses. T1wo: T1 nodule among cases without T2, T1w: T1 nodule among cases with T2

Table 2: Volume and distance of nodules from capsule and margin

Nodule	N	Volume (cc)	Capsule Distance (mm)	Margin Distance (mm)
T1	102 (100%)	16.7 ± 21.3	0.5 ± 0.6 (48)	0.9 ± 0.9 (75)
T1wo	34 (33%)	26.1 ± 30.9	0.5 ± 0.4	0.9 ± 1.0 (21)
T1w	68 (67%)	12.1 ± 12.2	0.5 ± 0.6	0.9 ± 0.9 (54)
Tumor 2	68 (67%)	2.9 ± 4.6	1.1 ± 1.1 (61)	1.7 ± 1.2 (62)
Tumor 3	32 (31%)	0.8 ± 1.2	1.2 ± 1.3 (32)	1.8 ± 1.5 (32)
Tumor 4	11 (11%)	0.5 ± 0.6	2.0 ± 1.3 (11)	2.3 ± 1.6 (11)

Table 3: T2 size (largest of multiple tumors per case)

T2 size (cm)	N (%)
≥ 2	6 (9%)
1.5 to 2	16 (24%)
1.0 to 1.5	18 (26%)
0.5 to 1.0	19 (28%)
<0.5	9 (13%)

Conclusions: 1. Two thirds of secondary tumor nodules are clinically significant based on Grade groups and warrant treatment. Although dominant tumor nodules are significantly larger than secondary nodules, we noted vast majority of secondary nodules to be greater than 0.5 cc in volume.

2. A significant difference is observed in distance of dominant tumor nodule from capsule compared to secondary nodules and this finding may be useful in more aggressive nerve sparing surgeries and focal therapy protocols were capsular tissue needs to be preserved.

1004 Expression of aromatase in tumor-related stroma is associated with human bladder cancer progression

Min Lu[1], *Shulin Wu*[2], *Zongwei Wang*[2], *Sharron X Lin*[2], *yingke liang*[3], *Aria F Olumi*[2], *Chin-Lee Wu*[4]. [1]Peking University Health Science Center, [2]Massachusetts General Hospital, [3]Massachusetts General Hospital, Boston, MA, [4]Newton Center, MA

Background: Putative gender difference in bladder cancer (BCa) has been proposed to result from sex hormone influence. Aromatase is the key enzyme catalyzing the conversion of androgens to estrogens which may result in an intratumoral microenviroment with increase of estrogen production. In this study, we investigated the pattern of aromatase expression in BCa and whether it is associated with BCa progression.

Design: Tissue samples from 88 BCa patients who underwent cystectomy were obtained. Using immunohistochemistry, expression of aromatase in tumor epithelium (TE) and tumor related stroma (TS) were evaluated separately, and the association of aromatase expression status with pathologic variables and overall survival (OS) outcome was examined.

Results: High aromatase expression was found in 33/88 (37.5%) of TE and in 65/88 (73.9%) of TS. Increased aromatase expression in TE was correlated with male gender. Increased aromatase in TS was significantly associated with adverse pathologic variables including higher pathologic pT, lymph node (LN) metastasis, lymphovascular invasion (LVI), and distant metastasis. In univariate analysis, high aromatase expression in TS was significantly associated with poor overall survival (p=0.014).

Conclusions: These results demonstrate that aromatase expression in TS may play a more critical role in BCa tumor progression than aromatase expression in TE. Our findings provide direct evidence of aromatase involvement in BCa and suggest endocrine therapy may have a potential role in the treatment of BCa.

1005 Immunohistochemical Characteristics of Renomedullary Interstitial Cell Tumor: A Study of 41 Tumors with Emphasis on Differential Diagnosis of Mesenchymal Neoplasms

Zhichun Lu[1], *Khaleel Al-Obaidy*[2], *Liang Cheng*[2], *David Grignon*[2], *Sean R Williamson*[3]. [1]Henry Ford Health System, Detroit, MI, [2]Indiana University School of Medicine, Indianapolis, IN, [3]Henry Ford Health System, Detroit, MI

Background: Renomedullary interstitial cell tumors (RMICT) are almost always incidentally identified either at autopsy or resection of the kidney for other reasons. However, rare cases have been reported which are large or clinically present as a mass lesion. The immunohistochemical phenotype of usual, incidental RMICT using modern soft tissue tumor markers in is largely unknown, however, providing little information to aid in classification of larger or atypical tumors.

Design: We retrieved 41 RMICTs from 37 patients who underwent kidney examination for other reasons (3/44 were no longer present on deeper sections and excluded). We studied pathologic characteristics including morphology, immunohistochemistry (S100, keratin AE1/AE3, smooth muscle actin, desmin, estrogen and progesterone receptors, calponin, CD34, CD35), and histochemical staining. Data collected included age, gender, tumor size, laterality, and indication for kidney examination.

Results: Forty-one RMICTs were identified in 24 male and 13 female patients, with mean age 57 years (range 24-83), tumor sizes ranged from <1 to 13 mm (median 4). Kidneys were resected for 33 tumors, 1 chronic pyelonephritis, 1 trauma, and 2 autopsies. Most (39, 95%) had entrapped renal tubules, 5 (12%) of which included cystic or dilated tubules. Most (35, 85%) had collagenous fibers that were negative for Congo red. Results are shown in Table 1.

IHC/HC Stains	-	+	++	+++	Positivity (%)
S100	41	0	0	0	0
AE1/AE3	41	0	0	0	0
α-SMA	12	17	11	1	71
Desmin	41	0	0	0	0
ER	16	22	3	0	61
PR	16	23	2	0	61
Calponin	2	6	32	1	95
CD34	31	8	2	0	24
CD35	41	0	0	0	0
Collagen	0	12	24	4	100
Alcian blue	5	7	25	4	88
Masson trichrome	0	1	17	23	100
Congo red	41	0	0	0	0

Conclusions: RMICT demonstrates a largely negative immunohistochemical phenotype with weak to moderate labeling for smooth muscle actin and calponin that is substantially less than myofibroblastic lesions. Positive staining for estrogen and progesterone receptor is common (61%), which could overlap with mixed epithelial and stromal tumor and other entities; however, staining is typically weak. CD34 is usually negative, with occasional weak labeling, in contrast to solitary fibrous tumor.

1006 Aggressive Chromophobe RCC (ChRCC) Are Molecularly and Immunochemically Separable From Indolent ChRCC

Shuhua Ma[1], *Nail Alouch*[2], *Monty Hawkins*[3], *Roberto Ruiz-Cordero*[2], *Lerong Li*[4], *Fumi Kawakami*[5], *Fadi Brimo*[6], *Jing Wang*[4], *Pheroze Tamboli*[7], *Kanishka Sircar*[7], *Priya Rao*[8]. [1]MD Anderson Cancer Center, Houston, TX, [2]MD Anderson Cancer Center, Houston, TX, [3]University of Texas MD Anderson Cancer Center, [4]MD Anderson Cancer Center, [5]The University of Texas MD Anderson Cancer Center, Houston, TX, [6]McGill University, Montreal, QC, [7]UT-MD Anderson Cancer Center, Houston, TX, [8]UT MD Anderson Cancer Center, Houston, TX

Background: Given the excellent oncologic outcomes associated with the large majority of ChRCC, the most germane question is determining which ChRCC are likely to recur or metastasize. Histologic assessment rarely provides useful information as to which ChRCC are likely to behave aggressively due to the absence of a validated grading system for ChRCC. Heretofore, molecular and immunohistochemcial characterization have only been performed on a handful of aggressive ChRCC. The aim of this study was to assess whether indolent ChRCC could be distinguished from aggressive ChRCC using molecular and immunohistochemical assays.

Design: We separated ChRCC into aggressive (defined as showing recurrence, local invasion, high stage, metastasis or sarcomatoid features) and indolent subtypes. We performed *in silico* analysis of public gene expression data to nominate the most differentially expressed genes between RO and ChRCC and genes associated with aggressive ChRCC. RNA was extracted from clinical FFPE tissues and the mRNA expression of these genes was assessed on 28 ChRCC (indolent = 14, aggressive = 14), using Nanostring's nCounter platform (Seattle, WA). Immunostains were performed with antibodies against CK7, CD117, CD10, vimentin and EMA.

Results: Aggressive ChRCC showed a distinctive gene expression profile that could be separated from indolent ChRCC using a limited number of mRNA (n=26 genes, P < 0.01) derived from clinical FFPE samples. Collagen genes (COL1A1, COL1A2, COL3A1, COL5A1, COL6A3) and matrix metalloproteinase genes (ADAM33, MMP2) were among the top 10 transcripts that were most overexpressed in aggressive ChRCC.

The immunohistochemical profile of aggressive ChRCC without sarcomatoid differentiation was different from that of indolent ChRCC in terms of CK7 expression. Among 4 aggressive ChRCC cases with

metastasis, CK7 expression is only present in rare cells in two cases, is negative in one case and strong and diffuse only in 1 case. Among 10 aggressive cases with high stage and local invasion but not metastasis yet, 5 cases showed focal expression of CK7.

Conclusions: Our data suggest that aggressive ChRCC can be distinguished from indolent ChRCC based on their immunohistochemical profiles and mRNA transcript expression profiles from clinical samples. Molecular profiling of ChRCC may help to stratify patients into surveillance (low risk ChRCC) versus treatment (high risk ChRCC) arms.

1007 Expanding the Clinicopathological Spectrum of Succinate Dehydrogenase-Deficient Renal Cell Carcinoma: 42 Novel Tumors in 38 Patients

Fiona Maclean[1], *Jesse McKenney*[2], *Ondrej Hes*[3], *Chia-Sui Kao*[4], *Carla L Ellis*[5], *John Turchini*[6], *Hemamali Samaratunga*[7], *Zwi Jonathan*[8], *Selina Bhattarai*[9], *Andrew Ryan*[10], *Michael Bonert*[11], *Xavier Leroy*[12], *L. Priya Kunju*[13], *Lauren Schwartz*[14], *Sean R Williamson*[15], *Admire Matsika*[16], *Priya Rao*[17], *Mukul Divatia*[18], *Rosa Guarch*[19], *Ferran Algaba*[20], *Fadi Brimo*[21], *Abbas Agaimy*[22], *Marcelo Balancin*[23], *Isabela W da Cunha*[24], *Ming Zhou*[25], *Kiril Trpkov*[26], *Anthony J Gill*[27]. [1]Douglass Hanly Moir Pathology, Macquaire Park, NSW, [2]Cleveland Clinic, Cleveland, OH, [3]Biopticka Laborator, Plzen, [4]Stanford University School of Medicine, Stanford, CA, [5]Emory University, Atlanta, GA, [6]University of Sydney, [7]Aquesta Pathology, Toowong, QLD, [8]adhb, [9]Leeds Teaching Hospital, Leeds, West Yorkshire, [10]Monash Medical Center, Melbourne, VIC, [11]McMaster University, [12]CHRU-LILLE, Lille, Hauts de France, [13]University of Michigan Hospital, Ann Arbor, MI, [14]University of Pennsylvania, [15]Henry Ford Health System, Detroit, MI, [16]Mater Hospital, [17]UT MD Anderson Cancer Center, Houston, TX, [18]Houston Methodist Hospital, [19]Complejo Hospitalario de Navarra, Pamplona, Navarra, [20]Fundacio Puigvert, Barcelona, [21]McGill University, Montreal, Quebec, [22]Friedrich-Alexander University Erlangen-Nuremberg, Erlangen, Bavaria, [23]University of Sao Paulo, Sao Paulo, [24]AC Camargo Cancer Center, Sao Paulo, SP, [25]Clements University Hospital, Dallas, TX, [26]University of Calgary, Calgary, AB, [27]University of Sydney, Greenwich, NSW, Australia

Background: Succinate dehydrogenase (SDH)-deficient renal cell carcinoma (RCC) is a rare subtype of renal cell carcinoma representing approximately 0.05-0.2% of all renal carcinomas (*Am J Surg Pathol* 2014; 38: 1588-602). As this is a relatively recently described tumor type, we sought to document additional cases seen across multiple institutions internationally.

Design: Collaborators with a special interest in urogenital pathology were invited to contribute RCCs with compatible morphology including intracytoplasmic inclusions, flocculent eosinophilic cytoplasm, cystic change and entrapped benign tubules. Following centralized review and SDHB IHC, only cases with loss of expression of SDHB were included. Putative prognostic factors including ISUP nucleolar grade, presence of coagulative necrosis and mitoses per 10 high power fields (hpfs) were recorded.

Results: The age range was 19 to 72 years, with a mean of 43.1 years, and a slight male predominance (male-to-female ratio 1.2:1). A relevant family history was identified in two patients only. Multifocal or bilateral tumors were identified in 4 patients. Tumors ranged in size from 10 to 200 mm in diameter (mean 81.2 mm). The morphologic growth patterns were in keeping with those previously described. Most tumors were of low ISUP nucleolar grade (Grade 1-2, 55%, Grade 3, 20%, and Grade, 4 25% [with focal pleomorphism only]), and had eosinophilic cytoplasm with the inclusion of at least focal cytoplasmic vacuoles or watery-appearing flocculent inclusions. Necrosis, which was often focal, was present in 26%. Loss of SDHA expression (implying SDHA mutation) was uncommon, being present in only 1 case. CK7 staining was only present focally in 1 case. Stage was pT1 in 36%, pT2 in 32% and pT3 or higher in 32%. One patient died of disease at 26 months after diagnosis. One patient was alive with lung metastases and another with retroperitoneal lymph nodes.

Conclusions: We document the clinicopathological spectrum of a novel series of 42 SDH-deficient RCCs occurring in 38 patients, which is the largest cohort assembled to date. We confirm that the recognition of these tumors rests on the morphology and the immunohistochemistry for SDHA and SDHB. Identification of such tumors necessitates long-term patient follow-up and surveillance, as well as potential genetic counselling and investigation of family members.

1008 A Series of 17 Cases of Primary MALT Lymphoma of the Bladder

Fiona Maclean[1], *Venu Chalasani*[2], *Warick Delprado*[3], *Migie Lee*[4], *Ross Brookwell*[5], *Jennifer J Turner*[6], *Ivan Burchett*[7]. [1]Douglass Hanly Moir Pathology, Macquaire Park, NSW, [2]University of Sydney, [3]Douglass Hanly Moir Pathology, McMahons Point, AUS, [4]Sydney University, [5]Sullivan Nicolades Pathology, [6]Douglass Hanly Moir Pathology and Macquarie University, Sydney, NSW, [7]Douglass Hanly Moir Pathology

Background: Primary lymphoma of the bladder is rare, with less than 100 cases of all types of lymphoma reported. Extranodal marginal zone lymphoma of mucosa-associated lymphoid tissue (MALT lymphoma) most commonly presents in the gastrointestinal tract (stomach in particular), but also occurs in other sites. Although it is the most common type of primary lymphoma reported in the bladder, the majority of reports are case reports or small case series. We aim to document further cases of MALT lymphoma of the bladder.

Design: Cases diagnosed as (or favouring) primary MALT lymphoma of the bladder were retrieved from the files of a single large institution over the period 2008-2017. The cases were reviewed and data including demographics, clinical presentation, histological appearances and immunoperoxidase findings were documented together with treatment given and the clinical outcome.

Results: 17 cases of primary MALT lymphoma of the bladder were identified - the largest series to date. The patients had an age range of 49 years to 93 years, and a male to female ratio of 1.4:1. Other series documented a female predominance. The majority had a long history of non-specific lower urinary tract symptoms or recurrent urinary tract infections. One patient had known sarcoidosis, and another had amyloidosis. In the majority of cases the cystoscopic appearance mimicked the red bladder seen in urothelial carcinoma-in-situ (CIS), with only 2 cases presenting as mass lesions. In our series the majority of cases showed plasmacytic differentiation (13 of 17, 76%). Lymphoepithelial lesions were present in only 42% of cases. Monotypic plasma cell differentiation was present in 72% (kappa in 43%, lambda in 29%). The cases were treated with chemotherapy, radiotherapy, surgical excision or a combination of modalities, with one patient refusing treatment. Although at other sites progression to diffuse large B cell lymphoma has been documented, in all of our cases in which follow up was available, the lymphoma behaved in an indolent fashion. FISH for MALT1 is proceeding.

Conclusions: This series of cases was presented with the aim of alerting the pathologist to a condition that may be readily overlooked. As the clinical impression is frequently one of Urothelial CIS, the pathologist might be tempted to focus on urothelial changes, thereby overlooking the atypical lymphoid infiltrate present. We document the histopathological features of 17 further cases, expanding the literature regarding this rarely reported entity.

1009 Correlation of PI-RADS in targeted prostate biopsy with pathologic features of prostate cancer

Andres G Madrigal[1], *Jenny Ross*[2], *Ximing Yang*[3]. [1]Northwestern University, Chicago, IL, [2]Feinberg School of Medicine, Chicago, IL, [3]Northwestern University, Chicago, IL

Background: Magnetic resonance imaging (MRI) of the prostate assists in the detection of lesions suspicious for malignancy to guide targeted biopsy. Lesions are scored from 1-5 in the Prostate Imaging Reporting and Data System (PI-RADS), with 1 as very low and 5 as very high suspicion for malignancy. Unlike standard prostate biopsies, involving 12 sites, MRI-targeted biopsies include less sites for pathology diagnosis and Gleason grading. We addressed the following questions; Is MRI based PI-RADS correlated with increased detection of prostate cancer? Are PI-RADS scores correlated with higher detection rates of higher grade cancer?

Design: We performed a 6 month review of all prostate biopsy cases and corresponding prostate MRI reports at our institution, including corresponding PI-RADS scores, type of biopsy procedure (standard 12 core biopsy, or targeted biopsy with or without non-target cores) and final pathology reports.

Results: The overall prostate cancer detection rate was 47% (226 cases /482 cases). Half of total cases had a prostate MRI prior to biopsy and had a cancer detection rate of 43% (102/240). Similarly, the cancer detection rate was 44% in patients without a prior prostate MRI (106/242). The cancer detection rate was 43% in the cases with targeted biopsy alone, and improved to 55% when additional non-targeted biopsies were collected. Radio-pathological correlation demonstrated increasing PI-RADS score was associated with increasing detection rates and PI-RADS scores (Table 1 and Figure 1). Importantly, a significant cancer detection rate of 38% (16/42) was also present in patients whose prostate MRI reports described no suspicious lesion or PI-RADS 1-2. High grade (Gleason≥7) and low grade (Gleason=6) prostate cancer was detected in 24% (10/42) and 14% (6/42), respectively, in this low suspicious group.

Table 1 Radiological pathological correlation of prostate MRI targeted imaging and Gleason score pathological diagnosis.

PI-RADS	Negative % (cases)	Gleason 6 (Grade 1) % (cases)	Gleason≥7 (Grade 2-5) % (cases)
0-2	62% (26/42)	14% (6/42)	24% (10/42)
3	64% (46/72)	10% (7/72)	26% (19/72)
4	42% (46/109)	19% (21/109)	39% (42/109)
5	18% (3/17)	18% (3/17)	65% (11/17)

PI-RADS: Prostate Imaging Reporting and Data System. PI-RADS 0 = no suspicious lesion and no PI-RADS score given.

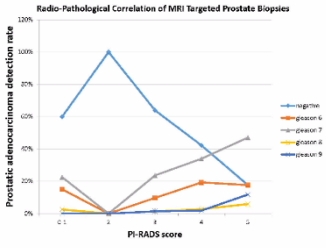

Conclusions: A higher PI-RADS score is correlated with a higher cancer detection rate and presence of high grade cancer. However, even no or low PIRADS scores have a significant cancer detection rate (38%), including the majority being with higher grade cancer (63%; 10/16) and presence of (24%) with high grade cancer. Relying on prostate MRI identified target biopsy alone is inferior to including additional non-targeted biopsies in detecting clinically significant cancer.

1010 Immunophenotypic Characterization of the Spectrum of Differentiation of Germ Cell Tumor-Derived Primitive Neuroectodermal Tumors

Martin J Magers[1], *Carmen M Perrino*[2], *Thomas Ulbright*[1], *Muhammad Idrees*[1]. [1]Indiana University School of Medicine, Indianapolis, IN, [2]Indiana University, Indianapolis, IN

Background: Primitive neuroectodermal tumors (PNETs) may arise as a secondary somatic-type malignancy in association with germ cell tumors (GCTs). In this setting, most PNETs resemble central nervous system PNETs and lack the chromosome 22 translocation of peripheral PNETs. However, description of the morphologic spectrum and differentiation potential of PNET arising from GCT is lacking in the literature. Here, we investigate the morphologic and immunohistochemical features of PNET, particularly with respect to neural and glial differentiation.

Design: Testicular PNETs were identified from the pathology archives of a large tertiary care academic center. Selected slides were reviewed by two study authors to identify whether a glial and/or neural component was present in association with the undifferentiated PNET. Immunohistochemistry for glial fibrillary acidic protein (GFAP), S100, synaptophysin, chromogranin A, and SOX11 was performed on tumors with available material; immunohistochemical stains were scored for both intensity (0-3) and quantity (0-3).

Results: Of 54 initially identified cases, 13 testicular PNETs with histologically identified differentiation were selected. The complete panel of GFAP, S100, synaptophysin, chromogranin A, and SOX11 was able to be performed in 10 tumors. SOX11 was the most sensitive marker with positive staining in the undifferentiated PNET component of all tumors (n=10, 100%) and was rarely positive in the differentiated component (n=1, 10%; focal & weak); synaptophysin was less sensitive in the undifferentiated component of tumors (n=12, 92%) versus SOX11 and was frequently positive in the differentiated component (n=5, 38%). GFAP and S100 were more frequently positive in the differentiated areas (83% and 77%, respectively) versus the undifferentiated areas (25% and 17%, respectively), and GFAP and S100 were usually both positive in the differentiated areas.

SOX11 is a sensitive immunohistochemical marker for testicular PNET, particularly PNETs which lack differentiation. Testicular PNETs may demonstrate glial and/or neural differentiation, and during the differentiation process S100 and GFAP expression are typically acquired while SOX11 is lost.

Conclusions: SOX11 is a sensitive immunohistochemical marker for testicular PNET, particularly PNETs which lack differentiation. Testicular PNETs may demonstrate glial and/or neural differentiation, and during the differentiation process S100 and GFAP expression are typically acquired while SOX11 is lost.

1011 Analysis of MYB-NFIB Gene Fusion in Prostatic Basal Cell Carcinoma/Adenoid Cystic Carcinoma: Clinicopathologic Correlates and Comparison with Basal Cell Hyperplasia/Adenoma

Martin J Magers[1], *Kenneth A Iczkowski*[2], *Rodolfo Montironi*[3], *David Grignon*[1], *Shaobo Zhang*[1], *Sean R Williamson*[4], *Ximing Yang*[5], *Mingsheng Wang*[6], *Adeboye O. Osunkoya*[7], *Ondrej Hes*[8], *John Eble*[1], *Liang Cheng*[1]. [1]Indiana University School of Medicine, Indianapolis, IN, [2]Medical College of Wisconsin, Milwaukee, WI, [3]Univ. Politecnica delle Marche /Medicine, Ancona, Marche, [4]Henry Ford Health System, Detroit, MI, [5]Northwestern University, Chicago, IL, [6]Indiana University, Carmel, IN, [7]Emory Univ/Medicine, Atlanta, GA, [8]Biopticka laborator, Plzen

Background: Prostatic basal cell carcinoma (BCC) is a malignant neoplasm composed of basaloid cells forming infiltrative nests and tubules which may potentially be misdiagnosed as florid basal cell hyperplasia/adenoma and also closely mimics adenoid cystic carcinoma (ACC) of the salivary gland. *MYB-NFIB* gene rearrangement occurs in 30-86% of salivary gland adenoid cystic carcinomas. We sought to further characterize *MYB* gene rearrangement in prostatic BCC and correlate *MYB-NFIB* fusion status with other clinicopathologic characteristics.

Design: FISH analysis for *MYB-NFIB* gene fusion using dual fusion probes was performed on formalin-fixed, paraffin-embedded tissue sections from BCC (n=30) and basal cell hyperplasia/adenoma (n=18).

Results: Fourteen of 30 (47%) cases of BCC were positive for *MYB-NFIB* gene dual fusion FISH, and no cases (0%) of basal cell hyperplasia/adenoma were positive ($p<0.05$). FISH-positive patients (mean age 61 years: range 35-81) tended to be younger than FISH-negative patients (mean age 69 years: range 55-93). Most FISH-positive cases demonstrated ACC-like morphology (67%, Figure 1), and most FISH-negative cases demonstrated non-ACC-like morphology (91%, Figure 2); one case (FISH-positive) demonstrated areas with both ACC-like and non-ACC-like morphology. FISH-positive cases more frequently demonstrated perineural invasion (58% vs 18%) compared to FISH-negative cases. Conversely, tall basal cells were more frequent in FISH-negative cases than FISH-positive cases (91% vs 33%, $p<0.05$, Figure 2).

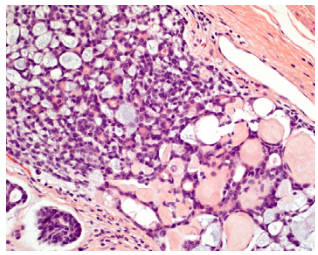

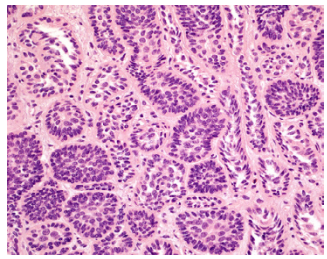

Conclusions: Approximately half of prostatic BCC harbor *MYB-NFIB* gene fusion. The majority of these cases were characterized by ACC-like morphology, perineural invasion, and lack of tall basal cells. Benign mimickers such as basal cell hyperplasia/adenoma are negative for *MYB-NFIB* gene fusion.

1012 Genomic Profile of Field Effects and Their Progression to Clinically Evident Bladder Cancer

Tadeusz Majewski[1], *Jolanta Bondaruk*[2], *Hui Yao*[3], *Sangkyou Lee*[3], *June-Goo Lee*[3], *Li Zhang*[4], *Charles Guo*[2], *Colin Dinney*[3], *David McConkey*[5], *Keith Baggerly*[3], *Bogdan Czerniak*[6]. [1]M. D. Anderson Cancer Center, Houston, TX, [2]UT-MD Anderson Cancer Center, Houston, TX, [3]The University of Texas MD Anderson Cancer Center, [4]University of Cincinnati, Cincinnati, OH, [5]Johns Hopkins University, [6]UT MD Anderson Cancer Ctr, Houston, TX

Background: Human bladder cancer is a model disease on which to perform the genomic characterization of mucosal field effects and how they evolve to clinically evident disease.

Design: We used a whole organ microscopic strategy coupled with exome sequencing, genome-wide copy number analysis and whole genome methylation to define the genomic profile of bladder cancer progression from field effects to clinically evident disease.

Results: We identified complex genomic alterations that involved areas of microscopically normal bladder mucosa adjacent to dysplasia and carcinoma *in situ*. They involved hypermethylated genes regulating several important oncogenic pathways such as RhoA and CDC42, as well as SIGIEC8 controlling inflammatory responses. Striking changes in the Senger mutational patterns were detected in field effects and involved those related to tobacco smoking, DNA missmatch, BRCA1/2, and APOBEC which competed in a manner of clonal evolution when the disease progressed to microscopically recognizable *in situ* changes and frank carcinoma. Reconstruction of the evolutionary tree disclosed at least 10 successive waves of clonal expansion in mucosal field effects which eventually evolved to a dominant clone of carcinoma *in situ*. Multifocal bladder cancers were closely related and originated from the same carcinoma *in situ* clone. Copy number variations were minimal in the field effects, but involved up to 200 genes including important oncogens such as SEPT14, GBAS, EPHB4 and CUX1 among others and increased dramatically in parallel to the disease progression.

Conclusions: The whole organ approach, combined with genomic characterization, provides unique insights into incipient events of bladder carcinogenesis and identifies novel mechanisms contributing to cancer initiation in its early clinical and microscopic occult phase. This strategy has significant implications for understanding the initiating events of bladder carcinogenesis and may provide novel targets for early cancer detection, treatment and prevention.

1013 Germ Cell and Trophoblastic Tumors Involving Kidney: Clinicopathologic Analysis With Proposed Classification

Faizan Malik[1], *Jatin S Gandhi*[2], *Ondrej Hes*[3], *Manju Aron*[4], *Michelle S Hirsch*[5], *Jae Y. Ro*[6], *Pilar Gonzalez-Peramato*[7], *Mahul Amin*[8]. [1]University of Tennessee Health Science Center, Memphis, TN, [2]University of Tennessee Health Science Center Memphis, Memphis, TN, [3]Bioptická laborator, Plzen, [4]Keck School of Medicine, University of Southern Ca, Los Angeles, CA, [5]Brigham and Women's Hospital, Boston, MA, [6]Houston Methodist Hospital, Cornell University, Houston, TX, [7]La Paz Hospital. Autonoma University of Madrid, Madrid, [8]Methodist University Hospital, Memphis, TN

Background: In recent years there has been considerable expansion of the spectrum of adult renal neoplasia with individual subtypes having clinical and therapeutic significance and recognition in the recent WHO classification of renal tumors. Little is known regarding germ cell tumors and trophoblastic differentiation in tumors involving the kidney.

Design: 12 putative cases involving the kidney were identified from the institutional and consultation files of the authors. Clinicopathologic and immunohistochemical analysis was performed to further understand these tumors.

Results: Germ cell and trophoblastic tumors involving the kidney were classified as: 1) primary germ cell tumors (GCT) of the kidney (n=2); 2) trophoblastic differentiation in primary carcinomas of the kidney (n=3); and 3) metastatic germ cell tumor to the kidney (n=1). 6 clear cell renal cell carcinomas (ccRCC) with nontumorous giant cells raising the possibility of ccRCC with syncytiotrophoblastic (ST) cells were excluded based on negative immunoreaction for β-hCG. Primary GCT of kidney included one case each of mature teratoma and placental site trophoblastic tumor (PSTT). The renal teratoma was diagnosed based on Beckwith criteria of the lesion confined within the renal capsule with absence of teratoma elsewhere, and with unequivocal heterotopic tissue other than renal tissue. The patient, a 57-year-old female with a 21 cm solid and cystic mass had histology of mature teratoma; with no evidence of metastatic disease (24 month follow-up). A 2.5 cm PSTT occurred in a 32-year-old female with elevated β-hCG levels. The patient had widespread metastases to lung, duodenum, and retroperitoneal space within 3 years of diagnosis. Trophoblastic differentiation occurred in three cases of invasive urothelial carcinomas of the renal pelvis (2 females, 1 male) which demonstrated numerous β-hCG positive STs. No other divergent differentiation was noted. The patient with metastatic germ cell tumor demonstrated exclusive choriocarcinoma histology in a 10 cm renal mass.

Conclusions: We describe herein the first series of germ cell and trophoblastic tumors involving the kidney with a proposed classification into 3 broad categories as outlined above. Although extraordinarily rare these tumors present as tumorous lesions, awareness of which is important while evaluating any renal tumor which is difficult to histologically classify based on the recently expanded WHO classification of renal tumors.

1014 Clinical, Morphologic, Immunohistochemical and Molecular Features of a Series of Primary Renal CIC-Rearranged Sarcomas

Shamlal Mangray[1], *David Kelly*[2], *Sophie Le Guellec*[3], *Eduard Fridman*[4], *Mary Shago*[5], *Andres Matoso*[6], *Rong Li*[2], *Kara A Lombardo*[1], *Jean-Michel Coindre*[7], *Siraj Ali*[8], *Gino R Somers*[5], *Evgeny Yakirevich*[1]. [1]Rhode Island Hospital, Providence, RI, [2]Children's of Alabama, Birmingham, AL, [3]Institut Claudius Regaud, Toulouse, Midi-Pyrrn, France, [4]Sheba Medical Center, Kfar-Sava, Israel, [5]The Hospital for Sick Children, Toronto, ON, Canada, [6]Johns Hopkins Hospital, Baltimore, MD, [7]Institut Bergonie, Bordeaux, France, [8]Cambridge, MA

Disclosures:
Siraj Ali: *Employee*, Foundation Medicine, Inc.

Background: Round and spindle cell sarcomas that resemble Ewing sarcoma/primitive neuroectodermal tumors (EWS/PNETs) of somatic soft tissues are recognized in the kidney. Examples of primary renal *CIC*-rearranged (*CIC*+) sarcomas, a form of *EWSR1* negative Ewing-like sarcomas characterized by fusion between the *CIC* and *DUX4* genes in the vast majority of cases, have also been described. Herein, we review the clinical, immunohistochemical and molecular features of a series of *CIC*+ sarcomas.

Design: The clinical presentation, imaging/gross, hematoxylin and eosin (H&E), immunohistochemical (IHC), molecular work-up, treatment and outcome of new cases along with our index case are reviewed. Semiquantitative IHC expression (intensity and extent) of markers reported to be useful in *CIC*+ sarcomas (WT-1, c-myc, ETV4, calretinin and DUX4) were compared to more widely used IHC stains (CD99 and NKX2.2) in the work-up of EWS/PNETs. Molecular testing included fluorescent in-situ hybridization (FISH), reverse transcriptase polymerase chain reaction (RT-PCR) and comprehensive genomic profiling (CGP) by next gene sequencing (NGS) on the FoundationOne platform.

Results: Three new cases in 3 females and the index case in a male occurring in a wide age range (9, 13, 32 and 83 years) were retrieved from multiple institutions (Table). Tumors ranged in size from 10-18 cm. There was a tendency for metastases and poor outcome, but treatment strategies differed (Table). Variable components of round cell (20-100%), spindle cell (0-80%) and plasmacytoid or rhabdoid morphologies (0-20%) were seen (Table). Two of 4 cases demonstrated WT1 nuclear positivity (3+, > 75%) while 2 demonstrated cytoplasmic positivity (3+ in 30% and >75%); DUX4 was positive in 2 of 4 cases (2+ and 3+, >75%); c-myc was positive in 1 case (2-3+, >75%); CD99 positivity was present in 3 cases (5%, 10% and 40-50%, and negative in 1 case; 1 case was focally calretinin (CAL) positive (2+, 30%) and all were NKX2.2 negative. CGP revealed a *CIC-DUX4* fusion in 2 cases, and a *CIC-NUTM1* fusion in 1 case that had been negative for *CIC-DUX4* fusion by RT-PCR. There was insufficient material for CGP in 1 case but it was DUX4 positive by IHC (Table).

Table. Clinical, immunohistochemical and molecular features in primary renal *CIC*-rearranged sarcomas.

Case Number	Age (years)/ Gender	Presentation and Gross/ Imaging Features	Histology	IHC Profile	Molecular Testing	Treatment and Course
Case 1 (index case)	9/male	Right 10 cm fleshy and myxoid cut surface, ~ 50% necrosis discovered in surveillance for previously treated stage 4 neuroblastoma	Round cells (~ 80%), spindle cells (~ 20 %), myxoid areas (~10%), no plasmacytoid or rhabdoid component, >20 mitoses/10 HPFs and necrosis	CD99+ (3+ 40-50%), WT-1+ (3+ >75% nu), CK+ (2+ 5%), CAL+ (2+ 30%), c-myc neg, ETV4 neg, DUX4 neg, NKX2.2 neg	CIC+ (193/200 cells) by FISH; CIC-DUX4 fusion (exon 18 of CIC, chr 19 and exon 1 of DUX4 on chr 10 by CG-P);EWSR1 neg and SYT neg by FISH	Primary resection (stage III, neg LNs), local radiation, chemotherapy (chemo) for Wilms tumor. Lung recurrence at 11 months, DOD at 18 months with lung and brain metastases (mets).
Case 2	13/female	Patient with history of juvenile rheumatoid arthritis found to have right 12.5 cm, 80% white fleshy and 20% cystic (blood) with associated hydronephrosis	Round cells (~ 80%), rhabdoid cells (~20%) with occasional nuclear pseudoinclusions, no spindle cells, 16 mitoses/10 HPFs and necrosis	CD99+ (3+ 10%), WT-1+ (3+ cyt, 30%), CK neg, c-myc, CAL neg, ETV4 neg, DUX4 neg, NKX2.2 neg	CIC-NUTM1 fusion (ex 16 chr 19 of CIC and exon 4-7 of NUTM1 on chr 15) by CGP; later CIC+ (161/200 cells) and NUTM1+ (128/200 cells) by FISH; CIC-DUX4 neg by RT-PCR	Primary resection showed involvement of renal sinus without renal vein (stage II) involvement. Chemo using Ewing protocol. Patient is alive 2 years after diagnosis
Case 3 (needle biopsy)	32/female	Right 18 cm by US with involvement of renal vein and IVC after presentation with hematuria	Spindle cells (80%) and round cells with prominent nucleoli (20%), and 13 mitoses in 10 HPFs on needle biopsy	WT1+ (3+ >75% nu), c-myc+ (2-3+ >75%), DUX4+ (3+ >75%), CD99 neg, CK neg, CAL neg, ETV4 neg, NKX2.2 neg	CIC+ (169/200 cells) by FISH Insufficient material for CGP by RNA sequencing	Resection post chemo using Ewing protocol with > 90% response but patient died of complications.
Case 4	83/female	Left 16 cm heterogenous mass with necrosis and thrombosis of renal vein. Increased from 5 cm on CT 3 months earlier for work-up of abdominal pain.	Round cell morphology (100%) with necrosis, 20 mitoses per 10 HPFs, and no spindle cell component	WT1+ (3+ >75% cyt), ETV4+ (3+ > 90%), DUX4+ (2+ >75%), CD99+ (5%), c-myc neg, CAL neg, NKX2.2 neg	CIC+ (>20% cells) by FISH; CIC-DUX4 (ex20 of CIC and ex 1 of DUX4 on chr 10) by CGP	Primary resection at 3 months from initial presentation, no evidence of mets, but mets to lung found a month later. No chemo and DOD 6 months after initial presentation.

Conclusions: *CIC*+ sarcomas rarely occur in the kidney and testing by FISH or NGS is optimal to avoid missing cases with variant fusion partners as demonstrated in our *CIC-NUTM1* case. Although this is a small series, these tumors tend to have an aggressive clinical course as is reported in peripheral soft tissue cases.

1015 RNA Expression Profiling of Lymphoepithelioma-like Carcinoma of the Bladder

Ujjawal Manocha[1], *Jordan Kardos*[2], *Jonathan Epstein*[3], *William Y Kim*[4], *Sara E. Wobker*[5]. [1]University of North Carolina, [2]University of North Carolina, Chapel Hill, NC, [3]The Johns Hopkins Med Inst, Baltimore, MD, [4]University of North Carolina at Chapel Hill, [5]UNC Chapel Hill, Chapel Hill, NC

Background: Lymphoepithelioma-like carcinoma of the bladder (LELC-B) is a rare variant consisting of undifferentiated epithelial cells within a dense lymphocytic infiltrate. Pure/predominant LELC has shown better overall survival, but the mechanism for this finding is not yet understood. The use of basal/luminal subtypes in urothelial carcinoma have emerged as prognostic markers and may predict response to treatment. Our aim was to profile and analyze the RNA expression of LELC-B tumors and identify prognostic markers that could better inform patient care.

Design: Cases were identified by a search of the pathology laboratory information system of two institutions for cases of "lymphoepithelioma-like carcinoma" involving the bladder from 2000-2017. Formalin-fixed paraffin-embedded tissue was retrieved for each case and initial H&E slide was cut followed by 10 unstained slides for RNA extraction. RNA was extracted with the Roche High Pure RNA Paraffin kit protocol, library prepped with the Illumina TruSeq RNA Access Library Prep Kit, sequenced on an Illumina NextSeq500, and processed through a STAR-Salmon data pipeline. The samples were analyzed in reference to TCGA Bladder Cancer dataset (n=408). Samples were then classified using BASE47 PAM bladder subtype predictor and subtype specific differences were identified.

Results: 16 cases were identified with FFPE tissue available for study. 14 cases had sufficient RNA yield following extraction. Sequencing analyses reconfirmed IHC results via expression of MMR proteins and PD-L1. BASE47 PAM Classification yielded an equal number of LELC-B cases correlating to the basal and luminal centroid, n=7. This result was consistent with hierarchical clustering performed on immune gene signatures. Further confirming the existence of innate subtypes, there were significant transcriptomic differences between the luminal LELC-B and the basal LELC-B samples.

Conclusions: Our prior work has shown that LELC-B shows high expression of PD-L1 by IHC, which was confirmed by RNA sequencing. While morphologically these tumors are highly immune infiltrated, transcriptomic profiling of the samples indicates they are more biologically heterogeneous than initially hypothesized. In other tumors, such as breast and bladder, basal and luminal subtypes predict outcomes and response to treatment. Our future studies will focus on elucidating whether subtype specific differences in LELC-B can better inform patient care.

1016 The Adverse Prognostic Impact of Cribriform Morphology in Prostatic Adenocarcinoma is Independent of PTEN Status

Alexander Maris[1], *Shanna A Arnold*[2], *Omar Hameed*[1], *Lan Gellert*[3], *Giovanna A Giannico*[1]. [1]Vanderbilt University Medical Center, Nashville, TN, [2]Vanderbilt University Medical Center, Nashville, TN, [3]Vanderbilt Univ Med Ctr, Nashville, TN

Background: Cribriform (CRIB) morphology is a strong predictor of aggressive clinical course and biochemical recurrence (BCR) in prostate cancer compared to other pattern 4 morphologies. Loss of tumor suppressor protein phosphatase and tensin homologue (PTEN) is implicated in progression to androgen independence and unfavorable clinical outcome. We explored the association between PTEN expression by immunohistochemistry (IHC) and CRIB vs. non-CRIB Gleason pattern 4 morphology.

Design: Seventy-six radical prostatectomies for adenocarcinoma Gleason 4+4=8 (Grade Group 4) were evaluated by IHC for PTEN. We have previously established concordance of our PTEN IHC and FISH status. Intraductal carcinoma was ruled out by p63 IHC in selected cases with CRIB morphology. PTEN in ≥ 10% of cells was defined as positive. Statistical analysis was performed with SPSS 23 for Windows.

Results: CRIB, poorly formed/fused (PF/F) and glomeruloid (GLOM) patterns were present in 57/67 (86%), 50/67 (75%) and 14/67 (21%) cases. Most cases presented multiple patterns [49/67 (73%)]. Mean percent CRIB was 43.7%. PTEN was positive in 35/57 (61%) CRIB, 30/50 (60%) PF/F and 10/14 (71%) GLOM cases with no significant difference between pattern 4 morphologies (P=0.725). Heterogeneous PTEN was present in 15/67 (22%) cases. Heterogeneous PTEN was associated with CRIB compared to non-CRIB morphology when controlling for presence or absence of PTEN (P=0.028). CRIB was associated with an increased risk of BCR compared to non-CRIB morphology after adjusting for pathologic stage (OR=1.93, P=0.002). Co-presence of GLOM morphology in patients with either CRIB (OR 0.298, P=0.088) or PF/F (OR 0.094, P=0.037) decreased risk of BCR after controlling for stage. Co-presence of PF/F did not affect BCR in patients with CRIB (P=0.244).

Conclusions: This study validates the current literature showing increased risk of BCR in patients with CRIB morphology. Although PTEN loss and CRIB morphology are both associated with unfavorable clinical outcome, we demonstrated that PTEN expression is not associated with any specific pattern 4 morphology, suggesting that the adverse effect of CRIB morphology is independent of PTEN loss. Heterogeneous PTEN expression was associated with CRIB morphology. Finally, we show that GLOM morphology is protective against BCR.

1017 Sensitivity and specificity of the biopsy diagnosis of intraductal carcinoma and invasive cribriform carcinoma and its impact on pathological staging using a prospectively collected dataset

Mehdi Masoomian[1], *Andrew J Evans*[2], *Joan Sweet*[1], *Carol Cheung*[3], *Theodorus van der Kwast*[1]. [1]University Health Network, Toronto, ON, [2]Toronto General Hospital, Toronto, ON, [3]Markham, ON

Background: Intraductal carcinoma (IDC) and invasive cribriform carcinoma (ICC) at biopsy are increasingly employed as independent prognosticators of tumour stage and prognosis. So far no studies were conducted on the concordance of biopsy and prostatectomy diagnosis of IDC and ICC. Information on the sensitivity and specificity of biopsy diagnosis of IDC and ICC using prostatectomy findings as a golden standard might impact the utility of these new parameters.

Design: Since November 2015, presence or absence of IDC and ICC were separate mandatory fields of synoptic reporting of prostate biopsies and radical prostatectomy (RP) specimens in our institution. Reporting on prostate samples is done by 4 dedicated subspecialty pathologists. A search of our laboratory information system revealed 141 patients who had both prostatic biopsy and the corresponding RP specimen diagnosed until September 2017. Patient age, ISUP grade group (GG), presence or absence of IDC and ICC in biopsies and prostatectomy specimens, pathological stage and lymph node status at RP were recorded. IDC and ICC recorded for RP were considered the gold standard.

Results: Median age at diagnosis was 62 years. GG distribution was GG1 in 15%, GG2 in 60%, GG3 in 15% and GG4-5 in 10%. IDC and ICC, respectively were reported in 14 (10%) and 33 (23%) of biopsies and in 36 (26%) and 62 (44%) of RP specimens. Sensitivity of the biopsy diagnosis of IDC was 36% (13/36), of ICC 44% (27/62), of both IDC and ICC 24% (6/25), and either IDC or ICC 52% (38/73). Specificity of biopsy diagnosis of IDC, ICC, IDC and ICC in combination and of IDC or ICC was 99%, 94%, 100% and 98%, respectively. Ten patients were N+ at RP. Of 6 patients with a biopsy reporting both IDC and ICC, 4 (biopsy GG2 in 1, GG3 in 3 patients) had a lymph node metastasis. Pathological stage distribution differed significantly (Chi-square p< 0.02) between the 65 patients with biopsy GG2 without (72% pT2, 18% pT3a and 9% pT3b) and the 19 patients with IDC or ICC (37% pT2, 42% pT3a and 21% pT3b).

Conclusions: Sensitivity of prostate biopsies for detection of IDC and ICC in this contemporary patient series is low, but specificity is very high (>90%). In spite of low sensitivity, biopsy IDC and ICC was strongly associated with extraprostatic extension at radical prostatectomy. Improved targeting of biopsies might improve the sensitivity of biopsy diagnosis for IDC and ICC.

1018 Assessment of Mismatch Repair, ERG and PTEN Status in Young Age Prostate Cancer Patients

Mehdi Masoomian[1], *Susan Prendeville*[2], *Theodorus van der Kwast*[1], *Michelle Downes*[3]. [1]University Health Network, Toronto, ON, [2]Cork University Hospital, Cork, Cork, [3]Sunnybrook Health Sciences Centre, Toronto, ON

Background: Prostate cancer is the most frequent solid organ malignancy in men but the incidence rate in males <50 is only 1%. Most young age patients who undergo radical prostatectomy have a favourable outcome and over-representation of mucinous histology has been reported. The molecular basis of this unusual subgroup has yet to be fully investigated. As an initial step we sought to evaluate the mismatch repair (MMR) status, ERG expression and PTEN loss by immunohistochemistry (IHC) in a cohort of patients treated with radical prostatectomy (RP).

Design: A retrospective search of the laboratory information system identified 159 males, <50 years with conventional acinar adenocarcinoma treated by RP between 2001-2015. A triplicate core microarray (0.6mm cores) was created with malignant and benign epithelium from each case. Sequential sections were stained using ERG, PTEN, MSH2, MSH6, MLH1 and PMS2 antibodies. ERG was scored as present/absent. PTEN was scored as positive when >90% of tumor showed cytoplasmic staining equal or greater in strength to background benign glands/stroma. The MMR proteins were assessed as retained/lost.

Results: The median age of the cohort was 47 years. The grade group distribution was: 1- 39%, 2-47.2%, 3-10%, 4-1.25%, 5-1.25% with two cases with marked hormone therapy effect (no Gleason score assigned). Negative staining for ERG was seen in 42.1% (n=67) with loss of PTEN expression in 41.7% (n=65). 22% of cases showed both ERG and PTEN loss. MLH-1 exhibited the highest level of loss of expression of the MMR proteins at 30.2% (n=48) and PMS2 the lowest at 3.1% (n=5). MSH2 and MSH6 loss were 8.8% (n=14) and 10% (n=16) respectively.

Four cases demonstrated combined MSH2/MSH6 loss and three cases combined MLH1/PMS2 loss.

Conclusions: Young age prostate cancer represents an uncommon disease with poorly understood molecular pathogenesis. Herein we

demonstrate a similar rate of ERG and PTEN loss by IHC which is somewhat lower than reported in the literature. Approximately 4% of cases have patterns of MMR deficiency suggestive of defective DNA repair and additionally loss of at least one MMR protein is noted in one third of patients. Further molecular investigation of this cohort is warranted.

1019 A Subset of Lipid-rich Urothelial Carcinoma Show MDM2 Immunostaining and Amplification by FISH

Andres Matoso[1], *Morgan L Cowan*[2], *Debra Saxe*[3], *Adeboye O. Osunkoya*[4], *Jonathan Epstein*[5]. [1]Johns Hopkins Hospital, Baltimore, MD, [2]Baltimore, MD, [3]Emory University School of Medicine, Atlanta, GA, [4]Emory Univ/Medicine, Atlanta, GA, [5]The Johns Hopkins Med Inst, Baltimore, MD

Background: Lipid-rich urothelial carcinoma is rare and characterized by the lipoblast-like cells and poor outcome. A previous study has shown that they share molecular alterations of urothelial carcinoma, express cytokeratins and have intracytoplasmic lipid ultrastructurally. Whether these tumors show molecular alterations characteristic of well-differentiated liposarcoma has not been previously studied.

Design: Review of the pathology files of 2 major academic institutions identified 19 cases of urothelial lipid-rich urothelial carcinoma from 1991 through 2017. All cases had at least one representative H&E slide for review. Additional material to perform immunohistochemistry (IHC) stains were available in 10 cases. FISH for MDM2 amplification was performed in 8 cases.

The cohort included 12 men and 7 women and the specimens included 17 TURBTs and 2 cystectomies. The mean age at presentation was 71 years old (range 54-93). All cases were invasive high-grade urothelial carcinoma. In 8 (42%) cases the tumor invaded the muscularis propria (MP), in 5 (26%) invasion limited to the lamina propria, and in 6 (32%) invasion was ambiguous for muscularis mucosae versus MP. Lymph nodes were negative in both cystectomy specimens. All cases had cells with vacuolated cytoplasm and large indented nuclei, often eccentrically located characteristic of lipoblasts. The percentage of the tumor involved by lipid-rich morphology varied from 2% to 30% (mean 8%) and was always surrounded by conventional urothelial carcinoma. An exophytic papillary component was present in 9 (53%) and in-situ carcinoma in 2 (11%). Additional variant morphologies included micropapillary (n=4), glandular (n=3), squamous (n=1), and sarcomatoid carcinoma (n=1). The lipid-rich areas were GATA3(+) in 7/7 (100%), adipophilin(+) in 7/7 (100%), AE1/AE3(+) in 4/7 (57%), p63(+) in 3/7 (43%), and MDM2(+) in 5/10 (50%). FISH for MDM2 amplification was positive in 4/5 (80%) cases that were MDM2(+) by IHC and negative in 3/3 (100%) of cases that were MDM2(-) by IHC.

A subset of lipid-rich urothelial carcinomas show MDM2 nuclear expression by IHC and amplification by FISH. Our findings raise the issue whether lipid-rich carcinomas should be classified as a sarcomatoid urothelial carcinoma with focal transdifferentiation to liposarcoma. However, in contrast to most sarcomatoid urothelial carcinomas the liposarcoma component tends to be focal and may still be best classified as a variant of urothelial carcinoma.

1020 Neuroglial Neoplasms in Testicular Germ Cell Tumors Lack Evidence of Mutations Characteristic of Their CNS Counterparts: An Immunohistochemical Study of 12 Cases

Andres Matoso[1], *Muhammad Idrees*[2], *Fausto Rodriguez*[3], *Carmen M Perrino*[4], *Thomas Ulbright*[2], *Jonathan Epstein*[5]. [1]Johns Hopkins Hospital, Baltimore, MD, [2]Indiana University School of Medicine, Indianapolis, IN, [3]Johns Hopkins Univ, Baltimore, MD, [4]Indiana University, Indianapolis, IN, [5]The Johns Hopkins Med Inst, Baltimore, MD

Background: Overgrowth of neuoglial tissue is rare in testicular germ cell tumors and mostly reported as isolated cases.

Design: We retrospectively reviewed 12 cases of testicular germ cell tumors from 2 institutions from 1995-2017. H&E slides were collected and reviewed. Immunohistochemistry (IHC) was performed in all cases with available material.

Results: The series included 3 primary tumors and 9 metastases, including 8 retroperitoneal and 1 axillary lymph node (LN). The average age was 35 (range 19-54). Four of the LN dissections were post-chemotherapy, with one a recurrence 5 years after the initial diagnosis. The average tumor size for primary tumors was 4.4 cm (range 1.7-7) and for metastases was 6.4 cm (range 0.6-15). The largest size of the neuroglial component was 0.9 cm in the primary tumors and 6.5 cm in metastatic sites. The neuroglial component in the primary site was associated with pure teratoma (n=2) and with a mixed germ cell tumor (teratoma, seminoma and embryonal carcinoma) (n=1). Cases involving lymph nodes were associated with teratoma (n=4), seminoma (n=2), rhabdomyosarcoma (n=2), PNET (n=1), and high grade sarcoma (n=1) (some with >1 other component). One case was a pure glial tumor. Histologically, the neuroglial components included low grade astrocytoma (n=2) (both with microcysts formation and pilocytic features), gemistocytic astrocytoma (n=3), anaplastic astrocytoma (n=2) (with gliosarcoma transformation in 1 case), diffuse astrocytoma (n=1), ganglioglioma (n=2), glioblastoma (n=1), and developing CNS (n=1). By IHC, 10/10 (100%) cases were GFAP(+), 9/9 (100%) cases showed retained ATRX, 9/9 were IDH1 pR132H (-), 1/9 (11%) was p53(+), 1/9 (11%) was BRAFmut p.V600E(+). No mutation was identified in the BRAF+ case by PCR. Follow-up was available in 5 patients; 4 were confirmed to have received chemotherapy with BEP; 1 had a local recurrence and the patient with gliosarcoma developed a lung metastasis of poorly differentiated sarcoma morphologically similar to the sarcomatoid component of the retroperitoneum.

Conclusions: Neuroglial tumors are rare in testicular germ cell tumors and are most commonly associated with teratomas; they can be seen in primary and metastatic sites. They exhibit the full range of neuroglial differentiation including developing CNS to glioblastomas, gliosarcomas and gangliogliomas. None of the cases showed results consistent with *ATRX*, *IDH* or *BRAF* mutation, suggesting they have different oncogenic mechanisms than their CNS counterparts.

1021 PD-L1 Expression Correlates with Lack of Response to BCG Therapy in Non-Muscle Invasive Bladder Cancer

Andres Matoso[1], *Alexander Baras*[2], *Max Kates*[3], *Trinity J Bivalacqua*[4], *Ashley Cimino-Mathews*[1], *Jonathan Epstein*[5]. [1]Johns Hopkins Hospital, Baltimore, MD, [2]Johns Hopkins, Baltimore, MD, [3]Johns Hopkins Hospital, [4]Johns Hopkins University, Baltimore, MD, [5]The Johns Hopkins Med Inst, Baltimore, MD

Background: Immunotherapy with BCG is the standard of care for patients with non-muscle invasive urothelial carcinoma (NMIUCa). Anti- PD-1/PD-L1 therapy is approved for patients with metastatic urothelial carcinoma who fail cisplatin. However, the role of PD-1/PD-L1 pathway and the immune microenvironment in NMIUCa has not been studied yet.

Design: Tissue samples from patients with NMIUCa, including pre- and post- BCG samples were used to construct tissue microarrays (TMAs) with 3 spots of tumor per case. Immunohistochemistry (IHC) for CK5/6, CK20, uroplakin, GATA3, CD4, CD8, POXP3, CD68, PD-1 were performed on sections from TMAs. Whole slide sections were used for PD-L1 IHC using the SP142 assay. Any stain of 5% of tumor area was considered positive.

Results: The cohort included 60 men and 6 women. Mean age was 69 (range 38-93). All specimens were TURBs. 38 (58%) patients responded favorably to BCG and 28 (42%) did not. There was no difference between BCG responders and non-responders in the expression of CK5/6, CK20, uroplakin, GATA3, CD4, CD8, FOXP3, PD-1 and CD68. All responders were PD-L1(-) in the pre- and in the post-BCG specimens. 7/28 (25%) of non-responders were PD-L1(+) in the pre-BCG specimens and 5 additional cases showed stain that was <5% (P=0.01). After BCG, 3/7 remained PDL-1(+), 1 converted to PD-L1(+), and 3 converted to PD-L1(-). Within non-responders PD-L1(+) cases, pre-BCG specimens had a similar number of CD8(+) and FOXP3(+) tumor infiltrating lymphocytes (TILs) but significantly lower number of CD4(+) TILs when compared to non-responders PD-L1(-) cases (P<0.01). After BCG, the non-responders PD-L1(+) showed similar number of CD4(+) and CD8(+) TILs but higher number of FOXP3(+) TILs than the non-responders PD-L1(-) cases (P=0.05).

Conclusions: Expression of common urothelial markers by IHC was not different in BCG-responders vs. non-responders. A subset of patients who do not respond to BCG therapy express PD-L1 in pre-BCG specimens, a finding not seen in responders. Higher FOXP3(+) TILs in non-responders post BCG samples suggests these subtypes of TILs may be involved in lack of response to BCG by suppressing antigen priming of T-lymphocytes. Overall, our results suggest that therapy targeting PD-1/PD-L1 pathway could be used alone or in combination with BCG to potentially delay or abort disease progression in patients who do not respond to conventional BCG therapy.

1022 p53 Status in the Primary Tumor Predicts Efficacy of Subsequent Abiraterone and Enzalutamide in Castration-Resistant Prostate Cancer

Benjamin Maughan[1], *Liana Benevides Guedes*[2], *Kenneth M Boucher*[3], *Emmanuel S Antonarakis*[4], *Tamara L Lotan*[5]. [1]Johns Hopkins School of Medicine, [2]Johns Hopkins University School of Medicine, Baltimore, MD, [3]Huntsman Cancer Center, Salt Lake City, UT, [4]Johns Hopkins University School of Medicine, [5]Johns Hopkins School of Medicine, Baltimore, MD

Background: We tested whether tissue-based analysis of p53 and PTEN genomic status in primary tumors is predictive for subsequent sensitivity to abiraterone and enzalutamide in castration-resistant prostate cancer (CRPC).

Design: We performed a retrospective analysis of 309 consecutive patients with CRPC treated with abiraterone or enzalutamide. Of these, 101 men (33%) had available primary tumor tissue for analysis. We screened for deleterious *TP53* missense mutations and *PTEN* deletions

using genetically validated immunohistochemical assays for nuclear accumulation of p53 protein and PTEN protein loss, with sequencing confirmation of *TP53* mutations in a subset. Overall survival (OS) and progression-free survival (PFS) were compared between patients with and without p53 and/or PTEN alterations.

Results: 48% of evaluable cases had PTEN loss and 27% had p53 nuclear accumulation. OS and PFS did not differ according to PTEN status, but were significantly associated with p53 status. Median OS was 16.7 months (95% CI, 14.00–21.9 months) and 31.2 months (95% CI, 24.5–43.4) for men with and without p53 nuclear accumulation, respectively (HR 2.32; 95% CI 1.19–4.51; P=0.0018). Similarly, median PFS was 5.5 months (95% CI, 3.2–9.9 months) and 10.9 months (95% CI, 8.0–15.2 months) in men with and without p53 nuclear accumulation, respectively (HR 2.14, 95%CI 1.20–3.81; P=0.0008). In multivariable analyses, p53 status was independently associated with PFS (HR 2.15; 95% CI 1.03—4.49; P=0.04) and a HR of 2.19 for OS (95% CI 0.89—5.40; P=0.087).

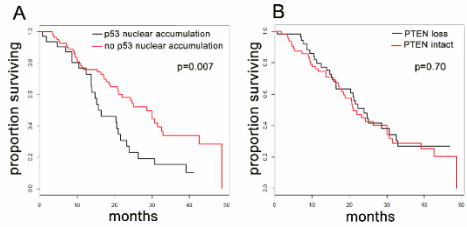

Conclusions: p53 inactivation in the primary tumor (but not PTEN loss) may be predictive of inferior outcomes to novel hormonal therapies in CRPC.

1023 PD-L1 Immunoreactivity and Immune Pathway Markers in Urothelial Carcinoma

Tristan F McKnight[1], *David Tacha*[2], *Ahmed Shabaik*[3], *Donna Hansel*[4]. [1]UC San Diego, San Diego, CA, [2]Biocare Medical, Pacheco, CA, [3]Univ. of California, San Diego, San Diego, CA, [4]UCSD, La Jolla, CA

Disclosures:
David Tacha: *Employee,* Biocare Medical

Background: PD-L1 immunoreactivity in tumor and immune cells has been used to predict response of cancers to checkpoint inhibition, although cases that lack PD-L1 expression have also been shown to respond at a lower frequency. Thus, other elements of the immune response pathway may be critical in regulating response to therapy independent from PD-L1 expression. To determine which immune response components could be potential candidates for future testing, we analyzed PD-L1, CD4, CD8, CTLA-4 and FoxP3 expression on tumor and/or immune cells in urothelial carcinoma, a cancer type in which checkpoint inhibition has been shown to improve overall survival in advanced disease.

Design: We analyzed 115 invasive conventional urothelial carcinomas from cystectomy specimens using predilute antibodies (Biocare Medical, Concord, CA) targeting PD-L1, CTLA-4, FoxP3, CD4 and CD8. Expression on lymphoctyes was scored as positive for negative for CTLA-4, FoxP3, CD4 and CD8 and as an H-score [intensity (0-3) x percent positive cells] for PD-L1 on immune cells and tumor cells. Correlation analysis was performed using Pearson's Correlation Coefficient and significance was designated as P<0.05.

Results: PD-L1 expression was identified in tumor cells in 60/115 cases (52%) and on immune cells in 78/115 cases (68%). Tumor cell and immune cell PD-L1 expression was correlated with other immune pathway markers. CTLA-4 was present in 36/115 cases (31%) and was not signficiantly associated with PD-L1 expression on tumor (r=-0.133) or immune cells (r=0.112). FoxP3, expressed by regulatory T cells, was present in 78/115 cases (65%) and was significantly correlated with CD8 tumor infiltrating lympocytes (TILs; r=0.349, P<0.05), but not PD-L1 tumor expression (r=0.212). CD4 and CD8 expressing lymphocytes were present in 95/115 cases (83%) and 105/115 cases (91%), respectively. The presence of CD4+ TILs significantly correlated positively with both PD-L1 expression in tumor cells (r=0.436; P<0.05) and PD-L1 H-score in tumor cells (r=0.451; P<0.05). Presence of CD8 positive lymphocytes did not signficantly correlate with PD-L1 expression.

Conclusions: PD-L1 expression in urothelial carcinoma demonstrates a range of expression in urothelial carcinoma, although the factors that influence expression in individual cases remains unclear. The current study demonstrates a potential relationship between CD4-positive TILs and expression and intensity of PD-L1 expression in tumor cells.

1024 PD-L1 Expression Highlights Key Differences in Expression between Urothelial Carcinoma Variants

Tristan F McKnight[1], *David Tacha*[2], *Ahmed Shabaik*[3], *Donna Hansel*[4]. [1]UC San Diego, San Diego, CA, [2]Biocare Medical, Pacheco, CA, [3]Univ. of California, San Diego, San Diego, CA, [4]UCSD, La Jolla, CA

Background: Quantitative expression of PD-L1 has been robustly studied in urothelial carcinoma (UCa), given its relative sensitivity to checkpoint inhibition. However, expression levels in UCa variants have not been extensively analyzed. This is critical given that several variants follow an aggressive course and/or may be less responsive to conventional forms of therapy. In addition, several variants have been historically excluded from clinical trials and these patients may benefit from immunotherapy options.

Design: We used a recently developed PD-L1 antibody (Biocare Medical, Concord, CA) at predilute concentrations to analyze PD-L1 expression in tumor cells using semi-quantitative (H-score; intensity (0 to 3) x % positive tumor cells; range 0-300) analysis over 4 tumor regions. Immune cell immunoreactivity was assessed as positive/negative irrespective of location relative to tumor cells. UCa variant morphology included 34 cases of divergent differentiation (29 cases squamous differentiation, 5 cases glandular differentiation), 12 cases of micropapillary UCa, 8 cases of sarcomatoid UCa, and 5 cases of plasmacytoid UCa.

Results: Expression of PD-L1 in tumor cells varied by UCa variant. Sarcomatoid UCa was robustly positive in tumor cells as compared to other variant subtypes (8/8; 100%; P<0.05) with an H-score of 212. The majority of cases of UCa with divergent differentiation were positive (21/34; 62%), although with a relatively lower H-score of 87. Micropapillary UCa and plasmacytoid UCa showed more restricted expression of PD-L1 in tumor cells, with both a low percentage of positive cases and a low H-score component. Immune cell infiltrate positive for PD-L1 included both lymphocytes and dendritic cells and included both tumor infiltrating immune cells and stromal-situated immune cells. All subtypes demonstrated some degree of immune cell expression in UCa subtypes, although micropapillary UCa demonstrated dense expression within stromal lymphocytes in all cases.

PD-L1 Expression in UCa Variants

Variant	Cases expressing PD-L1 in tumor cells	H-score (average)	Cases expressing PD-L1 in immune cells
Divergent differentiation	21/34 (62%)	87	17/34 (50%)
Micropapillary	3/12 (25%)	6.25	5/12 (42%)
Sarcomatoid	8/8 (100%)	212	1/8 (13%)
Plasmacytoid	1/5 (20%)	60	2/5 (40%)

Conclusions: UCa variants show a range of PD-L1 expression. Whereas tumor cell expression of PD-L1 is robust in sarcomatoid UCa, PD-L1 expression in lymphocytes is robust in micropapillary UCa. These two variants may be of especial interest to include as potential candidates in immunotherapy studies focused on UCa. Further analysis of immune cell subtype and location may be warranted in these cases.

1025 Solid pseudopapillary neoplasm (SPN) of the testis: Comprehensive mutational analysis of 4 testicular and 8 pancreatic SPNs

Kvetoslava Michalova[1], *Michael Michal*[2], *Monika Sedivcova*[3], *Dmitry Kazakov*[4], *Tatjana Antic*[5], *Ondrej Hes*[6], *Michal Michal*[7]. [1]Biopticka laboratory, Plzen, Czech Republic, [2]Charles University, Prague and Biomedical Center, in Pilsen, Charles University, Czech Republic, Plzen, [3]Biopticka laborator, s.r.o., Plzen, Czech Republic, [4]Bioptical Laboratory SVO, Pilsen, CZE, [5]The University of Chicago, Chicago, IL, [6]Biopticka laborator, Plzen, [7]Bioptical Laboratory s.r.o., Plzen

Background: Recently, we came with the theory of a possible relationship between a group of testicular and pancreatic tumors. We used one case of a testicular tumor termed „pancreatic analogue solid pseudopapillary neoplasm of the testis (PA-SPN)" which was composed partially of areas identical to solid pseudopapillary neoplasm (SPN) of the pancreas and partially of structures identical to the primary signet ring stromal tumor of the testis (PSRSTT) as a connecting link between these two entities. After demonstrating that PSRSTT and PA-SPN share the same immunoprofile and genetic features characteristic for pancreatic SPN, we came to conclusion that PSRSTT and PA-SPN represent a morphological spectrum of a single entity and that both are related to the pancreatic SPN.

Design: The aim of this study is to present a series of 4 cases of testicular tumors which lacked the signet ring cell component and were thus morphologically very similar to the SPN of the pancreas. Besides immunohistochemical analysis, our main goal is to compare the genetic background of these testicular tumors that are obviously

related to the PSRSTT/PA-SPN with the series of 8 pancreatic SPN.

Results: The mutational analysis revealed the oncogenic somatic mutation in the exon 3 of the *CTNNB1* (β-catenin) gene in all testicular (4/4) and pancreatic (8/8) tumors. The immunoprofile (positivity with β-catenin, CD 10, vimentin, NSE, CD56 and negativity with inhibin, calretinin, chromogranin) of the testicular and pancreatic tumors was the same as well.

Conclusions: This study expanded the morphological spectrum of the PSRSTT/PA-SPN by adding 4 cases without signet ring cell component. Considering the obvious analogy of PSRSTT/PA-SPN/SPN of the testis and their relationship to the pancreatic SPN we propose the collective term "solid pseudopapillary tumors of the testis" for these tumors. The genotype of the SPN of the testis and pancreas appeared to be the same in both groups of tumors which we consider as a final proof that SPN of the testis is identical to the SPN of the pancreas.

1026 Mixed germ cell sex cord-stromal tumors of the testis: 4 cases with features supporting the neoplastic nature of the germ cell component

Kvetoslava Michalova[1], *Michael Michal*[2], *Dmitry Kazakov*[3], *Ondrej Hes*[4], *Michal Michal*[5]. [1]Biopticka laborator, Plzen, Czech Republic, [2]Charles University, Prague and Biomedical Center in Pilsen, Charles University, Czech Republic, Plzen, [3]Bioptical Laboratory SVO, Pilsen, Czech Republic, [4]Biopticka laborator, Plzen, [5]Bioptical Laboratory s.r.o., Plzen

Background: The existence of the mixed germ cell sex cord-stromal tumors of the testis (MGSCT) has been repeatedly questioned. Some investigators consider these lesions sex cord stromal tumors with entrapped non-neoplastic germ cells, a standpoint based on the marked discrepancy between testicular and ovarian MGSCT, with the latter being a widely accepted entity. The "non-seminomatous" appearance of the germ cells and their immunohistochemical negativity with PLAP, c-kit and OCT4 in testicular MGCST allegedly support their non-neoplastic origin. We present 4 testicular MGSCT exhibiting either invasion into the adjacent structures and/or revealing atypical mitoses in the germ cell component, indicating that these are authentic neoplasms.

Design: 8 cases of testicular MGSCT were reviewed and 4 cases with either invasion into the adjacent structures and/or atypical mitoses in the germ cell component were selected. Immunohistochemistry for PLAP, c-kit and OCT3/4 was performed.

Results: All patients were karyotypically normal men with the age ranging 27-74 years. In 3 patients follow-up was uneventful, while the remaining patient died from an unrelated cause. All tumors had a similar biphasic morphology characterized by various proportions of the sex cord component resembling granulosa cell tumor of adult type and the germ cell component cytomorphologically akin to the spermatocytic tumor. Germ cells were haphazardly scattered throughout the tumor or arranged in larger groups, without tubular formation. In all cases, germ cells revealed atypical mitoses. Additionally, in 2 cases there was invasion into the funiculus spermaticus and into the tumor capsule, respectively. In each case, the invasive structures contained both tumor components. All cases were negative with PLAP, c-kit and OCT3/4.

Conclusions: The identification of the intrafunicular and intracapsular invasion of both components of MGSCT together with the finding of atypical mitoses in germ cells serve as a strong argument for the neoplastic nature of the germ cell component. The blastic appearance of the germ cells together with PLAP, c-kit and OCT4 negativity point towards their possible analogy with spermatocytic tumor cells rather that seminoma cells characteristic for the ovarian MGSCT.

1027 Therapy Resistant Metastatic Testicular Pure Seminoma: a Comprehensive Genomic Profiling Study

Sherri Z Millis[1], *Julia A Elvin*[2], *Jo-Anne Vergilio*[3], *James Suh*[4], *Shakti Ramkissoon*[5], *Laurie Gay*[6], *Eric Severson*[7], *Sugganth Daniel*[1], *Jon Chung*[1], *Alexa B Schrock*[8], *Siraj Ali*[9], *Ryan Hartmaier*[1], *Garrett M Frampton*[1], *Lee Albacker*, *Vincent A Miller*[1], *Philip M Stephens*[1], *Jeffrey S Ross*[1]. [1]Foundation Medicine, [2]Foundation Medicine, Inc, Cambridge, MA, [3]Foundation Medicine, Inc, Cambridge, MA, [4]Foundation Medicine, Inc., Morrisville, NC, [5]Foundation Medicine, Morrisville, NC, [6]Foundation Medicine, Cambridge, MA, [7]Foundation Medicine, Inc, Morrisville, NC, [8]Foundation Medicine, Cambridge, MA, [9]Cambridge, MA

Disclosures:
Sherri Millis: *Employee*, Foundation Medicine, Inc.
Jo-Anne Vergilio: *Employee*, Foundation Medicine, Inc.
James Suh: *Employee*, Foundation Medicine, Inc.
Shakti Ramkissoon: *Employee*, Foundation Medicine, Inc.
Laurie Gay: *Employee*, Foundation Medicine, Inc.
Eric Severson: *Employee*, Foundation Medicine, Inc.
Jon Chung: *Employee*, Foundation Medicine, Inc.
Alexa Schrock: *Employee*, Foundation Medicine, Inc.
Siraj Ali: *Employee*, Foundation Medicine, Inc.
Ryan Hartmaier: *Employee*, Foundation Medicine, Inc.
Philip Stephens: *Employee*, Foundation Medicine, Inc.
Jeffrey Ross: *Employee*, Foundation Medicine, Inc.

Background: Although pure seminomas (PS) of the testis are classically associated with a favorable prognosis, on occasion these tumors will pursue an aggressive clinical course. We performed comprehensive genomic profiling (CGP) to learn whether refractory metastatic PS (mPS) would harbor opportunities for targeted and immunotherapies.

Design: Tissue from 22 mPS patients was assayed by hybrid-capture based CGP evaluating all classes of genomic alterations (GA) including base substitutions, indels, amplifications, copy number alterations, fusions/rearrangements) and targeted therapy opportunities. Tumor mutational burden (TMB) was calculated from a minimum of 1.11 Mb sequenced DNA and reported as mutations/Mb. Microsatellite instability status (MSI) was determined by a novel algorithm from the sequencing data.

Results: The 22 mPS had a median age of 42 years (range 22 to 78 years). The primary tumor was sequenced in 9 (41%) and a metastasis biopsy in 13 (59%) including lymph nodes, bone, liver and lung. Four (18%) of mPS had syncytial trophoblast cells identified on routine histology and bHCH immunostaining. CGP identified three genomically defined subgroups. Group I: chromosome 12p12-13 amplicon GA, primarily amplification in at least 5 of 10 genes (*KDM5A, KRAS, CCND2, RAD52, FGF23,* F*GF6, PIK3C2G, CDKN1B, LRP6*, and/or *CHD4*), were seen in 36% (8) of the cohort. Group II: *KIT* GA found in 5 (23%) of mPS. Two of the *KIT* altered patients also had *KRAS* single base (SV) alterations, and one patient had a just a *KRAS* SV alteration. Group III: 8 (36%) of mPS were undefined by common alterations, with the exception of 2 patients with *PREX2* amplifications; however, 5 patients had either amplification or SV in a single gene in chromosome 12 (p or q). Demographic trends included a slightly younger age on average for the chromosome 12p group (39 yo) vs. the other two groups (43 yo). Two (9%) of mPS featured a TMB high status including a tumor in the chromosome 12p Group I and one in the ill-defined group III had an intermediate TMB; the remaining (91%) of the mPS were TMB-low. All (100%) of the mPS were MSI stable.

Conclusions: Genomic profiles of tumors from patients with mPS reveal genomically distinct subgroups, which may inform clinical trials and different treatment options. These findings may contribute to a better understanding of different pathways of oncogenesis of clinically aggressive pure seminomas and may ultimately define novel systemic treatment options.

1028 Reduced ERG expression in vascular endothelial cells of renal cell carcinoma; a novel marker of tumor progression and poor prognosis

Ahrim Moon[1], *Saetbyeol Lee*[2]. [1]Soonchunhyang University Bucheon Hospital, Bucheon, Gyeonggi-do, [2]Soonchunhyang University Bucheon Hospital

Background: Renal cell carcinoma (RCC) is the third most common urological malignancy. ERG, an ETS family transcription factor, is known to be expressed in endothelial cells, and oncogenic ERG gene fusions occur in subsets of prostatic carcinoma, acute myeloid leukemia, and Ewing sarcoma. ERG expressed throughout the life of the endothelium, regulates multiple pathways involved in vascular homeostasis and angiogenesis. We found that intratumoral vascular endothelial cells in some subset of RCC showed reduced ERG expression. The aims of this study were to evaluate ERG expression of endothelial cells in RCC specimen, and to determine the association of this protein with clinicopatholgic factors and its prognostic significance.

Design: Immunohistochemical staining for ERG and CD34 was performed for 184 cases of clear cell RCC (ccRCC), 14 cases of papillary RCC (pRCC), 13 cases of chromophobe RCC (ChRCC) and 3 cases of oncocytoma. The grade of ERG staining was defined as follow: negative, no staining or faint staining in ≤ 50% of intratumoral endothelial cells; equivocal, faint staining in > 50% of intratumoral endothelial cells; positive, strong staining in > 50% of intratumoral endothelial cells. We investigated whether ERG expression correlated with clinicopathological parameters and patient outcomes.

Results: The vascular endothelial cells of normal kidney showed consistently strong nuclear ERG immunoreactivity. ERG expression in ccRCC were 52.7% (n=97), 14.1% (n=26) and 33.2% (n=61) as negative, equivocal and positive staining, respectively. In 13 cases of ChRCC, 10 cases (76.9%) were ERG negative and 2 cases (15.4%) were ERG equivocal. Otherwise just 3 cases (21.3%) of pRCC were ERG negative and none of oncocytoma was ERG negative. ERG expression loss in ccRCC and ChRCC are more frequent than pRCC (p=0.027 in ccRCC vs. pRCC, p=0.007 in ChRCC vs. pRCC). In ccRCC, loss of ERG expression was significantly related to higher disease stage ($p = 0.011$). Univariate analysis showed that loss of ERG expression was significantly

associated with poor progression free survival and poor overall survival (p = .027 and .004, respectively).

ERG	ccRCC (n)	pRCC (n)	ChRCC (n)	Oncocytoma (n)
Negative	52.7% (97)	21.3% (3)	76.9% (10)	0% (0)
Equivocal	14.1% (26)	42.9% (6)	15.4% (2)	0% (0)
Positive	33.2% (61)	35.7% (5)	7.7% (1)	100% (3)
Total	100% (184)	100% (14)	100% (13)	100% (3)

Conclusions: Our results suggested that loss of ERG expression is associated with tumor progression and is a significant prognostic marker for patients with ccRCC.

1029 Prostate Specific Membrane Antigen (PSMA) Expression in Vena Cava Tumor Thrombi of Clear Cell Renal Cell Carcinoma Suggests a Role for PSMA-driven Tumor Neoangiogenesis

Giuliano Morgantetti[1], *Keng L Ng*[2], *Hemamali Samaratunga*[3], *Handoo Rhee*[4], *Glenda Gobe*[5], *Simon Wood*[4]. [1]University of São Paulo, Ribeirão Preto, SP, [2]University of Queensland, Annerley, QLD, [3]Aquesta Pathology, Toowong, QLD, [4]Princess Alexandra Hospital, [5]University of Queensland

Background: Clear cell renal cell carcinoma (ccRCC) is a malignant renal neoplasm with a peculiar propensity to propagate as tumor thrombus in the renal vein, inferior vena cava and occasionally up into the right atrium. Prostate specific membrane antigen (PSMA) is a glycoprotein extensively used in prostate cancer diagnostics. It is expressed in a variety of non-prostate cancers, including renal carcinomas. PSMA has been used in immunohistochemical and radiological studies as a useful vascular marker for solid tumors, but has not been investigated in tumor thrombi of the vena cava with ccRCC as the primary renal lesion.

Design: The objective of this study is to determine the differences of morphological patterns, microvessel density and immunohistochemical staining of PSMA in Clear Cell Renal Cell Carcinoma between tumor and vena caval tumor thrombi. 202 patients diagnosed with RCC were surgically treated at Princess Alexandra Hospital (Queensland, Australia). Of these cases, 131 consisted of ccRCC, of which ten presented with intravenacaval (IVC) tumor thrombus extension. Renal tumor and leading edge of the neoplastic thrombus (invasive front) tissues were collected from these patients. CD34 was the preferred pan endothelial immunohistochemical marker. Immunohistochemical reactions for CD34 and PSMA were performed using standard protocols.

Results: Immunostaining for PSMA and pan-vascular marker CD34 were noted in the neovasculature of tumor thrombi (Figures 1C and 1D, respectively) and renal tumor tissue (Figures 1A and 1B, respectively). A comparison between morphological patterns and microvessel density of tumor thrombi and its corresponding renal tumor mass was performed, with a posterior analysis of the difference between intensity and positive pixel counts of vascular marker CD34 and PSMA. There was a statistically significant increase (60%, Figure 2) in PSMA/CD34 positive pixel count ratio in tumor thrombus tissue when compared to renal tumor tissue, indicating increased neovascular expression of the protein in the tumor thrombi. No difference was noted between morphological patterns, necrosis or microvessel density.

Variables	Group	Average	St Dev	Median	Est diff	Confid Int (95%)		P-value*
Vessel Number (HotSpot)	Thrombus	74,3	47,38	52,5	-45,9	-102,9	11,114	0,1019
	Tumor	120,2	46,36	117,5				
Vascular Area (HotSpot)	Thrombus	52086,62	32302	49759,15	3308,4	-19564	26181	0,751
	Tumor	48778,21	20511	46933,07				
PSMA (HotSpot)	Thrombus	0,47	0,15	0,5	-0,025	-0,161	0,1113	0,6888
	Tumor	0,49	0,07	0,5				
CD34 (HotSpot)	Thrombus	0,29	0,11	0,28	0,0395	-0,057	0,136	0,3784
	Tumor	0,25	0,07	0,25				
PSMA/CD34 (HotSpot)	Thrombus	1,66	1,29	1,22	0,9469	0,1295	1,7644	0,0278
	Tumor	0,71	0,25	0,69				
PSMA (10 HPF Avg)	Thrombus	0,32	0,16	0,33	-0,049	-0,185	0,086	0,4309
	Tumor	0,37	0,08	0,39				
CD34 (10 HPF Avg)	Thrombus	0,19	0,11	0,16	0,0236	-0,064	0,111	0,556
	Tumor	0,16	0,06	0,18				
PSMA/CD34 (10 HPF Avg)	Thrombus	0,74	0,26	0,71	0,2704	0,0884	0,4523	<0,01*
	Tumor	0,47	0,16	0,46				
CD34 (Total)	Thrombus	0,3	0,17	0,28	-0,067	-0,202	0,0687	0,2937
	Tumor	0,37	0,07	0,37				
PSMA (Total)	Thrombus	0,18	0,11	0,18	0,0325	-0,063	0,1276	0,4593
	Tumor	0,15	0,06	0,14				
PSMA/CD34 (Total)	Thrombus	0,64	0,2	0,64	0,2323	0,0718	0,3927	<0,01*
	Tumor	0,4	0,15	0,39				

Legend: (1) HotSpot, the most vascular field analyzed; (2) Average values obtained from 10 high powered fields (10 HPF Avg); (3) Total slide section positive pixel analysis. St Dev – Standard Deviation; Est Diff – Estimated difference; Confid Int – Confidence interval.

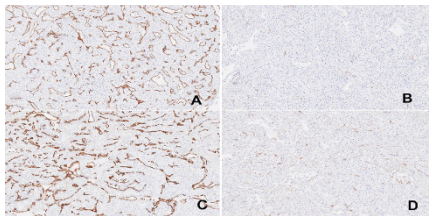

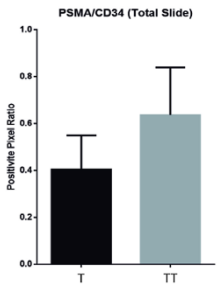

Conclusions: The leading tumor front (tumor thrombi) showed a proportional increase in PSMA expression in relation to CD34, when compared with the intraparenchymal renal neoplasm, supporting possible mechanism for PSMA in neoangiogenesis in ccRCC and therefore indicate its usefulness as a biomarker of neoangiogenesis and for future diagnostic and therapeutic advancements.

1030 A Molecular Profile of Clear Cell Papillary Renal Cell Carcinoma by Next Generation Sequencing

Diana Morlote[1], *Soroush Rais-Bahrami*[2], *Shuko Harada*[3], *Jennifer Gordetsky*[4]. [1]University of Alabama at Birmingham Dept. of Pathology, [2]University of Alabama at Birmingham, [3]Univ. of Alabama at Birmingham, Birmingham, AL, [4]The University of Alabama at Birmingham, Birmingham, AL

Background: Clear cell papillary renal cell carcinoma (CCP-RCC) is a rare entity comprising ~1% of all renal cell neoplasms. It was described in 2009 as being associated with end-stage renal disease, however, most cases have been found to be sporadic. As a result of its rarity, CCP-RCC is a poorly understood entity. The aim of this study is to explore the molecular characteristics of this tumor by performing targeted next generation sequencing (NGS) of 16 cases of CCP-RCC, which to our knowledge, is the largest cohort sequenced to date.

Design: Sixteen morphologically and immunohistochemically typical cases of CCP-RCC were selected and genomic DNA was extracted from tumor areas of FFPE samples. Ninety cancer-related genes were target-enriched using Agilent HaloPlexHS custom probe. Sequencing was performed on the Illumina MiSeq platform and the result was analyzed using PierianDX informatics pipeline. Known polymorphisms and variants of unknown significance (VUS) were excluded from the results.

Results: Fifteen somatic non-synonymous variants were identified across six of the 16 cases sequenced. Five variants (33%) were previously documented in other tumors (COSMIC database) (Table). Nine variants (60%) were predicted to be deleterious by either the SIFT or Condel prediction algorithms, three (20%) were predicted to be neutral or tolerated and three (20%) did not have a prediction score. The repeatedly found genes with significant variants were *ATM* (three cases, 19%), *BRCA2* and *VHL* (two cases, 13% each). One potentially actionable variant was identified in the *EGFR* gene (p.V765M, case#3), which has been reported in cases of lung adenocarcinoma as well as hematopoietic malignancies.

FOR TABLE DATA, SEE PAGE 403, FIG. 1030

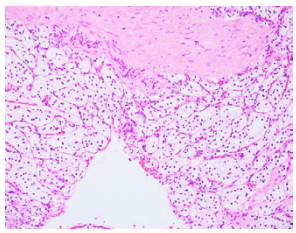

Conclusions: We identified 15 non-synonymous somatic variants in 16 CCP-RCC cases, none of which had been reported in CCP-RCC. No two cases shared the same variant. This may be a reflection of the lack of disease specific variants in CCP-RCC. The cases with *VHL* variants were clearly morphologically and immunophenotypically (strong diffuse positivity for CK 7 and CA 9) distinct from conventional clear cell renal cell carcinoma. Our study is the first one to report somatic *VHL* variants in cases of CCP-RCC. Further studies to characterize the molecular profile of CCP-RCC are warranted.

1031 Variation in Nuclear Size and PD-L2 Positivity Correlate with Aggressive Chromophobe Renal Cell Carcinoma

Mohamed Mostafa[1], *Anjishnu Banerjee*[2], *Daniel Rowan*[3], *Amrou Abdelkader*[4], *Kenneth A Iczkowski*[3]. [1]MCW, Wauwatosa, WI, [2]Medical College of Wisconsin, [3]Medical College of Wisconsin, Milwaukee, WI, [4]Wauwatosa, WI

Background: More frequent use of needle biopsy to sample renal tumors brings a need for prognostic measures. The Int'l Society for Urologic Pathology currently recommends against grading chromophobe carcinoma (PMID:24025520), although a nuclear grading scheme had been proposed (PMID:20679882). PD-L2 but not PD-L1, has been suggested to bear prognostic value in chromophobe cancer (PMID:28353093).

Design: Chromophobe cancers with adverse pathology or outcome were matched based on size to controls, all pT ≤3a and without recurrence/metastasis after >5 yr ("good outcome"). Any sarcomatoid component was an exclusion criterion.

Excluding any nuclei with degenerative features **(Fig.)**, the greatest dimensions of the largest and smallest nuclei in 5 random high-power fields were measured by linear micrometer; their ratio was expressed as variation in nuclear size (**VNS**). The % multinucleate (≥2 nuclei) cells (**PMC**) was counted among ≥300 cells in 3 random fields. % necrosis and mitotic activity were assessed. PD-L2 (mouse monoclonal, R&D Systems) result was dichotomized as weak to negative vs. strong membranous/cytoplasmic. These results were analyzed by linear mixed model, and PD-L2 positivity by Fisher's exact tests.

Results: 15 cases with adverse features included 8 women and 7 men ages 46-79: 5 primary (3 p3Ta, 2 p3Tb), 2 local recurrences, 4 metastatic sites only, 3 paired primary (Stages p1a, 3a, and 3b) and metastases, and 1 paired biopsy and metastasis. 15 controls were 5 women and 10 men ages 24-81 with stages pT1 (7), pT2 (7), and pT3a (1). Primary tumor size ranged from 5-15 cm in cases and 3-14 cm in controls. VNS and PMC results are shown (**Table**). VNS of 2.8 formed an absolute cut-point between adverse and non-adverse groups.

PD-L2 for those cases with available blocks was strong in 4/9 primary tumors with adverse outcome, 5/6 metastatic sites, and 3/15 primary tumors with good outcome. Metastatic site tumors alone (p=.01), or grouped with primary tumors with adverse outcome (p=.03), had stronger PD-L2 than controls. For adverse-outcome vs. good-outcome primary tumors, the difference was not significant (p=.2).

Tumor:	VNS	p	PMC	p
Primary tumor (adverse)	3.2±.2	<.001	5.5±1.0	.98
Metastatic site	3.4±.4	<.001	3.9±1.1	.17
Primary tumor (control)	2.3±.2		5.5±0.6	

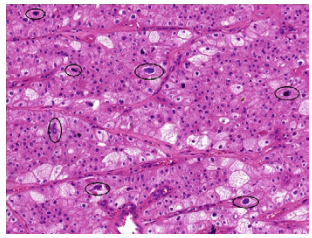

Conclusions: Variation in nuclear size may impart prognostic information in chromophobe renal cell carcinoma, suggesting that a basis for grading this tumor could be re-considered. We confirmed that strong PD-L2 staining correlated with outcome and, more strongly, with metastasis. However, its reactivity in < 50% of primary renal chromophobe carcinomas—good or adverse—may limit its use.

1032 PREVIOUSLY PUBLISHED

1033 Loss of Androgen Receptor Accompanied by Paucity of PD-L1 in Prostate Cancer is Associated with Clinical Relapse

Jerry Nagaputra[1], *Aye Aye Thike*[1], *Valerie Koh*[2], *Puay Hoon Tan*[3]. [1]Singapore General Hospital, [2]Singapore, [3]Singapore

Background: The incidence of prostate cancer has markedly increased in Asia, especially in Singapore. Programmed death-1 (PD-1) is an immune checkpoint molecule which is activated by binding to its ligand PD-L1 resulting in reduced T-cell activation facilitating disease progression. Androgen receptor (AR) is a nuclear receptor whose interaction with androgen modifies the biology of prostate cancer. Different studies investigating PD-1, PD-L1 and AR in prostate cancer have yielded conflicting results with regard to their expression and effect on prognosis.

Design: The cohort comprised 211 prostate cancers diagnosed from 2005 to 2008. Tissue microarrays (TMAs) were constructed from radical prostatectomy specimens. Immunohistochemistry was performed using antibodies to PD-1, PD-L1 and AR on TMA sections. Positive biomarker expression was defined as cytoplasmic membrane staining of 1% or more of tumor cells and tumor infiltrating lymphocytes (TILs) for PD-1 and PD-L1, and a H-score of 50 or more for AR nuclear expression. Follow-up data were obtained from case records and survival outcomes were estimated with the Kaplan–Meier method.

Results: PD-L1 expression in tumor cells and TILs was observed in 21% and 7% of cases respectively. PD-1 expressed only in TILs, accounting for 6% of cases. AR expression was detected in 39% of tumors. No significant correlation was observed between biomarker expression and clinicopathological parameters. Follow up ranged from 1 to 149 months (mean 92 months and median 109 months). Clinical recurrence was observed in 8 (3.8%) cases, of which 7 (3.3%) patients presented with bone metastasis and 1 case (0.5%) with metastasis to the lung, liver and kidney. Thirty (14.2%) patients had biochemical recurrence. Disease-specific death occurred in 4 (1.9%) patients. Although individual biomarkers were not associated with outcomes, patients whose tumors harbored negative expression of both AR and PDL-1 disclosed unfavorable disease-free survival (p=0.037) and a trend for poorer overall survival (p=0.055). These biomarkers, however, did not show significant impact on biochemical recurrence in our series.

Conclusions: Our study demonstrates that loss of both AR and PD-L1 expression in prostate cancer in a Singapore series is associated with unfavorable outcome. Expression of these biomarkers in combination may therefore serve as useful prognosticators of prostate cancer.

1034 Characterization of Male Urethral Strictures to Predict Recurrence

Manando Nakasaki[1], *Jill C Buckley*[2], *Donna Hansel*[3]. [1]UCI, San Diego, CA, [2]UC San Diego, San Diego, CA, [3]UCSD, La Jolla, CA

Background: Male urethral strictures are relatively uncommon but problematic, as many patients undergo extensive surgical management and still experience recurrence. Histopathological characterization of these strictures has been limited and it is unclear what factor(s) may predict recurrence.

Design: We evaluated 47 patients to determine features associated with recurrence. Histopathological features included extent of resection, inflammation score (0-3), fibrosis score (0-3), surface alterations, erosion, occlusion of subepithelial vessels, edema, and scar formation. Follow-up was 79 mo; no difference in follow-up was evident for recurrence (R) and non-recurrence (NR) patients (P=0.11).

Results: Most patients experienced stricture of unknown etiology (17/47; 36%); other major causes included trauma (15/47; 32%) and prior procedure (11/47; 23%). Of patients evaluated, 15 experienced recurrence and 32 remained disease-free on extended follow-up. There was no difference between R and NR patients for age (P=0.58), prior intervention (P=0.15), or etiology. Strictures most commonly affected the bulbar urethra (27/47; 57%), with other cases involving the membranous urethra (5/47; 11%), pendulous urethra (2/47; 4%); distal urethra/meatus (3/47; 6%); and bladder neck (1/47; 2%). Nine cases involved multiple regions of the urethra (20%). No significant difference in regional localization was present between R and NR groups. The majority of cases were treated with anastomotic urethroplasty (27/47; 57%), followed by urethroplasty with buccal graft (11/47; 23%). Histopathological review revealed the extent of resection was significantly associated with recurrence. Specifically, presence of resected corpus spongiosum was significantly greater in NR patients (24/32; 75%) versus in R patients (6/15; 40%); P=0.02. Similarly, specimens that contained extensive urethral (Littre) glands were also associated with reduced recurrence (R 1/15; 7% versus NR 13/32; 41%; P=0.02). No other significant differences in other histopathological features between these two groups were identified.

Conclusions: Male urethral strictures often represent clinically challenging cases in which little is known regarding factors predictive of recurrence. We identify that extensive resection of underlying inflammatory and fibrotic tissue to deeper layers is associated with reduced risk of recurrence. Further analysis on cellular factors associated with stricture formation may further define these risk factors in the future.

1035 Molecular Heterogeneity of Bladder Cancer: Identification and Clinico-Pathologic Evaluation of a Previously Uncharacterized Mixed Baso-Luminal Subtype Using CK5/6 and GATA3 Immunohistochemistry

Aejaz Nasir[1], *Beverly Falcon*[2], *Dan Wang*, *Mia Y Chen*[1], *Julia Carter*[3], *Larry Douglass*, *Bronislaw Pytowski*[4], *Rebecca Hozak*[2], *Amit Aggarwal*[1], *Katherine Bell-McGuinn*[1], *Richard Walgren*[2], *Aafia Chaudhry*[2], *Andrew Schade*[2]. [1]Eli Lilly & Co., Indianapolis, IN, [2]Eli Lilly & Co., [3]Wood Hudson Cancer Research Laboratory, NewPort, KY, [4]Eli Lilly, New York, NY

Background: Molecular subtyping of bladder cancer (BC) into basal, luminal and neuronal (latest TCGA data, Lerner S, ASCO 2017) has emerged as a major advance in the field. While development and validation of single-specimen classifiers is still under active investigation (Seiler R, ASCO-GU Cancers Symposium 2017), clinical implementation of broad molecular signatures will need cross-platform and clinical validation studies and refinement into smaller biomarker panels. Immunohistochemistry (IHC) is an important methodology to implement promising molecular subtyping biomarkers into surgical pathology reporting for bladder cancer.

Design: To identify main molecular subtypes of human BC, we used cytokeratin 5/6 (CK5/6) and transcription factor, GATA3 IHC on archival bladder cancer tissues from 117 adult patients in a custom-designed TMA. Unequivocal immunoreactivity in ≥20% tumor cells was used as cut-off for CK5/6 and GATA3 positivity. Molecular subtyping and clinico-pathologic data including demographics, histologic type, grade, stage, type of therapy (surgery, chemotherapy, other therapies), clinical follow-up (0-132 months) and overall survival (OS) were analyzed using Fisher's exact test, ANOVA and the Kaplan-Meier method with log-rank test.

Results: Of 117 adult BC patients, 83 (71%) were male and 34 (29%) were female, including 46 (39%) with muscle-invasive BC (MIBC) and 63 (54%) without muscle invasion (NMIBC). Patients with MIBCs had worse overall survival compared to NMIBC patients (HR: 5.13; 95% CI: 2.97-8.85; p<0.001). Among 112 evaluable BC tissues, the main molecular subtypes identified were basal (N=12[11%];CK5/6+/GATA3-), mixed baso-luminal (N=31 [28%];CK5/6+/GATA3+) and luminal (N=69[61%];CK5/6-/GATA3+). Fig. 1 illustrates baso-luminal bladder cancer with co-expression of GATA3 in tumor cell nuclei (lower left panel) and CK5/6 in tumor cell cytoplasm (lower right panel). Median OS for patients with basal, baso-luminal and luminal BCs was 18, 57, and 51 months respectively.

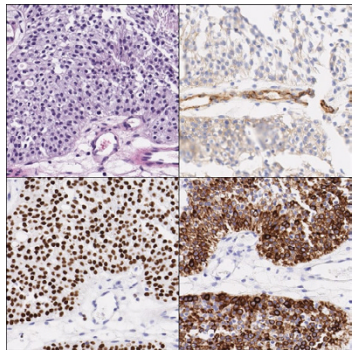

Conclusions: Unlike the mRNA expression signatures, which identified two main bladder cancer subtypes (basal, luminal), CK5/6 and GATA3 IHC revealed three predominant molecular bladder cancer subtypes. The newly characterized baso-luminal subtype seems to match the clinico-pathologic profile of luminal BCs. Independent validation of our molecular findings and data on the mixed baso-luminal and other main molecular subtypes (basal, luminal) of bladder cancer may have clinical and therapeutic implications.

1036 Computer-Extracted Nuclear Shape Features Distinguish Consensus High- and Low-Grade Non-Invasive Papillary Urothelial Carcinomas

Behtash G Nezami[1], *Mahmut Akgul*[2], *Patrick Leo*[3], *Holly Harper*[4], *Robin Elliott*[5], *Andrew Janowczyk*[6], *Anant Madabhushi*[5], *Gregory MacLennan*[6]. [1]University Hospitals, Cleveland Medical Center, Beachwood, OH, [2]Univ Hosp Case Med Ctr, Cleveland, OH, [3]Cleveland, OH, [4]University Hospitals Case Medical Center, Cleveland, OH, [5]University Hospitals Cleveland Medical Center, Cleveland, OH, [6]Case Western Reserve University, Cleveland, OH

Background: Nearly half of all bladder tumors are non-invasive papillary urothelial carcinomas (NIPUC). There are significant prognostic and clinical management differences between low-grade (LG) and high-grade (HG) NIPUC. However, morphological diagnosis of these categories has been challenging due to significant interobserver variability. By employing computerized measurements of attributes employed for pathologic grading we sought to create a quantitative and reproducible NIPUC grading model. In this study, we explored whether computer-extracted features of nuclear size, shape, architectural arrangement, and orientation can distinguish between consensus LG and HG NIPUC.

Design: The UHCMC Department of Pathology archives were searched for NIPUC 1987-2017, identifying 5605 cases. 201 cases with more than 5 years of available follow-up were selected and the H&E slides from these patients were blindly reviewed by three experienced genitourinary pathologists (GTM, HLH, RME). Of the cases with a consensus diagnosis of LG (40) or HG (40) carcinoma among all 3 reviewers, 67 (34 LG and 33 HG) were successfully digitized and processed. A Pathology Resident annotated a representative papillary lesion on each image. Nuclei were segmented from annotated regions using a deep learning model and 151 features of nuclear architecture, size, shape, and orientation were extracted. 13 HG and 13 LG cases were randomly selected for the training set. A linear discriminant classifier was trained on the training set using the top two features by the Wilcoxon rank-sum test. This model was then validated on the other 41 patients.

Results: The model achieved an area under the receiver operating characteristic curve (AUC) of 0.78 on the validation set. AUC ranges from 0 to 1 and describes the true and false positive rates as the classifier decision threshold is varied. The top two features were the mean of the second invariant moment and standard deviation of the first invariant moment of the nuclei boundaries. In the training set, the high-grade specimens had a significantly higher standard deviation of the first invariant moment (mean 0.0273 vs. 0.0215, p=1e-4), reflecting greater variation in nuclear shape. This is consistent with pleomorphism being a sign of higher grade cancer.

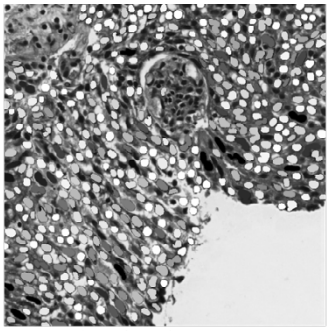

Figure 1: Cropped region of interest from an HG specimen. Nuclei are shaded according to the value of their second invariant moment, the standard deviation of which quantifies the nuclei pleomorphism. HG specimens had a higher standard deviation of second invariant moment, as seen by the variety of nuclei shading in this image.

Conclusions: We have demonstrated that quantitative histomorphometric features of nuclear shape can accurately distinguish between consensus LG and HG NIPUC. Our findings may be useful in developing an objective, automated NIPUC grading method.

1037 Immunohistochemical (IHC) Staining Patterns of Ki-67 and p53 in Florid Reactive Urothelial Atypia (RA) and Urothelial Carcinoma In Situ (CIS) Demonstrate Significant Overlap

Jane K Nguyen[1], *Jesse McKenney*[2], *Christopher Przybycin*[2], *Cristina Magi-Galluzzi*[2]. [1]Cleveland Clinic Foundation, Cleveland, OH, [2]Cleveland Clinic, Cleveland, OH

Background: Flat urothelial lesions with atypia may pose significant diagnostic challenges. Given our experience with increased proliferation rates in florid RA and limited studies on the interpretation of p53 stains in urothelium (following current standard guidelines for correlation with P53 mutation status), we sought to study their discriminatory value for RA versus CIS.

Design: Florid RA (n=21) and CIS (n=20) were assessed by IHC staining with antibodies for KI-67 (Ventana, rabbit monoclonal, 30-9, prediluted), p53 (Agilent, mouse monoclonal, DO-7, 1:20), CD44 (Agilent, mouse monoclonal, DF1485, 1:40), and CK20 (Agilent, mouse monoclonal, Ks20.8, 1:20). IHC was scored based on percent cells positive for Ki-67 and pattern of reactivity with p53 [aberrant: diffuse strong nuclear positive (DP) or negative; normal: patchy/wild type (WT)]. CD44 and CK20 IHC staining patterns were used as adjunctive internal validation controls for RA and CIS, as previously described.

Results: In RA, Ki-67 ranged from 0-75% (mean of 30% ± 22%) with 12 cases having ≥ 30%. In CIS, Ki-67 ranged from 20-90% (mean value of 58% ± 20%) with 18 cases having ≥ 30%. In RA, the p53 expression in all 21 cases (100%) had WT pattern. In CIS, p53 expression loss was identified in 10% (2/20) of cases, diffuse strong positive expression in 30% (6/20), and WT expression in 60% (12/20). 17 cases (81%) of RA demonstrated cytoplasmic CK20 immunoreactivity in superficial umbrella cells and 4 cases (19%) were negative. Additionally, CD44 was overexpressed in full thickness of RA in 17 cases (81%) and had expression confined to the basal/parabasal layers in 4 (19%). CK20 expression in CIS demonstrated diffuse strong en bloc positivity in 19 cases (95%) and patchy positivity in 1 case (5%). CD44 was not overexpressed in any case of CIS: no staining in 16 cases (80%) and focal expression in the basal cell layer in 4 cases (20%).

Conclusions: Ki-67 has poor discriminatory value for RA versus CIS, and adds little to CK20/CD44 immunophenotype. 30% of CIS showed distinctive strong and diffuse nuclear staining for p53, but we found the interpretation of p53 as either WT or negative to be challenging in this setting.

1038 An Audit of Pathologic Diagnoses in Urethral Biopsy Specimens

Odharnaith O'Brien[1], *Andrew J Evans*[2], *Joan Sweet*[3], *Carol Cheung*[4], *Theodorus van der Kwast*[3]. [1]Clonmel, [2]Toronto General Hospital, Toronto, ON, [3]University Health Network, Toronto, ON, [4]Markham, ON

Background: The urethra may harbor a variety of disease processes, both benign and malignant. These lesions may originate from the urethra mucosa or from the surrounding tissues, such as the prostate in men and uterine cervix in women. Generally, such lesions may be visualized by the urologist using urethral endoscopy and they may be removed for pathological diagnosis. Such samples, taken for histopathological diagnosis, are small in size and often very superficial and thus may prove challenging for the pathologist. Literature specific on the pathological diagnostics of urethral biopsies is scarce. We aimed to perform an audit of the pathological diagnoses made on urethral biopsies in our institution.

Design: We performed a retrospective search of our laboratory information system database for all urethral specimens over the period of 2001-2017. Urethral specimens taken at the time of prostatectomy and cystectomy to determine margin status were excluded. Patient demographics and pathological diagnosis were documented.

Results: A total of 127 specimens from 116 patients were identified that met our criteria; 99 specimens from 89 males and 28 specimens from 27 females. Patient age ranged from 22 years to 92 years (mean 65.8 years). Where recorded, the size of the urethral specimens (n=108) ranged from 0.05cm to 2.1cm (median 0.5cm). Reported diagnoses are summarized in the attached table. In specimens with a diagnosis of urothelial carcinoma (n=22), 9 (40.9%) had minimal or no stroma, precluding assessment of invasion and subsequent staging. Grading was not possible in 2/22 cases (9.1%) due to small biopsy size and presence of cautery artefact. Most striking was the occurrence of malignant melanoma in 4 females (2 representing primary urethral melanoma, 2 representing local recurrence of previous vulval melanoma), with no cases observed in males.

	Neoplastic specimens	No. specimens (n)	Benign Specimens	No. specimens (n)
Males	Urothelial carcinoma	23	Normal histology	27
	Carcinoma in situ	5	Inflammatory/ reactive	16
	Squamous cell carcinoma in situ	1	Metaplasia	9
	Dysplasia	3	Urethritis cystica et glandularis	1
	Urothelial atypia	2	Condyloma acuminatum	8
	Prostatic adenocarcinoma	2	Urethral stone	1
	PUNLUMP	1		
Females	Squamous cell carcinoma	2	Normal histology	2
	Basaloid adenosquamous carcinoma	1	Inflammatory/ reactive	8
	Malignant melanoma	4	Caruncle	5
	Clear cell adenocarcinoma	1	Squamous Hyperplasia	1
	Squamous cell carcinoma in situ	2	Papilloma	1
			Fibroepithelial polyp	1
Total no. specimens		47		80

Conclusions: Disease processes of the urethra are rare (mean 7.5 specimens/year). However, the pathology encountered is varied, ranging from benign to malignant with primary and secondary origins. Urethral pathology in the male frequently arises in conjunction with bladder pathology and occasionally in association with the prostate, while pathology arising in the female often arises in conjunction with vulvar pathology.

1039 TRIM24 as Independent Prognostic Marker in Prostate Cancer

Anne Offermann[1], *Felix Schneider*[2], *Marie Christine Hupe*[3], *Silke Hohensteiner*[4], *Finn Becker*[5], *Jessica Carlsson*[6], *Jutta Kirfel*[7], *Maria Svensson*[8], *Ove Andren*[9], *Axel Merseburger*[10], *Verena Lubczyk*[4], *Rainer Kuefer*[11], *Perner Sven*[1]. [1]University Medical Center Schleswig-Holstein, Leibniz Center for Medicine and Biosciences, Luebeck and Borstel, Germany, Luebeck, [2]Klinik am Eichert Alb Fils Kliniken, Goeppingen, Germany, [3]University Hospital Schleswig-Holstein, Campus Luebeck, Germany, [4]Klinik am Eichert Alb Fils Kliniken, Goeppingen, Germany, [5] University Medical Center Schleswig-Holstein, Leibniz Center for Medicine and Biosciences, Luebeck and Borstel, Germany, [6]Örebro University, Örebro, Sweden, [7]University Hospital Schleswig-Holstein, Leibniz Center for Medicine and Biosciences, Luebeck and Borstel, Germany, [8]Örebro University, Örebro, Sweden, [9]Örebro University, Örebro, Sweden, [10]University Hospital Luebeck, Luebeck, Germany, [11]Klinik am Eichert Alb Fils Kliniken, Goeppingen, Germany

Background: Simply applicable biomarkers for prostate cancer (PCa) predicting the clinical course are urgently needed. Recently, TRIM24 has been identified to promote androgen-receptor signaling and to correlate with poor outcome. Based on these data, we validated TRIM24 as a prognostic biomarker for PCa.

Design: We performed TRIM24 immunohistochemistry on two

independent cohorts including a total of 806 primary tumors, 26 locally advanced/recurrent tumors, 30 lymph node metastases, 30 distant metastases and 129 benign prostatic samples from 497 patients. Expression data were correlated with clinic-pathological data including biochemical recurrence free survival (bRFS) as endpoint.

Results: Benign samples show no/low TRIM24 expression in 94%, while tumors demonstrate significantly higher levels. Strongest expression is observed in metastatic tumors. In multivariate analyses, TRIM24 up-regulation correlates with shorter bRFS independent of other prognostic parameters. 5-(10-) year bRFS rates for TRIM24 negative, low, medium and high expressing tumors are 93.1(93.1)%, 75.4(68.5)%, 54.9(47.5)% and 43.1(32.3)%, respectively. Of interest, tumors diagnosed as indolent disease, TRIM24 expression stratifies patients into specific risk groups. Increased TRIM24 expression associates with higher Grade Group, positive nodal status and extraprostatic tumor growth.

Conclusions: Using two large independent cohorts, we found that TRIM24 expression predicts patients' risk to develop disease recurrence with high accuracy and independently from other established prognostic markers. To our knowledge, TRIM24 is the first prognostic biomarker to be independent, accurate and reproducible on three different primary PCa cohorts. Thus, we strongly suggest introducing TRIM24 in clinical routine as a simple immunohistochemical test.

1040 Collagen 1A1 Expression Is One of The Strongest Markers of Prostate Cancer Biochemical Recurrence in Several mRNA Databases, But Not By Immunofluorescence

Diana M Oramas[1], *Rami Hayajneh*[2], *Santiago Delgado*[2], *Andre Kajdacsy Balla*[3], *Virgilia Macias*[2]. [1]University of Illinois at Chicago, Chicago, IL, [2]University of Illinois at Chicago, [3]Univ. of Illinois, Chicago, IL

Background: In prostate carcinoma, as in many cancers, the tumor microenvironment plays a critical role and interactions between epithelium and stroma are known to be important for tumor progression and metastasis. Collagen 1 fibers are the main structural component of the extracellular matrix in prostate tumors. Analysis of Oncomine cancer microarray databases revealed that COL1A1 gene expression was significantly increased in prostate cancerbiochemical recurrence. In this study, our primary aim is to determine whether COL1A1 immunofluorescence predicts recurrence of prostate cancer.

Design: For this study, we used a prostate cancer outcome tissue microarray (TMA) from the Cooperative Prostate Cancer Tissue Resource. The TMA included 0.6 mm in diameter tissue core quadruplicates from 200 cases with biochemical recurrence after prostatectomy and 200 non-recurrent controls matched by age, year of surgery, race, Gleason grade and pathological stage. Fluorescent labels were targeted for COL1A1 and cytokeratins 8/18 to facilitate scoring of regions of interest at the tumor-stromal interface. COL1A1 was detected by multispectral scanning using the Vectra quantitative imaging system using a machine learning inForm algorithm (Perkin Elmer, Hopkinton, MA). The average COL1A1 intensity per subject was calculated by the sum of tumor-stromal interface COL1A1 total intensity of each quadruplicate and dividing by the total number of stromal pixels in all 4 cores. The paired Student's t- test was used for statistical analysis.

Results: Analysis of our data showed no statistically significant association of COL1A1 expression by immunohistochemistry with progression to recurrent prostate cancer (p value= 0.1054)

Conclusions: COL1A1 mRNA expression is a marker of poor prognosis in patients with recurrent prostate cancer. To our knowledge, this is the first study assessing the COL1A1 expression in the tumor-stromal interface. Our study showed non-significant association of COL1A1 when it is used as a biomarker by immunofluorescence.

1041 High Grade Prostatic Intraepithelial Neoplasia (HGPIN)- like Ductal Adenocarcinomas (PIN-Like Ductal PCa.): A Study of 193 Cases

Adina Paulk[1], *Jonathan Epstein*[2]. [1]Johns Hopkins Medical Institution, Baltimore, MD, [2]The Johns Hopkins Med Inst, Baltimore, MD

Background: PIN-Like Ductal PCa. are rare tumors characterized by crowded, often cystically dilated glands architecturally resembling HGPIN, lined by malignant pseudostratified columnar epithelium (Figures 1-2). The largest prior series studied 9 radical prostatectomies (RP) and suggested a behavior similar to Gleason score 6.

Design: We identified 193 PIN-like ductal PCa. between 2008-2017. Reports on 21 RPs were available. Slides are available on 11 RP cases with ongoing requests for the additional cases.

Results: The diagnoses were made on needle biopsies (n=186), TURs (n=4), and RP (n=3). In 29% (54/186) of biopsies there was an associated acinar PCa. Gleason scores of acinar cancer on biopsy were 3+3=6 (GG1) (24,44.4%), 3+4=7 (GG2) (n=15,27.8%), 4+3=7 (GG3) (n= 9,16.7%), 4+4=8 (GG4)(n=5,9.3%) and 4+5=9 (GG5) (n=1,1.8%). 4% (7/186) of needle biopsies also showed a cribriform/papillary ductal adenocarcinoma component. In patients potentially eligible for active surveillance [age ≤ 75 & GG1 on biopsy] with follow up data, 13/47 (27.6%) underwent RP, compared to 9/16 (56.2%) in the prior study (p=0.03). Of RP reports available for review, 16/21 (76.2%) were organ-confined. The grade at RP was 3+3=6 (7/21, 33.33%), 3+4=7 (10/21, 47.62%), and 4+3=7 (4/21, 19.04%); one 4+3=7 case with tertiary pattern 5. Features of RP with available slides are shown in Table 1. In all cases, PIN-like ductal PCa was in the peripheral zone, separate from the acinar PCa. In cases with a dominant acinar component, the PIN-like ductal PCa was small (<1 cm). In the 2 the largest PIN-like ductal tumors, there was EPE by the PIN-like ductal component. Two cases showed a peculiar pattern with focal large cystic cancer glands lined by benign appearing atrophic epithelium, in one case with EPE. One case had no PIN-like ductal tumor; this was a 73 gm prostate with representative sections submitted. No RPs showed an associated papillary/cribriform ductal PCa. Of the remaining 10 cases without available slides, reports showed Gleason 3+3=6 (n=3); 3+4=7 (n=4); 4+3=7 (n=3), with two cases (3+4=7; 4+3=7) showing both EPE and positive margins.

Table 1.

Case	Size of PLD (mm)	Acinar Gleason	Dominant Tumor	EPE	Other
1	7	3+4=7; GP4=5%	Acinar	0	
2	6	3+4=7; GP4=5%	Acinar	0	Paneth cell-like changes in PLD
3	10	3+4=7; GP4=5%	Acinar	0	
4	5	3+3=6	Acinar	0	
5	1	4+3=7; tertiary 5	Acinar	Acinar	
6	NT	3+4=7; GP4=10%	Acinar	0	
7	10	NT	PLD	0	
8	15	3+3=6	PLD	PLD	
9	4	3+4=7; GP4=5%	Acinar	0	Separate 4+5=9
10	18	3+3=6	PLD	PLD	Atrophic PLD cystic structures
11	3	3+3=6	Acinar	0	Atrophic PLD cystic structures

NT= No tumor; PLD= Pin-like ductal; GP=Gleason pattern

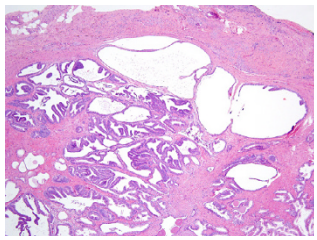

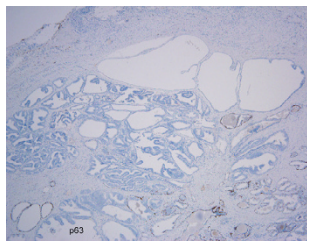

Conclusions: Patients diagnosed with PIN-like ductal PCa underwent RP at a decreased rate than in the previous study. PIN-like ductal PCa is frequently small, associated with acinar PCa of various Gleason scores, and located in the PZ, separate from the acinar PCa. Uncommonly is it associated with EPE or positive margins, consistent with Gleason score 3+3=6 behavior.

1042 Pathologic Characteristics of Magnetic Resonance Imaging/Ultrasound Fusion Targeted Biopsy Associated with Adverse Pathology at Radical Prostatectomy

Kevin T Pelland[1], *Kamyar Ghabili Amirkhiz*[1], *Sarah Amalraj*[1], *Alfredo Suarez-Sarmiento*[2], *Kevin A Nguyen*[2], *Jamil S Syed*[2], *Peter G Schulam*[2], *Peter Humphrey*[1], *Preston C Sprenkle*[2], *Angelique Levi*[3]. [1]Yale University, New Haven, CT, [2]Yale University, [3]Yale University, Fairfield, CT

Background: Among men with Gleason score 7 disease, the correlation between clinicopathologic characteristics at magnetic resonance imaging (MRI)/ultrasound fusion targeted biopsy (TB) and adverse pathology at radical prostatectomy (RP) has not been well documented. Recently, evidence has emerged that higher percent Gleason grade 4 (G4%) in systematic biopsy (SB) is associated with subsequent adverse pathology and biochemical recurrence. We

investigated whether clinicopathologic factors at TB and concurrent SB, including G4%, were associated with adverse pathology at RP.

Design: We retrospectively identified men who underwent RP for Gleason score 7 prostatic adenocarcinoma with MRI/US TB and concurrent systematic biopsy performed between January 2015 and July 2017. Adverse pathology was defined as primary Gleason 4 or ≥pT3 at RP. G4% was calculated as Gleason pattern 4 in positive TB or SB cores (mm)/total tumor in positive TB or SB cores (mm). Multivariable logistic regression was used to identify clinicopathologic features at biopsy predictive of adverse pathology at RP. Pathologic parameters included G4% (TB or SB), maximum percent biopsy core involvement, and proportion of cores positive for tumor.

Results: Sixty-one men underwent RP for grade group 2 (Gleason score 3+4=7; 64%) and grade group 3 (Gleason score 4+3=7; 36%) prostate cancer. Adverse pathology at RP was detected in 25 patients (41%). These men had greater maximum SB (*P*=0.03) and TB (*P*=0.003) core tumor involvement, a greater proportion of positive TB cores (*P*=0.04), and higher SB-G4% (*P*=0.009). In the logistic regression models, maximum percent TB core involvement (OR 1.04, 95% CI 1.005-1.080, *P*=0.02) and TB-G4% (OR 1.05, 95% CI 1.009-1.100, *P*=0.01) were predictors of adverse pathology at RP. Variables that failed to predict adverse pathology in the multivariable model included prostate specific antigen (PSA) and proportion of positive TB cores. On receiver operating characteristic analysis, the area under the curve for models including PSA, clinical stage, and biopsy Gleason score increased from 0.66 to 0.81 upon inclusion of maximum percent TB core involvement and TB-G4%.

Conclusions: G4% and extent of tumor involvement in TB specimens are important predictors of adverse pathology at RP in men with Gleason score 7 prostate cancer. These may be useful adjuncts to preoperative parameters commonly used to predict adverse pathology at RP.

1043 Pathologic Characterization of Speckle-Type POZ Protein (SPOP)-Mutated Prostate Cancer

Yu-Ching Peng[1], *Wassim Abida*[1], *Deborah DeLair*[1], *S. Joseph Sirintrapun*[2], *Ying-Bei Chen*[1], *Hikmat Al-Ahmadie*[1], *Samson W Fine*[1], *Satish Tickoo*[1], *Howard Scher*[1], *Victor Reuter*[1], *Anuradha Gopalan*[1]. [1]Memorial Sloan Kettering Cancer Center, New York, NY, [2]New York, NY

Background: Recurrent mutations (MUT) in SPOP gene are the most common somatic MUT in prostate cancer (PC), occurring in approximately 10% of primary PC. SPOP MUT PC has increased sensitivity to androgen deprivation therapy (ADT). Little is known about the histopathologic features of this distinct molecular subtype. We studied the morphologic features of SPOP MUT PC in the largest cohort known to date.

Design: We reviewed 80 primary PC with SPOP MUT from 1999 to 2017. This group included 53 radical prostatectomy (RP) specimens and 27 prostate biopsies. SPOP MUT status was determined using a CLIA-approved targeted Next Generation Sequencing platform for somatic alterations. 54 consecutive specimens that were SPOP wild-type (WT) (28 RP and 26 biopsies) from 2015 to 2016 were analyzed as comparison. 5 SPOP MUT and 1 WT cases were excluded from histologic analysis due to effects of ADT. Morphological features analyzed included ductal phenotype, intraductal carcinoma (IDC), cribriform architecture, cytoplasmic vacuolization and neuroendocrine (NE) features. Statistic analysis was performed using Chi-square test.

Results: The incidence of SPOP MUT primary PC in our institution is 11%. The Gleason scores of SPOP MUT and WT cases are in Table 1. The preponderance of grade group 4/5 in both MUT and WT groups reflects the clinical features of the sequenced cohort. The most frequently mutated residues were F133 (49%) and F102 (19%). The pathologic features are in Table 2. Significantly, 15% (11) of SPOP MUT cases showed ductal phenotype, compared to 2% (1) of WT cases (**p=0.01**). Also significantly, 55% (41) of SPOP MUT cases showed IDC based on H&E evaluation alone, compared to 36% (19) of WT cases (**p=0.04**). 67% (50) of SPOP MUT cases showed cribriform architecture, compared to 51% (27) of WT cases (p=0.07). Cytoplasmic vacuolization "Signet ring-like/ pseudo-lipoblast-like cells" were identified in 37% (27) of SPOP MUT cases (15% focal, 22% diffuse). 30% (16) of WT cases also showed similar vacuolization (11% focal, 19% diffuse, p=0.46). 1% (1) of the SPOP MUT case showed NE features.

Table 1 Grade groups in SPOP mutant and wild-type cases

SPOP	Grade Group (Gleason Score)					
	1 (3+3)	2 (3+4)	3 (4+3)	4 (4+4)	5 (4+5/5+4)	Total
Mutant	1 (1%)	8 (10%)	21 (26%)	19 (24%)	31 (39%)	80
Wild-type	0	7 (12%)	10 (19%)	10 (19%)	27 (50%)	54

Table 2 Morphologic features in SPOP mutant and wild-type cases

SPOP	Ductal	IDC	Cribriform	Vacuolization		NE
				Focal	Diffuse	
Mutant	11 (15%)	41 (55%)	50 (67%)	11 (15%)	16 (22%)	1 (1%)
Wild-type	1 (2%)	19 (36%)	27 (51%)	6 (11%)	10 (19%)	0
P-value	0.01	0.04	0.07	0.46		-

Conclusions: 1. This study is the largest histopathologic evaluation of prostatic carcinoma harboring SPOP mutations to date.

2. In this overwhelmingly high grade cohort, a significantly higher proportion of SPOP mutant prostatic carcinoma show ductal phenotype and intraductal carcinoma. Greater proportion of SPOP mutant cases show cribriform architecture than non-mutated cases, approaching significance in this cohort.

1044 Trabecular Angiomyolipoma: An Single Institution Morphologic and Immunohistochemical Study of 22 Cases

Carmen M Perrino[1], *John Eble*[2], *Liang Cheng*[2], *Muhammad Idrees*[2], *Shaoxiong Chen*[3], *David Grignon*[2]. [1]Indiana University, Indianapolis, IN, [2]Indiana University School of Medicine, Indianapolis, IN, [3]IU Health Pathology Laboratory, Indianapolis, IN

Background: Angiomyolipomas (AMLs) with a prominent smooth muscle component composed of epithelioid cells with plump nuclei that form trabeculae and cords on a background of variably sclerotic stroma have been ascribed several names in the literature. They are often a diagnostic dilemma given absent or minimal fat content and a unique morphologic appearance. We aim to describe a series of these cases primary to the kidney, which we refer to as trabecular AMLs.

Design: A search of the pathology database for renal AMLs was performed (2000-2017). Slides were re-reviewed to identify cases with a focal/pure trabecular pattern. 11 cases were submitted for a panel of 9 immunohistochemical (IHC) stains. IHC stains were scored for intensity (0: no staining; 1: weak; 2: moderate; 3: strong) and proportion of cells stained (0: 0%; 1: >0 to ≤25%; 2: >25 to ≤50%; 3: >50 to ≤75%; 4: >75 to 100%).

Results: Twenty-two primary renal AMLs with either focal (n=10) or pure (n=12) trabecular architecture were identified from 22 patients (17 F 5 M, median age 58 years, 15 R and 7 L kidney). One patient had a history of tuberous sclerosis (pure tumor). Specimens included needle core biopsies (2), partial nephrectomies (12), and radical nephrectomies (8). All areas with a focal trabecular pattern had markedly sclerotic vessels. Among the 11 cases submitted for staining, 4 had pure and 7 had focal trabecular architecture. Notably, desmin staining was absent in all cases with a focal trabecular pattern and was positive in 3 cases with a pure pattern (intensity 3, proportion 4). SMA was diffusely/strongly positive in all cases, and emphasized the trabecular pattern in pure cases. ERG stained cases showed an organized vascular pattern in the pure cases (highlighted the edges of trabeculae) in contrast to a disorganized pattern in the focal cases. Three pure cases showed absent or rare/weak staining for Melan A, while a greater proportion of cells stained in focal cases. All cases showed positivity for caldesmon, cathepsin K, collagen IV, and HMB45 (no significant difference between focal/pure cases). SOX10 was negative in all cases.

Conclusions: Trabecular AMLs rarely occur as primary kidney tumors and are often diagnostic dilemmas. While there is overlap between the IHC profile of classic and trabecular AMLs, the pure trabecular cases are more often positive for desmin and show a characteristic, organized pattern of ERG staining.

1045 A Unique Morphologic Entity: Metastatic Castration-resistant Neuroendocrine Carcinoma of the Prostate

Marie Perrone[1], *Lawrence D. True*[2], *Colm Morrissey*[3], *Xiaotun Zhang*[4]. [1]University of Washington, Seattle, WA, [2]Seattle, WA, [3]University of Washington, [4]Mayo Clinic, Rochester, MN

Background: Neuroendocrine (NE) carcinoma of the prostate is a rare, often aggressive, type of prostate cancer. It may arise de novo in the prostate or evolve following chemotherapy or androgen-deprivation treatment. The WHO Classification of Tumours of the ... Male Genital Organs, 2016, defines five morphologic subtypes of neuroendocrine carcinoma of the prostate: small cell carcinoma, large cell carcinoma, Paneth cell-like carcinoma, carcinoid, and mixed neuroendocrine-adenocarcinoma. In our work, we noticed a possible sixth histologic subtype of NE carcinoma in castration-resistant metastatic prostate cancer.

Design: H&E-stained tissue microarrays, with 420 samples of metastatic prostate cancer from a series of 81 patients, along with

paired immunohistochemical (IHC) data, were reviewed. All patients were on prolonged androgen deprivation therapy (ADT), including late-generation agents. IHC stains were done for androgen receptor (AR), chromogranin (CHGA), and synaptophysin (SYP). Cases were annotated with morphologic features, and were categorized based on expression of AR, CHGA, and SYP. We correlated histologic patterns with the immunophenotypes.

Results: 9% (N=39) of samples had a pure NE phenotype by IHC. An additional 19% (N=79) expressed both NE markers and AR ("amphicrine"). 56% (N=236) expressed AR, but not SYP or CHGA, consistent with an "adenocarcinoma" phenotype. 14% (N=59) lacked expression for all three markers ("null" phenotype). The pure NE carcinoma samples almost exclusively had the morphology of solid sheets of small, epitheloid cells with small to moderate amounts of cytoplasm, without gland formation. Unlike small cell carcinoma of the lung and prostate, there was no crowding or overlapping of cells, N:C ratios were relatively preserved and there were only rare mitoses. Of note, some metastases from different sites within the same patient have different IHC patterns.

Patients	81
Metastasis samples	420
Total pure NE metastasis	39 (9%)
Patients with at least one pure NE metastasis	13 (16%)
Patients with only pure NE metastasis	5 (6%)

Conclusions: Metastatic castration-resistant prostate cancer, following ADT, often develops a neuroendocrine phenotype. We observed a distinctive histology of tumors which have an NE immunophenotype. This histology also characterized metastases which had an amphicrine immunophenotype. We hypothesize that newer generation ADT's are driving the evolution of a biologically unique subtype of neuroendocrine prostate cancer that does not fit into the current prostatic neuroendocrine framework.

1046 Can Ki67 Predict Outcome for Prostatic Adenocarcinoma Patients on Androgen-Ablation Therapy? The Nigerian Experience

Adekoyejo Phillips[1], *Melanie Louw*[2], *Adekunbiola A Banjo*[3], *Charles C Anunobi*[4]. [1]Lagos University Teaching Hospital, Lagos, [2]National Health Laboratory Services, Johannesburg, Gauteng, [3]Lagos University Teaching Hospital, Nigeria, Lagos, [4]Lagos University Teaching Hospital / College of Medicine University of Lagos

Background: Prostate cancer is the fourth most common cancer in both sexes combined and the second most common cancer in men. The prognosis of prostate cancer depends on clinicopathological and biochemical factors. The most studied immunohistochemical factor is Ki-67 proliferative index (PI), despite this, little is known about the prognostic significance of this biomarker in prostatic adenocarcinoma patients in Nigeria.

Design: This is a retrospective study that was done on prostate cancer patients, on androgen ablation therapy (AAT), diagnosed between 2008 and 2011. The tumours from these patients were assigned to International Society of Urological Pathology (ISUP) grade groups and the proliferative index (PI) of each tumor was determined with Ki-67 antibodies. The associations between the Ki-67 PI and ISUP grade groups, diagnostic PSAs and age groups were assessed. A survival analysis was done to assess the association between PSA-defined biochemical recurrence and Ki-67 PI, diagnostic PSA, ISUP grades and age.

Results: Fifty-two cases were used in this study, the 60 – 69 age group was the most affected age group and ISUP grade group 4 was the most commonly diagnosed. Forty-five cases met the inclusion criteria for survival analysis of which 44 cases showed evidence of remission i.e PSA fell to a nadir after AAT and 21 cases showed biochemical recurrence. The mean PSA nadir was 2.2 ng.mL (0.2 to 20.3 ng/mL), the mean time to achieve biochemical remission was 13.5 months (5 – 23 months) and the mean follow-up period was 38.7 months. The mean diagnostic PSA was 98.95 ng/mL (5.23 ng/mL - 1000 ng/mL) and the mean Ki-67 proliferative index was 3.83% (0% - 35%). Based on the mean value, the Ki-67 cut-off was set at 4%. The Ki-67 PI showed statistically-significant association with only the ISUP grade group (p-value =0.038). On univariate analysis, using the Kaplan-Meier curve and log rank test, the PSA-defined biochemical recurrence showed statistically significance association with Ki-67 PI (p-value = 0.0007). There was no significant statistical association between biochemical recurrence and the diagnostic PSA and the ISUP grade group (p-value = 0.3051 and 0.3089 respectively). On multivariate analysis, Ki-67 PI was the only independent prognostic factor.

VARAIABLES	Ki-67

	0 – 0.9	1 – 3.9	≥ 4	TOTAL
ISUP GRADE GROUP	(Chi-square x^2 = 16.3471 and p-value = 0.038)			
1	5	1	0	6
2	4	3	1	8
3	6	1	2	9
4	4	3	11	18
5	6	0	5	11
TOTAL	25	8	19	52
PSA VALUE (ng/mL)	(Chi-square x^2 = 3.5138 and p-value = 0.476)			
0 - 10	1	0	0	1
11 - 100	19	6	11	36
101 - 1000	5	2	8	15
TOTAL	25	8	19	52
AGE	(Chi-square x^2 = 3.0710 and p-value = 0.930)			
40 - 49	1	0	1	2
50 - 59	3	0	2	5
60 - 69	10	5	7	22
70 - 79	9	3	8	20
80 - 89	2	0	1	3
TOTAL	25	8	19	52

Table 1: Showing the correlation between Ki-67 proliferative index and ISUP grade group, diagnostic PSA and Age.

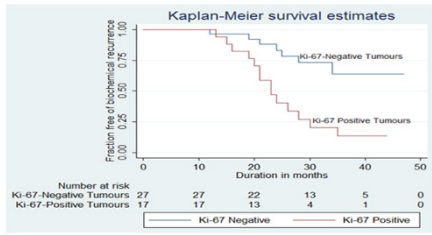

Figure 1: Shows the Kaplan-Meier curve for Ki-67 proliferative index.

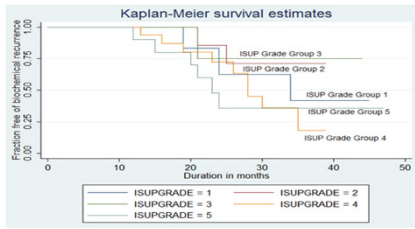

Figure 2: Shows the Kaplan-Meier curve for the ISUP grade groups.

Conclusions: Ki-67 PI is an important prognostic factor in AAT-managed prostatic cancer patient in Nigeria. Assessment of Ki-67 PI should be incorporated into routine clinical work-up for prostatic cancer patients who will be managed with AAT.

1047 Intratubular Germ Cell Neoplasia (ITGCN) in Testis-Sparing Surgery (TSS) for Small Testicular Masses (STMs

Francesco Pierconti[1], *Maurizio Martini*[2], *Luigi Maria Larocca*[3], *Esther Rossi*[4]. [1]Catholic University of Sacred Heart, Roma, Italy, [2]Catholic University of Sacred Heart, Roma, [3]Fondazione Policlinico Universitario A. Gemelli, Rome, Italy, [4]Catholic University, Rome, Italy

Background: The testis-sparing surgery (TSS) is a now well known accepted surgical technique for benign small testicular masses (STMs) but it can also be performed in the presence of malignant tumor in young but very selected patients. The enucleation of the mass must be accompanied by multiple biopsies of the surrounding tissue in order to rule out foci of intratubular germ cell neoplasia

Design: This retrospective study was conducted in our hospital between june 2010 and October 2014. A total of 35 patients underwent a radical orchiectomy for small testicular mass suspected to be malignant. Exclusion criteria from our study were testicular mass >2 cm at inspection and/or scrotal high frequency ultrasound (US). All the testis specimen was totally embedded and processed via the whole-mount method and the presence of ITGCN in the surrounding tissue were evaluated. Moreover the distance between lesion and the

foci of ITGCN were measured on the slides considering for the third dimension that each paraffin block were 5 mm of thickness. To identify the foci of ITGCN a confirmative immunoistochemical staining with PLAP and CD117 was performed.

Results: The diameter of the STMs was between 0,5 cm and 2 cm with a median value of 1,51 cm and the foci of ITGCN was identified near the SMTs up to a distance of 2,5 cm with a median value of 1,78 cm. The distance of ITGCN from the STMs was not related to dimension of the lesion. The foci of ITGCN were described in seminiferous tubules very closed to SMTs or as skip lesions in the sourrounding testicular parenchyma dispersed in normal testis. In any case, the foci of ITGCN were not observed beyond the 2,5 cm from the STMs.

Conclusions: In TSS after the enucleation of the mass, multiple biopsies of the surrounding tissue were performed and analyzed at the same time as frozen section in order to evaluate the presence of foci of ITGCN, the radicality of the procedure and sometimes to better diagnosize the testicular lesion. We demonstrated in this study that the ITGCN was found near the lesions, in a non-random distribution within the testicle and it was never observed beyond the 2,5 cm from the STMs. This indication could help the surgeons during the intraoperative procedures suggesting the best site to perform testicular biopsies, increase the ability of pathologist to make a correct diagnosis of (TGCT(s) in the STMs, reduce the false-negative biopsies mainly caused by the non-random distribution of TIN within the testicle and improve the radicality of the enucleation in TSS.

1048 Primary Adenocarcinoma of the Urinary Bladder: Next-Generation Sequencing (NGS) of Non-urachal Enteric-type Adenocarcinomas, Urachal Adenocarcinomas, Mucinous Adenocarcinomas, and Colonic Metaplasias/Adenomas

Ana Pires-Luís[1], *Petr Martinek*[2], *Jelena Filipovic*[3], *Reza Alaghehbandan*[4], *Kiril Trpkov*[5], *Eva Maria Comperat*[6], *Maria Delia Perez Montiel*[7], *Stela Bulimbasic*[8], *João Lobo*[9], *Rui M Henrique*[10], *Tomas Vanecek*[11], *Kristyna Pivovarcikova*[12], *Kvetoslava Michalova*[13], *Bohuslava Saskova*[14], *Michal Michal*[15], *Ondrej Hes*[15]. [1]Instituto Português de Oncologia do Porto Francisc, Porto, [2]Bioptical Laboratory, Pilsen, Czech Republic, Plzeň, Plzensky kraj, [3]University of Belgrade, Serbia, Belgrade, Serbia, [4]Royal Columbian Hospital, New Westminster, BC, [5]University of Calgary, Calgary, AB, [6]Paris, [7]Instituto Nacional de Cancerologia, Mexico City, [8]University Hospital Centre Zagreb, Zagreb, [9]Portuguese Oncology Institute - Porto, [10]Instituto Portugues de Oncologia do Porto Francisc, [11]Bioptical Laboratory, Pilsen, Czech Republic, [12]Biopticka Laborator Plzen, Plzen, West Bohemia, [13]Biopticka Laboratory, Plzen, Czech Republic, [14]Biopticka Laborator Plzen, Plzen, CZ, [15]Bioptical Laboratory s.r.o., Plzen, Biopticka Laboratory, Plzen

Background: Primary adenocarcinoma of the urinary bladder (enteric type) is uncommon and could present a challenging diagnostic dilemma in routine practice. These tumors overlap morphologically and immunohistochemically with other similar neoplasms found at various sites. The genetic background of such tumors is so far poorly understood. The aim of this study was to evaluate the mutational profile of the primary adenocarcinomas of the urinary bladder using NGS.

Design: 28 cases with detailed clinical data were included in the study, including 12 primary enteric adenocarcinomas (PEA), 10 urachal adenocarcinomas (UA), 2 primary mucinous/colloid adenocarcinomas (PMA), and 4 colonic-type metaplasia/villous adenomas (CMA). All cases were examined using NGS Comprehensive Cancer Panel of 275 genes.

Results: *KMT2C* was the most frequently mutated gene in all groups (PEA:83%, UA:90%, PMA and CMA:100%). In PEA other common mutated genes were *NOTCH2* (67%), *TP53 (58%), KDR* (58%), *BCR, NOTCH1* and *BRCA2* (50%). Among UA, *TP53* was mutated in 90%, followed by *NOTCH2* (50%) and *NF1* (50%). All 2 PMA cases demonstrated *NF1, MED12* and *ARID2* mutations. In all (4) CMA *RNF43* was mutated, followed by *LRP1B* (75%), *BCR* (75%), *ATR* (75%), *NOTCH2* (50%), *NF1* (50%) and *KDR* (50%). Frequency of *NF1* and *KDR* mutations differed between PEA and UA. Mutations in *APC, ATM, ARI1A* and *KRAS* were found in less than 50% of all study groups. Of note, the frequently mutated genes in colonic adenocarcinoma (*PIK3CA, FBXW7, SMAD4, NRAS, CTNNB1, SMAD2, SOX9*) and bladder urothelial carcinoma *(FGFR3, PIK3CA, HRAS, RB1, TERT*) were found in less than 33% of PEA, UA and CMA.

Conclusions: Despite similarities in the most frequently mutated genes between PEA and UA, these tumors seem to exhibit different mutational profiles. Importantly, the most commonly mutated genes (>50%) in all groups, did not overlap and were mostly different from the ones reported for colonic adenocarcinoma and bladder urothelial carcinoma, except for TP53.

1049 Fumarate-Hydratase Deficient Renal Cell Carcinoma Does not Demonstrate a Distinct Chromosomal Numerical Aberration Pattern

Kristyna Pivovarcikova[1], *Petr Martinek*[2], *Kiril Trpkov*[3], *Reza Alaghehbandan*[4], *Cristina Magi-Galluzzi*[5], *Enric Condom Mundo*[6], *Eva Maria Comperat*[7], *Dan Berney, Saul Suster*[8], *Anthony J Gill*[9], *Kvetoslava Michalova*[10], *Bohuslava Saskova*[11], *Michal Michal*[12], *Ondrej Hes*[13]. [1]Biopticka Laborator Plzen, Plzen, West Bohemia, [2]Bioptical Laboratory, Pilsen, Czech Republic, Plzeň, Plzensky kraj, [3]University of Calgary, Calgary, AB, [4]Royal Columbian Hospital, New Westminster, BC, [5]Cleveland Clinic, Cleveland, OH, [6]Bellvitge Hospital Barcelona, [7]Paris, [8]The Medical College of Wisconsin, Milwaukee, WI, [9]University of Sydney, Greenwich, NSW, Australia, [10]Biopticka Laborator, Plzen, Czech Republic, [11]Biopticka Laborator Plzen, Plzen, Czech Republic, [12]Bioptical Laboratory s.r.o., Plzen, [13]Biopticka Laborator, Plzen

Background: Several recent studies have examined various aspects of FH deficient RCC/Hereditary leiomyomatosis associated renal cell carcinoma syndrome associated renal cell carcinoma (FHRCC/HLRCC). It is evident that chromosomal numerical aberration pattern (CNAP) in FHRCC/HLRCC is more complex and heterogeneous than initially proposed. The aim of this study was to investigate CNAP in FHRCC/HLRCC, which to our knowledge has not been previously done.

Design: We evaluated 13 confirmed cases of FHRCC/HLRCC with genetically detected mutation/LOH of the FH gene for possible numerical chromosomal aberrations using array-CGH.

Results: Patient cohort included8 males and 5 females, with age range of 24-65 years (mean 50.8 years), and tumor size of 0.9-18 cm (mean 9.6 cm). The array-CGH analysis was successfully performed in 6/13 cases. The most frequent change was the loss of entire or part of chromosomes 1, 4, 19 (3/6 cases). Less frequently we observed gains of chromosome 17 (2/6) and 7 (1/6).

Case	sex	age (years)	size (cm)	FH mutation	CNAP
1	F	52	multiple 0.2-0.9	c.698G>A / p.(Arg233His)	NA
2	F	51	multiple 0.6-1.4	c.698G>A / p.(Arg233His)	-1,-4,-13,-14,-15,-19p
3	M	44	7	c.911_917delCTTTTGT /p.(Phe305Leufs*22)	NA
4	F	45	7	LOH	NA
5	M	42	10	c.395_398delTAAAT / p.(Leu132Ter)	NA
6	M	65	18	c.1189G>A / p.(Gly397Arg) +LOH	-8p,-9q,-13,-18q
7	M	60	8	c.174_177dupTGAAA / p.(Leu60Ter)	NA
8	F	50	10	c.139C>T, p.(Gln47Ter) +LOH	-1p,+1q,-3,-4,+5p,-5q,-7,-9,-17p,-18,-19p
9	M	60	8	c.496G>T, p.(Gly166Ter)	+2,-3q,+7,+10q,+16p,+17,-22q
10	M	52	14	c.1385_1390+6del	NA
11	M	54	14	c.239dupA / p.(Ile81Aspfs-Ter14)	-1,-4q,+16,+17
12	M	61	12	c.589A>T / p.(Ile197Phe) +LOH	NA
13	F	21	multiple 2.3-13	c.1118A>G / p.Asn373Ser	-5p15.33 - p15.2

Conclusions: CNAP in FHRCC/HLRCC appears to be highly variable. Despite the limited number of analyzable cases, we did not identify a characteristic CNAP associated with FHRCC/HLRCC that may have either a diagnostic utility or clinical significance in the routine practice. Immunohistochemical and molecular evaluation for *FH* gene mutations remain the gold standard in identifying FHRCC/HLRCC.

1050 Primary Renal Well-differentiated Neuroendocrine Tumor (Carcinoid): Next- Generation Sequencing Study of 12 Cases

Kristyna Pivovarcikova[1], *Petr Martinek*[2], *Reza Alaghehbandan*[3], *Maria Delia Perez Montiel*[4], *Isabel Alvarado-Cabrero*[5], *Joanna Rogala*[6], *Naoto Kuroda*[7], *Boris Rychly*[8], *Slavko Gasparov*[9], *Kvetoslava Michalova*[10], *Bohuslava Saskova*[11], *Michal Michal*[12], *Ondrej Hes*[13]. [1]Biopticka Laborator Plzen, Plzen, West Bohemia, [2]Bioptical Laboratory, Pilsen, Czech Republic, Plzeň, Plzensky kraj, [3]Royal Columbian Hospital, New Westminster, BC, [4]Instituto Nacional de Cancerologia, Mexico City, [5]Mexican Oncology Hospital, Mexico, MEX, [6]Wojewodzki Szpital Specjalistyczny, Wroclaw, [7]Kochi Red Cross Hospital, Kochi City, Kochi, [8]Bratischava, Slovakia, [9]School of Medicine, Zagreb, [10]Chotikov, [11]Biopticka Laborator Plzen, Plzen, Czech Republic, [12]Bioptical Laboratory s.r.o., Plzen, [13]Biopticka laborator, Plzen

Background: Primary well-differentiated renal neuroendocrine tumor (RNT) is a rare neoplasm with approximately 100 cases being reported in the literature. Limited information concerning the genetic background is available, with LOH3p being the most frequently mentioned feature.

Design: 20 RNTs were selected out of 21,000 renal tumors in our

registry. 12 cases with detailed clinical history were reviewed and further analyzed using Next-Generation Sequencing for the following genes: *CTNNB1, ERBB2, FGFR2, FLT4, GATA2, GREM1, HOXB13, KDR, NF1, NOTCH1, PIK3CA, PLCG1, PTEN, RUNX1, TNFAIP3,* and *VHL*.

Results: Patients were five males and seven females, with the mean age of 56.1 years, and the mean tumor size of 9.2 cm (size available in 10/12 cases). All cases were confirmed to be primary renal tumors. 5/12 tumors showed mutation in *NF1* gene, 2/12 mutation in *FLT4*, while only 3/12 carried LOH3p.

Conclusions: The most frequently observed genetic change in RNTs was mutation in *NF1* gene followed by LOH3p and mutation in *FLT4* gene. Our finding suggests that oncogenesis of RNTs is much more complex than originally thought, and that LOH3p may not be the most prevalent genetic change in RNTs.

1051 Multi-Scale Quantitative Tissue Phenotype Analysis of Prostate Cancer Biopsies: A New Diagnostic and Prognostic Tool for Pathologists

Miha Pukl[1], *Anita Carraro*[2], *Jagoda Korbelic*[3], *Alan Harisson*, *Zhaoyang Chen*[3], *Branko Palcic*, *Mira Keyes*[3], *Calum MacAulay*[4], *Metka Volavšek*[5], *Martial D Guillaud*[6]. [1]GH Celje, [2]BC Cancer Agency, Vancouver, BC, [3]BC Cancer Agency, [4]BC Cancer Agency, Vancouver, BC, [5]University of Ljubljana, Ljubljana, [6]BCCRC, Vancouver, BC

Background: Prostate cancer is the leading cause of cancer among elderly men in the Western world. Opportunistic screening has partially contributed to the increase in the incidence of prostate cancer by detecting many early-stage cancers that are low risk of progression. Even though active surveillance of such cancers is increasing, the majority of these cancers are still cured radically by surgery or radiotherapy. Gleason score (GS) is the most reliable diagnostic and prognostic tool for management of the disease. However, this subjective assessment results in inter-observer variability, particularly among general pathologists. There is a need for an objective and reproducible method that would produce reliable diagnosis and prognosis. As GS is defined by pathologists by visually screening tissue sections, we believe that a robust and in-depth quantitative evaluation of the tissue architecture could be of significant value for pathology.

Design: Our cohort consisted of 115 patients with GS 6 and GS 3+4=7 (later GS 7) cancers only. Tissue sections adjacent to the sections that contained the worst GS were stained with Feulgen stain, a quantitative DNA stain, and scanned with a whole slide scanner. Using an *in-house* software, several regions of interests were selected for analysis. Nuclei centers were automatically segmented and acini contours delineated. Multi-Scale Quantitative Tissue Phenotype Analysis (MSQTP) was performed using Voronoi diagrams and Minimum Spanning Trees to extract more than 300 features measuring changes in tissue architecture (Figure 1).

Results: There were 86 patients with GS 6 (75%) and 29 patients with GS 7 (25%). BCR was identified in 27 patients (23.5%) within an observation period of **9 years.** 13 patients with BCR had GS 6 (13% of GS 6 patients) and 14 patients had GS 7 (48% of GS 7 patients). Figure 2 illustrates the difference between patients with and patients without BCR with one of the most discriminate MSQTP features (mean length of the MST branches). Interestingly, the difference was the opposite for GS 6 and GS 7 patients. Using machine learning algorithms, we were able to correctly classify tumors from patients with BCR versus tumors from patients without BCR with an accuracy of 75%.

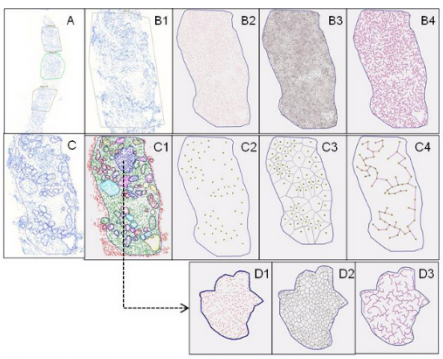

Figure 1. Multi-scale Quantitative tissue Phenotype Analysis of Prostate Biopsies. A) Feulgen-stained biopsy is scanned with a Whole Slide Scanner and several Regions of Interest are manually outlined (B1). **Nuclei based Tissue Architecture (Bx).** Automated extraction of nuclei centers (B2) Calculation of Voronoi diagram (B3) and Minimum Spanning tree (B4) based of nuclei coordinates. **Acini based Tissue Architecture (Cx)** Acini contour are manually outlined (C), automatically identified (C1), their centers of gravity automatically extracted (C2); Voronoi Diagram (C3) and MST (C4) are calculated. **Acini Architecure** : For each Acinus (C1), nuclei centers are extracted (D1) and Voronoi Diagram (D2) and MST (D3) are calculated.

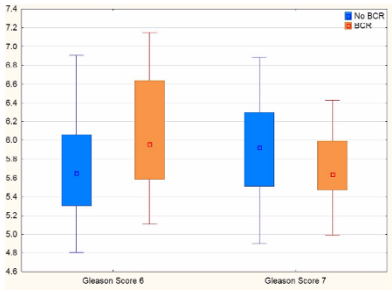

Conclusions: Our study indicates that MSQTP approach has the potential to be used in conjunction with the Gleason Score to further identify tumors with a more aggressive phenotype. Validation of these preliminary results on a larger cohort of patients is underway.

1052 Predictive Parameters of Prostate Needle Core Biopsies Associated with Seminal Vesicle Invasion at Radical Prostatectomy

Brian Radlinski[1], *Adeboye O. Osunkoya*[2]. [1]Emory University Hospital, Atlanta, GA, [2]Emory Univ/Medicine, Atlanta, GA

Background: Unilateral or bilateral seminal vesicle invasion (SVI) by prostatic adenocarcinoma (PCa) is typically characterized by poor clinical outcome. Identification of patients who are potentially at increased risk of having SVI at radical prostatectomy is therefore critical.

Design: A search was made through the urologic pathology files at our institution for radical prostatectomy cases of PCa with SVI. The laterality of the SVI was documented. Clinicopathologic parameters, including patient age, Gleason score (Grade group), percentage of involvement, laterality, and presence of perineural invasion (PNI), for the needle core biopsies were also obtained.

Results: Sixty-five patients were included in our study. Mean patient age was 61 years (range: 40-73 years). Twenty-three of 65 (35%) patients had bilateral SVI, and 42/65 (65%) had unilateral SVI (right 23/42 [55%] and left 19/42 [45%]). Sixty-one of 65 (94%) cases had PCa in the right and/or left base in the needle core biopsy (right 11/61 [18%], left 20/61 [33%], and bilateral 30/61 [49%]). PNI was present in the right and/or left base in 26/51 (51%) cases. The breakdown of Gleason scores (Grade groups) was as follows: Gleason score 3+3=6 (Grade group 1) 3/61 (5%) cases; Gleason score 3+4=7 (Grade group 2) 21/61 (34%) cases; Gleason score 4+3=7 (Grade group 3) 19/61 (31%) cases; Gleason score 8 (Gleason group 4) 9/61 (15%) cases; and Gleason scores 9-10 (Grade group 5) 9/61 (15%) cases. Fifty-eight of 65 (89%) cases showed concordance between the laterality of SVI at radical prostatectomy and PCa in the base needle core biopsy. Mean percentage of involvement in the base needle core biopsies that had subsequent ipsilateral SVI was 58.9% (95% confidence interval [CI]: +/- 10.4%). Mean percentage of involvement in the base needle core biopsies that had no subsequent ipsilateral SVI was 13.1% (95% CI: +/- 7.5%). The difference between these two groups was statistically significant ($p < 0.0001$).

Conclusions: This study demonstrates a statistically significant correlation between the percent involvement by PCa in the prostatic base in needle core biopsies, and the presence of ipsilateral SVI. Patients with greater than 50% involvement by PCa in the base have an increased likelihood of ipsilateral SVI. In addition, this study highlights one of the advantages of accurately reporting the percent involvement of individual cores on prostate needle core biopsies.

1053 PD-L1 Expression in Urothelial Carcinoma with Divergent Differentiation, Concordance among Three Antibodies

Henning Reis[1], *Rene N Serrette*[2], *Anuradha Gopalan*[2], *Ying-Bei Chen*[2], *Samson W Fine*[2], *Satish Tickoo*[2], *S. Joseph Sirintrapun*[3], *Gopa Iyer*[2], *Samuel A Funt*[2], *Min Yuen Teo*[3], *Jonathan E Rosenberg*[2], *Dean F Bajorin*[2], *David Solit*[2], *Guido Dalbagni*[2], *Bernard H Bochner*[2], *Victor Reuter*[2], *Hikmat Al-Ahmadie*[2]. [1]West German Cancer Center, University of Duisburg-Essen, University Hospital Essen, Essen, Germany, Essen, NW, [2]Memorial Sloan Kettering Cancer Center, New York, NY, [3]New York, NY

Background: Immune checkpoint blockade (ICB) is one of the most promising new treatments for advanced and metastatic urothelial carcinoma (UC) with several novel anti-PD1/PD-L1 agents currently approved to treat UC and other advanced cancers. However, as ICB therapy has been approved for classic UC (or NOS), patients with UC with divergent differentiation (UCDD) have been largely excluded from receiving ICB. The aim of this study is to investigate the expression of PD-L1 in UCDD and to compare such expression across three different clones for PD-L1.

Design: A total of 85 cases of UC with divergent differentiation (Table 1) were evaluated for PD-L1 expression using two clones currently approved as complementary tests with durvalumab (SP263) and atezolizumab (SP142). We also stained all cases with one of the earlier and commonly used clones, 22C3. PD-L1 expression in tumor cells (membranous pattern, total count, H-Score) and in the immune cell infiltrate were evaluated and compared.

Results: Detailed results are in Table 1. The majority of UCDD expressed PD-L1 in tumor cells, most commonly in areas with squamous, micropapillary and glandular differentiation, with the most extensive expression in squamous areas. The divergent differentiation with the most PD-L1 expression on infiltrating immune cells was squamous. There was strong correlation in detecting PD-L1 expression on tumor cells as well as infiltrating immune cells among the three antibodies used (p<0.001), with the highest expression detected with SP263 and the lowest with DP142

	SP263			SP142			22C3		
Histologic differentiation (n)	Tumors positive (n, %)	Mean expression on tumor cells (%)	Mean expression on tumor associated immune cells (%)	Tumors positive (n, %)	Mean expression on tumor cells (%)	Mean expression on tumor associated immune cells (%)	Tumors positive (n, %)	Mean expression on tumor cells (%)	Mean expression on tumor associated immune cells (%)
Micropapillary (19)	13 (68%)	6	14	6 (32%)	2	5	7 (37%)	3	9
Squamous differentiation (17)	16 (94%)	46	15	16 (94%)	25	11	16 (94%)	33	20
Nested (14)	5 (36%)	4	12	1 (7%)	3	5	4 (29%)	5	9
Plasmacytoid (14)	3 (21%)	5	11	3 (21%)	1	3	4 (29%)	2	4
Small cell carcinoma (12)	2 (17%)	9	7	2 (17%)	7	3	2 (17%)	7	6
Glandular differentiation (9)	6 (67%)	6	15	6 (67%)	1	5	6 (67%)	3	11
Total (85)	45 (53%)	14	12	34 (40%)	7	5	39 (46%)	10	10

PD-L1 expression in urothelial carcinoma with divergent differentiation is common, suggesting potential benefit from anti-PD1/PD-L1 therapies.

- PD-L1 expression is highest in urothelial carcinoma with squamous differentiation.
- Clone SP263 is associated with the highest expression rate, followed by 22C3 and SP142.
- Despite the variation in expression, there is significant correlation among these three clones, which applies to PD-L1 expression on both tumor cells and immune cell infiltrate.

1054 Potentially Targetable Molecular Alterations in 70 Cases of Urachal Cancer

Henning Reis[1], *Kristan E van der Vos*[2], *Christian Niedworok*[3], *Thomas Herold*[4], *Orsolya Módos*[5], *Attila Szendrői*[5], *Thomas Hager*[4], *Marc Ingenwerth*[4], *Daniël J Vis*[6], *Mark A Behrendt*[7], *Jeroen de Jong*[8], *Michiel S van der Heijden*[6], *Benoit Peyronnet*[9], *Romain Mathieu*[9], *Marcel Wiesweg*[10], *Jason Ablat*[11], *Krzysztof Okon*[12], *Yuri Tolkach*[13], *Felix Bremmer*[14], *Nadine T Gaisa*[15], *Piotr Chlosta*[12], *Joerg Kriegsmann*[17], *József Timar*[18], *Glen Kristiansen*[19], *Heinz-Joachim Radzun*[14], *Ruth Knüchel*[15], *Martin Schuler*[10], *Peter C Black*[20], *Herbert Rübben*[3], *Boris Hadaschik*[3], *Kurt Werner Schmid*[4], *Bas W van Rhijn*[21], *Péter Nyirády*[5], *Tibor Szarvas*[3]. [1]University of Duisburg-Essen, University Hospital Essen, Essen, Germany, Essen, NW, [2]Netherlands Cancer Institute, [3]West German Cancer Center, University of Duisburg-Essen, University Hospital Essen, Essen, Germany, [4]West German Cancer Center, University of Duisburg-Essen, University Hospital Essen, Essen, Germany, [5]Semmelweis University, Budapest, Hungary, [6]Netherlands Cancer Institute – Antoni van Leeuwenhoek Hospital, Amsterdam, Netherlands, [7]Netherlands Cancer Institute – Antoni van Leeuwenhoek Hospital, Amsterdam, Netherlands, [8]Amsterdam, Netherlands, [9]University of Rennes, Rennes, France, [10]West German Cancer Center, University of Duisburg Essen, University Hospital Essen, Essen, Germany, [11]Vancouver Prostate Centre, University of British Columbia, Vancouver, Canada, [12]Jagiellonian University, Cracow, Poland, [13]University of Bonn, Bonn, Germany, [14]University of Göttingen, Göttingen, Germany, [15]RWTH, [16]Aachen University, Aachen, Germany, [17]MVZ für Histologie, Zytologie und Molekulare Diagnostik, Trier, Rheinland-Pfalz, [18]Semmelweis University, Budapest, Hungary, [19]University of Bonn, Bonn, Germany, [20]Vancouver Prostate Centre, University of British Columbia, Vancouver, Canada, BC, [21]Netherlands Cancer Institute – Antoni van Leeuwenhoek Hospital, Amsterdam, Netherlands

Background: Urachal cancer (UrC) is a rare but aggressive cancer. While prospective clinical studies can hardly be conducted, rationale-based targeted therapeutic treatment approaches become more important for treatment in advanced disease. We therefore investigated the distribution of candidate molecular targets for potential therapeutic intervention in a large cohort of UrCs in context with clinicopathological and survival data.

Design: A total of 70 UrCs were analyzed by targeted next-generation sequencing in an international and multi-institutional approach and in situ and protein expression analyses were performed. Clinicopathological and survival data were collected and analyzed for statistical associations. Univariable/multivariable Cox regression and Kaplan-Meier analyses were conducted.

Results: The majority of patients were male (66%) and the mean age was 50 years. The 5-year recurrence-free (RFS) and overall survival (OS) rates were 45% and 58%. A genetic alteration was detected in 79% of samples (55/70). Gene sequence alterations were found in TP53 (66%), KRAS (21%), PIK3CA (4%), BRAF (4%), NRAS (1%), MET (1%), PDGFRA (1%), and FGFR1 (1%). In EGFR, ERBB2, and MET gene amplifications were identified. No alterations were detected in DDR2, FGFR3, HRAS, KIT, and RET.

Conclusions: With implications for anti-EGFR therapy, alterations in intracellular signal transduction pathways (RAS/RAF/PI3K) were identified in 31% of UrCs. In ERBB2 (HER2), FGFR1, MET, and PDGFRA also less frequent potentially actionable genetic alterations were detected. The molecular profile gives support to the concept that UrC at the genomic level more closely resembles colorectal cancer than urothelial carcinoma.

1055 The Grade Group in the New Grading System for Prostate Carcinoma Could be Predicted by the PCA3 urine test

Natalia Rodon[1], *Isabel Trias*[2], *Montse Verdu Artufel*[3], *Miquel Calvo*[4], *Josep Maria Banus*[5], *Olga Díaz Castello*[2], *Yessica Anahi No Garbarino*[2], *Xavier Puig Torrus*[6]. [1]BIOPAT. Biopatologia Molecular SL., Barcelona, Spain, [2]BIOPAT. Biopatologia Molecular SL., [3]Barcelona, [4]Department of Statistics. Biology Faculty. Universitat de Barcelona., [5]ICUN. Institut Català d'Urologia i Nefrologia., [6]BIOPAT, Biopatologia Molecular SL, Barcelona

Background: In this study the association between the Grade groups in the new Grading System for prostate cancer (PCa) proposed by the International Society of Urological Pathology (WHO Classification of Tumours. 4th ed. 2016) and the PCA3 urine test was evaluated.

Design: This retrospective study included data from consecutive patients with suspected PCa who presented to the urology office between November 2009 and April 2016 and were candidates for prostate biopsy. A total of 1038 urine samples were tested with a kit that generated a PCA3 score (s-PCA3). A prostate biopsy (Pbx) was recommended only in those patients with sPCA3 ≥ 35. When a PCa was diagnosed the following variables were recorded: the percentage of cylinders affected by tumor, the Gleason score and its corresponding Grade group. When associations with aggressiveness parameters were evaluated a cut-off of 50 was used for the s-PCA3 and a 33% for the affected cylinders. Associations between variables were analyzed using the R software.

Results: In patients with a positive s-PCA3 (44.5%), a subsequent Pbx was recommended. A total of 151 Pbx were studied, 56.3% yielded a diagnosis of PCa. The probability of a positive Pbx increased as the sPCA3 increased (p=0.041). A statistically significant relationship was observed between the Grade groups and the s-PCA3 (p=0.008). The 68.8% of patients with a positive sPCA3 lower than 50 were in the Grade group 1 (Figure 1). The best loglinear models and a logistic model confirmed the relationships between sPCA3 and Grade groups shown previously with Fisher's exact tests. A statistically significant relationship was also observed between the sPCA3 and the Gleason score (p=0.001). The percentage of affected cylinders increased as the sPCA3 increased (p=0.015) and no patient with a positive sPCA3 lower than 50 had more than the 33% of cylinders affected.

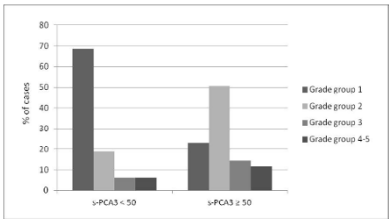

Conclusions: To our knowledge this is the first time that an association has been demonstrated between Grade group in the new Grading System and the PCA3 score. The PCA3 score may avoid overdiagnosis and overtreatment of PCa. The sPCA3 prognostic significance was also supported by its association with tumor volume and Gleason score.

1056 Single Nucleotide Copy Number Array Analysis of Unclassified Renal Cell Carcinoma (URCC): Can URCC be "Re-Classified" with Updated Immunohistochemical Stains and Application of Reported Molecular Abnormalities?

Catherine Roe[1], *Jennifer Hauenstein*[2], *Debra Saxe*[3], *Stewart Neill*[4], *Lara R Harik*[5], *Adeboye O. Osunkoya*[6], *Carla L Ellis*[7]. [1]Decatur, GA, [2]Emory University, [3]Emory University School of Medicine, Atlanta, GA, [4]Emory Univ/Medicine, Decatur, GA, [5]Emory University Hospital, Atlanta, GA, [6]Emory Univ/Medicine, Atlanta, GA, [7]Emory University, Atlanta, GA

Background: "Unclassified" Renal Cell Carcinoma (URCC) is a pathologic diagnosis that is rendered when the morphologic features and immunohistochemical profile of a renal cell carcinoma do not precisely fit into a specific, recognized World Health Organization/International Society of Urological Pathology (WHO/ISUP) category. We sought to determine if cytogenetic analysis of a subset of URCC using single nucleotide polymorphism copy number array analysis (SNP-CN) combined with re-evaluation of morphology and additional immunohistochemical stains (IHC) would aid in more accurate classification of these tumors.

Design: We analyzed 27 cases diagnosed as URCC ranging from 2007 to 2017 after a search of our pathology data system. A representative formalin-fixed, paraffin-embedded tissue block from each case was selected and SNP-CN was performed on isolated genomic DNA. We re-evaluated the morphology of the lesions by H & E staining and performed additional IHC as recommended by the ISUP. We categorized SNP-CN results as either "cardinal", "useful" or "non-contributory", based on their observed ability to re-classify each tumor in concert with IHC and morphology. Two classified cases (Papillary and Tubulocystic RCC) as well as a lymph node metastasis from one of the URCC cases were submitted as controls.

Results: Of 27 cases diagnosed as URCC, 12 of 27 (44.4%) were re-classified into a recognized WHO/ISUP or literature reported category, based on cardinal SNP-CN results and supplementary IHC. The re-classified cases were designated as follows: Clear Cell RCC (N=3), Clear Cell Papillary RCC (N = 3), SDHB-Deficient RCC, Chromophobe RCC, FH-deficient RCC, Eosinophilic Solid and Cystic RCC (N = 1 each) and two recently described TFEB-VEGFA co-amplified RCC. The remaining 15 cases (55.6%) remained unclassified by the same criteria. Another notable finding was the absence of consistent cytogenetic abnormalities in clear cell papillary and tubulocystic RCC.

Conclusions: In the appropriate histopathologic context, SNP-CN is useful in classifying RCCs that would otherwise be "unclassified" by morphology and IHC alone, based on its ability to demonstrate cardinal (known) genetic alterations that have been reported in the literature. This finding may aid in improved treatment strategies with directed/personalized therapeutic regimens.

1057 Should targeted prostate biopsy replace standard prostate biopsy?

Jenny Ross[1], *Andres G Madrigal*[2], *David Casalino*[3], *Ximing Yang*[4]. [1]Feinberg School of Medicine, Chicago, IL, [2]Northwestern University, Chicago, IL, [3]Northwestern Memorial Hospital, [4]Northwestern University, Chicago, IL

Background: With advances in imaging studies, MRI-guided "targeted" prostate needle biopsies are becoming more frequent. It has been suggested that targeted biopsy could increase diagnostic accuracy and reduce unnecessary biopsies because target should detect more clinically significant prostate cancer.

Design: We searched recent files for all targeted prostate biopsies performed over a six month period (March to September 2017) at our institution and compared the results of targeted biopsy sets with standard sextant biopsy sets. Prostatic adenocarcinomas were graded as Gleason 6 or low (Group1), Gleason 3+4=7 (Group 2), Gleason 4+3=7 (Group 3), Gleason 8 (Group 4), or Gleason 9 or higher (Group 5).

Results: In the six month period, there were 482 prostate biopsies, of which 142 had targeted biopsies including 121 with both standard sextant biopsies and targeted biopsies (S+T), and 21 with targeted biopsies only (T). Out of 121, 66 (54.5%) were positive for prostatic adenocarcinoma including 46/121 (38%) in Group 2 or above.

Of 121 targeted biopsies, 9 (7.4%) had carcinoma discovered only on targeted biopsies, including 4/9 (44.4%) in Group 2 or above. In 4 separate cases, targeted biopsies had higher grade cancer (Group 2 or higher) than the standard set (Group 1).

In 16 (13.2%) of the 121 targeted biopsies, the results were benign, but standard biopsies (S) contained adenocarcinomas including 9/16 (56.3%) cases with Group 2 or higher. In 3 separate cases, standard biopsies had cancers of Group 2 or higher, while the targeted biopsies had Group 1.

Typically, each targeted area produced 2-5 tissue cores, the average for all targeted cores is 4.5, while the standard set contained 11.3 cores on average. The combination of standard biopsies and targeted biopsies leads to increased tissue sampling by almost 39.8%. Performance of targeted biopsy alone would remove 11.3 cores of standard biopsy, reducing core tissue sampling by 71.5%.

	S	T	Total positive cases	Groups 2-5 carcinomas	Percentage of higher grade carcinomas of positive cases
121	121	121	66 (54.5%)	46	46/66 (69.7%)
	Positive	Positive	41 (33.9%)	33	33/41 (80.5%)
	Negative	Positive	9 (7.4%)	4	4/9 (44.4%)
	Positive	Negative	16 (13.2%)	9	9/16 (56.3%)
21	0	21	11/21 (52.4%)	8	8/11 (72.7%)

Conclusions: Based on our study, targeted prostate needle core biopsy cannot replace the standard prostate biopsy. Targeted biopsy will be complementary to standard biopsy by detection of additional cases of prostate cancer including higher grade cases. However, targeted biopsies without the standard sextant sets, reducing tissue sampling by 70%, would fail to detect nearly 13% of prostatic adenocarcinoma including 10% of higher grade (Group 2 or above) adenocarcinomas.

1058 Clear cell cluster in the kidney: Is this a precursor lesion of renal cell carcinoma?

Jenny Ross[1], *Huiying He*[2], *Xiaoqi Lin*[3], *Ximing Yang*[4]. [1]Feinberg School of Medicine, Chicago, IL, [2]Beijing, China, [3]Northwestern University, Chicago, IL, [4]Northwestern Univeristy, Chicago, IL

Background: Premalignant lesions of renal cell carcinoma (RCC), particularly clear cell renal cell carcinoma (CCRCC) are mostly unknown.

Design: A series of 11 partial or total nephrectomies were identified to contain clusters of epithelial cells with abundant clear cytoplasm similar to CCRCC. Primary tumor type, number and size of clusters, and numbers of cells within each cluster were recorded. Immunohistochemistry was performed for Carbonic Anhydrase IX (CA-IX), CK7, AMACR, PAX8, and Vimentin and presence or absence of marker expression evaluated.

Results: The histologic subtypes of main tumor included 7 CCRCC, 2 papillary RCCs, and 2 multilocular cystic renal cell neoplasms of low malignant potential. The size of the CCC ranged from a few micrometers to 2 mm. The number of clear cells in each cluster ranged from a handful to hundreds of cells (Fig. 1). Immunohistochemistry was successful in 8 of 11 cases. Results showed that the CCC were positive for both PAX8 and CK7 in 8 of 8 cases, and were negative for CA-IX, AMACR, and Vimentin in 8 of 8 cases.

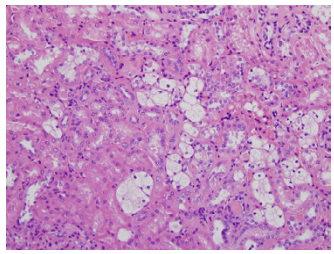

Conclusions: In this study, we reported pathologic features of clear cell clusters in the kidney harboring RCC. Although their histologic features are similar to those of CCRCC, the immunoprofile of CCC is different from that of CCRCC or PRCC. Based on our study, it is not conclusive that these clear cell clusters are indeed a precursor lesion of CCRCC. However, caution should be exercised when clear cell

clusters are encountered on a limited specimen, particularly needle biopsies, as this lesion may be confused with CCRCC.

1059 Contributory and Noncontributory Factors in Accuracy of MRI Guidance in Detecting Prostate Cancer versus Systematic Biopsy in Patients with Radical Prostatectomy

Omid Rouhi[1], *Shaun Boyes*[1], *Maria Picken*[2]. [1]Loyola University Medical Center, Maywood, IL, [2]Loyola Univ. Med. Ctr., Maywood, IL

Background: Despite improvements in cancer detection, prostate biopsy lacks the ability to aacurately map locations of cancer. The current diagnostic procedure for prostate cancer is systematic (sextant) biopsies (SBx). Unlike many other solid tumors for which image-guided biopsy is common, prostate cancer has traditionally been detected by randomly sampling the entire organ. Use of mutiparametric MRI (mpMRI) for targeted biopsy (TBx) allows for imaging-based identification of prostae cancer, which may improve prostate biopsy efficiency. The aim of our study was to evaluate the biopsy efficiency of TBx vs SBx in patients undergone both standard and targeted prostate needle biopsy and subsequent radical prostatectomy (RP).

Design: This single-institution retrospective study included 24 patients with concomitant SBx and TBx needle core biopsies who subsequently underwent radical prostatectomy from July-2015 to July-2017. The mean age of the patiets was 60 years (range: 43-71). The median time between core biopsy and radical prostatectomy was 2.5 months (range: 1.5-7 months). A mean of 6 standard and 2.1 targeted biopsies were obtained from each patient.

Results: 62% of patients showed an agreement in the results of SBx and TBx. There was 38% discrepancy between the results of TBx and SBx. This agreement was statistically significant in the cases with higher cancer burden in RP (9.5% vs 20%, p: 0.02) However, the weight, size, and density of prostate gland and patient's age did not have any significant effect on the biopsy result. The cancer staging distribution was: T2a (8%), T2c (62%) and T3a (30%). None of the discrepancy cases was seen in T3a stage patients.

A total of 45% of cases had matching Gleason score at SBx and RP (62% at TBx). 20% of cases were upgraded from SBx to a higher grade at RP (8% at TBx). 25% of cases were downgraded from SBx to a lower grade at RP (0% at TBx).

	SBx (no Pca)	SBx (Pca)
TBx (no Pca)	0 (0%)	7 (30%)
TBx (Pca)	2 (8%)	15 (62)%

Conclusions: Targeted biopsy (TBx) is more accurate than systematic biopsy (SBx) in determining the Gleason score. The weight, size and density of prostate gland do not interfere with the diagnostic ability of TBx. Our data suppots the efficiency of targeted biopsy in prostate cancer. However, there are pitfalls in this technique such as inflammation and prostatic atrophy which lead to false positive results and need to be studied further.

1060 Automated Clear Cell Renal Carcinoma Grade Classification with Prognostic Significance

Christopher Rubadue[1], *Katherine Tian*[1], *Humayun Irshad*[1], *Yujing Jan Heng*[1]. [1]Beth Israel Deaconess Medical Center, Boston, MA

Background: Clear cell renal cell carcinoma (CCRCC) is the most common malignant kidney tumor. Accurately classifying CCRCC Fuhrman grade and stage is important for clinical management. Fuhrman's 4-tier nuclear grading system is the current gold standard which provides significant prognostic value. The high subjectivity of Fuhrman grade assignments has led to the proposal of simplified 2- or 3-tiered systems, which improves inter-observer reliability and retains prognostic ability. Computational pathology can potentially improve reproducibility and introduce objectivity for pathology practice. We developed a computer pipeline to automatically classify CCRCC whole slide images (WSIs) in low or high grades and evaluate the prognostic efficacy of our predicted CCRCC Fuhrman grade.

Design: Regions of interests (ROIs) on WSIs from The Cancer Genome Atlas (TCGA) CCRCC dataset (*n*=395) were annotated and assigned a grade. For each ROI, nuclear segmentation was performed using Fiji, and 72 quantitative nuclear morphological, intensity and texture features were extracted. Cases were stratified into low (grades 1 & 2) and high grade (grades 3 & 4). Concordant cases between TCGA and our internally assigned grade were randomly spilt into a training (85%) or test (15%) set to build the classification model (Lasso regression). Cox proportional hazard model evaluated if the predicted CCRCC grade was associated with overall survival (OS), adjusting for age at diagnosis, gender and stage.

Results: There were 276 concordant and 119 discordant cases. Two hundred and thirty-five concordant cases (85%) were used to train the classification model. Lasso algorithm identified 14 unique features related to the size and shape of nuclei associated with CCRCC grade. This model was evaluated on the remaining 41 concordant cases where it predicted low or high grade with an AUC of 0.86. This classification model was subsequently applied to an extended test set created by combining those 41 cases and 119 discordant cases. In this extended test set of 160 cases, cases predicted as high grade had a hazard ratio of 2.0 compared to low grade (95% CI 1.2-3.5, p<0.01).

Conclusions: We developed an automated 2-tier CCRCC grading system and demonstrated that our predicted grades are associated with OS. This is algorithm may improve the reproducibility in the diagnosis and grading of CCRCC.

1061 Hybrid Oncocytic Renal Tumors Display A Molecular Profile Intermediate Between Oncocytoma And Chromophobe Renal Cell Carcinoma

Roberto Ruiz-Cordero[1], *Lerong Li*[2], *Yuan Qi*[2], *Fumi Kawakami*[3], *Nail Alouch*[1], *Wei Lu*[2], *Ken Chen*[2], *Fadi Brimo*[4], *Jing Wang*[2], *Pheroze Tamboli*[5], *Priya Rao*[6], *Kanishka Sircar*[5]. [1]MD Anderson Cancer Center, Houston, TX, [2]MD Anderson Cancer Center, [3]The University of Texas MD Anderson Cancer Center, Houston, TX, [4]McGill University, Montreal, QC, [5]UT-MD Anderson Cancer Center, Houston, TX, [6]UT MD Anderson Cancer Center, Houston, TX

Background: Hybrid oncocytic/chromophobe tumors (HOCT) of the kidney represent a poorly understood clinicopathologic entity with histologic features that overlap between benign renal oncocytoma (RO) and potentially malignant chromophobe renal cell carcinoma (ChRCC). We initially performed next generation sequencing of HOCT and identified a low mutational frequency without mutations in known cancer driver genes. Herein, we describe copy number alteration (CNA) results in HOCT and we compare the mRNA expression profile of HOCT to that of RO and ChRCC.

Design: DNA from paired tumor/normal HOCT (n=14 samples from 11 patients) was subjected to targeted sequencing of coding regions from 261 cancer related genes (HiSeq3000, Illumina, San Diego, CA) spanning all chromosomes. An in house pipeline was used to assess arm level CNA from sequencing data. Subsequently, we performed *in silico* analysis of public gene expression data to nominate the 85 most differentially expressed genes (DEG) between RO and ChRCC. The mRNA expression of these foregoing genes was assessed on 71 samples, including 24 HOCT (mean diameter: 5.3 cm; metastatic, n=1), 19 RO (mean diameter: 5.6 cm; metastatic, n=0), and 28 ChRCC (mean diameter: 7.5 cm; metastatic, n=9) using Nanostring's nCounter platform (Seattle, WA).

Results: Among HOCT, 9 samples showed CNA with 5 samples lacking arm level chromosomal gains or losses. Copy alterations included: 1p deletion (n = 3); whole chromosome 1 deletion (n=6); deletions in 2q, 5p, and 6q (n=1); 22q deletion (n=1); polysomy chromosome 7 (n=1); Y chromosome deletion (n=4) and X chromosome deletion (n=1). RNA transcript data of DEG revealed HOCT to generally show values intermediate between RO and ChRCC; however, a greater contrast was noted between HOCT vs ChRCC (n=58 genes, P< 0.01) compared to HOCT vs RO (n=25 genes, P<0.01).

Conclusions: HOCT display a molecular profile characterized by a lack of cancer driver gene mutations, predominant chromosome 1 and sex chromosome deletions, and a gene expression profile that is separable from RO and ChRCC. Hence, HOCT appear to be molecularly distinct and to occupy an intermediate position between RO and ChRCC.

1062 Prospective Comparison of ISUP and Fuhrman Grading for Renal Cell Carcinoma on Resection Specimens

Stephen T Ryan[1], *Donna Hansel*[2]. [1]University of California at San Diego, [2]UCSD, La Jolla, CA

Background: The International Society of Urological Pathology (ISUP) grading system for renal cell carcinoma has been in recent use as an alternative for the Fuhrman grading system. However, the changes in grading of clear cell and papillary RCC and prognostic implications have not been analzyed in detail. Prospective interpretation of the two systems has yet to elucidate if there are any key differences.

Design: A prospective data collection of all renal mass lesions that underwent extirpative surgery was performed by two experienced genitourinary pathologists. Both the Fuhrman and ISUP grading systems were recorded.

Results: Ninety-eight renal cell carcinomas that underwent resection were prospectively analyzed from 3/2015 - 7/2017, including 50 partial nephrectomies (51%) and 48 radical nephrectomies (49%). Average patient age was 60.2 yrs (median 61.0 yrs) and average tumor size was 4.9 cm (median 3.9 cm). Cases consisted of 86 clear cell RCCs and 12 papillary RCCs. The majority of cases (84/98; 85.7%) showed

concordance of ISUP and Fuhrman grading (Table). However, 14 cases were discordant and included 1 case (8%) of papillary RCC and 13 cases (15%) of clear cell RCC. In all instances of discordance, Fuhrman nuclear grade 2 was assigned alongside an ISUP nucleolar grade of 1, suggesting a potential downgrading of 14% of all renal cell carcinomas during this time period. Three cases were lost to follow-up. Average follow-up was 268 days. At the time of follow-up, there were 2 recurrences (208 and 172 days, both ISUP grade 4) and 4 deaths (2 disease related and 2 other-cause mortalities, ISUP grades 3 and 4). All cancer and overall survival events had concordant pathology in the ISUP 3 and 4 groups.

Assigned Grade	Papillary RCC	Clear Cell RCC
Concordant		
ISUP1/Fuhrman 1	0	4
ISUP2/Fuhrman 2	5	41
ISUP3/Furhman 3	6	19
ISUP4/Furhman 4	0	9
Discordant		
ISUP1/Furhman 2	1	13

Conclusions: In a prospectively collected cohort of patients with renal mass resection, Fuhrman and ISUP renal grades were discordant 14% in the overall cohort, with the primary discordance reflecting a downgrading from Fuhrman grade 2 to ISUP grade 1 in clear cell RCCs. No discordance of grades 3 or 4 were noted, suggesting the histopathological features associated with both Furhman and ISUP grading of higher grade lesions are less prone to variability. No differences in oncologic or overall survival were observed over our short follow-up period. Further study with longer follow-up is needed to understand the clinical implications of the discordant grade interpretations at the lower grade categories.

1063 Tumor Micro-environment of Seminoma and Non Seminomatous Germ Cell Tumors (NSGCT) Show Differential Involvement by Tumor Associated Macrophages and Tumor Infiltrating Lymphocytes

Sam Sadigh[1], *Sahar J Farahani*[2], *Amanda Lisby*[3], *Priti Lal*[4]. [1]Hospital of the University of Pennsylvania, Philadelphia, PA, [2]Hospital of the University of Pennsylvania, Philadelphia, PA, [3]Hospital of the University of Pennsylvania, [4]University of Pennsylvania, Philadelphia, PA

Background: Recent strides in our understanding of the role of tumor micro-environment in cancer progression have led to the rapid development of immunotherapy. One of the targets of immunotherapy is the signaling pathway of programmed death ligand-1 (PD-L1) binding to programmed death 1 receptor (PD-1) on the surface of tumor-infiltrating lymphocytes (TILs). Additionally, tumor associated macrophages (TAMs) are thought to be involved in immune suppression and tumor invasion, and are potential candidates for immunotherapeutics. We sought to characterize the tumor microenvironment of recurrent (R) and non-recurrent (NR) seminoma and NSGCT with respect to PD-1, PD-L1, activated TILs and subtypes of TAMs.

Design: A total of 42 orchiectomy cases including 30 seminomas (23 NR-Seminoma; 7 R-Seminoma) and 12 NSGCTs (8 NR-NSGCT and 4 R-NSGCT) were identified from the archives. Clinicopathologic data was collected for each patient. H&E and immunohistochemical stains for PD-1 (clone NAT105; Abcam), PD-L1 (clone E1J2J; Cell Signaling), FOXP3 (clone 206D; BioLegend), CD68 (clone KP1: Dako), and CD163 (clone 10D6; Leica) were evaluated. Percentage of TILs positive for FOXP3 and PD-1 and TAMs positive for CD68 and CD163 were calculated. Membranous PDL-1 expression was evaluated on tumor cells.

Results: A statistically significant increase in membranous PDL-1 expression was noted in seminoma as compared to the NSGCT ($p<0.001$). The tumor micro-environment of NR-Seminoma revealed statistically significant increase in FOXP3 positive TILs ($p<0.001$) and CD163 positive TAMs ($p<0.001$) as compared to NR-NSGCT. CD163 positive TAMs were more abundant in R-Seminoma when compared to NR-Seminoma. The cohort for NR-NSGCT was limited, and no specific comparisons could be definitively drawn.

Conclusions: Our study suggests that the TAMs in primary seminoma may play a role in subsequent disease recurrence. In addition, our finding that NSGCTs had significantly less PD-L1 staining when compared to seminomas, raises the potential difference in immunogenicity of these tumor groups and the need for larger study cohorts. The immune micro-environment in testicular neoplasms involves dynamic and complex interplays, and the promise of stratifying patients in anticipation of immune-therapies requires further delineation of these.

1064 Downregulation of HOXB13 Expression in Ductal Adenocarcinoma of Prostate

Faisal Saeed[1], *Jonathan Epstein*[2], *Minghao Zhong*[3]. [1]New York Medical College at Westchester Medical Center, Valhalla, NY, [2]The Johns Hopkins Med Inst, Baltimore, MD, [3]Westchester Medical Center/ New York Medical College

Background: Recent studies identified *HOXB13* (G84E) mutation is the most common germline mutation associated with prostate cancer. Men with this mutation have a 10-20-fold increased risk of prostate cancer. *HOXB13* maintains a high expression level into adulthood in normal prostate. Additionally, studies also show HOXB13 is a sensitive and specific marker of prostate cells, and can be useful in distinguishing between carcinomas of prostatic and urothelial origin.

Design: We collected 13 cases of ductal adenocarcinoma composed of either cribriform or papillary carcinoma lined by tall pseudostratified columnar cells. All 13 cases of ductal and 89 cases of acinar carcinoma from a TMA were subjected to HOXB13 immunostaining.

Results: All benign prostatic luminal cells were positive for HOXB13 [Figure. A]. 81/89 (91%) cases of acinar carcinoma were positive for HOXB13 [Figure. B], similar to a prior study. However, only 4/13 (31%) ductal prostate adenocarcinomas were positive for HOXB13. An acinar carcinoma component associated with the ductal carcinoma was positive in 6/13 (46%) cases [Figure. C & D].

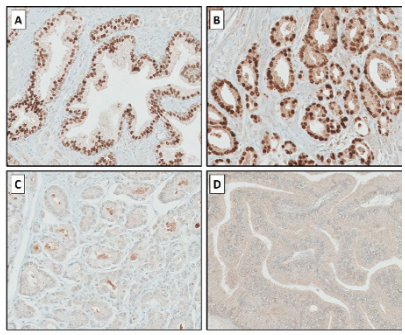

Figure. HOXB13 expression. A) Benign prostatic glands. B) Acinar carcinoma of prostate. C & D) Acinar carcinoma associated with ductal adenocarcinoma of prostate.

Conclusions: This is the 1st study of *HOXB13* expression in ductal adenocarcinoma of the prostate. Compared to usual acinar carcinoma, ductal carcinomas showed loss or decrease of *HOXB13* expression. The acinar carcinoma component associated with ductal carcinoma was also down regulated for *HOXB13* compared to pure acinar prostate cancer. Our data suggest that down regulation of *HOXB13* is important for prostatic ductal adenocarcinoma carcinogenesis. Further studies including sequencing of *HOXB13* in ductal adenocarcinoma is warranted.

1065 Integrated Molecular Analysis of Papillary Renal Cell Carcinoma and Precursor Lesions Unfolds an Evolutionary Biological Process From Kidney Progenitor Cells

Rola Saleeb[1], *Mina Farag*[2], *Qiang Ding*[3], *Michelle Downes*[4], *Georg Bjarnason*[5], *Fadi Brimo*[6], *Pamela Plant*[3], *Fabio Rotondo*[3], *Zsuzsanna Lichner*[7], *George M Yousef*[8]. [1]University of Toronto, Toronto, ON, [2]Li Ka Shing Knowledge Institute, St. Michael's Hospital, Toronto, ON, Canada, [3]St. Michael's Hospital, [4]Sunnybrook Health Sciences Centre, Toronto, ON, [5]Sunnybrook Health Sciences Centre, [6]McGill University, Montreal, QC, [7]Toronto, ON, [8]The Li Ka Shing Knowledge Institute of St. Michael's Hospital, Toronto, Canada

Background: Papillary renal cell carcinoma (PRCC) is the most common type of RCC in end stage kidney disease (ESK). It is known to have multiple subtypes with distinct molecular and clinical profiles. Papillary adenomas (PAs) are small benign papillary lesions that are thought to be PRCC precursors and are also very prevalent in ESK. The evolution of PAs to PRCCs and their relationship to ESK are poorly understood.

Design: Samples selected for the study were 20 PAs, 5 normal kidneys, 7 ESK and 108 PRCCs. Molecular analysis of the different groups was performed using miRNA expression analysis (n=12), Copy number variations CNV (n=21), and whole exome sequencing WES (n=12). Immunohistochemical (IHC) markers BCL2, CK7, LGR5 were performed on the different groups. Image analysis software was used for IHC scoring .

Results: The CNV analysis exhibited similarities between the ESK and PA. IHC markers of renal tubular progenitor cells showed a significant increase in their number in ESK (score=0.24, p value <0.0001) and PAs (score=0.2, p value 0.02) in comparison to the normal kidney(score=0.046). CNV and WES revealed common gains and mutations between the PA and the different PRCC subtypes that highlight an embryonic developmental theme. Lysine

methyltransferase 2C (KMT2C) an epigenetic regulator on Chr7 was found to have a common frameshift insertion among all papillary lesions. Each subtype had its own additional set of common mutational changes highlighting their unique identity. Pathway analysis showed an evolutionary interconnected model from ESK as a first stage to the different PRCC tumor subtypes as final stage.

Conclusions: This study uncovers evidence that correlates PRCCs with the normal kidney progenitor cells as likely cells of origin. These cells increase in ESK and hence the frequency of PRCCs in ESK. We clarify the sequence of molecular events that underlie the transformation of ESK to PAs to the different PRCC subtypes, as well as highlight the molecular differences between the subtypes. The results shed light on previously unknown biological aspects of PRCC development and are extremely significant regarding the clinical management and early prevention of these tumors.

1066 Modulating ATP binding cassette (ABC) transporters in papillary renal cell carcinoma type 2 enhances its response to targeted molecular therapies

Rola Saleeb[1], *Mina Farag*[2], *Zsuzsanna Lichner*[3], *Fadi Brimo*[4], *Fabio Rotondo*[5], *Michelle Downes*[6], *George M Yousef*[7]. [1]University of Toronto, Toronto, ON, [2]Li Ka Shing Knowledge Institute, St. Michael's Hospital, Toronto, ON, Canada, [3]Toronto, ON, [4]McGill University, Montreal, QC, [5]St. Michael's Hospital, [6]Sunnybrook Health Sciences Centre, Toronto, ON, [7]The Li Ka Shing Knowledge Institute of St. Michael's Hospital, Toronto, Canada

Background: Papillary renal cell carcinoma (PRCC) is the most common non-clear cell RCC and is known to comprise two histological subtypes. PRCC2 is more aggressive tumor and is molecularly distinct from PRCC1. Despite this PRCCs are clinically treated as one entity, with a complete lack of evidence-based management recommendations for these tumors. We have previously detected ABCC2 (an ABC transporter) and the mTOR pathway to be enriched in PRCC2. In this study we assess the value of targeting these pathways as therapeutic potentials for PRCC2

Design: Comprehensive bioinformatics analysis was performed on twenty RCC cell lines from the cancer cell line encyclopedia and compared to the PRCC2 signature derived from cancer genome atlas cohort (290 cases). Selected cell lines were grown in vitro in culture plates as well as harvested and injected subcutaneously in immune-compromised mice. Cells were treated both in vitro (in corresponding growth media) and in vivo (oral gavage) with five different conditions, untreated, anti-VEGF (Sunitinib), ABCC2 blocker (MK571), mTOR inhibitor (Everolimus) and Sunitinib + MK571. Sunitinib uptake and apoptosis were measured by flow cytometry. Mice tumors were examined histologically and Ki67 was quantified with digital analysis for the different treatment groups.

Results: CAKI-2 cell line was selected as most representative of PRCC2. The Sunitinb+ABCC2 blocker treated group showed significant response to therapy both in vitro (p value <0.0001) and in vivo (p value 0.0132). ABCC2 blockage resulted in almost double the uptake of Sunitinib, both in vitro (p value 0.0016) and in vivo (p value 0.0031). The Everolimus treated group demonstrated second best response in vivo, but the results were not reproducible in vitro. The dual treatment group showed the highest apoptotic, and lowest ki67 proliferation rate.

Conclusions: There is an urgent need for individualized therapies of RCC subtypes that take into account their specific biology. Our study demonstrates that targeting ABC transporter ABCC2 in PRCC2 has great therapeutic potential. The results are also significant for similar ABCC2 high tumors. Clinical trials are needed to confirm these effects in PRCC2 patients.

1067 Molecular Profiling of Urothelial Papilloma and Inverted Papilloma of the Bladder

Judy Sarungbam[1], *Sumit Isharwal*[2], *Ying-Bei Chen*[3], *Anuradha Gopalan*[3], *Samson W Fine*[3], *Satish Tickoo*[4], *S. Joseph Sirintrapun*[5], *Sana Jadallah*[6], *Florence Loo*[7], *Eugene J Pietzak*[2], *Eugene K Cha*[2], *Guido Dalbagni*[2], *Bernard H Bochner*[2], *Gopa Iyer*[8], *Michael F Berger*[9], *David Solit*[2], *Victor Reuter*[3], *Hikmat Al-Ahmadie*[3]. [1]Montefiore Medical Center, New York, NY, [2]Memorial Sloan Kettering Cancer Center, [3]Memorial Sloan Kettering Cancer Center, New York, NY, [4]Memorial Sloan Kettering CC, New York, NY, [5]New York, NY, [6]NYPQ, Ridgewood, NJ, [7]New York Presbyterian Queens, Flushing, NY, [8]MSKCC, New York, NY, [9]MSKCC

Background: Urothelial papilloma (UP) and inverted papilloma (IP) are benign urothelial neoplasms with exophytic and endophytic growth pattern, respectively. Hotspot mutations in *FGFR3, HRAS* and *TERT* promoter have been reported in these entities at various rates but no comprehensive molecular analysis has been reported. We performed next generation sequencing to characterize the molecular profiles of UP and IP.

Design: All cases were re-reviewed to confirm diagnosis. DNA was extracted from formalin fixed paraffin embedded tissue. Tumor and matched germline DNA (when available) were analyzed for somatic point mutations, truncations, copy number alterations, and insertions/deletions using a next generation sequencing platform assay that detects alterations in all exons and select introns of 468 oncogenes and tumor suppressor genes including the entire *TERT* promoter region.

Results: Data were available from 9 UP and 7 IP. Age ranged form 51 to 71 years. There were 13 males and 3 females. Mutation count ranged from 1 to 15 (median 4.5). In UP, 4 of 9 tumors harbored hotspot *KRAS* mutations (all in codon 12), 2 harbored hotspot *HRAS* mutations (G13R, Q61K) and one harbored an oncogenic *BRAF* mutation (T599dup). Two UP harbored *TERT* promoter mutations and one harbored an *FGFR3* hotspot mutation (S249C) taken from a patient with multiple recurrences of low grade papillary carcinoma.

In IP, 6 of 7 tumors harbored hotspot *HRAS* mutations (five Q61K, one G13R) and the remaining tumor harbored a hotspot *KRAS* mutation (G12V). No *TERT* promoter or *FGFR3* mutations were detected in any IP. In both UP and IP, *KRAS*, *HRAS* and *BRAF* mutations were mutually exclusive. Mutations in chromatin remodeling genes were less common in both UP (4 cases) and IP (2 cases) with only one *KDM6A* mutation and no *ARID1A* mutations detected. Alterations in genes involved in cell cycle regulation were rare (no *TP53* mutations and only one mutation in each of *RB1* and *CDKN1A*).

Conclusions: - Unlike in urothelial carcinoma, activating *KRAS* and *HRAS* mutations are the most common alterations in urothelial papilloma and inverted papilloma, and are mutually exclusive.

- In this cohort, activating RAS mutations are detected all inverted papillomas (6 *HRAS,* 1 *KRAS*) and in the vast majority of urothelial papillomas (4 *KRAS*, 2 *HRAS*, 1 *BRAF*).

- Compared to urothelial carcinoma, in this cohort of urothelial papilloma and inverted papilloma, *FGFR3* and *TERT* promoter mutations are rare, and mutations in chromatin modifiers are less common.

1068 Prostate Cancer of Biopsy Gleason Score 3 + 4 = 7 with Less than 5% of Gleason Pattern 4 Component Is Associated with Significantly Lower Incidence of Adverse Pathology in Japanese Cohort: Suggestion for Active Surveillance Criteria

Shun Sato[1], *Takahiro Kimura*[2], *Takashi Yorozu*[3], *Masahiro Ikegami*[2], *Hiroyuki Takahashi*[4]. [1]The Jikei University School of Medicine, Minato-ku Tokyo, [2]The Jikei University School of Medicine, [3]The Jikei University School of Medicine, Tokyo, [4]The Jikei University School of Medicine, Tokyo

Background: Active surveillance (AS) has been broadly accepted as an option for management of prostate cancer. Many inclusion criteria for AS have been proposed. In the majority of the criteria, only cancers of Gleason score (GS) 3 + 3 = 6 or less are candidates for AS. Recently, some AS criteria have included cancers of GS 3 + 4 = 7 with minimal proportion of Gleason pattern 4 (%GP4), although it is not yet universally accepted and evidence especially from Asian population is limited. This study was performed to investigate the possibility to include GS 3 + 4 = 7 cancers with small proportion of GP4 in AS.

Design: A total of 314 radical prostatectomy cases with prior prostate biopsy of GS 3 + 3 = 6 or 3 + 4 = 7 were utilized. Clinical follow up data as PSA failure were available in all cases. All biopsy specimens were reviewed and length of cancer, GS and %GP4 in each biopsy core were recorded. Cancers with GS 3 + 4 = 7 were divided as %GP4<5%, %GP4 of 5-10%, %GP4<10%, or %GP4≥10% by its highest/overall %. Relationship between highest/overall %GP4 in biopsy and adverse pathology (AP) in radical prostatectomy specimen was statistically analyzed. Subsequently, relationship between AP and PSA failure was analyzed by log-rank test. The highest %GP4 for each case was defined as the highest %GP4 among all cores of the case. Overall %GP4 for each case was calculated by (sum of cancer length of each core × %GP4)/ (sum of each cancer length). The AP was defined as GS upgrade to 4 + 3 = 7 or higher, or pT3 cancer, or positive surgical margin.

Results: The cohort included 115 GS 3 + 3 = 6 and 199 GS 3 + 4 = 7 cancers. In the setting of highest %GP4, GS 3 + 4 = 7 cancers were divided by its %GP4 as shown in Table 1. The frequency of AP in GS 3 + 3 = 6 cancers was significantly lower than GS 3 + 4 = 7 cancers with %GP4 of 5-10% and %GP4<10% (p=0.0435 and 0.0463, respectively), although there was no significant difference between GS 3 + 3 = 6 and GS 3 + 4 = 7 cancers with %GP4<5% (Table 1). Similar tendency was not identified in the setting of overall %GP4. Cancers with AP were significantly associated with higher risk of PSA failure compared to those without AP (p<0.0001).

Table 1. Relationship between highest %GP4 and AP

Highest %GP4	Case number	Number with AP (%)	P-Value
0% (GS 3 + 3 = 6)	115	47 (40.8%)	
<5%	45	23 (51.1%)	0.288 (NS)
5-10%	40	24 (60.0%)	0.0435
<10%	85	47 (55.3%)	0.0463
≥10%	114	80 (70.2%)	<0.0001

P-Value shows result of comparison between GS 3 + 3 = 6 cancers and cancers with %GP4 in each row.

Conclusions: Our results suggest that GS 3 + 4 = 7 cancers with highest biopsy %GP4<5% have similar clinical significance with GS 3 + 3 = 6 cancers, and they may be eligible in AS category. On the other hand, GS 3 + 4 = 7 cancers with highest biopsy %GP4≥5% may show more aggressive behavior and exclusion from AS criteria have to be considered.

1069 Immunohistochemical characterization of locally aggressive sarcomatoid/rhabdoid renal cell carcinoma

Jessica Saunders[1], *Chris Conklin*[2], *Cheng-Han Lee*[3]. [1]UBC, Vancouver, BC, [2]BC Cancer Agency, [3]British Columbia Cancer Agency, Vancouver, BC

Background: Sarcomatoid differentiation and rhabdoid feature are associated with aggressive clinical behavior in renal cell carcinoma (RCC). To gain better insight into the tumor biology, we performed immunohistochemical analysis on locally aggressive RCC with these features.

Design: We included 31 RCC (nephrectomy specimen) showing either sarcomatoid differentiation or rhabdoid features by histology and locally aggressive growth with extension into perinephric adipose tissue. A tissue microarray was constructed that contains duplicate cores from sarcomatoid/rhabdoid area and corresponding carcinoma area of each tumor. We evaluated the expression of PAX8, p53, MDM2, BRG1, INI1 and BAP1 by immunohistochemistry.

Results: Among the 31 tumors, 22 showed sarcomatoid and 9 showed rhabdoid features. 25 tumors contained a carcinoma component, with 15 being conventional clear cell, 3 collecting duct, 2 papillary, 2 chromophobe, 2 mixed and 1 unclassified type. PAX8 expression was uncommon in carcinoma component with 13.7% of cases showing positive staining while the sarcomatoid component was negative in all cases. 2 cases with rhabdoid features showed PAX8 expression in the rhabdoid component. Strong diffuse nuclear p53 staining indicative of *TP53* mutation was seen in the sarcomatoid component of 4 cases while the corresponding carcinoma component showed wild-type p53 expression. Two sarcomatoid RCC with wild-type p53 staining showed strong nuclear MDM2 expression in the sarcomatoid component. There was a complete loss of BAP1 nuclear expression (with internal positive stromal control) in the rhabdoid component of two cases while the corresponding carcinoma component showed retained expression. BRG1 and INI1 expression was intact in all areas of the 31 tumors examined.

Conclusions: Locally aggressive RCC showing sarcomatoid or rhabdoid features frequently lack PAX8 expression in the carcinoma component. The acquisition of *TP53* mutation and MDM2 overexpression may be associated in sarcomatoid transformation in a subset of sarcomatoid RCC, while and the loss of BAP1 expression appears to represent a potential mechanism that results in rhabdoid histology. The findings of occasional MDM2 overexpression in sarcomatoid RCC also suggest that MDM2 overexpression is not specific for well-differentiated/dedifferentiated liposarcoma in a retroperitonel location unless an underlying renal mass can be excluded radiologically.

1070 Primary Somatic Transformation of Testicular Germ Cell Tumors. Pathology and Outcome

Glenda Scandura[1], *Jonathan Shamash*[2], *Luis Beltran*[3], *Daniel Berney*[4]. [1]Barts Cancer Institute, [2]Queen Mary University of London, [3]Barts Health NHS Trust, London, [4]Queen Mary University of London, London

Background: While men with somatic transformation (ST) of testicular germ cell tumours (GCT) identified in metastases have a genally very poor prognosis, the prognosis of patients with primary somatic transformation of GCTs, when first identified within the testis, is not well understood. We here describe clinical and pathological factors of a cohort of men identified with PST to determine the optimal method of treatment of these rare cases.

Design: The database of a tertiary referral centre for testicular GCT was searched between 2003 and 2016. Pathology and clinical databases were investigated to reveal the initial and late pathology, tumor marker levels including tumor type and stage as well as any recurrences. The presenting pathology was reviewed as well as any recurrences. This was correlated with treatments given and survival data as well as cause of death.

Results: 15/1015 (1.5%) of patients were identified as having a diagnosis of primary somatic transformation. The presenting pathological GCT transformation included 7 sarcomas (4 rhabdomyoblastomas, 1 osteosarcoma, 1 chondrosarcoma and 1 sarcoma NOS), 4 carcinomas, 3 PNETs and 1 nephroblastoma.

The mean age was 34.6 years with a range of 21-51. Complete follow up was available in 13 patients. Tumour markers at presentation were available in 10/13 (77%) cases and 6/10 (60%) were normal, while the remaining 4 (40%) showed raised tumour markers. At presentation, 9/13 (69%) patients had radiologically proven metastases. 7/13 (54%) patients had chemotherapy, 4 (31 %) underwent surveillance, 1 had an RPLND and 1 had palliative Radiotherapy. To date only 3/13 (23%) of patients have relapsed.

11/13 (85%) patients are disease free after treatment including 1 patient with nephroblastoma who underwent multiple rounds of chemotherapy. 5/11 underwent RPLND. 4 of these showed teratoma and 1 showed seminoma: therefore all discordant with the primary pathology. 2/13 (15%) patients have died because of disease (1 adenosquamous and 1 rahbdomyosarcoma).

Conclusions: When compared with somatic transformations which present after initial diagnosis in metastases, primary somatic tranformations show a more favourable outcome. Metastases often show discordant and more favourable pathology. We suggest that treatment should presume these tumours to be similar to germ cell tumours without somatic transformation, unless this is proven histologically. Biopsy of metastatic deposits in this situation might asssist in tailoring treatmnent.

1071 Integrated Analyses of Gene, Protein and miRNA Expression in Bladder Cancer Patients Reveals a Link Between mTOR and Differentiation

Luciana Schultz[1], *Claudia Camillo*[2], *André Schultz*[3], *Renato Puga*[4], *Isac de Castro*[5], *Darshan S Chandrashekar*[6], *Samuel J Spagnul*[6], *Isabela W da Cunha*[7], *Sooryanarayana Varambally*[8], *George J Netto*[9], *Luiz F Onuchic*[10], *Fernando Soares*[11]. [1]Instituto de Anatomia Patológica, AC Camargo Cancer Center, Santa Barbara dOeste, SP, [2]AC Camargo Cancer Center, [3]Rice University, Houston, TX, [4]Hospital Israelita Albert Einstein, [5]Hospital Sirio Libanez, São Paulo, São Paulo, [6]The University of Alabama at Birmingham, [7]AC Camargo Cancer Center, Sao Paulo, SP, [8]University of Alabama at Birmingham, [9]University of Alabama at Birmingham (UAB), Birmingham, AL, [10]University of São Paulo School of Medicine, São Paulo, SP, [11]São Paulo

Background: Tumor differentiation has prognostic potential and impact in treatment choice, that can be enhanced by molecular knowledge. mTOR pathway, which is frequently mutated in urothelial carcinoma, regulates processes that require a substantial amount of matter and energy, such as cell metabolism, proliferation and differentiation.

Design: Expression of genes and proteins involved in mTOR and its interacting pathways (hypoxia-inducible pathway and cell cycle) were quantified in the same cohort of patients by IHC (n=99), RT-PCR (n=78) and miRNA profiling (n=72), in neoplastic and non-neoplastic urothelial tissue. Density plots of gene expression and IHC values were calculated using kernel density estimate and interactions were analyzed by clustering using correlation coefficients. Using *t*-test followed by cluster analyses, miRNA expression was compared between tumors with detectable and undetectable phosS6 (Ser 235/236) expression, as a surrogate for mTOR activation. Gene interaction network (UALCAN plattform) was built over 16 differentially expressed miRNA (Fig2).

Results: Cohort included 19 non-muscle invasive and 82 muscle invasive urothelial carcinomas (M:F 1.7:1, 10 Neoadjuvant Tx). Papillary and squamous features were present in 47% and 25% of tumors, respectively. mTOR and hypoxia pathways were highly correlated at gene (r>0.83) and protein (r>0.32) expression levels, while cell cycle was not. pS6 expression was lower in tumor compared to non neoplastic urothelium (p<0.0001) and decreased with stage (p=0.048). It was preferentially expressed by superficial cells (in non-neoplastic urothelium and in papillary structures), areas of mature squamous differentiation and at the invasive front of infiltrative nests (Fig 1). pS6, HIF1α and VEGF were higher in tumors of basal subtype and associated with DSS, however only pS6 remained an independent predictor by multivariate analyses (p=0.022; HR: 0.46). miRNAs were involved in pS6 loss of expression and this relationship showed clinical, pathological and morphological differences (Table).

	Cohort N=72	miRNA clusters I+II N=41	miRNA cluster III+IV N=31	p value (chi2)
Male : female	2:1	3 : 1	1 : 1	0,022
Age <60	17 (24)	12 (29)	05 (16)	0,214
NMIBC on 1st TURB	28 (38)	19	09	0,262
multifocal disease	15 (21)	04 (09)	11 (35)	0,008
papillary morphology	14 (19)	03 (07)	11 (35)	0,003
squamous differentiation	18 (25)	14 (34)	04 (13)	0,039
Basal subtype	15 (21)	8 (20)	7 (23)	0,504
Luminal subtype	33 (46)	20 (49)	13 (42)	0,993
pTa/pTis/pT1 pT2 pT3/pT4	10 (14) 19 (26) 43 (60)	02 (05) 13 (32) 26 (63)	08 (26) 06 (19) 17 (55)	0,033
positive lymph nodes	29 (40)	16 (39)	13 (42)	0,740
positive surgical margins	19 (26)	14 (34)	05 (15)	0,086
disease specific survival	60%	49%	74%	0,028

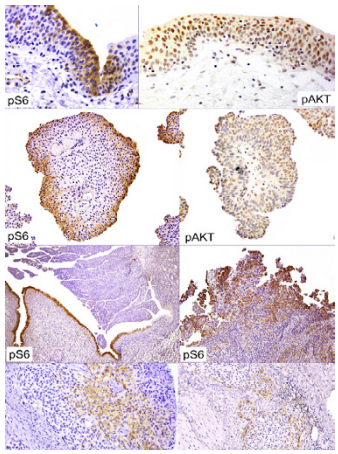

Gene interaction network between down-regulated miRNA and its mTOR pathway targets

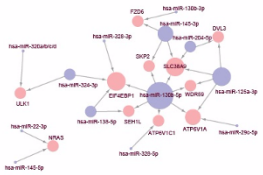

Gene interaction network between up-regulated miRNA and its mTOR pathway targets

Conclusions: pS6 under-expression in tumors, although apparently not directly related to gene expression, showed evidence of miRNA regulation. This post-transcriptional association correlated with morphological parameters classically associated with differentiation. mTOR interaction with the hypoxia pathway seems to cooperate in this phenomenon. Our findings suggest that mTOR activation in urothelial carcinoma is linked to differentiation status.

1072 ETS Genes (ERG, ETV1, ETV4 and ETV5) Overexpression and PTEN Loss in Prostate Cancer

Laura Segalés Tañà[1], *Josep Lloreta*[2], *Nuria Juanpere*[3], *Marta Lorenzo*[2], *Lluís Fumadó*[2], *Lluís Cecchini*[2], *Belen Lloveras*[4], *Silvia Hernández-Llodrà*[5]. [1]Universitat Pompeu Fabra, Barcelona, Catalunya, [2]Hospital del Mar-Parc de Salut Mar-IMIM, [3]Hospital del Mar-Parc de Salut Mar, Barcelona, Spain, [4]Hospital del Mar, Barcelona, [5]Pompeu Fabra University

Background: *ERG* is overexpressed in most of the rearranged prostate tumors (PrCa) and *PTEN* loss is often found as a concomitant event. Other *ETS* members as *ETV1*, *ETV4* and *ETV5* have been shown to be overexpressed with a lower frequency, but the relationship between this overexpression and the consequences on the clinical-pathological features of the respective prostate tumors are incompletely understood. The aim of the present study has been to investigate the relationship of *ETS* gene overexpression and *PTEN* loss with the main clinical-pathological parameters of PrCa.

Design: The mRNA expression of *ETS* genes (*ERG*, *ETV1*, *ETV4* and *ETV5*) was analyzed by RT-qPCR in 101 PrCa, and *PTEN* in 97 of the same series of cases (Parc de Salut MAR-Biobank, Barcelona, Spain). *GADPH* was used as internal control and 3 benign frozen prostate samples were used to normalize the thresholds for both *ETS* genes and *PTEN* (ΔΔCt). *ETS* overexpression cut-off was ≥ 2.2 and *PTEN* loss of expression cut-off was ≤ 0.35.

Results: *ETS* gene overexpression was found in 69.3% of PrCa: *ERG*, *ETV1*, *ETV4* and *ETV5* were increased in 55.4%, 18.8%, 7.9% and 5.9%, respectively, and *PTEN* loss in 39.2% of tumors. Fifty-eight tumors (57.4%) overexpressed only one *ETS* gene and 12 (11.8%) more than one. *ETS* gene overexpression plus *PTEN* loss was found in 37.1%, and only 2 cases (2.1%) presented with only *PTEN* loss. There is a strong correlation between single *ETS* overexpression and *PTEN* loss (P<0.0001). In addition, *PTEN* loss is mutually exclusive with multiple *ETS* gene overexpression (P=0.046). *ETS* overexpression (either single or multiple) plus *PTEN* loss was found in a 28.3% of GG1-2 and in a 48.9% of GG3-5 PrCa (P=0.04). On the other hand, overexpression of a single *ETS* gene was found to be associated with *PTEN wt* in a 34.6% of GG1-2 and in a 9.3% of GG3-5 PrCa (P=0.0036).

Conclusions: In our PrCa series, *ETS* overexpression is present in a high percentage of tumors, mostly as a single *ETS* gene overexpression. Single *PTEN* loss is a rare event. *PTEN* loss is significantly associated with *ETS* overexpression. But, interestingly seems to be mutually exclusive with overexpression of multiple *ETS* genes. Combined *ETS* overexpression/*PTEN* loss is associated with GG3-5 and single *ETS* overexpression/*PTEN wt* with GG1-2. (FIS/Carlos III/FEDER/PI15/00452, Spanish Ministry of Health).

1073 Clinicopathologic Characteristics of Patients Undergoing Radical Prostatectomy (RP) with High-Risk (PI-RADS 5) Lesions by Prostate Multiparametric Magnetic Resonance Imaging (mpMRI)

Tanmay Shah[1], *Aaron M Udager*[2], *Rohit Mehra*[1], *Madelyn Lew*[3], *Scott Tomlins*[1], *Angela Wu*[4], *L. Priya Kunju*[5], *Matthew Davenport*[3], *Jeffrey Montgomery*[3]. [1]University of Michigan, Ann Arbor, MI, [2]University of Michigan Medical School, Ann Arbor, MI, [3]University of Michigan, [4]Ann Arbor, MI, [5]University of Michigan Hospital, Ann Arbor, MI

Background: mpMRI utilizes the PI-RADS v2 system to detect clinically significant [Grade Group (GG) 2 or higher] prostate cancer (PCa), with PI-RADS 5 lesions typically corresponding to high-risk disease. Our prior prostate biopsy (PBx) study showed that GG2 or higher PCa is detected in 79% of PI-RADS 5 lesions. Here, we analyzed clinicopathologic characteristics of RP specimens in patients with PI-RADS 5 lesions.

Design: All RP patients with ≥1 PI-RADS 5 lesion(s) on mpMRI between 1/1/15-6/30/16 at a large academic institution were retrospectively identified. All available cases were re-reviewed to assess stage and index tumor nodule parameters, including: location, size, GS, %Gleason pattern (GP) 4, and presence of cribriform architecture. Correlation between RP and mpMRI and PBx results was assessed.

Results: Of 199 patients with ≥1 PI-RADS 5 lesions, 120 underwent PBx and 68 underwent RP. Of 54 patients available for review (Table 1), one showed GG1, while the rest showed GG2 or higher (median %GP4=40). There was very high concordance (*n*=52; 96%) and moderate positive correlation (*P*<0.0001) between location and size of the index tumor nodule and the PI-RADS 5 lesion respectively. The majority (*n*=30; 56%) of tumors were pT3a or higher; there was moderate to strong positive correlation for extraprostatic extension (EPE) and seminal vesicle invasion (SVI) (*P*<0.0001). The sensitivity of prostate mpMRI for detecting EPE or SVI was relatively low (<65%) and specificity was 89% and 100% respectively. The majority (*n*=30; 56%) of index tumor nodules showed cribriform architecture, including 11 (20%) cribriform-predominant tumors (defined as >50% of tumor volume). The %GP4 in RP demonstrated strong positive correlation with highest %GP4 in prior PBx (*P*<0.0001). Overall, half of tumors demonstrated concordance between RP and PBx highest GG, with 16 (30%) showing GG upgrade (including 7/8 GG1 on PBx) and 11 (20%) showing GG downgrade; only one clinically-significant upgrade (>1 GG) was identified; 7 tumors showed novel GP5 at RP (minor tertiary pattern in all but one case).

RP	n=54
Age	Median = 64 (range = 46-75)
Grade Group	GG 1: 2% GG 2: 44% GG 2 with tertiary 5: 9% GG 3: 20% GG 3 with tertiary 5: 11% GG 4: 4% GG 5: 9%
Size of index nodule (cm)	Median = 2.6 (range = 0.8-4.3)
%GP4 (n=53)	Median = 40 (range = 10-100)
Presence of cribriform architecture in index nodule	56%
Cribriform-predominant index nodule (n=30)	20%
Anterior-dominant index nodule	38%
Multifocality	77%
EPE	57%
SVI	17%

Conclusions: The vast majority (98%) of patients with PI-RADS 5 lesions on mpMRI who undergo RP have clinically-significant PCa, with cribriform architecture present in more than 50% cases and 20% being cribriform- predominant. Significant moderate to strong positive correlation with several standard pathologic RP variables and mpMRI is observed. %GP4 on prior PBx is strongly correlated with %GP4 in the RP index tumor nodule.

1074 Morphological Correlates of PTEN Tumor Suppressor Gene Loss in Prostate Cancer

Rajal Shah[1], *Karen T Shore*[2], *Ji Yoon Yoon*[1], *Wei Tian*[1], *Savvas Mendrinos*[3]. [1]Miraca Life Sciences, Irving, TX, [2]Rice University, Houston, TX, [3]East Orange, NJ

Background: The loss of *PTEN* tumor suppressor gene is one of the most common somatic genetic aberrations in prostate cancer (PCa) and is frequently associated with high risk disease. Deletion or mutation of at least one *PTEN* allele has been reported to occur in 20%-40% of localized PCas and up to 60% of metastases. The goal of this study was to determine if this somatic alteration is associated with a morphological phenotype.

Design: We assessed 246 cases with PCa in core needle biopsies for loss of *PTEN* status using an analytically validated immunohistochemical assay. PTEN status was analyzed on PCa cores with the highest Gleason score (GS) and/or volume. Blinded to the PTEN status, each tumor was assessed for the presence or absence of 9 epithelial and 2 stromal morphological features. Stromal morphological features included the presence of reactive stroma and determination of epithelial and stroma ratio (Grade 0, absent or up to 5% reactive stroma; Grade 1, 6% to 15% reactive stroma; Grade 2, 16% to 50% reactive stroma; Grade 3, > 50% reactive stroma). Statistical analysis was performed to determine significant associations between morphological features and PTEN protein loss status. Both partial and complete loss of PTEN staining in cancerous glands was considered PTEN loss.

Results: Thirty-three percent of cases had GS 3+3, 37% 3+4 and 30% ≥ 4+3. Thirty-three percent of PCa cases exhibited PTEN loss while 67% had intact PTEN. Three morphological features were significantly associated in PCa exhibiting PTEN loss compared to intact PTEN: intraductal tumor spread (71% versus 12%), reactive stromal grade ≥ 2 (68% versus 30%), and invasive cribriform growth pattern (30% versus 6%), all with p-values < 0.05. Majority (56%) of stromogenic PCas were defined as grade 3 reactive stroma exhibiting PTEN loss. Finally, at least one of three morphological features was present in 93% of PCa cases exhibiting PTEN loss.

Conclusions: Our results lend further support that PTEN loss in PCa is a late genetic event that is associated with an aggressive morphological phenotype. Furthermore, we demonstrate that stromal microenvironment plays an important role in PCa progression. These morphological features may also be helpful in diagnosing PTEN loss PCa, which have both prognostic and therapeutic implications.

1075 Pre-operative serum β-HCG, syncytiotrophoblasts and tumor tissue β-HCG levels are associated with more aggressive clinical behavior in testicular seminoma

Daniel D Shapiro[1], *Ying-Hsia Chu*[2], *E. Jason Abel*[3], *Wei Huang*[4]. [1]University of Wisconsin-Madison, Madison, WI, [2]University of Wisconsin Madison, Madison, WI, [3]University of Wisconsin-Madison, [4]Univ. of Wisconsin, Madison, WI

Background: It is controversial if pre-operative serum β-HCG levels predict clinical behavior of classic seminoma. Syncytiotrophoblasts (STB) in seminoma are considered "innocent" bystanders. In this study, we examined if there is a correlation among pre-operative serum β-HCG, STB, tissue β-HCG levels and tumor behavior.

Design: Twenty-eight pure seminoma cases from Pathology archive at the University of Wisconsin were studied. Serum β-HCG levels were measured as part of clinical care for the patients. Patients were divided into three groups according to their pre-operative β-HCG levels (Table 1).

Orchiectomy slides were reviewed. One representative block for each case was selected for tissue β-HCG immunohistochemical staining (IHC) following standard protocol. Four image cubes from each IHC slide were acquired at 20x using Nuance 3.0.2 microscope (Perkin Elmer), and β-HCG expression levels (mean optical density (OD) per pixel) were analyzed using inForm software 2.1.1 (Perkin Elmer). Student t-test was used for data analysis.

Results: We found that some seminoma tumor cells, particular STB express β-HCG. Serum β-HCG levels correlated with overall tissue β-HCG levels and associated with more aggressive behavior (Table 1, 2).

Table 1. Correlation of serum **β**-HCG, STB and tissue **β**-HCG

Group (n)	Age (yrs)	Tumor size (cm)	Serum β-HCG (mIU/mL)	Tissue STB (n/n)	Tissue β-HCG (mean OD/pixel)	*p-value
1 (13)	34.5 (22-67)	3.1 (1.4-6.5)	<2.5	0/13	0.037*	
2 (7)	30 (24-44)	5.0 (1.8 -10)	2.5 -10	3/7 (43%)	0.061*	<0.001[a]
3 (8)	41.3 (23-66)	5.4 (1.2 -9.5)	>10	3/8 (40%)	0.117*	<0.01[a], 0.1[b]

[a]p-value (tissue β-HCG): group 2 and 3 vs. group 1, [b]p-value: group 2 vs. group 3.

Table 2. Tumor characteristics and outcome in three groups.

		Tumor involvement (n/n)						
Group (n)	FU (m)	Rete testis (pT1)	Epididymis (pT1)	Vaginalis (pT2)	Cord (pT3)	LN+	Recurrence	Death
1 (13)	29.7	9/13 (69%)	0/13	1/13 (8%)	0/13	1/13 (8%)	1/13 (8%)	0/13
2 (7)	9.1	5/7 (71%)	1/7 (14%)	0/7	0/7	1/7 (14%)	0/7	0/7
3 (8)	71.6	5/8 (62%)	1/8 (13%)	0/8	2/8 (25%)	3/8 (38%)	0/8	0/8

FU: follow-up, LN: lymph node, cord: spermatic cord; Vaginalis: Tunica vaginalis

Conclusions: STB in seminoma may signify early transformation/differentiation towards more aggressive form. Serum β-HCG could be used to stratify patients with seminoma for clinical management.

1076 Clinical Significance of Perivesical Lymph Node Metastasis in Radical Cystectomy for Bladder Cancer

Meenal Sharma[1], *Jerome Jean-Gilles*[1], *Hiroshi Miyamoto*[2]. [1]University of Rochester, [2]University of Rochester, Rochester, NY

Background: It is well documented that pelvic lymph node (LN) metastases in bladder cancer (BC) are associated with a poor prognosis. By contrast, little is known about the prognostic implications of the involvement of perivesical LNs (PVLNs) that are occasionally isolated during grossing of cystectomy specimens.

Design: We searched the Surgical Pathology database of our institution from July 2004 to December 2016 and identified 107 radical cystectomy cases where PVLNs (mean: 3.9; median 3; range: 1-14) had been assessed.

Results: Of the 107 patients, 18 (17%) and 29 (27%) had metastases to the PVLNs and other pelvic LNs, respectively. 14 (13%) patients showed concurrent metastases to both LNs. We then compared

clinicopathologic data in isolated PVLN(+) (n=4) *vs.* concurrent pelvic LN(+) (n=14) or only non-PVLN(+) (n=15) diseases. There were no significant differences in age [mean: 71.0 *vs.* 68.9 (P=0.741) or 70.2 (P=0.894) yr] or sex [3 *vs.* 13 (P=0.405) or 12 (P=1.000) males] of patients or histology [4 urothelial carcinomas (UCs) *vs.* 12 UCs + 2 non-UCs (P=1.000) or 15 UCs (P=1.000)] or stage [1 pT2 + 3 pT3 *vs.* 1 pT2 + 13 pT3-4 (P=0.405) or 5 pT2 + 10 pT3-4 (P=1.000)] of primary tumors. Similarly, the number of positive PVLNs (mean: 2.0 *vs.* 2.4; median: 1.5 *vs.* 2; range: 1-4 *vs.* 1-12; P=0.738) and largest tumor focus (mean: 0.7 *vs.* 0.8; median: 0.8 *vs.* 0.8; range: 0.1-0.9 *vs.* 0.2-2.4 cm; P=0.542) or the presence of extracapsular extension [1 (25.0%) *vs.* 5 (35.7%); P=1.000] in the PVLNs were not significantly different between the first two groups. Kaplan-Meier analysis revealed patients with isolated positive PVLN tended to have a lower risk of disease progression (P=0.075), but not cancer-specific mortality (P=0.136), compared to those with concurrent positive pelvic LN. No significant difference in progression-free (P=0.389) or cancer-specific (P=0.776) survival was seen between isolated PVLN(+) and non-PVLN(+) diseases.

Conclusions: PVLN metastasis is less commonly identified compared to positive LN in other locations, but isolated BC metastasis to the PVLNs can occur. While PVLN metastasis is associated with aggressive disease, slightly better outcomes in patients with isolated positive PVLN than in those with concurrent PVLN and other pelvic LN metastases following radical cystectomy are implied. Our findings also indicate the importance of pathologic analysis of PVLNs in cystectomy specimens and further support the AJCC 8th edition BC staging system where PVLN metastasis is staged as pN1 or pN2.

1077 FOXA2 Protein Expression Is Associated with Neuroendocrine Phenotype and Androgen Receptor Status in the Metastatic Castration-Resistant Prostate Cancer

Mingxia Shi[1], *Zachary Connelly*[2], *Shu Yang*[1], *Xiaotun Zhang*[3], *Colm Morrissey*[3], *Eva Corey*[3], *Runhua Shi*[2], *Xiuping Yu*[2]. [1]LSU Health Shreveport, Shreveport, LA, [2]LSU Health Shreveport, [3]University of Washington

Background: Transformation to a neuroendocrine (NE) phenotype is one proposed mechanism of resistance to contemporary androgen receptor (AR) targeted therapies in prostate cancer. More knowledge concerning NE differentiation process and its association with castration-resistant prostate cancer (CRPC) is needed. We have previously shown that activation of Wnt/beta-Catenin signaling promotes the development of CRPC with increased NE phenotype. Our study has also shown that activation of Wnt/beta-Catenin signaling induces the expression of FOXA2, a member of the family of forkhead transcription factors. FOXA2 is expressed in embryonic prostate and its expression diminished after birth. In adult prostate, FOXA2 is expressed in the rare neuroendocrine cells of normal prostates and a subset of neuroendocrine prostate cancer. In the present study, we have examined the expression of FOXA2 on metastatic CRPC tissues and analyzed the association of FOXA2 expression with expression of NE marker synaptophysin and AR.

Design: By immunohistochemistry staining, the expression of FOXA2, synaptophysin and AR was examined on serial sections from a set of tissue microarrays (UWTMA22) that consist of CRPC metastasis samples. Evaluation of both the percentage of cells stained and intensity of nuclear (FOXA2) or cytoplasmic (synaptophysin) staining was performed. An overall expression score was calculated as the product of the intensity and percentage of stained cells. Nuclear immunoreactivity of AR in more than 10% tumor cells was considered as positive. Statistical analysis was performed by using the Spearman correlation test and Cochran-Armitage Trend Test. A P-value of <0.05 was considered statistically significant.

Results: Among 204 metastatic CRPC samples, FOXA2 protein expression was detected in 43 samples (21%). FOXA2 expression was highly correlated with synaptophysin (Rho = 0.35, p<0.0001), a NE phenotypic marker. FOXA2 protein expression was inversely correlated with the expression of AR (Rho = -0.18, p=0.0126). Inverse correlation between the expression of synaptophysin and AR (Rho = -0.31, p<0.0001) was observed with a negative trend.

Conclusions: Our findings suggest that FOXA2, a Wnt/beta-Catenin downstream target gene, is actively involved in the progression to castrate resistance via a NE differentiation. Identifying this gene and the pathway that are active in these processes can improve our understanding on prostatic NE tumor and associated CRPC transition and provide potential therapeutic targets.

1078 Clinical Utility and Concordance of Upper Urinary Tract Cytology and Biopsy in Predicting Clinicopathologic Features of Upper Urinary Tract Urothelial Carcinoma

Caroline T Simon[1], *Stephanie L Skala*[1], *Martin J Magers*[2], *Arul Chinnaiyan*[3], *Alon Weizer*[4], *Samuel D Kaffenberger*[4], *Daniel Spratt*[4], *Jeffrey Montgomery*[4], *Aaron M Udager*[5], *Madelyn Lew*[6], *Rohit Mehra*[1]. [1]University of Michigan, Ann Arbor, MI, [2]Indiana University School of Medicine, Indianapolis, IN, [3]Plymouth, MI, [4]University of Michigan, [5]University of Michigan Medical School, Ann Arbor, MI, [6]Dexter, MI

Background: Upper tract urothelial carcinoma (UTUC) can be diagnosed on biopsy or upper tract washings. High-grade biopsy or positive cytology in the upper tract often results in radical nephroureterectomy (RNU) or ureterectomy (UT). Endoscopic access to UTUC can be difficult, so pre-operative biopsy and cytology are often suboptimal. Herein, we investigate the concordance between endoscopic biopsy/cytology and surgical resection with respect to grade and stage.

Design: UTUC cases with RNU or UT performed between 2000-2016 were retrospectively identified at a single large academic institution. 130 cases had biopsy and/or cytology material available for review. Biopsy, cytology, and resection materials were re-reviewed, and pre- and post-operative diagnoses were examined for concordance.

Results: Results of upper tract biopsy and/or cytology influenced the decision to proceed to RNU or UT in 83/130 (63.8%) cases. 104 and 81 resections had upper urinary tract biopsies and upper tract cytology available for review, respectively. 13 patients lacked in-house pre-operative pathologic material diagnostic of carcinoma prior to resection (5 with negative cytology and no biopsy, 8 with negative cytology and non-diagnostic or benign biopsy). Among the 104 resections containing UTUC with in-house pre-operative endoscopic biopsy, 14 biopsies were negative for neoplasm. Biopsies lacking neoplastic diagnoses were most commonly from the renal pelvis (9/14, 64.3%). The concordance rates of biopsy with subsequent RNU or UT are shown in Table 1.

64 surgical resections with high-grade UTUC had pre-operative upper tract cytology. The majority (51/64; 79.7%) of patients had abnormal cytology results prior to surgery, including 33 (51.6%) positive, 6 (9.4%) suspicious, and 12 (18.8%) atypical diagnoses. 17 surgical resections with low-grade UTUC had pre-operative upper tract cytology. While most cases had negative pre-operative cytology (9/17; 52.9%), abnormal results included 6 (35.3%) atypical and 2 (11.8%) positive diagnoses.

	Downgraded	Concordant	Upgraded	Total
Biopsy				104
Grade	3 (3.3%)	80 (88.9%)	7 (7.8%)	90
Invasion	1 (1.1%)	61 (67.8%)	28 (31.1%)	90

Conclusions: Although the decision to proceed to RNU or UT for treatment of UTUC is typically based on endoscopic upper tract biopsy and/or cytology, surgical resections often result in reclassification of tumor stage and grade and frequently confirm the presence of neoplasms not detected on pre-operative biopsy/cytology.

1079 BK Viral integration in Urologic Malignancies

Deepika Sirohi[1], *Steven C Smith*[2], *Michelle Don*[3], *Kathryn G Lindsey*[4], *Mahesha Vankalakunti*[5], *Jamie Koo*[6], *Shikha Bose*[7], *Mariza de Peralta-Venturina*[7], *Jessica Van Ziffle*[8], *James Grenert*[9], *Steve Miller*[10], *Mahul Amin*[11], *Jeffry Simko*[12], *Bradley Stohr*[13], *Daniel Luthringer*[7], *Charlie Vaske*[14], *Zack Sanborn*[14], *Scot Federman*[10], *Charles Chiu*[15]. [1]University of Utah, Salt Lake City, UT, [2]VCU School of Medicine, Richmond, VA, [3]West Hollywood, CA, [4]Medical University of South Carolina, Charleston, SC, [5]Manipal Hospital, Bangalore, India, [6]Cedars-Sinai Dept of Pathology, West Hollywood, CA, [7]Cedars-Sinai Med Ctr, West Hollywood, CA, [8]University of California, San Francisco, [9]University of California, San Francisco, CA, [10]UCSF, [11]Methodist University Hospital, Memphis, TN, [12]Univ. of California, San Francisco, San Francisco, CA, [13]UCSF, San Francisco, CA, [14]NanotOmics, Santa Cruz, CA, [15]USCF

Background: In recent years, increased attention has focused on polyoma virus associated urologic malignancies (PVAUMs) in immunocompromised (IC) patients. We report viral integration data in PVAUMs by next generation sequencing (NGS).

Design: Targeted genomic profiling using a capture based NGS assay of 500 cancer related genes, 10 polyoma viruses and 6 other viruses was performed on paired tumor and normal or tumor only samples of 8 PVAUMs (7 urothelial & 1 collecting duct carcinoma) occurring in IC setting. A control group comprised of 4 post-transplant cases of UMs negative for SV-40. Viral detection was done using SURPI ("sequence-based ultra-rapid pathogen identification") computational pipeline for pathogen detection. Viral integration analysis was performed by BamBam and GATK was used for indel realignment. Viral integration sites were verified in Integrated genomic viewer.

Results: BK virus was detected in both normal and tumor samples in all PVAUMs; other viruses were not detected. In 5 cases, an average of 3 clonal chimeric viral and human reads were identified in the tumor samples and absent in normal. The breakpoints in the human genome included exonic, intronic and intergenic regions. In the viral genome breakpoints were distributed across the genome, including within VP-1, VP-2, VP-3 and small and large T-antigens.

Conclusions: The BK viral integration sites were clonal in PVAUM but not site specific and randomly distributed across both the viral and the human genome. While the functional significance of random integration with multiple breakpoints remains uncertain, it could potentially predispose to a background of genomic instability and oncogenic transformation.

1080 Frequent Structural Variants of TP53 gene in Metastatic Prostate Carcinoma

Deepika Sirohi[1], *Jessica Van Ziffle*[2], *James Grenert*[3], *Jeffry Simko*[4], *Bradley Stohr*[5]. [1]University of Utah, Salt Lake City, UT, [2]University of California, San Francisco, [3]University of California, San Francisco, CA, [4]Univ. of California, San Francisco, San Francisco, CA, [5]UCSF, San Francisco, CA

Background: Aberrant immunohistochemical (IHC) expression of p53 protein is well recognized in prostatic carcinomas with increased expression reported in aggressive disease. The underlying molecular mechanisms are thought to be missense or truncating mutations and copy number changes. In this study, we report complex structural variants (SVs) of *TP53* gene as a frequent mechanism of gene inactivation in metastatic prostatic carcinomas. SVs of *TP53* have very recently been reported in the context of primary prostate carcinomas and may be a feature related to aggressive biology.

Design: Targeted genomic profiling using a capture-based next generation sequencing assay of about 500 cancer related genes was performed on paired tumor and normal samples or tumor-only samples of 10 primary and 17 metastatic prostate carcinomas. To understand the functional significance of *TP53* alterations, IHC analysis for p53 protein expression was done in 15 cases with available blocks.

Results: *TP53* was the most frequently altered gene in a series of 27 prostate carcinomas, seen in 11 cases (40.7%) and including 6 missense variants or small insertions/deletions; 4 SVs and 1 copy number loss. While 4 of 6 missense variants were identified in metastatic prostate carcinomas, all SVs and copy number loss were seen in metastatic carcinomas. The SVs were enriched in metastatic prostatic carcinomas, being present in 4 of 17 cases (23.5%). The breakpoint in the rearrangements involved intron 1 of *TP53* in all cases, which is predicted to result in complete disruption of gene expression and has been reported in patients with Li Fraumeni syndrome and osteosarcoma. This was confirmed by IHC analysis showing complete lack of nuclear staining consistent with loss of function. Concurrent *PTEN* loss was identified in 3 of 4 cases, *TMPRSS2-ERG* fusion in 2 and *AR* and *FOXA1* amplification in 1 case each.

Conclusions: In this small series, we report recurrent structural variants in *TP53* as a frequent mechanism of inactivation in metastatic prostatic carcinomas. Alone or in combination with loss of function of other tumor suppressor genes, it may serve as a potential biomarker of aggressive disease amenable to detection by increasingly employed targeted gene sequencing and widely available IHC assays. These findings need to be validated in a larger cohort of metastatic prostate carcinomas.

1081 Genomic profiling of Unclassified Renal Cell Carcinomas

Deepika Sirohi[1], *Jessica Van Ziffle*[2], *James Grenert*[3], *Nancy Joseph*[4], *Boris Bastian*[5], *Karuna Garg*[6], *Bradley Stohr*[7], *Jeffry Simko*[6]. [1]University of Utah, Salt Lake City, UT, [2]University of California, San Francisco, [3]University of California, San Francisco, CA, [4]University of California San Francisco, San Francisco, CA, [5]Memorial Sloan-Kettering CC, New York City, NY, [6]Univ. of California, San Francisco, San Francisco, CA, [7]UCSF, San Francisco, CA

Background: Unclassified renal cell carcinoma (URCCs) preclude accurate classification with conventional diagnostic tools, limiting the clinical decisions for patient management. They comprise up to 5% of RCCs and are characterized by higher rate of metastases and lower overall survival rates.

Design: Targeted genomic profiling using a capture-based next generation sequencing assay of about 500 cancer related genes was performed on paired tumor and normal samples of 10 unclassified RCCs and 5 cases with established histopathologic diagnosis.

Results: Targeted gene sequencing confirmed the diagnosis in 5 of 5 cases with a prior established diagnosis (Table-1). In the unclassified RCCs, sequencing results helped establishing the diagnosis in 9 of 10 cases (Table-2). A BRD4-NUTM1 fusion was identified in 1 case establishing a diagnosis of nuclear protein in testis (NUT) carcinoma, the second reported case of this diagnosis in the kidney. Additionally, in 4 cases pathogenic germline alterations were identified.

Table-1: Genomic alterations in classified RCCs

Case #	Histopathologic diagnosis	Pathogenic genetic alterations
1	Hybrid oncocytoma/chromophobe tumor (HOCT)	TSC2 p.R905Q homozygous
2	pRCC 1	Copy number changes
3	ccRCC	BAP1 p.Q483*, VHL p.L118P
4	Metastatic pRCC	Copy number changes
5	Unclassified RCC, favor TSC associated	TSC2 splicing (c.3132-2A>G)

Table- 2: Genomic alterations in URCCs

Case #	Histopathologic diagnosis	Pathogenic genetic alterations	Final Diagnosis	Clinical utility
6	Unclassified	VHL p.C77*	ccRCC	D
7	Favor ChRCC	TP53 p.M237K with LOH, Copy number changes	ChRCC	D
8	Likely TFE3	MED15-TFE3 gene fusion	TFE3 RCC	D
9	Unclassified	None	Unclassified RCC	ND
10	Unclassified	TERT Promoter VHL p.I151T	ccRCC	D
11	Unclassified	NF2 p.E530fs- hemizygous	pRCC	D
12	Unclassified	BRD4-NUTM1 fusion	NUT Carcinoma	D
13	Unclassifed metastatic RCC	FH c.267+1G>T, hemizygous	FH deficient RCC	D
14	Unclassified	PTEN p.Q17*, TFE3 rearrangement (with C10orf11 or LRMDA)	TFE3 RCC	D
15	pRCC 2	TFE3-PRCC gene fusion	TFE3 RCC	D

Abbreviations: ChRCC- chromophobe RCC, D- Diagnostic, ND- Not diagnostic, pRCC- papillary RCC, ccRCC- Clear cell RCC, TSC- Tuberous sclerosis, LOH- loss of heterozygosity

Conclusions: Targeted sequencing of URCCs provides a clinically useful ancillary modality to establish a definitive diagnosis, provide prognostic and therapeutic information and potentially identify new subsets of tumors.

1082 FOXI1 is a Sensitive and Specific Marker for Detection of Primary and Metastatic Chromophobe Renal Cell Carcinoma

Stephanie L Skala[1], *Lisha Wang*[1], *Yuping Zhang*[2], *Xuhong Cao*[3], *Fengyun Su*[3], *Javed Siddiqui*[3], *Cieślik Marcin*[3], *Arul Chinnaiyan*[4], *Saravana M Dhanasekaran*[3], *Rohit Mehra*[1]. [1]University of Michigan, Ann Arbor, MI, [2]Michigan Center for Translational Pathology, [3]University of Michigan, [4]Plymouth, MI

Background: The immunohistochemical (IHC) stains commonly used to support the diagnosis of chromophobe renal cell carcinoma (RCC) are not lineage-specific and are expressed by various tumor types. Discovery of cancer-specific markers will alleviate diagnostic challenges, particularly when it comes to evaluation of metastases or tumors with unusual morphology. We analyzed RCC next generation sequencing (RNAseq) data to identify novel cancer and lineage-specific biomarkers to enhance existing diagnostic panels and to identify potential cell of origin of chromophobe RCC.

Design: We performed integrative analysis of RNAseq data on a combined cohort of 1049 RCC specimens from The Cancer Genome Atlas and several in-house studies, as well as RNAseq data from microdissected rat nephron to identify cancer/lineage-specific biomarkers. We built a webportal ("Renaissance") for data visualization and nominated several novel lineage-specific biomarkers including FOXI1. For validation, we investigated RCC retrieved from the surgical pathology database at our large academic institution including classic chromophobe RCC (n= 33), eosinophilic chromophobe RCC (n=10), unclassified RCC with oncocytic features (n= 6), clear cell RCC (6 grade 2, 10 grade 3, 14 grade 4), clear cell papillary RCC (n=5), mucinous tubular and spindle cell carcinoma (MTSCC, n=1), and papillary RCC (6 type 1, 4 type 2). All available chromophobe RCC metastases were retrieved (n=17), as well as clear cell RCC (n=16) and papillary RCC metastases (n=5) from various sites. All cases were re-reviewed and interrogated for IHC expression of FOXI1 using an anti-FOXI1 antibody.

Results: We performed in-depth characterization of protein expression of the transcription factor FOXI1 in this RCC tissue validation cohort. All primary and metastatic chromophobe RCC demonstrated diffuse nuclear FOXI1 expression. Eosinophilic chromophobe RCC and

unclassified RCC with oncocytic features also demonstrated positive nuclear FOXI1 expression. In contrast, no clear cell RCC (primary or metastatic), clear cell papillary RCC, papillary RCC (primary or metastatic), or MTSCC showed nuclear FOXI1 expression.

Conclusions: Based on our findings, nuclear FOXI1 expression is highly sensitive and specific for variants of chromophobe RCC and other RCC with oncocytic features in primary and metastatic settings. Our results suggest that the cell of origin for chromophobe RCC resides in the connecting tubule/collecting duct of the nephron.

1083 Comprehensive Immunophenotypic Profiling of High Grade Renal Adenocarcinomas, including Renal Medullary Carcinoma (RMC), Collecting Duct Carcinoma (CDC), and Fumarate Hydratase-Deficient Renal Cell Carcinoma (FH-deficient RCC)

Steven C Smith[1], *Mark Mochel*[1], *The HDNA Consortium*[2], *Mahul Amin*[3]. [1]VCU School of Medicine, Richmond, VA, [2]Collaboration, [3]Methodist University Hospital, Memphis, TN

Background: Recent advances have defined key clinicopathologic and molecular differences between high grade RCCs classified as RMC, CDC, and FH-deficient RCC. However, the immunophenotype of these tumors has not been compared systematically in a meaningful number of cases.

Design: A tissue microarray was constructed from a large cohort of archival tissues of well-characterized high grade RCCs (N=50), contributed by an international consortium. These included RMCs (SMARCB1-deficient; N=17), CDCs (SMARCB1+, FH-retained, urothelial carcinoma excluded; N=23), and FH-deficient RCC (FH- &/or 2SC+ &/or *FH* mutation; N=10). The microarray was stained under routine CLIA-compliant conditions for several antibodies, many routinely used in RCC workup, including PAX8, AMACR, CK7, CK20, CK5/6, HMWCK, CK17, CK19, p63, CAIX, GLUT1, OCT4, SALL4, c-KIT, and RCC antigen. Each immunostain was scored by two pathologists for proportion and intensity of positivity.

Results: Table 1 summarizes findings, highlighting statistically significant differences in proportions of tumors showing positivity for AMACR, CK7, CD10, and OCT4. Notably, no case demonstrated diffuse membranous CAIX expression; CAIX positivity reported below represents any patchy positivity, often involving incipient necrosis.

Table 1

	CDC	FH-deficient RCC	RMC	X^2 Test
Antibody	% Positive	% Positive	% Positive	P-value
PAX8	87	100	88	0.49
AMACR	61	80	6	0.0001
CK5/6	9	0	6	0.63
CK7	39	0	76	0.0005
CK17	26	30	29	0.96
CK19	50	90	53	0.07
CK20	13	0	0	0.15
HMWCK	17	0	6	0.26
CD10	61	20	24	0.02
CAIX	43	30	12	0.09
GLUT1	100	100	88	0.12
RCC Antigen	22	10	0	0.11
c-KIT	0	0	0	~
OCT4	0	0	18	0.05
SALL4	0	0	6	0.37

Conclusions: We recommend close correlation of morphology with clinical, hematologic, immunophenotypic, and syndromal features for diagnosis of RMC, CDC, and FH-deficient RCC. Though study of additional markers is ongoing, the present findings serve to establish the as yet unknown ranges of expression of routine markers in these increasingly recognized, exceptionally aggressive tumors.

1084 Prostate Cancers in Filipino Men Have Greater Adverse Pathologic Risks at Radical Prostatectomy: A Study Comparing with US Prostate Cancer Cohort

Jeffrey So[1], *Bonnie Choy*[2], *Gladell P Paner*[2], *Mayen T Grageda*[3]. [1]St. Luke's Medical Center Philippines, Quezon City Metro Ma, [2]University of Chicago, Chicago, IL, [3]St. Luke's Medical Center -Global City

Background: The race long known to be most at risk for prostate adenocarcinoma (PCa) is African-Americans. However, Asians have traditionally been considered to be at the opposite end of the spectrum. Although some studies have compared different ethnicities to support this claim, few have specifically looked into the histopathologic characteristics of PCa among Filipinos. To our knowledge, this is the first study that investigates the histopathologic differences between Filipino and US patients with PCa.

Design: We compared the different histopathologic & prognostic findings at radical prostatectomy (RP), plus pre-operative prostate specific antigen (pre-op PSA) in 351 patients (179 Philippines, 172 US). Philippine data includes those who underwent RP from April 2013-Dec 2016, while US data includes those from Sept 2012-July 2014.

Results: At diagnosis, patients from the Philippines (PH) were older than US patients (mean 64y PH vs 59y US, p<0.01), & have significantly higher pre-op PSA (21.4 ± 46.4 ng/mL PH vs 7.6 ± 9.2 ng/mL in US, p <0.01). Gleason score (GS) 9 (4+5 and 5+4) was significantly higher among Filipinos (10.6% PH vs 2.3% US, and 2.8% PH vs 0% US, respectively) while a sizeable proportion of GS 7 (3+4) is seen in US patients (62.2% US vs 38.5% PH). In terms of grade group (GG), US patients showed lower grade PCa, GG 1 to 2 (18.6% US vs 14.5% PH and 62.2% US vs 48.6% PH, respectively), while Filipinos harbor more advanced grades, GG 3, 4 & 5 (15.1% PH vs 10.5% US, 7.8% PH vs 6.4% US, and 14% PH vs 2.3% US, respectively). In line with this, margin involvement among Filipinos(51.4% PH vs 23.8% US), specifically multifocal involvement, is considerably higher (35.2% PH vs 4.7% US). A significant difference in extraprostatic extension(EPE) is noted (47% PH vs 38% US), as well as seminal vesicle (SV) involvement(16.8 % PH vs. 5.3% US). The percentages of positive & negative lymph node were not significantly different.

Conclusions: Filipinos with PCa present at an older age, which may be due to a less stringent PSA screening protocol. Filipinos notably had significantly higher pre-op PSA levels, higher GGs (3 to 5), greater margin positivity, EPE, & SV involvement. This study, the first to directly compare PH and US RP findings, highlights a vital racial difference of Filipinos from other Asian ethnicities, that have repeatedly been shown to be at low risk for PCa. A more stringent PCa screening protocol maybe warranted for Filipinos whose risk profiles may have been greatly underestimated.

1085 UroSEEK: A Novel Non-Invasive Molecular Method for Early Detection of Bladder Cancer

Simeon Springer[1], *Maria Del Carmen Rodriguez Pena*[2], *Yuxuan Wang*[3], *Diana Taheri*[4], *Aline C Tregnago*[5], *Stephania M Bezerra*[6], *Christopher VandenBussche*[7], *Kazutoshi Fujita*[8], *Dilek Baydar*[9], *Isabela W da Cunha*[10], *Lijia Yu*[11], *Trinity J Bivalacqua*[12], *Kathleen G Dickman*[13], *Rachel Karchin*[14], *Ralph Hruban*[15], *Cristian Tomasetti*[16], *Nickolas Papadopoulos*[3], *Kenneth W Kinzler*[3], *Bert Vogelstein*[17], *George J Netto*[18]. [1]The Ludwig Center for Cancer Genetics and Therapeutics and Sidney Kimmel Comprehensive Cancer Center, Baltimore, MD, [2]University of Alabama at Birmingham, Birmingham, AL, [3]The Ludwig Center for Cancer Genetics and Therapeutics and Sidney Kimmel Comprehensive Cancer Center, Baltimore, MD, [4]Tehran University of Medical Sciences, Tehran, [5]The Johns Hopkins Med Inst, Baltimore, MD, [6]AC Camargo Cancer Center, Sao Paulo - SP, [7]The Johns Hopkins Hospital, Baltimore, MD, [8]Department of Pathology, Osaka University, Osaka, Japan, [9]Hacettepe University, Ankara, [10]AC Camargo Cancer Center, Sao Paulo, SP, [11]University of Alabama at Birmingham, Birmingham, AL, [12]Johns Hopkins University, Baltimore, MD, [13]Stony Brook University, Stony Brook, NY, [14]Institute for Computational Medicine, Johns Hopkins University, Baltimore, MD, [15]Johns Hopkins Medical Institutions, Baltimore, MD, [16]Sidney Kimmel Cancer Center, Johns Hopkins School of Medicine, Baltimore, MD, [17]The Ludwig Center for Cancer Genetics and Therapeutics and Sidney Kimmel Comprehensive Cancer Center, Baltimore, MD, [18]University of Alabama at Birmingham (UAB), Birmingham, AL

Background: Current non-invasive approaches for bladder cancer (BC) detection are suboptimal. We report the development of a non-invasive molecular assay (UroSEEK) for detection of BC in patients with hematuria using DNA recovered from cells shed into urine. UroSEEK incorporates assays for assessment of mutations in 11 genes and copy number changes on 39 chromosome arms.

Design: Patients urine samples were collected prospectively in four institutions. The patients selected were referred for hematuria or lower urinary tract symptoms that prompted urine cytology examination to rule out BC. Urine samples were analyzed for mutation using three component assays: A multiplex PCR was used to detect mutations in regions of *CDKN2A, ERBB2, FGFR3, HRAS, KRAS, MET, MLL, PIK3CA, TP53*, and *VHL*. An amplification primer was used to amplify a 73-bp segment containing the region of *TERT* promoter. Aneuploidy was assessed with FastSeqS, which uses a single primer pair to amplify ~38,000 loci scattered throughout the genome. Follow up data was obtained for each patient.

Results: 570 patients were included in the study, 175 developed BC. The multiplex assay detected mutations in 68% of patients that developed BC. The most commonly altered genes were *TP53* and *FGFR3* (45% and 20% of the total mutations). Mutations in the T*ERT* promoter were detected in 57% and aneuploidy was detected in

46% of patients that developed cancer, the most commonly altered chromosome arms were 5q, 8q, and 9p. **Fig. 1.** When all 3 assays were combined, the sensitivity of UroSEEK was 83%.

Combined with cytology UroSEEK was 95% sensitive and 93% specific. A total of 105 patients had "atypical" diagnosis on cytology. Eighteen patients developed a biopsy proven tumor. UroSEEK was positive in all 18 (100% sensitivity) with a mean lead time of 4 months (range 0 - 18) from biopsy diagnosis.

Cytology did not detect any of the low-grade tumors while UroSEEK detected 67% of these tumors. Cytology detected 50% of high-grade carcinomas while UroSEEK detected all of them. **Fig 2.**

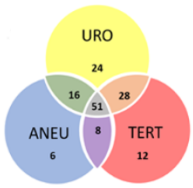

Fig 1. Venn diagram of the distribution of samples that were positive by each of the three assays. URO = Ten gene panel, *TERT* = *TERT* promoter region, ANEU = Aneuploidy test.

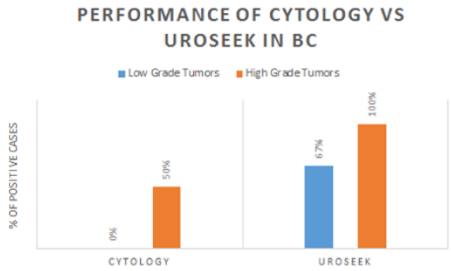

Fig 2. Bar graphs showing the performance of Cytology Vs. UroSEEK in diagnosis of low and high grade urothelial neoplasms.

Conclusions: UroSEEK raised the sensitivity of cytology from 43% to 95% for early detection of BC. UroSEEK was positive in all cases with atypical cytology that were subsequently diagnosed with BC. Prospective trials will be required to further demonstrate the utilty of integrating UroSEEK in screening strategies for BC detection in patients at risk.

1086 UroSEEK: A Novel Non-Invasive Molecular Assay for Surveillance of Bladder Cancer

Simeon Springer[1], *Maria Del Carmen Rodriguez Pena*[2], *Yuxuan Wang*[3], *Diana Taheri*[4], *Aline C Tregnago*[5], *Stephania M Bezerra*[6], *Christopher VandenBussche*[7], *Kazutoshi Fujita*[8], *Dilek Baydar*[9], *Isabela W da Cunha*[10], *Lijia Yu*[11], *Trinity J Bivalacqua*[12], *Kathleen G Dickman*[13], *Arthur P Grollman*[14], *Ralph Hruban*[15], *Cristian Tomasetti*[16], *Nickolas Papadopoulos*[3], *Kenneth W Kinzler*[3], *Bert Vogelstein*[17], *George J Netto*[18]. [1]The Ludwig Center for Cancer Genetics and Therapeutics and Sidney Kimmel Comprehensive Cancer Center, Baltimore, MD, [2]University of Alabama at Birmingham, Birmingham, AL, [3]The Ludwig Center for Cancer Genetics and Therapeutics and Sidney Kimmel Comprehensive Cancer Center, Baltimore, MD, [4]Tehran University of Medical Sciences, Tehran, [5]The Johns Hopkins Med Inst, Baltimore, MD, [6]AC Camargo Cancer Center, Sao Paulo - SP, [7]The Johns Hopkins Hospital, Baltimore, MD, [8]Department of Pathology, Osaka University, Osaka, Japan, [9]Hacettepe University, Ankara, [10]A.C Camargo Cancer Center, Sao Paulo SP, [11]University of Alabama at Birmingham, Birmingham, AL, [12]Johns Hopkins University, Baltimore, MD, [13]Stony Brook University, Stony Brook, NY, [14]Stony Brook University, Stony Brook, NY, [15]Johns Hopkins Medical Institutions, Baltimore, MD, [16]Sidney Kimmel Cancer Center, Johns Hopkins School of Medicine, Baltimore, MD, [17]Ludwig Center for Cancer Genetics and Therapeutics and Sidney Kimmel Comprehensive Cancer Center, Baltimore, MD, [18]University of Alabama at Birmingham (UAB), Birmingham, AL

Background: Current non-invasive approaches for bladder cancer (BC) detection are suboptimal. In this study, we report the development of a non-invasive molecular assay (UroSEEK) for detection of BC recurrence during disease surveillance using DNA recovered from cells shed into urine. UroSEEK incorporates assays for mutations in 11 genes and copy number changes on 39 chromosome arms.

Design: Urine samples were collected prospectively from patients with previously established diagnosis of BC from two institutions. Patients with a known history of malignancy other than BC were excluded. Urine samples were analyzed for mutation in three component assays: First, a multiplex PCR was used to detect mutations in regions of *CDKN2A, ERBB2, FGFR3, HRAS, KRAS, MET, MLL, PIK3CA, TP53,* and *VHL*. Second, an amplification primer was used to amplify a 73-bp segment containing the region of the *TERT* promoter. Aneuploidy was assessed with FastSeqS, which uses a single primer pair to amplify ~38,000 loci scattered throughout the genome. Follow up data was obtained from medical records.

Results: 322 patients were identified, 187 had biopsy proven recurrence. The multiplex PCR assay detected mutations in 52% patients that developed recurrent BC. The most commonly altered genes were *TP53* and *FGFR3* (38% and 29% of the 200 mutations; respectively). Mutations in *TERT* promoter were detected in 57% of samples and aneuploidy was detected in 28% of samples from patients with recurrent disease. The most commonly altered chromosomal arms were 8p, 8q, and 9p. **Fig 1.** In patients with BC recurrence, 127/187 samples were positive for at least one of the three UroSEEK componont assays for a sensitivity of 68% and a specificity of 80%.

In combination with cytology UroSEEK demonstrated 71% sensitivity and 82% specificity. One-hundred patients had "atypical" diagnosis on cytology. Among the latter, UroSEEK was positive in 68% of 71 patients that recurred with a 83% specificity and a mean lead time from biopsy proven recurrence of 6 months (range 0 - 35).

Cytology did not detect recurrent low-grade tumors while UroSEEK detected 67% of them. Cytology detected 41% of high-grade tumors while UroSEEK detected 71%. **Fig 2.**

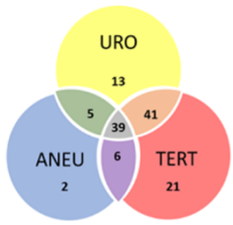

Fig 1. Venn diagram of the distribution of samples that were positive by each of the three assays for the surveillance cohort. URO = Ten gene panel, TERT = TERT promoter region, ANEU = Aneuploidy test.

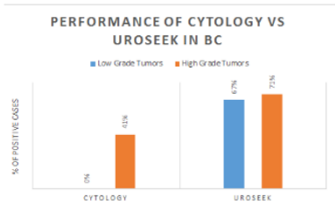

Fig 2. Bar graphs showing the performance of Cytology Vs. UroSEEK in diagnosis of low and high grade urothelial neoplasms.

Conclusions: UroSEEK raised the sensitivity of cytology from 25% to 71% and detected recurrence in 68% of atypical cytology patients. UroSEEK positivity preceded clinical diagnosis by months to years. Prospective trials are required to demonstrate the ability of UroSEEK to improve outcome in BC surveillance.

1087 Immunohistochemical profiling of recurrent prostate cancer following radiotherapy and androgen ablation

Catherine Suen[1], *Kyle Hurth*[2], *Ashley Hagiya*[3], *Christina Wei*[4], *Wafaa Elatre*[5], *Guang-Qian Q Xiao*[6]. [1]Keck Hospital of USC and LAC-USC Medical Center, Los Angeles, CA, [2]Washington University, Saint Louis, MO, [3]Pasadena, CA, [4]USC/ LAC+USC Pathology and Laboratory Medicine, Los Angeles, CA, [5]USC-Keck Medical Center, Los Angelos, CA, [6]USC-Keck Medical Center, Los Angeles, CA

Background: Radiotherapy and androgen ablation are the two principal non-surgical modalities for prostate cancer (PCa). Histologically, post-therapy recurrent PCa displays treatment and/or no treatment effect (TE). 30-50% of high-risk and 10% of low-risk PCa recur following radiotherapy and almost 100% PCa recur after hormonal therapy. The recurrent PCa often present a more aggressive clinical course. Although a variety of biomolecules have been associated with increased aggressiveness of recurrent PCa, their immunohistochemical (IHC) profiles and morphologic association following these therapies have not been well studied.

Design: TMA made from salvage prostatectomies for post-therapy recurrent PCa was immunostained with prostate specific markers (AR, NKX3.1 and Prostein), oncogenic biomarkers (Bcl-2, c-Myc, and EZH2) and p53. Their expression in PCa was evaluated and correlation with

morphologic changes was made.

Results: Strong expression of AR and NKX3.1 was retained in all the cases regardless of the treatments and histomorphology. Expression of Prostein was significantly decreased in PCa with TE compared with those without TE. Expression of oncogenic markers and p53 was both increased, and expression levels of c-Myc, Bcl-2 and EZH2 were higher in PCa with TE than PCa without TE. Expression of p53 was more common in PCa without TE than those with TE (see Table 1).

	PCa-postradiotherapy						PCa-androgen ablation					
	No treatment effect			Treatment effect			No treatment effect			Treatment effect		
	n	Pos. cases	Neg. cases	n	Pos. cases	Neg. cases	n	Pos. cases	Neg. cases	n	Pos. cases	Neg. cases
AR	39	39/39 (100%)	0	7	7/7 (100%)	0	8	8/8 (100%	0	29	29/29 (100%)	0
NKX3.1	39	39/39 (100%)	0	7	7/7 (100%)	0	8	8/8 (100%)	0	29	29/29 (100%)	0
Prostein	39	36/39 (92%)	3/39 (8%)	7	1/7 (14%)	6/7 (86%)	7	7/7 (100%)	0	27	12/27 (44%)	15/27 (56%)
p53	36	11/36 (31%)	25/36 (69%)	10	1/10 (10%)	9/10 (90%)	10	4/10 (40%)	6/10 (60%)	41	9/41 (22%)	32/41 (78%)
c-Myc	31	7/31 (23%)	24/31 (77%)	7	3/7 (43%)	4/7 (57%)	8	0	8/8 (100%)	29	4/29 (17%)	25/29 (83%)
BCL-2	41	1+: 2/41 (5%) 2+: 3/41 (7%)	36/41 (88%)	10	1+: 2/10 (20%) 2+: 0/10 (0%)	8/10 (80%)	12	1+: 0/12 (0%) 2+: 1/12 (8%)	11/12 (92%)	41	1+: 10/41 (24%) 2+: 2/41 (5%)	29/41 (71%)
EZH2	33	1+: 23/33 (70%) 2+: 10/33 (30%)	0	7	1+: 0/7 (0%) 2+: 7/7 (100%)	0	7	1+: 4/7 (57%) 2+: 3/7 (43%)	0	38	1+: 19/38 (50%) 2+: 19/38 (50%)	0

Conclusions: Expression of AR and NKX3.1 was not altered by either radiotherapy or androgen ablation. Their utility in diagnosis and future potential targeted therapy is therefore still applicable in post-therapy recurrent PCa. Expression of Prostein was downregulated with therapy and its utility in PCa, particularly those with TE, is limited. The higher prevalence of p53 mutation in PCa without TE effect than those with TE and higher level of expression of oncogenic markers in PCa with TE than those without TE may reflect biologic differences between the two morphologies. Not all the cases present with overexpression of oncogenic markers and/or p53, implying a molecular complexity and potential involvement of many other pathways in the process of PCa recurrence. Compared to published data for untreated PCa, the significant over-expression of oncogenic c-Myc, Bcl-2 and EZH2 and mutant p53 in PCa following these therapies supports increased aggressiveness of recurrent PCa. This raises important questions as well as fuels the debate on the benefit of radiation and androgen ablation in the treatment of PCa, especially, low grade PCa.

1088 ERBB4 and RB1 Immunohistochemical Stains and Fluorescence in Situ Hybridization Are Helpful in Distinguishing Chromophobe Renal Cell Carcinoma from Oncocytoma

Tong Sun[1], *Amy G Zhou*[1], *Qingqing Liu*[2], *Ediz Cosar*[3], *Maryann St.Cyr*[4], *Nicole Ninteau*[1], *Karen Dresser*[5], *Zhong Jiang*[4], *Lloyd Hutchinson*[6], *Kristine M Cornejo*[7]. [1]UMass Medical School, Worcester, MA, [2]Icahn school of Medicine at Mount Sinai, New York, NY, [3]University of Massachusetts, UMass Memorial, Worcester, MA, [4]UMass Medical School, [5]UMass Memorial Healthcare, Worcester, MA, [6]UMass Memorial Healthcare, Worcester, MA, [7]University of Massachusetts Medical School, Worcester, MA

Background: Differentiating renal oncocytoma (RO) from chromophobe renal cell carcinoma (ChRCC) can be challenging at times for surgical pathologists. CK7 and colloidal iron have traditionally been the only potentially useful markers, which often yield variable results. The aim of this study was to evaluate the expression of RB1 and ERBB4 in RO and ChRCC and to compare the immunohistochemistry (IHC) results to *RB1* and *ERBB4* gene abnormalities by fluorescence in situ hybridization (FISH).

Design: A total of 53 kidney resections (ChRCC, n=28; RO, n=25) were retrieved from the surgical pathology files of a tertiary medical center from 2000 to 2015. Slides were stained for RB1and ERBB4 IHC. Staining in >5% of tumor cells was considered positive and <5% of tumor cells or no staining was considered a loss or negative. FISH analysis was performed to evaluate gene copy number in parallel unstained slides in the same cohort.

Results: A loss of RB1 staining was identified in 18 of 28 (64%) ChRCC cases, and none of the RO cases (0/25; P<0.001). FISH analysis revealed that 10 of 28 (36%) ChRCC contained a hemizygous deletion of the *RB1* gene, with a 56% (10/18) concordanceof between the IHC and FISH findings. No *RB1* gene copy number variations were detected in any of the RO cases (0/25; P<0.001), and all cases retained expression of RB1 by IHC. ERBB4 showed cytoplasmic/membranous staining in all cases of RO and ChRCC. However, 21 of 28 (75%) ChRCC cases also contained nuclear positivity for ERBB4, which was much less common in the RO cases (3/25; 12%) (P< 0.001). A hemizygous *ERBB4* gene deletion was detected in nearly half of the ChRCC cases (13/28; 46%) by FISH analysis, but in none of the RO cases (0/25; 0%). The concordance of ERBB4 nuclear staining and *ERBB4* gene deletion by FISH was not statistically significant (P>0.05).

Diagnosis	RB1 Loss by IHC	Hemizygous **RB1** Gene Deletion	Nuclear ERBB4 IHC	Hemizygous **ERBB4** Gene Deletion
ChRCC (n=28)	18 (64%)	10 (36%)	21 (75%)	13 (46%)
RO (n=25)	0 (0%)	0 (0%)	3 (12%)	0 (0%)

Fig. 1

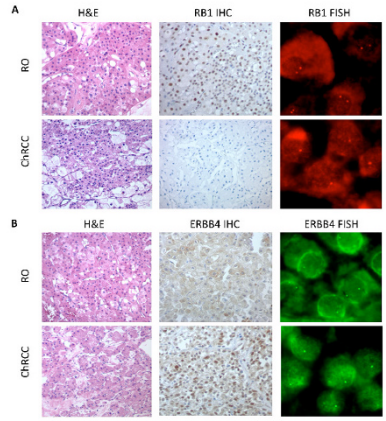

Conclusions: In summary, the loss of RB1 expression, which in part appears to be due to genetic loss at the chromosome level, is a highly specific diagnostic biomarker in distinguishing ChRCC from RO. The nuclear ERBB4 expression appears to be a sensitive diagnostic biomarker for ChRCC.

1089 Acquired Cystic Disease-Associated Renal Cell Carcinoma (ACKD-RCC)-Like Cysts

Yue Sun[1], *Pedram Argani*[2], *Satish Tickoo*[3], *Jonathan Epstein*[4]. [1]Johns Hopkins Medical Institutions, Baltimore, MD, [2]Johns Hopkins Hospital, Ellicott City, MD, [3]Memorial Sloan Kettering CC, New York, NY, [4]The Johns Hopkins Med Inst, Baltimore, MD

Background: ACKD-RCC, originally described by Tickoo et al., is found exclusively in patients with end stage renal disease (ESRD). Tickoo et al. noted: "Many of the tumors (16 of 24 dominant tumors) appeared to arise in a cyst, most often completely filling the cystic space. The cells lining such cysts were morphologically similar to those in the rest of the tumor." Subsequent literature lacks analysis of cysts lined by cells identical to ACKD-RCC, yet lacking areas of solid growth.

Design: Of 18 cases in our system diagnosed with ACKD-RCC-like cysts, we were able to review slides on 16 cases which formed the basis of this study.

Results: All specimens were nephrectomies and occurred in the setting of ESRD. Of the 16 cases, 12 were in men. Patient's ages ranged from 32 to 66 years (median 57). We defined ACKD-RCC-like cysts as cysts lined by vacuolated cells with eosinophilic cytoplasm identical to those seen in ACKD-RCC, yet lacking areas of solid growth. The cysts ranged in size from 0.2 to 2.5 cm. 12 cases had unilateral cysts with the remaining 4 seen in both kidneys. 8 cysts were multilocular, 6 unilocular, and 2 consisted of closely clustered cysts. The atypical cysts showed architectural variation. One cyst was lined with a single layer of atypical cells (1/16), whereas the majority of the cases were

focally lined by 2-4 cell layers of atypical cells (6/16) with occasional short papillary formations (9/16). Calcium oxalate crystals were noted in cyst walls and stroma in 9/16 cases. 14/16 cases had separate RCCs (2 cases with 2 RCCs; 1 case with 3 RCCs). Carcinoma ranged in size from 3 mm to 5 cm in the largest dimension: 4 were pT1 ACKD-RCC; 5 were pT1 papillary RCC; 5 were pT1 clear cell papillary RCC; 1 was pT3 clear cell RCC; and 3 pT1 unclassified.

Conclusions: Although the majority of RCC variants can be found in the background of ESRD, only ACKD-RCC is exclusively found in patients with ESRD. Our study formally analyzes for the first time in the literature atypical cysts lined with vacuolated cells with eosinophilic cytoplasm that are likely the earliest precursors of ACKD-RCC. When these cysts are encountered, especially ones that are multilocular or clustered, they may be misdiagnosed as ACKD-RCC. ACKD-RCC-like cysts should be recognized as a distinct entity from ACKD-RCC, defined by the lack of any solid growth within the cyst.

1090 Alterations of the p53 and MDM2 pathway are Frequent in Sarcomatoid Renal Cell Carcinoma

David Suster[1], *Shira Ronen*[2], *Jess F Peterson*[2], *Alexander Mackinnon*[3], *Ondrej Hes*[4], *Saul Suster*[5], *Douglas I Lin*[6]. [1]Boston, MA, [2]Medical College of Wisconsin, Milwaukee, WI, [3]Medical College/WI, Milwaukee, WI, [4]Biopticka laborator, Plzen, [5]The Medical College of Wisconsin, Milwaukee, WI, [6]Beth Israel Deaconess Medical Center, Boston, MA

Background: Sarcomatoid renal cell carcinoma (sRCC) is an aggressive RCC with propensity for metastasis and accurate diagnosis may be challenging. In contrast to the underlying parent clear cell, chromophobe and papillary RCCs, the molecular features of sRCC are not well defined. Here, we evaluate the immunohistochemical and molecular features of a cohort of both primary and metastatic sRCC with emphasis on members of p53/MDM2 and RB pathways.

Design: Immunohistochemistry (IHC) and FISH were performed on sections from 49 patients with sRCC (30 primary, 19 metastatic). Each case was reviewed by 3 pathologists to confirm sarcomatoid differentiation. IHC was performed on TMAs for cytokeratin AE1/3, Cam5.2, Pax8, RCC, CD10, p53, MDM2, p16, and CDK4 and were evaluated by a semiquantitative method. *MDM2* gene amplification was assessed by FISH. Altered p53 IHC (mutant type) was assessed by either diffuse, strong positivity in the majority of cells or complete absence of any staining in tumor cells (null-pattern). TCGA and MSK IMPACT genomic data on non-sarcomatoid RCC was retrospectively analyzed via online data mining tools.

Results: sRCC expressed Cytokeratin, Cam5.2 or Pax8 in 44/49 (90%) cases, 27/49 (55%) cases and 30/49 (61%) cases respectively. Altered p53 IHC (mutant pattern) was observed in 18/49 (37%) cases. MDM2 nuclear expression was observed in 30/49 (61%) cases. 15/19 (78%) metastatic sRCC and 15/30 (50%) primary sRCC showed nuclear MDM2 expression. In the RB pathway, CDK4 was expressed in 11/49 (22%) cases,and p16 in 23/39 (59%) cases. Of 49 sRCC cases, 5 (10%) showed *MDM2* gene amplification and 7 (14%) contained polysomy 12 (extra MDM2 and centromere 12 signals). Analysis of TCGA and MSK IMPACT studies of non-sarcomatoid RCC revealed that our *MDM2* amplification frequency in sRCC is higher than that seen in clear cell (0.2%, 1/418), chromophobe (0%, 0/65), papillary (0.4%, 1/280), and advanced metastatic RCCs (0.6%, 2/323 cases).

Conclusions: Alterations of the p53 and MDM2 pathway are frequent in sRCC, which may display nuclear MDM2 and mutant p53 staining patterns. A subset of cases may also harbor *MDM2 gene* amplification, which may represent a potential diagnostic pitfall when a sarcoma (such as de-differentiated liposarcoma) is also in the differential diagnosis. In addition, our results may also have therapeutic implications for sRCC since MDM2 and CDK4 specific inhibitors are currently in clinical trials for cancer.

1091 Next-Generation Sequencing-Based Molecular Characterization Of Urothelial Carcinoma

Sahr Syed[1], *Stephanie Mercurio*[2], *Wayne L Ernst*[3], *Thu Tran*[4], *Marina Nikiforova*[3], *Sheldon I Bastacky*[4], *Rajiv Dhir*[5], *Somak Roy*[6]. [1]UPMC, Pittsburgh, PA, [2]University of Pittsburgh Medical Center, Verona, PA, [3]University of Pittsburgh Medical Center, [4]University of Pittsburgh Medical Center, Pittsburgh, PA, [5]UPMC, Shadyside, Pittsburgh, PA, [6]University of Pittsburgh Medical Center, Allison Park, PA

Background: Muscle-invasive and metastatic urothelial carcinoma (UC) is a major cause of morbidity and mortality amongst cancer patients in the United States. Despite improvements in overall management of bladder cancer, a significant subset of muscle-invasive and metastatic UC is associated with treatment failures and progression. While there are established guidelines for molecular testing and targeted therapy in other cancers (e.g. lung, melanoma), routine clinical molecular testing is currently not standard of care for patients with UC. The aim of this study is to identify genomic alterations of clinical significance using next-generation sequencing (NGS) in UC.

Design: Seventy-two cases of high-grade urothelial carcinoma (HGUC), diagnosed between February 2016 and July 2017, were sequenced using a targeted NGS panel as part of routine clinical workup. The NGS panel analyzed for DNA mutations and copy-number changes in 50 cancer-related genes (AmpliSeq Hotspot V2, ThermoFisher, Carlsbad, CA). DNA was isolated after microdissection from formalin-fixed paraffin embedded tissue (FFPE). The raw sequencing data was analyzed using Torrent Suite v4.2.1 (ThermoFisher, Carlsbad, CA) and human genome reference sequence (GRCh37). Variant calling and copy number analysis was performed using Variant Caller v4.4.3.3 plugin and custom developed bioinformatics pipeline, respectively. A minimum coverage of 300x was required to reliably identify variants at 3% allelic fraction.

Results: All cases of HGUC were muscle-invasive with nodal disease in 78% (56/72) of cases. Sixty-two of 72 HGUC harbored at least one genomic alteration, with *TP53* being the most commonly mutated gene, followed by *FGFR3* (18%), *PIK3CA* (14%), *RB1* (13%), *FBXW7* (7%), *PTEN* (6%), *HRAS* (6%), *KRAS* (4%), *FGFR1* (4%), *ERBB2* (3%), and *BRAF* (3%), amongst others (Figure 1). Mutations and/or copy number alterations of potential therapeutic significance in HGUC were identified in at least 20% (10/50) of the genes in the panel, including *PIK3CA, FGFR3, FGFR1, BRAF, FBXW7, ATM, HRAS, and KRAS*. Correlation with clinicopathologic details and statistical analysis is under progress.

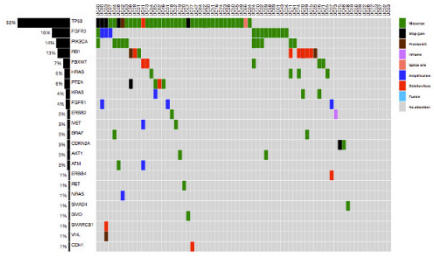

Conclusions: Our data suggests considerable molecular heterogeneity in HGUC. Targeted NGS assays can help identify genetic alterations of clinical and therapeutic significance for personalized management of HGUC. Muscle invasive UC that are resistant to conventional chemotherapy may potentially benefit from targeted mutational analysis.

1092 Analysis of genomic alterations of the EGFR gene family in advanced urothelial carcinomas by deep NGS sequencing and in situ hybridization

Cristina Teixidó[1], *Iban Aldecoa*[2], *Pedro Jares*[1], *Juan A Virizuela*[3], *Miguel A Climent*[4], *Alejo Rodríguez-Vida*[5], *Albert Font*[6], *Juan F Rodriguez-Moreno*[7], *Javier Puente*[8], *Begoña Perez*[8], *Enrique Gallardo*[10], *Aranzazu Gonzalez del Alba*[11], *Enrique Grande*[12], *Pablo Maroto*[13], *Josep Serra*[14], *Neil Gibson*[15], *Francisco Real*[16], *Pedro L Fernandez*[17]. [1]Hospital Clinic of Barcelona, Spain, [2]Hospital Clinic of Barcelona, [3]Hospital Universitario Virgen Macarena, Sevilla, Spain, [4]Instituto Valenciano de Oncología(IVO), Valencia, Spain, [5]Hospital del Mar, Barcelona, Spain, [6]ICO, Hosp. Germans Trias i Pujol, Badalona, Spain, [7]Clara Campal Comprehensive Cancer Center, Madrid, [8]Hosp. Clinico San Carlos, Madrid, Spain, [9]Hosp. Virgen del Rocio, Sevilla, Spain, [10]Hosp. Parc Tauli, Sabadell, Spain, [11]Hosp. Son Espases, Mallorca, Spain, [12]Hosp. Ramon y Cajal, Madrid, Spain, [13]Hosp. Sant Pau, Barcelona, Spain, [14]Boehringer Ingelheim España, S.A., Barcelona, Spain, [15]Boehringer Ingelheim Pharma GmbH & Co. KG, Biberach, Germany, [16]CNIO, Madrid Hospital Clinic, [17]FCRB and University of Barcelona, Spain

Disclosures: Pedro Fernandez: *Research Support*, Boehringer-Ingelheim

Background: Urothelial carcinoma comprises approximately 5% of newly diagnosed cancer and prognosis is dismal once in advanced stages. Therefore, new therapeutical approaches are needed and targeted therapy is still in its infancy for this type of tumors. The EGFR family of receptors could represent therapeutical targets in urinary tract as in other types of cancers, but the precise prevalence of their structural alterations is not well known in urothelial carcinoma.

Design: Locally advanced and metastatic urothelial carcinomas (n= 203) were analyzed for structural genomic alterations of the four members of the EGFR tyrosine kinase receptor family (EGFR, HER2, HER3, HER4). Samples included either primary or metastatic sites. Fluorescence in situ hybridization (FISH) for EGFR and HER2 as well as NGS sequencing with a 256 amplicons panel covering almost the entire coding regions of the four genes (AmpliSeq and PGM from Life Technologies) were performed in all cases. Four small regions, three in HER2 and one in HER3, were analyzed by Sanger sequencing. Nine cases were considered not evaluable due to poor DNA quality or insufficient material. Similarly to other cancers, FISH amplification of HER2 was considered when HER2/CEP17 ratio was $\geq$2. Cases were considered amplified for EGFR when $\geq$ 6 EGFR copies were found in >20% of the $\geq$50 evaluated cells.

Results: EGFR and HER2 FISH analyses showed 20 (10,3%) and 24 (12,3%) amplified cases respectively, and were coincidental in 4. Point mutations were observed in 6 cases for EGFR (3%), 12 cases for HER2 (6,1%),16 for HER3 (8,2%) and 10 for HER4 (5,1%). Coincidental mutations were observed in one case for HER2 and 3, HER2 and 4 and HER3 and 4. Two cases had coincidental mutations for EGFR and HER2. All point mutations were different except for one in HER2 (c.929C>T; p. Ser310Phe) which appeared twice. Coincidence of FISH amplification and mutation occurred in 4 cases.

Conclusions: We conclude that genomic alterations in the EGFR family occur in a significant proportion of urothelial carcinomas which could represent abnormalities in the tyrosine kinase receptor pathway and therefore potential targets for specific therapy.

1093 ETS2 is Highly Expressed in Prostate Cancers Aberrantly Expressing p63 and is a Prostate Basal Cell Marker

Alba Torres[1], *Mohammed Alshalalfa*[2], *Tamara L Lotan*[3]. [1]Johns Hopkins School of Medicine, [2]GenomeDx Biosciences Inc, Vancouver, BC, [3]Johns Hopkins School of Medicine, Baltimore, MD

Background: A rare subset of prostate carcinomas aberrantly express p63, and we have previously shown that these tumors have an immunophenotype intermediate between prostatic basal and luminal cells. Here, we performed gene expression profiling on p63-expressing prostatic carcinomas and compared them to usual-type adenocarcinoma.

Design: A total of 8 p63-expressing prostate carcinomas were compared to 358 usual-type adenocarcinomas by gene expression profiling performed on formalin fixed paraffin embedded tumor tissue using Affymetrix 2.0 ST microarrays. For validation, ETS2 *in situ* hybridization was performed using the Advanced Cell Diagnostics platform on a total of 19 p63-expressing prostate carcinomas arrayed on tissue microarrays (TMA).

Results: Differential gene expression profiling identified 104 genes that differed significantly in expression levels between usual-type adenocarcinoma and p63-expressing prostate carcinomas. Among the genes with the highest area under the curve (AUC) for distinguishing usual-type adenocarcinoma and p63-expressing prostate carcinomas were TP63, TRIM29, MIR206 and ETS2. TRIM29 is a previously described basal cell marker and MIR206 is positively regulated by the p63 transcription factor. *ETS2* is related and closely located to the *ERG* gene, and is lost in interstitial deletions resulting in *ERG* gene rearrangements. Though rarely mutated in advanced prostate cancer, little is known about its function. We found that ETS2 gene expression is highly correlated with P63 expression and is significantly higher in benign prostate tissues compared to usual-type adenocarcinoma tissues. By *in situ* hybridization, ETS2 expression was high in benign basal cells, and rarely detectable in benign luminal cells and or usual-type adenocarcinoma. In contrast, ETS2 was highly expressed in 95% (18/19) of p63-expressing prostate carcinomas.

Conclusions: ETS2 is highly expressed in benign basal cells and rare p63-expressing prostate carcinomas, but shows much lower expression in benign luminal cells and usual-type adenocarcinomas. Thus, the significance of *ETS2* deletion in usual-type adenocarcinomas that rearrange *ERG* and its mutation in advanced prostate carcinomas is uncertain.

1094 PTEN and ERG Status of Intraductal Carcinoma of the Prostate Occurring with Invasive Gleason Score 6 Carcinoma at Needle Biopsy

Aline C Tregnago[1], *Jessica L Hicks*[2], *Angelo DeMarzo*[3], *Jonathan Epstein*[1], *Tamara L Lotan*[4]. [1]The Johns Hopkins Med Inst, Baltimore, MD, [2]Johns Hopkins University School of Medicine, [3]Johns Hopkins University, Baltimore, MD, [4]Johns Hopkins School of Medicine, Baltimore, MD

Background: When intraductal carcinoma of the prostate (IDC-P) occurs in needle biopsies with only low grade, Gleason score 6 carcinoma, about 80% men have Gleason 7 or higher invasive carcinoma at radical prostatectomy. Thus, many of these cases of IDC-P may represent retrograde spread of the invasive high grade tumor into prostatic ducts. In this setting, the sampled Gleason 6 tumor may represent a low grade clone unrelated to the IDC-P or an under-sampled area of the high grade invasive tumor. Here, we examined ERG and PTEN status for IDC-P sampled on needle biopsy with Gleason 6 invasive tumor.

Design: We queried our consultation archives for cases of IDC-P occurring with only concurrent Gleason 6 carcinoma at needle biopsy and were able to retrieve unstained tissue on 22 cases of IDC-P, with 15 having adequate concurrent Gleason 6 carcinoma after re-cutting for immunostaining. Immunostaining was performed with genetically validated protocols for PTEN and ERG.

Results: Overall, 59% (13/22) of the IDC-P lesions expressed ERG and 52% (11/22) had PTEN loss. Of the concurrent invasive Gleason score 6 carcinoma, 60% (9/15) expressed ERG and 14% (2/14) had PTEN loss. 29% (4/14) of cases with matched IDC-P and Gleason score 6 carcinoma were discordant for ERG status (3 were ERG-negative in IDC-P and ERG-positive in the invasive tumor) and 38% (5/13) were discordant for PTEN status (all had PTEN loss in the IDC-P and intact PTEN in the invasive tumor and all of these cases were concordant for ERG in both the invasive and IDC-P components). In all, 64% (9/14) were discordant for PTEN or ERG status.

Conclusions: Based on discordant ERG status, in at least 29% of cases, the IDC-P and Gleason score 6 carcinoma are derived from separate tumor clones. In these cases, the IDC-P may represent retrograde spread of a separate un-sampled higher grade tumor clone or a true *in situ* precursor lesion. In an additional 38% of cases, the IDC-P had PTEN loss, while the Gleason 6 carcinoma retained PTEN, suggesting that the IDC-P is almost certainly not a precursor lesion to the sampled invasive carcinoma clone. Based on concordant ERG status in these cases, it could be that the IDC-P is a further evolved sub-clone of the invasive tumor undergoing retrograde intraductal spread, though we cannot exclude the possibility that it represents a separate tumor clone.

1095 Skene's Glands Adenocarcinoma: A Series of Four Cases

Aline C Tregnago[1], *Jonathan Epstein*[1]. [1]The Johns Hopkins Med Inst, Baltimore, MD

Background: Skene's (periurethral) gland adenocarcinoma is very rare, with only 7 cases reported in the literature. This is the first series of cases on this entity.

Design: We describe the histologic, immunohistochemical and clinical findings of 4 patients with Skene's gland adenocarcinoma from our consult service from 1984 to 2017.

Results: The average age at diagnosis of the four women was 74.5 years (range, 61-87 y). Diagnostic specimens included 1 biopsy and 3 limited resections. Tumor size ranged from 1.0 to 2.0 cm (mean, 1.5 cm). Average follow-up time was 10.3 months (range, 4-19 months). Three of our cases were morphologically consistent with prostatic acinar adenocarcinoma with variable cribriform, fused, and poorly-formed glands, analogous to Gleason score 4+4=8. Of these, one had mixed ductal features with neoplastic cells showing papillary carcinoma with columnar cytology. These 3 cases were positive for PSA, P501S, NKX3.1 and AMACR. Focal goblet cells positive for CK20 and negative for prostatic markers were seen in one of these cases, suggesting intestinal differentiation (although negative for CDX2 and SATB2). One case was in-situ and had glandular and papillary formations with pseudostratified columnar epithelium and mucin secretion, showing positivity for CK7, ER and P16, and negativity for prostatic markers, suggesting Mullerian differentiation (although negative for PAX8, WT1, and RNAscope ISH high risk cocktail for HPV). PIN4 cocktail confirmed the origin in pre-existing paraurethral glands in all cases. All patients were alive and free of recurrence or metastatic disease at the time of last follow-up.

Conclusions: Our findings demonstrate that most Skene's gland adenocarcinomas recapitulate morphologies and immunohistochemical markers seen in prostatic adenocarcinoma, yet not all have this morphology. It is unknown whether applying the same grading criteria for prostatic adenocarcinomas to Skene's gland adenocarcinoma is valid given the small number of cases with variable treatment and limited follow-up. Because of the rarity of Skene's gland adenocarcinomas, there is no consensus regarding their treatment. Serum PSA should be performed at the time of diagnosis and treatment, since decreased levels have been shown after successful therapy.

1096 Predicting Higher Clinical Stage in Testicular Germ Cell Tumors: Do the Same Factors Matter for Seminomas and Nonseminomas?

Karen Trevino[1], *Alaleh Esmaeili Shandiz*[2], *Thomas Ulbright*[1], *Muhammad Idrees*[1]. [1]Indiana University School of Medicine, Indianapolis, IN, [2]Indianapolis, IN

Background: Testicular germ cell tumors are categorized into seminomas or nonseminomas, and this classification affects the prognosis and recurrence risk of the tumor. It has been established that certain pathologic criteria lead to higher stage in seminomas and also in nonseminomas. However, it is not clear whether these criteria carry the same significance when the group is examined as a whole.

Design: We performed a slide and chart review of 249 cases of testicular germ cell tumors (144 seminomas and 105 nonseminomas). Patient age, tumor size, and invasion into lymphovascular spaces, rete testis, hilar soft tissue, epididymis, and spermatic cord were recorded. We divided rete testis and epididymal invasion into direct invasion versus pagetoid spread. We then compared clinical stage I patients to higher clinical stage patients (stage II and III) in reference to these factors.

Results: Of the 249 cases, 173 cases were clinical stage I and 76 cases were clinical stage II or III. Statistical analysis demonstrated a significantly increased risk of higher stage disease in patients with increased tumor size (p=0.0014) and invasion into lymphovascular spaces ($p=7.87x10^{-8}$), rete testis (p=0.002), hilar soft tissue ($p=2.53x10^{-6}$), epididymis (p=0.0001), and spermatic cord ($p=6.90x10^{-5}$). Age (p=0.69) and pagetoid spread (p=0.125) were not significantly associated with higher stage disease. When comparing rete testis invasion to lymphovascular invasion (LVI), LVI is a significantly better predictor of higher stage disease (p=0.04). However, soft tissue invasion was not found to be statistically different from LVI (p=0.951).

Conclusions: The same predictors of higher stage disease are significant when looking at testicular germ cell tumors as a whole as when dividing these groups into seminomas and nonseminomas. In the combined group though, rete testis invasion was significantly different from LVI in its risk for higher stage disease, which varies from what has been seen in the groups individually. However, there were more cases with rete testis invasion in the seminoma group and more with LVI in the nonseminoma group, which may skew the data when combined. Additionally, we found that increased tumor size was associated with increased clinical stage, a criterion that is currently only used in seminomas. In conclusion, the pathologic criteria used to upstage testicular germ cell tumors are primarily the same between seminoma and nonseminomas and staging should remain the same for both.

1097 Men with Intraductal Carcinoma of Prostate Benefit from Adjuvant Radiotherapy: A New Stand-Alone Indication From a Multi-Cohort Study of Localized Prostate Cancer

Vincent Quoc-Huy Trinh[1], *Nazim Benzerdjeb*[2], *Ségolène Chagnon-Monarque*[3], *Nicolas Dionne*[3], *Guila Delouya*, *Roula Albadine*[4], *Mathieu Latour*[6], *Anne-Marie Mes-Masson*[6], *Alain Bergeron*[7], *Hélène Hovington*[8], *Kevin Zorn*[3], *Fred Saad*[8], *Yves Fradet*[7], *Daniel Taussky*[3], *Dominique Trudel*[9]. [1]Centre Hospitalier de l'Université de Montréal, Montreal, QC, [2]Centre de recherche du CHUM/Institut du cancer de Montréal, Montréal, QC, [3]Centre hospitalier de l'Université de Montréal, [4]Montreal, [5]St-Eustache, QC, [6]Centre de recherche du CHUM, [7]Centre hospitalier universitaire de Québec-Université Laval, Québec, QC, [8]Centre hospitalier universitaire de Québec-Université Laval, Quebec, QC, [9]CHUM, Montreal, PQ

Background: Intraductal carcinoma of the prostate (IDCP) is a prevalent finding in prostate cancer (PCa), affecting 20% of patients. Though IDCP is clearly associated with poor prognosis, no targeted management exists. Radiotherapy (RT) is associated with better outcomes in aggressive PCa. Here, we studied IDCP in the context of adjuvant radiotherapy (ART), and aimed to predict response as a stand-alone indication.

Design: PCa patients with first-line RP with or without ART (1993-2015) were extracted from 2 cohorts (exclusion criteria: any other form of treatment prior to biochemical recurrence (BCR), N1/M1, detectable post-treatment PSA, and <75% of material available) with up to ten years of follow-up. Main outcome was BCR (2 PSA >0.2ng/ml). Pathology material was reviewed for staging, Gleason score (GS) and IDCP status. Patients were grouped into one or more indication for ART (ARTIndi≥1) or ARTIndi=0. ARTIndi are GS=8-10, extraprostatic extension (EPE), seminal vesicle invasion (SVI), and positive margins (PM).

Results: We reviewed 293 eligible RP specimens, 39 from center 1 and 254 from center 2. 48 patients were treated by RP+ART, 97 treated by RP only with ARTIndi≥1, and 148 treated by RP only with ARTIndi=0. Men with ARTIndi=0 had significantly lower grade and stage than men with ARTInd>=1 (P<0.001 and P <0.001). Mean follow-up time was 3184 days (d) (SD=1639). IDCP was found in 30.5% of patients, 37.5% if ARTIndi≥1, and 13% if ARTIndi=0. In multivariate analysis, Cox regression showed IDCP (HR=2.65 (95%CI:1.57-5.57, P<0.001)) and ART (HR=0.32 (95%CI:0.14-0.75, P=0.008)) predicted BCR (Table 1). Patients with IDCP+/RP only/ARTIndi≥1 had the worst BCR-free survival, even though they had lower rates of EPE, LVI and SVI when compared to patients treated by ART (Figure 1). To see if IDCP can be a stand-alone ARTIndi, we compared IDCP+/RP only/ARTIndi=0 vs IDCP–/RP only/ARTIndi≥1: they did not differ in BCR-free survival (mean survival 2959d (95%CI=2473-3445) vs 2945d (95%CI=2661-3228), median not calculable, P=0.959).

Table 1. Cox regression for biochemical recurrence up to 10 years of follow-up of 293 men with localized PCa undergoing first-line RP.

	Hazard-ratio (95% C.I.)	P
Adjuvant radiation therapy	0.32 (0.14-0.75)	0.008
Intraductal carcinoma of prostate	2.65 (1.57-4.47)	<0.001
ISUP grade (Gleason score)	1.29 (1.01-1.65)	0.042
Extraprostatic extension	2.03 (1.16-3.54)	0.013
Positive margins	2.24 (1.33-3.77)	0.002
Seminal vesicle invasion	1.36 (0.68-2.71)	0.390

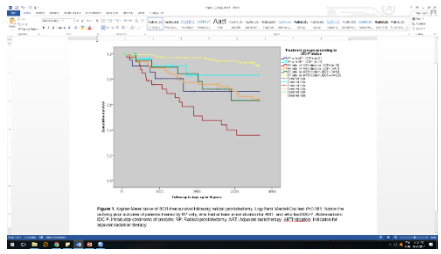

Conclusions: In this study of 293 RP of localized PCa treated by RP or RP+ART, we find IDCP+ patients only treated by RP showed significantly lower BCR-free survival against other groups. Furthermore, isolated IDCP confers the same BCR-free survival as current ART indications. Our results strongly suggest that IDCP has the same aggressive potential as current ART indications, and would benefit from the same treatment. This is the first report of a targeted treatment for IDCP.

1098 Oncocytic Renal Tumors with CD117 Negative, Cytokeratin 7 Positive Immunoprofile are Different from Eosinophilic Chromophobe Renal Cell Carcinoma (ChrRCC) and Oncocytoma

Kiril Trpkov[1], *Sean R Williamson*[2], *Petr Martinek*[3], *Liang Cheng*[4], *Pilar San Miguel Fraile*[5], *Asli Yilmaz*[6], *Ondrej Hes*[7]. [1]University of Calgary, Calgary, AB, [2]Henry Ford Health System, Detroit, MI, [3]Bioptical Laboratory, Pilsen, Czech Republic, Plzeň, Plzensky kraj, [4]Indiana University School of Medicine, Indianapolis, IN, [5]Hospital Álvaro Cunqueiro, Vigo (Pontevedra), Spain, [6]Calgary Laboratory Services, Calgary, AB, [7]Biopticka laborator, Plzen

Background: Positive staining for CD117 is often used to support diagnoses of oncocytoma or ChrRCC. Greater extent of cytokeratin 7 (CK7) labeling is generally considered in favor of ChrRCC; however, the extent of CK7 labelling in oncocytic tumors is usually limited compared to classic ChrRCC. We have encountered occasional oncocytic tumors that are unexpectedly CD117 negative, but diffusely CK7 positive.

Design: Prompted by 2 index cases with oncocytic morphology that were CD117 negative and CK7 diffusely positive, we searched 4 large renal tumor archives for similar cases. In particular, we reviewed the cases labelled as "consistent with (or favor) eosinophilic ChrRCC", "oncocytic tumor, favor oncocytoma, or with hybrid features" and "low-grade oncocytic tumor (unclassified)", all of which showed negative CD117 and diffusely positive CK7. We collected clinicopathologic and follow-up (F/U) data and, in addition to CD117 and CK7, we performed the following immunostains: PAX8, CD10, AMACR, e-cadherin, CK20, CA9, AE1/AE3, vimentin, BerEP4, and MOC31. Muller-Mowry colloidal iron stain was also done. In 7 cases with available paraffin tissue, we performed array CGH (aCGH) evaluation.

Results: We identified 19 cases with male-to-female ratio of 1:1.7, and median age of 66 years (range 53-78y). Median tumor size was 30 mm (range 11-135 mm); all were single tumors. Grossly, the cut surface was tan-brown and solid. On microscopy, all cases showed solid or compact nested growth and often loosely arranged tumor cells in areas of edematous stroma. The cells exhibited oncocytic cytoplasm with uniformly round to oval, but not irregular or crumpled nuclei, with focal delicate (or absent) perinuclear halos, as shown in Figures 1 and 2. Uniform reactivity was found for: AE1/AE3, PAX8, e-cadherin, BerEP4 and MOC31. Negative stains included: CA9, CK20, and vimentin; CD10 and AMACR were either negative or focal. Muller-Mowry stain was either negative or apical positive. aCGH showed common deletions on 19p (7/7), 1p36 (5/7) and 19q (4/7), but no other consistent gains or losses. F/U was available for 15/19 patients (median 21 mo, range 3-118); all were alive with no disease progression.

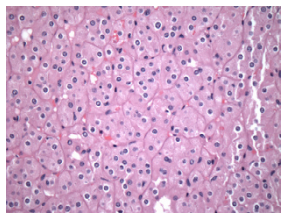

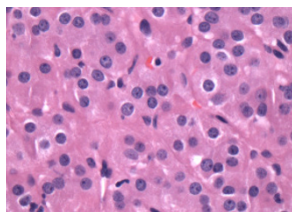

Conclusions: Oncocytic tumors that are CD117 negative and CK7 positive show remarkably consistent morphology and immunoprofile, which does not fit completely into either oncocytoma or eosinophilic ChrRCC. These tumors are indolent and show frequent losses of 1p36 and 19q, and uniform loss of 19p, but no other consistent losses or gains.

1099 Biopsy Global Grade Group vs. Highest Grade Group vs. Largest Volume Cancer Grade Group: Concordance of Biopsy 'Case Level' and Radical Prostatectomy Grade Groups

Kiril Trpkov[1], *sakkarn sangkhamanon*[2], *Asli Yilmaz*[3], *Shaun Medlicott*[4], *Panche Zdravkovski*[5], *Tarek Bismar*[6], *Melissa A Shea-Budgell*[7]. [1]University of Calgary, Calgary, AB, [2]University of Calgary, [3]Calgary Laboratory Services, Calgary, AB, [4]Calgary, AB, [5]Institute of Pathology - Medical Faculty, University "Ss. Cyril and Methodius" - Skopje, Macedonia, Skopje, Macedonia, [6]Rockyview General Hosp, Calgary, AB, [7]University of Calgary, Calgary, AB

Background: The practice of assigning 'case level' biopsy Gleason Score (GS) or Grade Group (GR) is variable. To our knowledge, a comparison of concordance between different biopsy 'case level' GR/GS with the radical prostatectomy (RP) GR/GS, has not been done in a contemporary, post-2005 prostate cancer cohort.

Design: We evaluated the GR/GS in 2,527 patients who had biopsy and RP performed at our institution between 2005 and 2014. We compared the agreements, the upgrades and the downgrades of 3 different 'case level' biopsy GR, with the final RP GR: 1) Global GR, based on the most prevalent and the highest grade (in any biopsy specimen); 2) Highest GR (in any biopsy specimen); and 3) Largest Volume Cancer GR (in any biopsy specimen). We evaluated separately the concordance for cases with tertiary pattern 5 (T5) on RP, particularly in the setting of GR2 T5 (GS3+4 T5) and GR3 T5 (GS4+3 T5). Weighted kappa (κ) was used to assess the overall biopsy-RP GR concordance.

Results: The overall biopsy Global GR, Highest GR, and Largest Volume Cancer GR were identical with the RP GR in 60.4%, 57.1% and 54.3% cases, respectively; weighted κ values: 0.49, 0.48, and 0.44, respectively (see Table). All biopsy GR showed highest and comparable agreements for GR2 (GS3+3) and GR5 (GS9-10) and lowest for GR4 (GS8). GR1 (GS3+3) agreement was moderate for all GR with comparable rates of upgrade. In GR3 (GS4+3), there was better agreement and less downgrading for the Global GR vs. the Highest and the Largest Volume Cancer GR. When RP GR contained T5, the overall biopsy-RP grade agreement decreased: Global GR 41.5%, Highest GR 40.3%, and Largest Volume Cancer GR 37.1% (weighted κ: 0.22, 0.21, and 0.18, respectively). In RP with T5, the RP findings (pT stage, tumor volume, lympho-vascular invasion, positive nodes) for GR2 T5 (GS3+4 T5) and GR3 T5 (GS4+3 T5) were not significantly different than the RP findings in GR4 (GS8) and GR5 (GS9-10), respectively.

Biopsy GR (GS)	Upgrade (%)	No Change (%)	Downgrade (%)
Global GR (GS)	31.8	60.4	7.8
GR1 (GS3+3)	51.6	48.4	-
GR2 (GS3+4)	16.2	75.9	7.9
GR3 (GS4+3)	19	47.3	33.7
GR4 (GS8)	38.3	21.7	40
GR5 (GS9-10)	-	82.7	17.3
Highest GR (GS)	30.2	57.1	12.7
GR1 (GS3+3)	51.6	48.4	-
GR2 (GS3+4)	15	76	9
GR3 (GS4+3)	11.7	36.5	51.8
GR4 (GS8)	20.5	17.3	62.2
GR5 (GS9-10)	-	81.4	18.6
Largest Vol. Ca GR (GS)	38	54.3	7.7
GR1 (GS3+3)	57.6	48.4	-
GR2 (GS3+4)	17.3	75.3	7.4
GR3 (GS4+3)	17.6	46.1	36.3
GR4 (GS8)	31.6	20.3	48.1
GR5 (GS9-10)	-	82.2	17.8

Conclusions: Assigning biopsy 'case level' Global GR, rather than the Highest GR and Largest Volume Cancer GR, resulted in slightly improved overall agreement with the final RP GR. All biopsy GR had good and comparable agreements for GR2 and GR5 and moderate for GR1. The agreement for GR4 was fair for all biopsy GR. For GR3, the biopsy Global GR showed better agreement and less downgrading than the Highest GR and the Largest Volume Cancer GR. When T5 was present on RP in GR2 and GR3, the RP findings were not significantly different than those in GR4 and GR5, respectively.

1100 Intraductal Carcinoma of the Prostate: Incidence on biopsies and Concordance with Radical Prostatectomy

Dominique Trudel[1], *Nazim Benzerdjeb*[2], *Alain Bergeron*[3], *Hélène Hovington*[4], *Yves Fradet*[3], *Bernard Tetu*[5], *Theodorus van der Kwast*[6]. [1]CHUM, Montreal, [2]Centre de recherche du CHUM/Institut du cancer de Montréal, Montréal, QC, [3]Centre hospitalier universitaire de Québec-Université Laval, Québec, QC, [4]Centre hospitalier universitaire de Québec-Université Laval, Quebec, QC, [5]CHAUQ-Hopital St. Sacrement, Quebec City, [6]University Health Network, Toronto, ON

Background: Intraductal carcinoma is predicting poor prognosis in men with prostate cancer. Found in approximately 20% of radical prostatectomy, its incidence on biopsies is not well known. Furthermore, the concordance rate between biopsies (BX) and radical prostatectomies (RP) has not yet been explored, as well as the BX factors influencing such concordance.

Design: Men who underwent first line RP after a BX at the Centre hospitalier universitaire de Québec-Université Laval between 1993 and 2003 were included in the cohort. RP slides were reviewed to update grade, stage and IDC-P status. In view of its relationship with IDC, large cribriform (LC) carcinoma was also recorded as present or absent. BX slides were reviewed to record tumor length (mm), grade and IDC/LC status. Incidences and concordances were evaluated using descriptive statistics.

Results: A total of 283 men were included in the cohort. BX ISUP grade distribution paralleled RP ISUP grade (1: 43%/46%; 2: 32%/36%; 3: 14%/12%; 4: 9%/3%; 5: 1%/3%). IDC was present in 7.4% of the BX and in 22.6% of the RP. When combined with LC, the incidences were 24.7% (BX) and 61.1% (RP). As 81.3% of the cases were concordant for IDC status, 93% of those cases were negative for IDC. 17% of the cases were negative for IDC at BX but positive at RP. Overall, positive and negative predictive values of presence of IDC at RP as evaluated at BX were of 76.2 (95% confidence interval, CI: 55.0-89.4% and of 81.7% (95% CI: 79.44-83.72%), respectively. When combined with LC, only 57.2% of the cases were concordant, with overall positive and negative predictive values of IDC/LC as evaluated at BX were of 87.1% (95% CI: 77.8-92.9%) and of 47.4% (95%CI: 44.7-50.5%). Whether IDC status was assessed alone or with LC, total BX length did not differ according to concordance status (p>0.05). However, tumours which were concordant for IDC status were either longer (IDC positive, mean length=25.8 mm) or shorter (IDC negative, mean length=9.2 mm) compared to discordant cases (mean length=16.0mm) (p<0001). Similar results were obtained when IDC was evaluated in combination with LC.

Conclusions: BX is a better indicator of absence of IDC at RP than of its presence. Longer and shorter tumours are more likely to be concordant for IDC/LC status than tmours of intermediate length, but BX length does not impact concordance. Lastly, to increase our capacity to predict the presence of aggressive carcinoma (IDC/LC) at RP, IDC should be evaluated in combination with LC at BX.

1101 Primary Mixed Epithelial and Stromal Tumors (MEST) of the Seminal Vesicles: A Report of Two Cases

Lawrence D. True[1], *Jose Mantilla*[2], *Thomas H Norwood*[3]. [1]Seattle, WA, [2]University of Washington, Seattle, WA, [3]University of Washington

Background: Primary neoplasms of the seminal vesicles are exceedingly rare. Of these neoplasms one of the rarest is the epithelial and stromal neoplasm (MEST). Little is known of their long-term biology or molecular phenotype.

Design: Our Pathology laboratory information system was reviewed for cases with a diagnosis of mixed epithelial stromal tumor of the prostate or seminal vesicle, and of permutations of these terms, between 1995 and 2017. Immunohistochemical and cytogenetic features of the identified cases were reviewed.

Results: Two cases of MEST of the seminal vesicles were found.

Case 1: An incidentally identified (by imaging studies) right seminal vesicle mass (7 cm) was resected from a 70-year old.

Case 2: A radical cystoprostatectomy was done for an 8.5 cm complex mass prostate-associated mass in a 26 year-old man. Microscopically, the mass was associated with the seminal vesicles and abutted the prostate.

The histology of both cases was similar. Both had a phylloides-like architecture with solid and cystic regions. Within the case 2 tumor were areas of necrosis. The stromal component was hypercellular, composed of cytologically bland, mitotically inactive spindle cells. The epithelial component consisted of cuboidal to columnar cells with no more than moderate nuclear atypia, but virtually no mitoses. Epithelial cells in case 2 had variable amounts of cytoplasmic lipochrome pigment.

Karyotype studies of Case 2 mass showed multiple alterations, including loss of chromosomes 1, 7, 16 and 22; partial loss of 9p, and a 1p;10q22 translocation. On follow-up, the patient had no evidence of

disease at 22 years. Immunohistochemical findings are summarized in the table.

	Case 1	Case2
PAX-8	NEG (stroma) POS (epithelium)	Not performed
ER	POS (stroma) NEG (epithelium)	NEG (stroma) NEG (epithelium)
PR	POS (stroma) NEG (epithelium)	NEG (stroma) NEG (epithelium)
PSA	NEG (stroma) NEG (epithelium)	NEG (stroma) NEG (epithelium)
PSAP	NEG (stroma) NEG (epithelium)	NEG (stroma) NEG (epithelium)

Conclusions: Our two cases add to what is known of the phenotype and biology of MESTs. The immunophenotype (PAX 8 positive, PSA and PSAP negative) suggests that the epithelial component is of müllerian origin, consistent with the embryology of seminal vesicles. Stromal expression of ER and PR is indicative of ovarian-type stroma. Accordingly, these tumors appear to represent a fusion of 2 developmental pathways. The cytogenetic abnormalities are consistent with MEST's being neoplastic, though they do not point to a specific tumorigenic lineage. Based on the 22 year disease free outcome of patient 2, we have evidence that MESTs which have a bland cytology with little mitotic activity are likely to have a benign outcome.

1102 Integrating the Presence of Intraductal Carcinoma of the Prostate into the Grade Group System Improves Prediction of biochemical Failure in Radical Prostatectomy Patients

Toyonori Tsuzuki[1], *Mashashi Kato*[2], *Naoto Sassa*[2], *Ryohei H Hattori*[3], *Momokazu Gotoh*[2]. [1]Aichi Medical University Hospital, Nagakute, Aichi, [2]Nagoya University Hospital, [3]Japanese Red Cross Nagoya Daiichi Hospital

Background: The ISUP2014 and WHO2016 proposed a grade group system for prostate cancer. Although the presence of the intraductal carcinoma of the prostate (IDC-P) influences biochemical failure in radical prostatectomy patients, only a few studies have mentioned the utility of integrating the presence of IDC-P into the grade group system.

Design: We retrospectively evaluated 1000 patients who underwent radical prostatectomy between 2005 and 2013 at the authors' institutions. No patients received neoadjuvant and/or adjuvant therapy before biochemical failure. HE slides for each patient were reviewed by a single genitourinary pathologist (T.T.) according to ISUP2014 criteria. Cox proportional hazard regression models were developed to predict biochemical failure.

Results: The median patient age was 67 (range, 49–77) years. The median initial PSA was 6.9 ng/ml (range, 0.4–82 ng/ml). The median follow-up period was 69 (range, 0.7–134) months. The grade group were as follows: Group 1 without IDC-P, 16.3% (n=163); Group 2 without IDC-P, 47.2% (n=472); Group 2 with IDC-P, 5.4% (n=54); Group 3 without IDC-P, 15.9% (n=159); Group 3 with IDC-P, 8.9% (n=89); Group 4 without IDC-P, 2.6% (n=26); and Group 5 without IDC-P, 4.3% (n=43); any grade Group with IDC-P, 15.6% (n=157; Group 2 (n=31); Group 3 (n=58); Group 4 (n=13); Group 5 (n=55)). Any grade Group with IDC-P showed a significantly worse prognosis than any other groups without IDC-P (p=.00001).

Conclusions: *Integrating the presence of IDC-P into the grade group system will improve the accuracy of patient outcome predictions.*

1103 Integrating Tertiary Gleason Pattern 5 into the Grade Group System Improves Prediction of Biochemical Failure in Radical Prostatectomy Patients

Toyonori Tsuzuki[1], *Mashashi Kato*[2], *Naoto Sassa*[2], *Ryohei H Hattori*[3], *Momokazu Gotoh*[2]. [1]Aichi Medical University Hospital, Nagakute, Aichi, [2]Nagoya University Hospital, [3]Japanese Red Cross Nagoya Daiichi Hospital

Background: The ISUP2014 and WHO2016 proposed Gleason grade groups for prostate cancer. Although the presence of the tertiary Gleason pattern 5 (TP5) influences biochemical failure in radical prostatectomy patients, only a few studies have mentioned the utility of integrating TP5 into the grade group system.

Design: We retrospectively evaluated 1000 patients who underwent radical prostatectomy between 2005 and 2013 at the authors' institutions. No patients received neoadjuvant and/or adjuvant therapy before biochemical failure. HE slides for each patient were reviewed by a single genitourinary pathologist (T.T.) according to ISUP2014 criteria. Cox proportional hazard regression models were developed to predict biochemical failure.

Results: The median patient age was 67 (range, 49–77) years. The median initial PSA was 6.9 ng/ml (range, 0.4–82 ng/ml). The median follow-up period was 69 (range, 0.7–134) months. The grade group were as follows: Group 1, 16.3% (n=163); Group 2, 43.6% (n=436); Group 2 with TP5, 5.4% (n=54); Group 3, 12.1% (n=121); Group 3 with TP5, 8.9% (n=89); Group 4, 3.9% (n=39); and Group 5, 9.8% (n=98). Group 2 with TP5 showed a significantly worse prognosis than Group 2 (p<.0001). Similarly, Group 3 with TP5 demonstrated a significantly worse prognosis than Group 3 (p=.0001). In contrast, Groups 2 with TP5 and 3 and Group 3 with TP5 and 4 showed the same prognosis (p=0.916 and p=0.854).

Conclusions: Integrating TP5 into Gleason grade groups will improve the accuracy of patient outcome predictions.

1104 Clinicopathological Features of Renal Cell Carcinomas in Patients with End-Stage Kidney Disease

Toyonori Tsuzuki[1], *Tsunenori Kondo*[2], *Naoto Sassa*[3], *Momokazu Gotoh*[3]. [1]Aichi Medical University Hospital, Nagakute, Aichi, [2]Tokyo Women's Medical University, [3]Nagoya University Hospital

Background: New disease entities were proposed in the 2016 WHO classification for renal cell carcinoma (RCC) in patients with end-stage renal disease (ESRD), such as acquired cystic disease (ACD)-associated and clear cell papillary RCC. However, their accurate incidence in RCC patients with ESRD has not yet been documented. We aimed to determine its clinicopathological features based on data obtained from three Japanese institutions.

Design: We retrospectively evaluated 315 RCC patients with ESRD between 1987 and 2015. At the time of nephrectomy, patients were either undergoing chronic dialysis therapy or had a previous history of long-term (more than 6 months) dialysis therapy before renal transplantation. All H&E stained slides with were reviewed and classified based on the 2016 WHO classification by a single uropathologist (T.T.).

Results: The mean age of patient's was 56.1 years (range 23–80 years). The male to female ratio was 5.60 (265:51). The mean hemodialysis period was 13.6 years (range 1–36 years). The incidence of acquired cystic kidney disease (ACDK) was 238 (76%). The ratios of histological subtypes are shown in Figure 1. The incidence of the RCC subtypes depending on the duration of hemodialysis is shown in Figure 2. The multivariable analysis for predictive factors for occurrence of ACD-associated RCC is shown in Table 1.

Multivariable Analysis for Predictive Factors for Occurrence of ACD-associated RCC

	HR	CI	p value
Presence of ACDK	$1.7X10^9$	10-	<0.001
Dialysis duration (years)	1.10	1.04-1.16	<0.001
Patient age	0.95	0.92-0.98	0.01
Male gender	2.45	0.85-8.16	0.09
Diabetic nephropathy	1.18	0.27-4.59	0.80

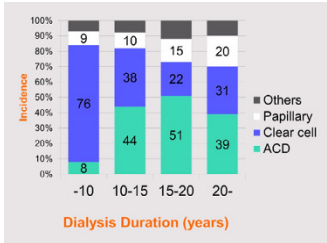

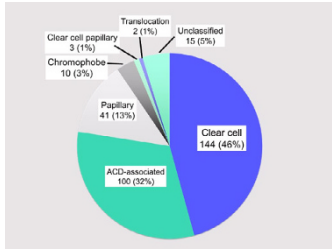

Conclusions: The incidence of ACD-associated RCC was dependent on the presence of ACDK and hemodialysis duration; while the incidence of clear cell papillary RCC in this study was lower than that of reports from western countries.

1105 Histologic Findings Associated with False Positive Multiparametric MRI Performed for Prostate Cancer Detection

David Ullman[1], *Luciana Schultz*[2], *Carli Calderone*[1], *Kristin Porter*[1], *Jeffrey Nix*[1], *Soroush Rais-Bahrami*[1], *Jennifer Gordetsky*[3]. [1]University of Alabama at Birmingham, [2]Instituto de Anatomia Patológica, AC Camargo Cancer Center, Santa Barbara dOeste, SP, [3]The University of Alabama at Birmingham, Birmingham, AL

Background: Multiparametric MRI/Ultrasound (US) targeted biopsy has been shown to more accurately identify higher grade prostate cancers compared to the standard extended sextant prostate biopsy. However, this technique is imperfect, creating occasional false positive imaging results. We aimed to investigate the histologic findings associated with false positive MRI performed for prostate cancer detection.

Design: A retrospective review was performed on our surgical pathology database from 2014-2017 selecting patients, with previous standard negative biopsy, who then underwent MRI/US targeted biopsy (TB) and concurrent 12-core extended standard biopsy (SB). Histologic features evaluated included percentage of core involvement by chronic inflammation, percentage of core composed by stroma, percentage of glands involved by atrophy and presence of the following features: acute or granulomatous inflammation, stromal hyperplasia, adenosis, squamous metaplasia, basal cell hyperplasia and presence of skeletal muscle. Histologic findings on TB were compared to SB (located at least two quadrants away from the TB) and also to corresponding MRI PIRADS score for each lesion.

Results: We identified 544 patients who underwent MRI/US TB. Of these, 40 patients had no tumor on all SB and TB cores, and a maximum of 2 targeted lesions on MRI. We evaluated a total of 61 TBs and compared them to 40 controls taken from the concurrent SB. Compared to SB tissue, the mean percentage of stroma and chronic inflammation were found to be increased on the TB; 59.3 vs 67.5 for stroma and 11.1 vs 16.1 for chronic inflammation, respectively (p=0.01, p=0.02). Of the other binary histological parameters evaluated, acute inflammation was found in 18/61 (29.5%) TB and 5/40 (12.5%) SB, p=0.46. A score composed of one point for each of the three most relevant parameters (high chronic inflammation [>10%, median on TB], acute inflammation, and basal cell hyperplasia) was significantly associated with with TB (p=0.015). Interestingly, atrophy and percentage of stroma showed a positive correlation (r=0.75), which was restricted to high PIRADS lesions.

Conclusions: There are specific benign histologic findings associated with false positive findings on Multiparametric MRI prostate imaging. A high percentage of stroma and chronic inflammation, as well as presence of acute inflammation is associated with false positive lesions. Adenosis and areas with increased stroma and atrophy may be associated with higher PIRADS scores.

1106 Prognostic Value of Microscopic Linear Length and Gleason score of the Tumor at Positive Margin in Robot Assisted Radical Prostatectomy Specimens: A study of 127 whole mount cases

Beena Umar[1], *Mohamed Alhamar*[2], *Kanika Taneja*[3], *Mireya Diaz-Insua*[4], *Sean R Williamson*[1], *Nilesh Gupta*[5]. [1]Henry Ford Health System, Detroit, MI, [2]Henry Ford Health System, Dearborn, MI, [3]Henry Ford Health System, Detroit, Michigan, [4]Henry Ford Health System, [5]Henry Ford Hospital, Detroit, MI

Background: Localized prostate cancers (PCa) are usually treated with radical prostatectomy (RP) to improve cancer specific survival. Presence of positive surgical margins (PSM) is an independent prognostic factor as well as a reason for adjuvant therapy. Currently there is heterogeneous data about the significance of extent of PSM. Some studies have used the term focal and extensive and others have done exact quantification of the PSM. Some studies have questioned if extent of positive surgical margin provides any additional prognostic significance. On this background, we wanted to assess the correlation of linear length of PSM in RP specimens with the risk of biochemical recurrence (BCR). In addition, we also evaluated other pathologic parameters such as Gleason score (GS) of the tumor at the positive margin, location of positive margin, and positivity within or outside of the prostatic capsule.

Design: We reviewed 127 cases of PCa with PSM on patients who underwent RP at our institution between 2012-2014. Microscopic linear length (LL) of positive margin was measured and cases were stratified as follows, LL <1mm, 1-3mm and >3mm. Following parameters were also assessed: Gleason score and stage of the main tumor, tumor volume, location of positive margin, GS at the positive margin, capsular incision with positive margin (CI) versus extraprostatic extension with positive margin (EPE-M).

Results: After pathologic review, 127 patients were grouped as follows,

1. 26 with LL of <1mm, 41 with LL of 1-3 mm and 60 with LL of > 3. During the 4.5 years of follow up 0, 9, 20 patients had BCR in each group respectively. Our data suggest that LL is associated with an increased risk of BCR (p<0.001) (table 1).

2. Patients were further stratified according into two groups: CI and EPE-M, and association between LL and BCR was retained for EPE-M (p=0.036) but did not exist for CI (p=0.432).

3. Statistical significant association was also found between increasing GS of the tumor at margin and BCR (p=0.001). (table 2)

4. Apex was the most common positive margin (49%) and three fourths of the PSM were present in posterior half of prostate gland. No significant associations were seen in location of PSM and BCR.

Table 1. Association of Linear Length with BCR

	Linear length < 1 mm n=26	Linear length 1-3 mm n=41	Linear length > 3 mm n=60
BCR absent	26	32	40
BCR present	0	9	20

Table 2. Association of Increasing Gleason score at positive margin with BCR

	GS at the margin: 6 n=38	GS at the margin: 7 n=60	GS at the margin: 8 n=17	GS at the margin: 9 n=12
BCR absent	37	49	8	4
BCR present	1	11	9	8

Conclusions: In summary, linear length of positive surgical margin and Gleason score of the tumor at margin are significant predictors of biochemical recurrence in radical prostatectomy specimens. EPE-M carries worse prognosis than CI. We recommend reporting these three margin parameters in RP cases with PSM.

1107 Are Certain High Grade Prostatic Intraepithelial Neoplasia Subtypes Associated with Increased Risk of Prostatic Adenocarcinoma?

Beena Umar[1], *Kanika Taneja*[2], *Mohamed Alhamar*[3], *Mehrnoosh Tashakori*[4], *Ifeoma N Onwubiko*[5], *Nallasivam Palanisamy*[1], *Sean R Williamson*[1], *Nilesh Gupta*[6]. [1]Henry Ford Health System, Detroit, MI, [2]Henry Ford Health System, Detroit, MI, [3]Henry Ford Health System, Dearborn, MI, [4]Detroit, MI, [5]Henry Ford Health System, [6]Henry Ford Hospital, Detroit, MI

Background: High grade prostatic intraepithelial neoplasia (PIN) is a presumed precursor lesion of prostatic adenocarcinoma (PCa). Studies have shown that extensive sampling of prostatic tissue and multifocal PIN are better predictors of cancer than unifocal PIN diagnosed on limited samples. However, currently there is no consensus on overall management and subsequent follow-up of PIN. Moreover, to the best of our knowledge, there are only a few studies on the morphologic patterns of PIN to stratify men with an increased risk of PCa. Thus, we aimed to study the correlation of the morphologic patterns of PIN with the subsequent progression to PCa.

Design: We reviewed 323 patients who underwent transrectal needle biopsies and diagnosed with isolated PIN without current or prior diagnosis of carcinoma or atypical glands at our institution from 2009 to 2016. The following parameters were recorded: 1. Morphologic pattern of PIN which were divided into 4 categories with increasing complexity - flat, tufted, micropapillary and cribriform. When more than one pattern was present the more complex pattern was assigned. 2. Extent of PIN: Focal (1 core); multifocal (>1 to 3 cores) and extensive (> 3 cores).

Results: Out of 323 patients, 7 patients were re-categorized as being negative for PIN and were excluded from final analysis. The distribution of the pattern and extent of PIN in the remaining 316 cases is provided in Table 1 & 2 respectively.

No cancer was seen in cases with flat PIN, 10% of cases with tufted morphology progressed to PCa, 18% of cases with micropapillary morphology progressed to PCa and 25% of cases with cribriform morphology progressed to PCa. Out of 9 cases with micropapillary morphology, 4 cases were multifocal, 3 cases were extensive and 2 cases showed focal involvement. When only multifocal or extensive involvement was noted, 25% of the cases with micropapillary morphology progressed to PCa.

Our data suggest that morphologic patterns of PIN are associated with progression to PCa (χ^2 =17.850; df=3; p<0.0005). We further observed higher rate of micropapillary and cribriform patterns in biopsies that progressed to PCa.

Table 1: Morphologic patterns of HGPIN

	Tufted	Micropapillary	Cribri-form	Flat
Progressed to cancer (n=38)	25 (66%)	9 (24 %)	4 (10%)	0 (0%)
Remained benign (n=278)	222 (80%)	41(15%)	12(4%)	3(1%)

Table 2: Extent of HGPIN

	Focal	Multifocal	Extensive
Progressed to cancer (n=38)	19 (50%)	14(37%)	5(13%)
Remained benign (n=278)	146(52%)	103(37%)	29(10%)

Conclusions: In summary, we found that morphologic patterns of PIN are associated with progression to PCa with micropapillary and cribriform being the most worrisome patterns, especially if these are multifocal or extensive. We recommend reporting micropapillary and cribriform patterns of PIN in pathology reports for closer surveillance of these patients.

1108 PREVIOUSLY PUBLISHED

1109 How Do Clinicians Interpret Contemporary Prostate Biopsy Reports?

Murali Varma[1], *Jon Oxley*[2], *Krishna Narahari*[3], *Malcolm Mason*[4], *Daniel Berney*[5]. [1]University Hosp of Wales, Cardiff, Wales, [2]North Bristol NHS Trust, Bristol, Bristol, [3]University Hospital of Wales, Cardiff, UK, [4]Cardiff University, Cardiff, UK, Cardiff, Wales, [5]Queen Mary University of London, London

Background: Recent years have seen significant changes in prostate biopsy technique and reporting practice but there is limited information on how clinicians use pathological data in prostate needle biopsy reports.

Design: A survey was circulated to urologists and oncologists to investigate how they use data in prostate needle biopsy reports.

Results: Responses were received from 114 respondents (88 urologists, 26 oncologists). 97 (94%) use the number of positive cores from each side and 43 (42%) use the % number of positive cores. 72 (71%) would not differentiate between the number of positive cores in targeted and non-targeted samples (2/10 standard biopsies and 3/3 targeted biopsies from a single lesion assessed as 5 cores positive for patient management). 87 (84%) use % core involvement while 62 (60%) use mm linear involvement. If multiple Gleason Scores were included in a report, 77 (78%) would use the worst score even if it was present in a core with very little tumour, 12% would use the global score and 10% the score in the core most involved by tumour. 55 (55%) either never or rarely used perineural invasion for patient management.

1. The number of cores is an important parameter for clinicians (whether using overall number or % positive) but may be difficult to determine in the laboratory (for example due to core fragmentation). Hence, the biopsy-taker must indicate the number of biopsies taken and the pathologist must ensure that number of positive cores from each site/side is not greater than the number of biopsies taken from that site/side.

2. Multiple biopsies taken from a single site are often interpreted by clinicians as separate cores when determining the number of positive cores so pathologists should report "number of SITES positive" rather than "number of CORES positive".

3. Clinicians have a non-uniform approach to the interpretation of multiple Gleason Scores in a prostate biopsy report. The reporting pathologist is in a better position to determine which of the Gleason Scores is most representative in an individual case so we suggest that pathologists also include a single "bottom-line" Gleason Score for each case to direct the clinician's treatment decision.

4. Perineural invasion is uncommonly used by clinicians so this parameter does not need to be a mandatory data item in prostate needle biopsy reports.

5.

6.

1110 Molecular Characterization and Clinical Outcome of Clear Cell Papillary Renal Cell Carcinoma

Kartik Viswanathan[1], *Kyung Park*[2], *Francesca Khani*[3], *Juan Miguel Mosquera*[4], *Brian Robinson*[3]. [1]New York Presbyterian Hospital - Weill Cornell Medicine, [2]New York, NY, [3]Weill Cornell Medicine, New York, NY, [4]Weill Cornell Medical College, New York, NY

Background: Clear cell papillary renal cell carcinoma (CCP-RCC) represents the fourth most common renal cell carcinoma (RCC) after conventional clear cell, papillary and chromophobe RCC. Although patients with CCP-RCC behave in an indolent fashion in reported cases, long-term clinical outcomes remain unclear. Also, only limited molecular information is available in CCP-RCC, which has primarily been focused on *VHL* alterations. In this study we aimed to better understand the mutational landscape of CCP-RCC and provide extended follow up information.

Design: A retrospective search of our institutional database from 1997-2017 yielded 64 cases of CCP-RCC treated by surgical resection. Follow up was obtained for all patients. All H&E and, when available, immunostained slides were reviewed. A subset of 17 cases that showed classic morphology and immunoprofile of CCP-RCC was selected for molecular testing. We used the Oncomine Comprehensive Assay v3 (ThermoFisher) that covers 161 cancer-related genes including 51 fusion drivers, 91 copy number variants, 48 full-length genes and 87 hotspot mutations. HDx positive controls were used and ≥ 90% of expected variants were detected. Average read depth per sample was 1418.

Results: For the cohort of 64 CCP-RCC, the mean patient age was 60 years (range 34-82) with a 1.6:1 male:female ratio. The racial distribution was 37.5% Caucasian, 20.3% African American, 6.3% Asian, 1.6% Other and 34.4% Unknown. CCP-RCC was identified in the context of end-stage renal disease in 29.7% of the cases. No recurrence or metastasis was detected in any case after a mean follow up of 57 months (range 1-240 months). In the subset of 17 CCP-RCC that underwent sequencing, seven cases (41.1%) showed no mutations in the cancer-related genes tested, eight (47.1%) cases had a single mutation, and only two (11.8%) cases had 2 mutations (Table 1). No fusion drivers were detected.

TABLE 1: Molecular characterization of 17 cases of CCP-RCC

Mutation identified	Frequency (%)
No mutations	7/17 (41.1%)
ARID1A*[a]	4/17 (23.5%)
NOTCH3[a]	3/17 (17.6%)
TSC1[a]	2/17 (11.8%)
KIT[b]	2/17 (11.8%)
ATM[a]	1/17 (5.9%)

* Two cases with *ARID1A* mutations also showed a second *NOTCH3* or *TSC1* mutation

[a] Loss-of-function mutation

[b] Gain-of-function mutation

Conclusions: All 64 patients with CCP-RCC had indolent behavior after a maximum follow up of twenty years. Targeted sequencing of 17 cases showed recurrent somatic mutations in *ARID1A*, *NOTCH3*, *KIT* and *TSC1* in subsets of tumors. Nearly half of the cases had no detectable mutation at all. This study is the largest and most comprehensive molecular characterization of CCP-RCC to date and reports the longest available follow up. Our findings support the notion that CCP-RCC harbors a unique mutational landscape and follows an indolent clinical course.

1111 SPINK1 Loss in Upper Tract Urothelial Carcinoma is Associated with Advanced Stage Disease

Kartik Viswanathan[1], *Kyung Park*[2], *Aram Vosoughi*[3], *Peyman Tavassoli*[4], *Juan Miguel Mosquera*[5], *Francesca Khani*[6], *Brian Robinson*[6]. [1]New York Presbyterian Hospital - Weill Cornell Medicine, [2]New York, NY, [3]Weill Cornell Medicine / Englander Institute for Precision Medicine New York, NY, [4]BC Cancer Agency, Vancouver, BC, [5]Weill Cornell Medical College, New York, NY, [6]Weill Cornell Medicine, New York, NY

Background: Although urothelial carcinoma is a common cause of death in the United States, useful prognostic markers are lacking. Serine peptidase inhibitor Kazal type 1 (SPINK1) was recently described as a novel prognostic marker and was associated with higher stage malignancies and lymph node metastasis in patients who underwent radical cystectomy for lower tract urothelial carcinoma. However, little is known of the SPINK1 expression status and its prognostic significance in upper tract urothelial carcinoma. Here we assess SPINK1 levels in upper tract urothelial carcinoma (UTUC) and correlate the expression status to clinicopathologic parameters.

Design: We identified 34 cases of UTUC from 2012-2014 in our institutional archives for tissue microarray construction. TMAs were then stained for SPINK1 and interpreted as follows: staining in <= 50% of the cells was considered altered (loss of) expression while staining in >50% of the cells was considered retained. Clinical follow up was obtained for all patients.

Results: Mean patient age was 75 years (range 39-89) with a 1.3:1 male:female ratio. The average length of patient follow-up for our cases is 30 months (range 3 to 68 months). SPINK1 loss was associated with a higher tumor stage (stage pT2-T4) compared to patients with retained SPINK1 expression (14/17 vs. 5/15; p=0.01). We did not find any significant association between SPINK1 expression loss and tumor grade (p=0.091), nodal metastasis (p=0.14), smoking (p=0.52), or distant metastasis (p=0.265). There was a trend toward shorter overall survival in patients with SPINK1 loss (p=0.066). Of note, SPINK1 expression was concordant in 8 of 11 cases that had both invasive and non-invasive components available for evaluation. In 7 of these 11 cases, SPINK1 was lost in both the invasive and non-invasive components, suggesting that loss of SPINK1 may be an early event in UTUC and a useful prognosticator on biopsy.

Conclusions: SPINK1 expression loss was more frequently seen in invasive upper tract urothelial carcinoma and retained in non-invasive upper tract urothelial carcinomas. SPINK1 loss is associated with high stage (pT2-T4) disease in our cohort, and there was a trend toward decreased overall survival in patients with SPINK1 loss. Our findings are comparable to those of SPINK1 in the lower urinary tract, suggesting that SPINK1 may serve as a useful adjunct prognostic marker in both upper and lower urinary tract urothelial carcinoma.

1112 Identification of Characteristic Immune Profiles from Gene Expression Data in Renal Cell Carcinoma Gene Expression TCGA Data Sets

Konstantin Volyanskyy[1], *Minghao Zhong*[2], *Robert Lucito*[3], *Michael Fanucchi*[4], *John T Fallon*[5], *Nevenka Dimitrova*[6]. [1]Larchmont, NY, [2]Westchester Medical Center/ New York Medical College, [3]Hofstra Northwell School of Medicine, Hofstra University, [4]New York Medical College, WMCHealth Cancer Institute, [5]Westchester Medical Center, Valhalla, NY, [6]Pelham, NY

Background: The immune system is designed to identify antigens, including tumor antigens, and attack diseased cells. However, more often than not, the tumor cells can suppress the immune system from performing its vital role of attacking the tumor. The study of this misregulation of the immune system is at the forefront of basic and clinical science research since understanding this phenomenon will lead to better treatments for patients where their own immune system will fight the aberrantly growing tumor cells.

Design: We have studied renal cell carcinoma (RCC) and specifically looked at the gene expression profiles of immune related genes to determine if; first, the subtypes had different immunoregulatory protein profiles and second, to determine if any of the profiles could be used to identify possible treatment options or possibly new targets for future treatment development. Specifically, we used Level III RNASeq gene expression data in 889 tumor samples of RCC across three major subtypes – clear cell renal cell carcinoma (ccRCC), papillary renal cell carcinoma (prRCC), chromophobe carcinoma (chRCC), and 129 normal samples from The Cancer Genome Atlas (TCGA) and studied the expression patterns of 800 immune related genes selected from InnateDB public database.

Results: We characterized immune-related gene expression profiles associated with each cancer subtype by generating predictive models using Random Forest algorithm.

We identified highly predictive genes in each experiment. For example, upregulated SCARB1, TNFRSF10B, TNFRSF14, CD40, CD276 distinguishes ccRCC vs normal; upregulated CD63, ITGAX, TAPBP and down-regulated TEK, CD34 distinguishes prRCC vs normal; upregulated BSG, CLIP1, CR1L and down-regulated FGFR3, THY1, TNFSF10 characterize chRCC vs normal; CD34 , KDR, CD36 are high rank predictors of RCC subtypes, as well as are CDH5, CD93, CXCR7, INSR, and EBF2 in all subtypes and normal prediictions.

We have identified well known targets of immune misregulation that are currently being therapeutically targeted such as CTLA4. We have also identified other genes such as the B-Cell co-activator CD137 (4-1BB) as well as its ligand (CD137) which s

Conclusions: Our findings show heterogeneous patterns in immune profiles and can be further used for analysis and characterization in connection with proteomic and mutations data. With further investigations, these results will be helpful for identifying current treatment options as well as new potential therapeutic targets to improve patient outcomes.

1113 VSTM2A Over-expression is a Sensitive and Specific Biomarker for Mucinous Tubular and Spindle Cell Carcinoma (MTSCC) of the Kidney

Lisha Wang[1], *Yuping Zhang*[2], *Stephanie L Skala*[1], *Xuhong Cao*[3], *Brendan A Veeneman*[3], *Jin Chen*[3], *Cieślik Marcin*[3], *Javed Siddiqui*[3], *Fengyun Su*[3], *Pankaj Vats*[3], *Ming Zhou*[4], *Ankur Sangoi*[5], *Kiril Trpkov*[6], *Adeboye O. Osunkoya*[7], *Giovanna A Giannico*[8], *Jesse McKenney*[9], *Arul Chinnaiyan*[10], *Saravana M Dhanasekaran*[3], *Rohit Mehra*[1]. [1]University of Michigan, Ann Arbor, MI, [2]Michigan Center for Translational Pathology, [3]University of Michigan, [4]Clements University Hospital, Dallas, TX, [5]El Camino Hospital, Mountain View, CA, [6]University of Calgary, Calgary, AB, [7]Emory Univ/Medicine, Atlanta, GA, [8]Vanderbilt University Medical Center, Nashville, TN, [9]Cleveland Clinic, Cleveland, OH, [10]Plymouth, MI

Background: Next-generation RNA sequencing (RNA-seq) of tumors allows biomarker and therapeutic target discovery, provides insight into disease mechanisms, and enables identification of cells of origin. Our recent RNA-seq study revealed recurrent chromosomal losses and somatic mutations of genes in the Hippo signaling pathway in the majority of MTSCC (PMID: 27604489).

Design: We performed an integrative analysis of 1,049 renal cell carcinoma (RCC) RNA-seq samples (combined from The Cancer Genome Atlas and in-house studies) and the Knepper dataset of microdissected rat nephrons (PMID: 25817355) to identify cancer- and lineage-specific biomarkers. We then utilized an RNA *in situ* hybridization (RNA-ISH) platform to examine top ranked candidates in 60 whole tissue sections, including 21 MTSCC cases, 24 type 1 papillary renal cell carcinoma cases (PRCC), 5 type 2 PRCC cases, 5 clear cell renal cell carcinoma cases (CCRCC), and 5 chromophobe renal cell carcinoma cases (ChRCC).

Results: Our integrative RNA-seq analysis identified *VSTM2A* and *IRX5* as novel cancer-specific and cell type/lineage-specific biomarkers in MTSCC. All 21 MTSCC showed high expression of *VSTM2A* (mean ISH product score = 265; range = 165 to 350). There was a strong correlation of *VSTM2A* gene expression assessed by both RNAseq and RNA-ISH product score (Spearman's correlation coefficient R^2 = 0.81, P = 0.00016). The majority of type 1 PRCC, type 2 PRCC, CCRCC, and ChRCC showed negative/low expression of *VSTM2A* (mean ISH product score = 10; range = 0 to 80). Four out of nine PRCC tumors with low-grade spindle cell foci showed low to moderate expression of *VSTM2A* (mean ISH product score = 65; range = 0 to 180). *IRX5*, a marker of the loop of Henle, was moderate to highly expressed in all 21 MTSCC tumors (mean ISH product score = 165; range = 75 to 350). *IRX5* gene expression strongly correlated with the RNA-ISH product score (Spearman's correlation coefficient R^2 = 0.69, P = 0.00291). In MTSCC, *VSTM2A* over-expression was more sensitive (100% vs. 95.24%) and specific (94.87% vs. 79.49%) than *IRX5.*

Conclusions: We validated *VSTM2A* over-expression as a sensitive and specific marker for MTSCC. *VSTM2A* may also serve as a potential diagnostic marker to clinically distinguish cases with overlapping histology (MTSCC vs. PRCC). Our results also suggest the loop of Henle as a putative cell of origin for MTSCC.

1114 PD-L1 Expression in Upper Tract Urothelial Carcinomas Associated with Higher Pathological Stage

Michael Ward[1], *Dan Albertson*[2], *Larissa Furtado*[3], *Georgios Deftereos*[3]. [1]University of Utah, Cottonwood Heights, UT, [2]University of Utah, [3]University of Utah, Salt Lake City, UT

Background: Upper tract urothelial carcinomas (UTUCs) are a subset of urothelial carcinomas which, compared to urothelial carcinomas (UCs) of the bladder, are associated with increased morbidity, in part due to treatment by radical nephroureterectomy and the resulting loss of renal function. Immune checkpoint inhibitors are showing promise in the treatment of UC the bladder and UTUC alike. There are conflicting data in recent literature regarding the utility of PD-L1 expression as a biomarker for predicting response to immune checkpoint therapy. PD-L1 28-8 was recently approved by the US Food and Drug Administration (FDA) as complementary diagnostic for the use of nivolumab in UC. While several large studies have looked at PD-L1 expression in UC in general, to our knowledge none of them have looked at expression of PD-L1 in upper tract urothelial carcinomas as a separate group.

Design: This is a retrospective study of 37 cases of UTUC collected by the department of pathology at the University of Utah between 2005 and 2014. Representative tumor cores from each case were compiled into tissue microarrays and immunohistochemical stains for PD-L1 223C and 28-8 clones were performed. The percentage of tumor cells showing positive staining was recorded and possible clinicopathological correlations were investigated. Cases with ≥1% tumor cells showing membranous staining were considered as positive.

Results: 11 out of 37 cases (29.7%) of cases stained positive for PD-L1, and there was 100% concordance between 22C3 and 28-8 in terms of positivity rate. 10 out of 18 (55.6%) cases with higher pathological

stage (pT3/4) were positive for PD-L1, compared to only 1 out of 19 (5.3%) cases of lower pathological stage (pTis/1/2) UTUC (p=0.0011). No correlations were found between rates of PD-L1 positivity and grade (low vs. high) or location (involvement of renal pelvis alone vs. ureteropelvic involvement).

Conclusions: Our study shows that 29.7% of UTUCs are positive for PD-L1 expression, comparable to the 20-30% reported in bladder UCs. Our results suggest that higher pathological stage UTUCs are more often associated with PD-L1 expression, which may reflect an immune response evasion mechanism that UC cells acquire later in disease progression. Finally, PD-L1 22C3 and 28-8 clones show similar patterns of staining in this setting.

1115 Microscopic Bladder Neck Invasion Re-Visited: Correlation with Tumor Topography, Staging and Grading

Vitor Werneck Krauss SIlva[1], *Hikmat Al-Ahmadie*[1], *Ying-Bei Chen*[1], *Anuradha Gopalan*[1], *S. Joseph Sirintrapun*[1], *Satish Tickoo*[1], *Victor Reuter*[1], *Samson W Fine*[1]. [1]Memorial Sloan Kettering Cancer Center, New York, NY

Background: In the 7th edition AJCC staging system, microscopic bladder neck invasion (BN+) was re-assigned to pT3a. BN+ is defined as tumor involving discrete smooth muscle bundles in the absence of benign prostatic glandular tissue in the BN section(s). The topography of tumors displaying BN+ and related pathologic features has not been well studied.

Design: We identified entirely-submitted and whole-mounted radical prostatectomies having BN+ with or without prostatic tissue in the BN section, over a 12-year period. 177 had all slides available for review and constitute the current cohort. We performed detailed histopathologic analysis, including: confirmation of "true" BN+, topography of the dominant prostatic tumor, as well as grading and staging parameters.

Results: 12/177 (7%) cases had BN section involvement adjacent to benign prostatic tissue and were excluded, leaving 165 cases with "true" BN+. In 5 (3%) cases, BN+ was the sole stage-determining (pT3a) factor, while 160 (97%) cases had other sites of extraprostatic extension (EPE), 94 (57%) showed seminal vesicle invasion (SVI) and 83 (50%) had positive lymph nodes (LNI). In 90 (56%) cases, BN was the sole positive margin.

45 (27%) BN+ cases had anterior-dominant tumors, 36 (22%) posterior-dominant tumors and 84 (51%) had tumor either involving both anterior+posterior or diffusely involving the gland.

In 4/45 anterior-dominant tumors, BN+ was the stage (pT3a) determining factor; 38 (84%) cases also had anterior EPE (exclusively [n=25] or with other non-anterior EPE [n=13]) and 3 (7%) had non-anterior EPE only. 6/94 SVI and 14/83 LNI cases were in the anterior-dominant group. Grading distribution for anterior-dominant v. other tumors is detailed in Table 1, with Grade Group ≥ 3 seen in 42% of anterior-dominant versus 82% of other tumors (p<0.01).

	Anterior-Dominant Tumors [n=45]	Other Tumors [n=120]
Grade Group 1	2 (4.5%)	0 (0%)
Grade Group 2	24 (53%)	14 (11.5%)
Grade Group 3	8 (18%)	26 (22%)
Grade Group 4	3 (6.5%)	13 (11%)
Grade Group 5	8 (18%)	59 (49%)
Not graded (profound treatment effect)	0 (0%)	8 (6.5%)

Microscopic BN invasion is rarely the sole factor determining pT3a stage, but is the sole positive margin in ~50% of tumors with BN+.

- Topographic location of tumors exhibiting microscopic BN involvement is heterogeneous.
- In the BN+ group with anterior-dominant tumors, the overwhelming majority also showed anterior extraprostatic extension.
- Grade Group ≥ 3, SVI and LNI are less frequently seen in anterior-dominant tumors with BN+.

1116 Challenges in Pathologic Staging of Renal Cell Carcinoma: An Interobserver Variability Study of Urologic Pathologists

Sean R Williamson[1], *Priya Rao*[2], *Ondrej Hes*[3], *Jonathan Epstein*[4], *Maria Picken*[5], *Ming Zhou*[6], *Maria Tretiakova*[7], *Satish Tickoo*[8], *Ying-Bei Chen*[9], *Victor Reuter*[8], *Stewart Fleming*[10], *Fiona Maclean*[11], *Nilesh Gupta*[12], *Naoto Kuroda*[13], *Brett Delahunt*[14], *Rohit Mehra*[15], *Christopher Przybycin*[16], *Liang Cheng*[17], *John Eble*[17], *David Grignon*[17], *Holger Moch*[18], *Jose Lopez*[19], *L. Priya Kunju*[20], *Pheroze Tamboli*[21], *John Srigley*[22], *Mahul Amin*[23], *Guido Martignoni*[24], *Michelle S Hirsch*[25], *Kiril Trpkov*[26]. [1]Henry Ford Health System, Detroit, MI, [2]UT MD Anderson Cancer Center, Houston, TX, [3]Biopticka laborator, Plzen, [4]The Johns Hopkins Med Inst, Baltimore, MD, [5]Loyola Univ. Med. Ctr., Maywood, IL, [6]Clements University Hospital, Dallas, TX, [7]University of Washington, Seattle, WA, [8]Memorial Sloan Kettering CC, New York, NY, [9]Memorial Sloan Kettering Cancer Center, New York, NY, [10]University of Dundee, Dundee, [11]Douglass Hanly Moir Pathology, Macquaire Park, NSW, [12]Henry Ford Hospital, Detroit, MI, [13]Kochi Red Cross Hospital, Kochi City, Kochi, [14]Wellington School/Medicine, Wellington South, New Zealand, [15]University of Michigan, Ann Arbor, MI, [16]Cleveland Clinic, Cleveland, OH, [17]Indiana University School of Medicine, Indianapolis, IN, [18]Institute for Klinische Pathologie der Universitat, Zurich [19]Hospital de Cruces-Osakidetza, Barakaldo, [20]University of Michigan Hospital, Ann Arbor, MI, [21]UT-MD Anderson Cancer Center, Houston, TX, [22]Trillium Health Partners - Credit Valley Hospital, Mississauga, ON, [23]Methodist University Hospital, Memphis, TN, [24]Verona, Italy, [25]Brigham and Women's Hospital, Boston, MA, [26]University of Calgary, Calgary, AB

Background: Staging criteria for renal sinus, perinephric fat, and sinus vein invasion were defined more precisely at the ISUP Consensus Conference in 2012 (*Am J Surg Pathol* 2013;37:1505-17). However, renal cell carcinoma differs from many other cancers, in that tumors are often spherical with subtle tongue-like extensions into veins, renal sinus, or perinephric tissue, in contrast to infiltrative and desmoplastic growth prototypical of cancer. We sought to study whether urologic pathologists have uniform criteria for assigning pathologic stage categories in this setting.

Design: An online survey was constructed and circulated to urologic pathologists with interest in kidney tumors, aiming to evaluate interobserver agreement, emphasizing challenging or borderline cases for renal staging. Response rate was 86% (30/35) of the invited pathologists with broad geographic distribution. Most questions included 1-4 images, divided into categories of: vascular and renal sinus invasion (n=24), perinephric tissue invasion (n=9), and gross pathology/specimen handling (n=17). Responses were collapsed for analysis into positive and negative for upstaging. Equivocal responses were included in the latter. Consensus was regarded as 67% (2/3) of participants.

Results: Consensus was reached in 16/24 (67%) questions for sinus and vascular invasion (13 positive and 3 negative for pT3a, with 80% or greater consensus in 12), and 4/9 (44%, with 3 at 80% or greater consensus) for perinephric invasion. Lack of agreement was especially encountered regarding small tumor protrusions into possible vascular lumina, close to the tumor leading edge or within the tumor. For gross photographs, the most common response was that findings were "suspicious for venous invasion," but required histologic confirmation. Most participants (60%) rarely used special stains to evaluate vascular invasion, usually endothelial markers (80%). Most agreed that a spherical mass bulging well beyond the kidney parenchyma into the renal sinus (70%) or perinephric fat (90%) did not necessarily indicate invasion. Criteria for assessment of biopsy site artifact were also incompletely agreed upon.

Conclusions: Interobserver agreement in pathologic staging of renal cancer is relatively good among urologic pathologists interested in kidney tumors, even when selecting cases that test the earliest thresholds for extrarenal extension. Disagreements however remain, particularly for tumors with small, finger-like protrusions, closely juxtaposed to the main mass.

1117 Whole Genome Sequencing of Matched Prostate Cancer and High-Grade Prostatic Intraepithelial Neoplasia Demonstrates Both Shared and Private Mutations

Parker Wilson[1], *Wade Schulz*[2], *Xiaoling Guo*[3], *Kaya Bilguvar*[4], *Peter Humphrey*[5]. [1]Hamden, CT, [2]Roseville, MN, [3]Harrison, NY, [4]Yale Center for Genome Analysis, [5]Yale University, New Haven, CT

Background: High-grade prostatic intraepithelial neoplasia (HGPIN) is a well-established risk factor for the development of prostatic adenocarcinoma. It's unclear whether prostate cancer arises from HGPIN or if the acquisition of additional somatic variants can lead to invasion. We report the first whole genome sequencing (WGS) study in matched HGPIN and prostate cancer samples to demonstrate overlapping and unique somatic variants.

Design: FFPE tissue cores were collected from 3 radical prostatectomy specimens containing separate foci of HGPIN and adenocarcinoma. High-depth WGS was performed on tumor,

HGPIN and corresponding normal in each patient. Sequences were aligned and somatic variants were called using SomaticSniper (SNV) and Breakdancer Max (structural variants). Functional annotation (VEP), transcription factor analysis (Enrichr) and clonality analysis (SciClone) were performed.

Results: Approximately 25% of somatic variants in prostate cancer were detected in corresponding HGPIN. The overlap represents 9-11% of total SNV (Figure 1A) and 6-13% of structural variants (Figure 1B).

The majority of SNV were located in intronic or intergenic sites with fewer than 1% affecting protein coding regions. Individual samples of HGPIN or adenocarcinoma harbored 15-35 non-synonymous SNVs in exons or splice sites. Genes affected by somatic SNV unique to prostate cancer included NRIP1 and NCAN. Somatic SNV affecting genes unique to HGPIN, included: OR56B4, MMEL1, GAB4 and PKNOX2.

Prostate cancer and HG-PIN shared numerous deletions, inversions and translocations (Figure 2); some of which implicated well-known oncogenes. A 13Mb PTEN inversion was detected in both HGPIN and prostate cancer in patients 1 and 3 suggesting that PTEN loss occurs prior to invasion. Patients 1 and 3 had additional translocations involving the ETS family member, FLI1, that were shared between HGPIN and prostate cancer. TMPRSS2:ERG and ETV family translocations were not detected.

Transcription factor pathway analysis demonstrated increased enrichment of androgen receptor signaling in prostate cancer compared to corresponding HG-PIN. Clonality analysis suggests that prostate cancer arises from a HGPIN clone.

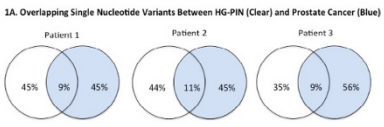

Figure 2. Genomic Rearrangements Seen in Corresponding HGPIN and Prostate Cancer Samples in Patient 1 (HGPIN=Red, Adenocarcinoma=Blue)

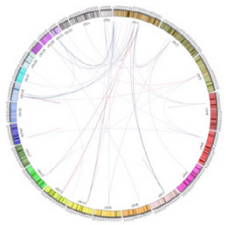

Conclusions: HGPIN and prostate cancer are genetically related but both proliferations harbor private mutations. PTEN inversion, ETS family member translocation and somatic variantion in androgen receptor signaling genes occur in HGPIN prior to invasion.

1118 Comprehensive Genomic Profiling of Adult Renal Sarcomas Provides Insight into Disease Biology and Opportunities for Targeted Therapies

Evgeny Yakirevich[1], *Eduard Fridman*[2], *Shamlal Mangray*[1], *Kara A Lombardo*[1], *Russell Madison*[3], *Matthew Cooke*[3], *Jennifer Webster*[3], *Jeffrey S Ross*[4], *Siraj Ali*[5]. [1]Rhode Island Hospital, Providence, RI, [2]Sheba Medical Center, Kfar-Sava, Israel, [3]Foundation Medicine, Inc, [4]Foundation Medicine, Cambridge, MA, [5]Cambridge, MA

Disclosures:
Russell Madison: *Employee*, Foundation Medicine, Inc.
Matthew Cooke: *Employee*, Foundation Medicine, Inc.
Jeffrey Ross: *Employee*, Foundation Medicine, Inc.
Siraj Ali: *Employee*, Foundation Medicine, Inc.

Background: Primary adult renal sarcoma (RS) is a rare aggressive kidney neoplasm. We queried whether comprehensive genomic profiling (CGP) could uncover characteristic genomic alterations (GA) and guide therapy for patients with RS.

Design: Hybrid capture-based CGP was performed on FoundationOne platform including 315 cancer-related genes and introns from 28 genes frequently rearranged in cancer in 13 adult RS with various histologic types, none with rhabdoid features. Tumor samples were analyzed for all classes of GA, including base substitutions, small indels, rearrangements, and copy number alterations. High-level amplifications were defined as >6 copies. Tumor mutational burden (TMB) was determined on 1.1 Mbp of sequenced DNA and microsatellite instability (MSI) was determined on 114 loci.

Results: There were 6 female and 7 male patients with a median age of 62 years (range 18 to 82 years). The primary RS tissue was used for CGP in 12 RS and a metastasis biopsy in 1 RS. CGP revealed 57 GA (4.38 per tumor), 29 of which were clinically relevant genomic alterations (CRGA) (2.23 per tumor). At least one CRGA was detected in 9 (69%) cases. High-level amplifications involving 4q12 amplicon (4q12 amp) of the *KIT* and *PDGFRA* genes, were identified in 4 (31%) cases (three undifferentiated pleomorphic sarcomas and 1 high-grade myxofibrosarcoma). Two of these undifferentiated pleomorphic sarcomas had *KDR* gene co-amplification in addition to *KIT* and *PDGFRA*. Additional CRGA were found in *NF1* (23%) and *MET* (8%). The mean tumor mutational burden (TMB) was 3.51 mutations per megabase with a median of 2.5 mutations per Mb. None (0%) of RS featured TMB > 10 mutation/Mb and all (100%) of RS were MSI-stable.

Conclusions: Renal sarcomas are primary renal malignancies with diverse histology and genomic profiles including 31% of cases with 4q12 amplification involving the *KIT/PDGFRA* genes. Although, based on their low TMB, RS are not likely candidates for immunotherapies, as many as 69% of RS harbor clinically relevant genomic alterations which could lead to potential benefit from targeted therapies.

1119 Clinicopathologic and Molecular Characteristics of Urothelial Carcinoma of the Ureter

Qiqi Ye[1], *Samuel Barasch*[2], *Humayun Islam*[3], *Minghao Zhong*[4]. [1]Westchester Medical Center, Valhalla, NY, [2]Westchester Medical Center, Poughkeepsie, NY, [3]Westchester Medical Center, Valhalla, NY, [4]Westchester Medical Center/ New York Medical College

Background: Upper urinary tract urothelial carcinoma comprises only 5-10% of all urothelial carcinomas (UCs). UCs involving ureter only are even rare. To date, literature on characteristics of UC of the ureter is limited. The aim of the study is to investigate clinicopathologic features and *TERT* promoter mutation status in UC of the ureter.

Design: Retrospective review of all UC cases (~ 2000 cases) at our institution between 2005 to 2017 was done and cases involving ureter only are included in this study. *TERT* promoter mutation status was determined by PCR amplification and bidirectional Sanger sequencing.

Results: 18 UC cases with involvement of ureter only were identified. The median age of patients was 73 years (range: 62 to 90 years) with the majority being males (72.2%). Of the 18 patients, 12 underwent radical nephroureterectomy and 6 segmental ureterectomy. Concomitant lymph node dissection was performed in 7 patients, and the median number of lymph nodes removed was 4.5. The tumor ranged in size from 1 mm to 17.5 cm (median, 4.15 cm). Histologically high-grade disease was present in 14 cases. 4 of them exhibited architectural pattern other than papillary: 3 solid growth pattern, and 1 flat pattern. 5 of them showed invasion into muscularis propria (pT2) and 4 into periureteral tissue (pT3). Histologic variation was observed in 3 cases with glandular and squamous differentiation as well as sarcomatoid changes. The other pathologic features included lymphovascular invasion in 2 cases, lymph nodes metastasis (N3) in 1 case, necrosis in 2 cases, and concomitant carcinoma *in situ* in 3 cases. Clinical follow-up was available in 9 of the 18 cases with follow-up time ranging from of 4-133 months (mean, 46.7 months). Subsequent to their definitive surgery, 5 of the 9 patients had recurrent urothelial carcinoma: two in the bladder, 10 and 57 months after nephroureterectomy, respectively for pT2 stage carcinoma; one in the kidney, ureter and bladder 5 months after ureterectomy for pT3 stage carcinoma; one in the bladder and kidney 32 months after ureterectomy for pTis stage carcinoma; and one in the bladder and kidney 26 months after ureterectomy for pT2 stage carcinoma. *TERT* mutations were found in 61.1% of cases.

Conclusions: Our study focuses exclusively on UC of ureter. The data demonstrated that clinicopathologic features of ureter UC are slightly different from those of bladder UC: higher incidence of high grade disease, more aggressive clinical behavior and relatively lower *TERT* mutation rate.

1120 PD-L1 As A Prognostic Indicator In Renal Cell Carcinoma: Study Of A Mixed Ethnicity Asian Cohort

Joe Yeong[1], *Huihua Li*[1], *Chee Keong Toh*[2], *Puay Hoon Tan*[1], *Li Yan Khor*[1]. [1]Singapore General Hospital, Singapore, [2]National Cancer Centre, Singapore

Background: Expression and distribution of PD-L1 in renal cell carcinoma (RCC) and its role in prognosis are still not clear. We investigate PD-L1 protein expression as a prognostic marker by two antibody clones in a RCC cohort of mixed ethnicity Asian patients.

Design: Three hundred and twenty-two cases of various RCC subtypes diagnosed at our institution between 1995 and 2008 were scored "PD-L1 positive" or "PD-L1 negative" based on 1% tumor proportion score cut-off for PD-L1 protein expression by two anti-PD-L1 antibodies, E1L3N (Cell Signaling Technology, Danvers, MA) and SP263 (Ventana

Medical System, Tucson, AZ). Disease-free survival (DFS) and overall survival (OS) were correlated with protein expression.

Results: Two hundred and sixty-seven cases (83%) of clear cell RCC and 55 (17%) cases of non-clear cell RCC were studied. Overall PD-L1 expression rates for the entire cohort were 8% and 13% for E1L3N and SP263 clones, respectively. PD-L1 immunoreactivity was not noted in tumor infiltrating lymphocytes. Patients bearing PD-L1-positive tumors experienced significantly worse DFS (E1L3N: HR 1.89, 95% CI 1.15-3.09, p=0.01; SP263: HR 1.97, 95% CI 1.08-3.61, p=0.02) but not OS compared to those with PD-L1-negative tumors. Multivariable survival analysis further confirmed the results of the E1L3N clone, but not SP263, as significant after adjusting for pathologic stage, histologic grade and histologic subtype (E1L3N: HR 1.86, 95% CI 1.10-3.13, p=0.02; SP263: HR 1.65, 95% CI 0.81-3.34, p=0.16). Intriguingly, in multivariable analysis, the H score of E1L3N was also significantly associated with worse DFS (based on single increment level of H score; HR=1.02, 95% CI 1.00-1.02, p=0.030). Furthermore, E1L3N was an independent prognostic marker in the 267 cases of clear cell RCC in the cohort (HR=1.885, 95% CI 1.13- 3.14, p=0.015). Additionally, the Kendall concordance coefficient, calculated to evaluate agreement between the two clones, showed a κ coefficient of 0.786, indicating substantial concordance. The addition of PD-L1 E1L3N tumor proportion score to clinicopathological features significantly increased the prognostic value for DFS ($\Delta LR\chi 2=5.25$, p=0.022), compared to clinicopathological features alone.

Conclusions: PD-L1-positive RCCs in our study cohort showed unfavorable prognosis. PD-L1 E1L3N was an independent prognostic indicator of clinical outcome either by a 1% expression cutoff or as a continuous parameter. Validation with a larger prospective cohort is warranted.

1121 Mitotic Index and Recurrence of Non-Invasive Papillary Urothelial Cell Carcinoma

Michael P Zaleski[1], *Augustyna Gogoj*[2], *Jay Raman*[3], *David DeGraff*[3], *Joshua I Warrick*[4]. [1]Penn State Hershey Medical Center, Hershey, PA, [2]Penn State College of Medicine, [3]Penn State Hershey Medical Center, [4]Penn State Health

Background: Non-invasive papillary urothelial carcinoma (NIPUC) is biologically and clinically diverse. Criteria state that NIPUC is to be graded as high- or low-grade. Tumor grade informs on prognosis and dictates treatment. Several studies have shown high cell cycle activity predicts recurrence and progression of NIPUC. Yet, mitotic counts are not emphasized in contemporary grading of NIPUC.

Design: We set out to determine if mitotic index predicts recurrence of NIPUC, while controlling for tumor grade. To investigate, we assembled a retrospective cohort of 63 NIPUCs, each a primary diagnosis made at TUR. Slides were methodically reviewed and assigned a high/low grade. Mitotic index was determined in all cases, as mitotic figures per 10 high-power fields (HPF). Clinical data were obtained by chart review. Recurrence risk was compared using Kaplan-Meier methods and Cox regression.

Results: Of the 63 cases of NIPUC, 23 (36.5%) were high-grade and 40 (63.5%) were low-grade. Intravesical Bacillus Calmette-Guerin (BCG) had been given in 24 (38%) of the cases. 21 (33.3%) tumors had recurred. Median follow-up time was 36 months (lower and upper quartiles 14 and 60 months). We chose a cutoff of >1 mitotic figure per 10 HPF based on manual review, separating tumors into mitotic-high and mitotic-low groups. Among patients who had not received intravesical BCG, recurrence at 60 months was 80% in those with mitotic-high tumors, and 20% in those with mitotic-low tumors (p=0.02, log rank test). This association held when controlling for high/low tumor grade (multivariate Cox regression, p=0.02 for mitotic group, p=0.54 for high/low tumor grade). Among patients who had received intravesical BCG, there was no difference in recurrence between mitotic-high and mitotic-low tumors (p=0.76).

Conclusions: The findings suggest mitotic index may predict recurrence in patients with NIPUC who do not receive intravesical BCG, adding information beyond that given by high/low tumor grade. Thus, it may be useful to add a metric of mitotic activity to current grading schema.

1122 Gleason Grade 4 Expansile Cribriform Pattern is Associated with Poor Prognosis in Prostate Cancer

Xiaotun Zhang[1], *Laureano J Rangel Latuche*[2], *John Cheville*[1]. [1]Mayo Clinic, Rochester, MN, [2]Mayo Clinic Rochester

Background: The Gleason grade is one of the key factors guiding prostate cancer (PCa) clinical treatment decisions and predicting patients' prognosis. The recently described Grade Group (GG) system further simplifies the interpretation of Gleason scores. Gleason grade 4 glands can be found in GG 2 to 5; however, the clinical-pathological correlations among different patterns of Gleason grade 4 glands are poorly understood.

Design: Pathology files were searched for post-radical prostatectomy patients with diagnoses of GG2 or higher PCa. All cases were re-reviewed to verify the Gleason scores and to determine the percentage of Gleason grade patterns. Cases of disagreement were solved by consensus. Medical record search was performed and clinicopathologic factors were collected. The association between the Gleason grade 4 histological patterns (including poorly formed/fused glands, small uniform cribriform, expansile cribriform, mucinous, and glomerulations), and the risk of biochemical recurrence (BCR) and systemic progression (SP) was assessed by Cox proportional hazard regression.

Results: A total of 262 cases with a median follow-up time of 14.3 years were included in this study. In univariable hazard ratio analyses, the expansile cribriform pattern had a significantly higher risk of BCR and SP ($p<0.0001$). There was no evidence of the other Gleason grade 4 patterns showing a significant association with the outcomes.

In multivariable hazard ratio analyses, expansile cribriform pattern remained significantly associated with BCR and SP ($p<0.0001$). Interestingly, poorly formed/fused Gleason grade 4 pattern appeared to be relevant to BCR with cribriform pattern increasing ($p=0.0164$). The combined effect of expansile cribriform and poorly formed/fused patterns became stronger when associated with SP ($p<0.0001$).

Conclusions: Our data suggest that the expansile cribriform pattern of Gleason grade 4 carcinomas is associated with worse prognosis. One limitation of this study is due to the biological nature of PCa, in which most cases were composed of a mixture of at least 2 Gleason grade 4 patterns of variable percentages. Therefore, data based solely on histology may not reflect the biological features of expansile cribriform pattern entirely. This study will be followed by molecular tests to determine the underlying genetic differences of individual Gleason grade 4 histological patterns, with a focus on expansile cribriform glands.

1123 Metastatic Renal Cell Carcinoma to the Brain: A Contemporary Clinicopathologic Analysis of 33 Cases

Wei Zheng[1], *Kar-Ming Fung*[2], *Adeboye O. Osunkoya*. [1]Emory Univ/Medicine, Atlanta, GA, [2]Univ of OK HSC, Oklahoma City, OK

Background: Renal cell carcinoma (RCC), especially clear cell RCC is known to metastasize to several sites. However, there are only few large series in the pathology literature specifically analyzing the clinicopathologic features of patients with metastatic RCC to the brain.

Design: A search was made through a multi-institutional Urologic Pathology database and consult cases for patients with metastatic RCC to the brain. Multiple clinicopathologic parameters were analyzed. The location, focality, and size of brain metastases were also obtained.

Results: Thirty-three cases of primary RCC with brain metastasis were identified. Twenty (61%) patients were male. Mean age at diagnosis of primary RCC was 59 years (range: 37-82 years). The mean interval from primary RCC diagnosis to brain metastasis was 39 months (range: 4-156 months). All primary tumors were unilateral with 57% right sided. The mean size of primary RCC was 7.9 cm (range: 2.5-19.5 cm). The histologic subtypes were conventional clear cell RCC (69%), sarcomatoid variant of clear cell RCC (14%), and unclassified RCC (17%). Most cases were Fuhrman nuclear grade 3 or 4. Pathologic stage of primary tumor was as follows: 3% pT1 (1 case pT1b), 59% pT3 (17 cases pT3a and 2 cases pT3b), 3% pT4. Seven of 24 (29%) patients had brain metastases at the time of initial diagnosis of primary RCC. The metastatic RCC in brain was right-sided (53%), left-sided (41%) and bilateral (6%). The mean size of brain metastasis was 2.3 cm (range: 0.3-5.5 cm). Twenty of 33 (61%) patients had a single brain metastasis and 13 patients (39%) had multifocal lesions at the time of diagnosis of the first brain metastasis. The regional distribution of brain metastases of RCC was as follows: frontal (29%), parietal (28%), temporal (18%), occipital (3%), cerebellum (10%), pontine (3%), pineal (3%), basal ganglia (3%) and periventricular area (3%). Seventeen of 33 (52%) patients also had metastases to other sites, with lung (67%) and bone (20%) being the most common sites.

Conclusions: This is one of the largest contemporary studies on the clinicopathologic findings of patients with metastatic RCC to the brain. Clear cell RCC is the most common variant of RCC to metastasize to the brain. A solitary brain mass on imaging does not exclude metastatic RCC. Future molecular studies including gene expression profiling of these tumors may play a role in predicting the likelihood of patients who are at increased risk of developing brain metastasis.

1124 Vascular Tumors of the Adrenal Gland: A Multi-institutional Clinicopathologic Analysis of 27 Cases

Wei Zheng[1], *Liang Cheng*[2], *Feng Yin*[3], *Kar-Ming Fung*[4], *Adeboye O. Osunkoya*. [1]Emory Univ/Medicine, Atlanta, GA, [2]Indiana University School of Medicine, Indianapolis, IN, [3]University of Oklahoma HSC, Edmond, OK, [4]Univ of OK HSC, Oklahoma City, OK

Background: Vascular tumors of the adrenal gland (VTAG) are relatively uncommon and may pose a diagnostic challenge. The frequency of the detection of these tumors is increasing due to high resolution imaging studies. However, there is very limited data in the literature regarding the clinicopathologic features of these tumors.

Design: A search was made through a multi-institutional Urologic Pathology database and consult cases for VTAG. Clinicopathologic features and follow-up data were obtained.

Results: Twenty-seven cases of VTAG were identified. Fifteen (65%) patients were female. Mean age was 60 years (range: 25-81 years). The most common clinical presentation was abdominal/flank/back pain in 16/27 (60%) cases. The tumors were incidentally detected on imaging in 6/27 (22%) cases, and signs of Cushing's syndrome or pheochromocytoma were present in 5/27 (19%) cases. All tumors were unilateral and 16/27 (60%) cases were right sided. In all cases, imaging studies revealed a solid and/or cystic adrenal mass. Grossly, the mean tumor size was 5.3 cm (range: 0.6-12.0 cm). The tumors were mainly located in the cortex, with larger ones also replacing most of the medulla. Seventeen of 27 (63%) cases were hemangioma (13/17 of which were associated with cystic features), 5/27 (19%) cases were malignant vascular tumors (4 cases of angiosarcoma and 1 case of adrenal venous leiomyosarcoma), 4/27 (15%) cases were lymphangioma, and 1/27 (3%) cases was vascular leiomyomatosis. Of the hemangioma cases, 2/17 (12%) were associated with adrenal cortical adenoma and 3/17 (18%) were isolated, but interestingly had associated elevated mineralocorticoid, glucocorticoid or normetanephrine levels. Calcifications were present in 4/27 (15%) cases. Additional findings included thrombosis, hemorrhage, and necrosis. Mean follow up duration was 63 months (range: 7 to 139 months). All cases except leiomyosarcoma and angiosarcoma showed no evidence of recurrence or metastasis after adrenalectomy. Sites of distant metastasis were kidney and lung.

Conclusions: This is one of the largest studies to date of VTAG. Although benign vascular tumors accounted for the majority of the cases, a subset of these tumors are malignant. Intratumoral heterogeneity with associated cystic features is common. In addition, the fact that some cases of adrenal hemangioma had elevated mineralocorticoid, glucocorticoid or normetanephrine levels without other associated entities, highlights a potential clinical/radiological diagnostic pitfall.

1125 Renal Cell Carcinoma with leiomyomatous stroma: Pathologic and Genomic Features

Ming Zhou[1], *Fang-Ming Deng*[2], *Cristina Magi-Galluzzi*[3]. [1]Clements University Hospital, Dallas, TX, [2]New York University Medical Center, New York, NY, [3]Cleveland Clinic, Cleveland, OH

Background: Renal cell carcinoma (RCC) with leiomyomatous stroma constitutes a group of uncommon renal epithelial tumors with clear cells and prominent fibromuscular stroma. It is unclear whether it is a distinct type of RCC with distinct genomic changes, or whether it is related to clear cell RCC (CCRCC) or clear cell papillary RCC (CCPRCC).

Design: 11 RCC with leiomyomatous stroma were selected based on morphology (clear cells with prominent fibromuscular capsule and stroma and positive CK7/CD10/CA9). Three of these tumors along with 13 CCRCC and 11 CCPRCC were subject to array-based comparative genomic hybridization. Genomic DNA was extracted from formalin-fixed, paraffin-embedded tumor and adjacent normal tissue and hybridized to Affymetrix SNP 6.0 Array chips, which contained 1.8 million genetic markers, including 906,600 single nucleotide polymorphisms (SNPs) and 946,000 probes for copy number variation (CNV) detection. Selected immunohistochemical stains were also performed.

Results: For patients with RCC with leiomyomatous stroma, mean age was 50.3 (48-84) years. Mean tumor size was 1.9 (0.9-3.5) cm. Grade was 1, 2 and 3 in 2, 5 and 4 cases, respectively. Pathologic stage was T1a in all cases. The dominant morphological feature was clear cells forming arborizing glands and acini with branching contour and basally oriented nuclei and abundant apical cytoplasm with blebs. All tumors had prominent fibromuscular capsule and stroma with various amounts of smooth muscle fibers. The epithelial cells were positive for CK7, CD10 and CA9. The following genomic changes were present in at least 2 of 3 RCC with leiomyomatous stroma: loss-8p12-q21.11 (containing TCEB1 gene), 7q11.21-22, 19p12-13; gain-18q21.1-22.1. None of these changes was, however, present in CCRCC and CCPRCC. In 13 CCRCC, the dominant genomic changes (in $\geq$7/13 tumors) included loss of 3p, 9p, Yp and gain of 11q. In 11 CCPRCC, the dominant genomic changes (in $\geq$6/11 tumors) were gain of 3p.

Conclusions: This study provides evidence that RCC with leiomyomatous stroma, CCRCC and CCPRCC are distinct tumors in their morphological, immunohistochemical and genomic features. RCC with leiomyomatous stroma comprises CK7/CD10/CA9 positive clear cells forming arborizing glands and acini with branching contour and basally oriented nuclei and abundant apical cytoplasm with blebs, and prominent fibromuscular capsule and stroma. Loss of 8p12-q21.11 (containing TCEB1), 7q11.21-22, 19p12-13, and gain of18q21.1-22.1 are seen in 2 of 3 tumors.

1126 How are Gleason Scores (GS) Categorized in the Current Literature

Amy G Zhou[1], *Jonathan Epstein*[1]. [1]The Johns Hopkins Med Inst, Baltimore, MD

Background: How are published studies categorizing Gleason grades after the 2014 ISUP recommendation to classify prostate cancer according to 5 Gleason grade groups?

Design: A PubMed search included all studies with "Gleason" published in 2016. We excluded review articles, case reports, meta-analyses, non-English articles, and articles without full text, leaving 822 articles for the study.

Results: Radiology (57.0%), Pathology (55.6%), and Urology (42.7%) journal articles were more likely than Oncology journal articles (27.3%, $p<0.05$) to grade GS 3+4 and 4+3 separately compared to lumping them as GS7. Articles authored by North Americans (45.8%) and Europeans (40.1%) separated GS 3+4 and 4+3 more than those authored by Asians (20.4%, $p<0.05$). When pathologist authors were included, GS 4+3 and 3+4 were graded separately in 52.8% of studies vs. in 27.8% without a pathologist ($p<0.001$). Clinical articles more often separated GS 3+4 and 4+3 (40.6%) compared to research articles (32.4%, p= 0.03). Articles with a pathologist more often separated GS 8 from 9-10 (42.3% vs. 26.1%, $p<0.001$). Radiology articles more often separated GS 8 from 9-10 (60%) compared to Urology (31.3%), Oncology (28.5%) and Rad. Onc. (23.1%) articles, $p<0.05$. Pathology journals separated 8 vs. 9-10 in 9/22 (40.9%) articles. We categorized the 5 Grade Groups as "Ideal" with all other grading as "Not Ideal". The only significant difference was between Pathology (20.4% Ideal) and Oncology articles (6.4% Ideal, p=0.017), compared to Urology (11.9%), Radiology (13.4%), and Rad. Onc. (3.4%) articles. N. American authors were more likely to use Ideal grouping (11.7%) compared to Asians (4.2%, p= 0.014); Europeans was 9.3%. When a pathologist was included, Ideal grouping was more likely (16.3%) in articles vs. no pathologist (5.3%, $p<0.001$). We then separated the Not Ideal groupings, arranging them in decreasing order from ideal (Table). When a pathologist was included, articles were more likely to be classified closer to Ideal ($p<0.001$). N. American ($p<0.001$) and European (p = 0.016) authored articles were more likely to classify cases closer to the Ideal than those by Asian authors. Journal types were not different in this analysis.

Gleason category	No Pathologist	Pathologist	Total
≤6, 3+4, 4+3, 8, 9-10 (ideal)	24 (6.8%)	46 (19.7%)	70
≤6, 3+4, 4+3, 8-10	45 (12.7%)	58 (24.9%)	103
≤6, 7, 8, 9, 10	26 (7.3%)	16 (6.9%)	42
≤6, 7, 8- 10	148 (41.7%)	68 (29.2%)	216
≤7, 8-10 OR ≤6, 7-10	112 (31.5%)	45 (19.3%)	157
Total	355	233	588

Conclusions: There is still wide variation in how Gleason scores are grouped world-wide. Although there are some differences in grading based on whether pathologist are co-authors, geographic location, and type of journal, only a minority of published articles are grouping Gleason scores accurately.

FIG. 895

	Gleason score	HGPIN	Lower grade IT	Higher grade IT	IDCP
Case 1	4+5=9	HRAS	APC, PTEN, MED12	Failed QC due to large quantity of necrosis	APC, PTEN, TP53, TP53
Case 2	4+5=9	ATM, HRAS, STK11	ATM, ATM, CSNK2A1, STK11	APC, ATM, ATM, FGFR1,MYC, STK11, GNAS, ZNF217	APC, APC, ATM, ATM, FGFR1, MYC, STK11, GNAS, ZNF217
Case 3	4+5=9	PTEN, STK11	STK11	CTNNB1, PTEN, P53, P53, STK11	PTEN, P53, P53, STK11
Case 4	4+5=9	HRAS, STK11, U2AF1	STK11, U2AF1	STK11, U2AF1	FBXW7, PTEN, STK11, U2AF1
Case 5	4+5=9	TMPRSS2(1)-ERG(2), BRAF, U2AF1	TMPRSS2(1)-ERG(2), TP53, TP53, STK11, U2AF1	TMPRSS2(1)-ERG(2), FGFR1, MYC, GATA3, PTEN, TP53, TP53, TIAF1, NF1, BRCA1, U2AF1	TMPRSS2(1)-ERG(2), MYC, GATA3, TP53, TP53, TIAF1, NF1, BRCA1, ERBB2, U2AF1

Amplification, deletion, gain of function missense mutation, loss of function missense mutation, nonsense mutation, frameshift INDEL, gene fusion. Repeated gene names of identical color represent the presence of two distinct defects belonging to the same general category of genetic abnormalities within a particular lesion. IT = invasive tumor (lower grade corresponds to Gleason 4 and higher grade to Gleason 5). Small areas of Gleason 3 present in case 1 were sequenced together with Gleason 4 components (lower grade IT).

FIG. 1030

Table. Summary of Next Generation Sequencing Results of 16 Cases of CCP-RCC

Gene	Variant	Cosmic ID	Predictive algorithms (SIFT/Condel)	1	2	3	4	5	6	7	8	9	10	11	12	13	14	15	16
ATM	p.V2915M		Deleterious/ Deleterious												X				
ATM	p.E641G		Neutral/ Tolerated															X	
ATM	p.C2464R	COSM758329	Neutral/ Tolerated														X		
APC	p.L2039F		Deleterious/ Deleterious														X		
BCORL1	p.S56C		Deleterious/ Unknown												X				
BRCA2	p.S976I		Unknown/ Unknown					X											
BRCA2	p.E3053G		Deleterious/ Deleterious														X		
EGFR	p.V765M	COSM28603	Tolerated/ Deleterious			X													
ERBB2	p.S427L		Unknown/ Deleterious												X				
JAK1	p.Q565*		Unknown/ Unknown					X											
PHF6	p.I33M		Neutral/ Tolerated														X		
SMC1A	p.A73D		Deleterious/ Neutral										X						
VHL	p.V74G	COSM3364888	Unknown/ Deleterious														X		
VHL	p.N78S	COSM17855	Unknown/ Deleterious			X													
ZRSR2	p.R448_ R449insSR	COSM5762985	Unknown/ Unknown							X									